

# **B**urnup Credit Criticality Benchmark Phase IID

Burnup Calculations of Gadolinium-  
Bearing Fuel Rods in Boiling Water  
Reactor Assemblies for Storage and  
Transportation



**Unclassified**

**English text only**

31 August 2023

**NUCLEAR ENERGY AGENCY  
NUCLEAR SCIENCE COMMITTEE**

**Cancels & replaces the same document of 29 August 2023**

## **Burnup Credit Criticality Benchmark Phase IIID**

### **Burnup Calculations of Gadolinium-Bearing Fuel Rods in Boiling Water Reactor Assemblies for Storage and Transportation**

Please note that this report was initially published in November 2022 (NEA/NSC/R(2022)3) under erroneous benchmark number IIB; in this updated version (NEA/NSC/R(2022)3/CORR) this has been corrected into IIID.

**JT03524516**

## ORGANISATION FOR ECONOMIC CO-OPERATION AND DEVELOPMENT

The OECD is a unique forum where the governments of 38 democracies work together to address the economic, social and environmental challenges of globalisation. The OECD is also at the forefront of efforts to understand and to help governments respond to new developments and concerns, such as corporate governance, the information economy and the challenges of an ageing population. The Organisation provides a setting where governments can compare policy experiences, seek answers to common problems, identify good practice and work to co-ordinate domestic and international policies.

The OECD member countries are: Australia, Austria, Belgium, Canada, Chile, Colombia, Costa Rica, the Czech Republic, Denmark, Estonia, Finland, France, Germany, Greece, Hungary, Iceland, Ireland, Israel, Italy, Japan, Korea, Latvia, Lithuania, Luxembourg, Mexico, the Netherlands, New Zealand, Norway, Poland, Portugal, the Slovak Republic, Slovenia, Spain, Sweden, Switzerland, Türkiye, the United Kingdom and the United States. The European Commission takes part in the work of the OECD.

OECD Publishing disseminates widely the results of the Organisation's statistics gathering and research on economic, social and environmental issues, as well as the conventions, guidelines and standards agreed by its members.

## NUCLEAR ENERGY AGENCY

The OECD Nuclear Energy Agency (NEA) was established on 1 February 1958. Current NEA membership consists of 34 countries: Argentina, Australia, Austria, Belgium, Bulgaria, Canada, the Czech Republic, Denmark, Finland, France, Germany, Greece, Hungary, Iceland, Ireland, Italy, Japan, Korea, Luxembourg, Mexico, the Netherlands, Norway, Poland, Portugal, Romania, Russia (suspended), the Slovak Republic, Slovenia, Spain, Sweden, Switzerland, Türkiye, the United Kingdom and the United States. The European Commission and the International Atomic Energy Agency also take part in the work of the Agency.

The mission of the NEA is:

- to assist its member countries in maintaining and further developing, through international co-operation, the scientific, technological and legal bases required for a safe, environmentally sound and economical use of nuclear energy for peaceful purposes;
- to provide authoritative assessments and to forge common understandings on key issues as input to government decisions on nuclear energy policy and to broader OECD analyses in areas such as energy and the sustainable development of low-carbon economies.

Specific areas of competence of the NEA include the safety and regulation of nuclear activities, radioactive waste management and decommissioning, radiological protection, nuclear science, economic and technical analyses of the nuclear fuel cycle, nuclear law and liability, and public information. The NEA Data Bank provides nuclear data and computer program services for participating countries.

This document, as well as any data and map included herein, are without prejudice to the status of or sovereignty over any territory, to the delimitation of international frontiers and boundaries and to the name of any territory, city or area.

Corrigenda to OECD publications may be found online at: [www.oecd.org/about/publishing/corrigenda.htm](http://www.oecd.org/about/publishing/corrigenda.htm).

---

### © OECD 2022

You can copy, download or print OECD content for your own use, and you can include excerpts from OECD publications, databases and multimedia products in your own documents, presentations, blogs, websites and teaching materials, provided that suitable acknowledgement of the OECD as source and copyright owner is given. All requests for public or commercial use and translation rights should be submitted to [neapub@oecd-nea.org](mailto:neapub@oecd-nea.org). Requests for permission to photocopy portions of this material for public or commercial use shall be addressed directly to the Copyright Clearance Center (CCC) at [info@copyright.com](mailto:info@copyright.com) or the Centre français d'exploitation du droit de copie (CFC) [contact@cfcopies.com](mailto:contact@cfcopies.com).

---

## *Foreword*

The Working Party on Nuclear Criticality Safety (WPNCS), under the Nuclear Science Committee (NSC) of the Nuclear Energy Agency (NEA), has organised several international benchmarks to assess variations in predicted  $k_{inf}$  and nuclide concentrations in burnup calculations by different code systems. The Phase IIIC burnup credit (BUC) benchmark results for 9×9 “STEP-3” boiling water reactor (BWR) fuel assembly design, organised by the NEA Expert Group on Burnup Credit (EGBUC), showed that modelling options, i.e. spatial resolution of gadolinium pins and depletion step size, can cause significant variations in predicted  $k_{inf}$  and assembly average nuclide concentrations. A Phase IIID BUC benchmark was subsequently organised by the NEA Expert Group on Used Nuclear Fuel criticality (EGUNF) to re-examine code and nuclear data performance for BWR lattice calculations and focus on the depletion modelling of gadolinium fuel in the burnup region near peak reactivity. Modelling of the gadolinium pins was specified in the benchmark to limit some of the modelling variations observed in the Phase IIIC benchmark and to better isolate differences caused by code methods and nuclear data relevant to gadolinium depletion in the burnup range important to gadolinium depletion. This report presents the results of the Phase IIID benchmark approved at the meeting of the WPNCS in July 2018. Results of 37 depletion calculations from 14 organisations in 13 countries are compared and analysed in detail.

## *Acknowledgements*

The NEA Secretariat would like to extend its sincere gratitude to the members of the Expert Group on Used Nuclear Fuel criticality for their contributions to this report, as well as for the valuable time and effort dedicated to this field of work. Special thanks go to Dr Ugur Merturek, Ian Gauld and B.J. Marshal of Oak Ridge National Laboratory for developing the benchmark specifications, performing the data analysis and preparing the final report. Thanks also go to Meraj Rahimi of the US Nuclear Regulatory Commission for initially proposing and championing the benchmark, and Shadi Ghayeb for initially developing the software used to assist in data analysis.

## *List of authors*

Ugur Merturek (Oak Ridge National Laboratory, United States)

Ian C. Gauld (Oak Ridge National Laboratory, United States)

B.J. Marshall (Oak Ridge National Laboratory, United States)

## *Table of contents*

<b>List of abbreviations.....</b>	<b>10</b>
<b>Executive summary .....</b>	<b>11</b>
<b>1. Introduction .....</b>	<b>13</b>
<b>2. Benchmark problem.....</b>	<b>14</b>
2.1 Geometry .....	14
2.2 Materials .....	14
2.3 Depletion conditions .....	17
2.4 Requested data .....	19
<b>3. Participants and codes .....</b>	<b>20</b>
3.1 Codes .....	21
3.2 Nuclear data library .....	22
<b>4. Comparisons of results from participants.....</b>	<b>24</b>
4.1. Web interface .....	24
4.2. Neutron multiplication factor, $k_{inf}$ , by all codes.....	25
4.3. Neutron multiplication factor by Monte Carlo codes .....	30
4.4. Neutron multiplication factor by deterministic codes.....	33
4.5. Burnup and distribution of gadolinium isotopes.....	37
4.6. Actinide concentrations in UO <sub>2</sub> rods .....	51
4.7. Fission product distribution in UO <sub>2</sub> rods .....	73
4.8. Comparison of SCALE code results .....	95
4.9. Effect of nuclear data libraries .....	99
<b>5. Conclusions .....</b>	<b>101</b>
<b>References .....</b>	<b>103</b>
<b>Annex A. Participant list.....</b>	<b>103</b>
<b>Annex B. Results from all participants.....</b>	<b>104</b>

### List of tables

Table 2.1. Gadolinia ring dimensions	16
Table 2.2. Fuel and absorber number densities	17
Table 2.3. Water and Zircaloy number densities	17
Table 2.4. Depletion steps	18
Table 2.5. Nuclides to report	19
Table 2.6. Burnup and decay times for reporting	19
Table 3.1. List of participants	20
Table 3.2. List of codes used in the benchmark	22
Table 3.3. List of nuclear data libraries	23
Table 4.1. Statistics for $k_{inf}$ reported by all participants	27
Table 4.2. Peak $k_{inf}$ and corresponding burnup by all participants	29
Table 4.3. Statistics for $k_{inf}$ reported by CE MC codes	32

Table 4.4. Statistics for $k_{inf}$ reported by deterministic codes, excluding results with ENDF/B-V and ENDF/B-VI libraries	36
Table 4.5. Statistics for rod average $^{154}\text{Gd}$ concentrations	38
Table 4.6. Statistics for rod average $^{155}\text{Gd}$ concentrations	41
Table 4.7. Statistics for rod average $^{156}\text{Gd}$ concentrations	42
Table 4.8. Statistics for rod average $^{157}\text{Gd}$ concentrations	44
Table 4.9. Statistics for rod average $^{158}\text{Gd}$ concentrations	45
Table 4.10. Statistics for rod average $^{160}\text{Gd}$ concentration	46
Table 4.11. Statistics for $^{155}\text{Gd}$ concentration at 8 GWd/MTU	48
Table 4.12. Statistics for $^{157}\text{Gd}$ concentration at 8 GWd/MTU	48
Table 4.13. Statistics for gadolinia rod burnup	51
Table 4.14. Statistics for $^{238}\text{U}$ concentration	53
Table 4.15. Statistics for $^{234}\text{U}$ concentration	54
Table 4.16. Statistics for $^{235}\text{U}$ concentration	55
Table 4.17. Statistics for $^{236}\text{U}$ concentration	56
Table 4.18. Statistics for $^{237}\text{Np}$ concentration	58
Table 4.19. Statistics for $^{238}\text{Pu}$ concentration	60
Table 4.20. Statistics for $^{239}\text{Pu}$ concentration	62
Table 4.21. Statistics for $^{239}\text{Pu}$ concentration (KENOREST and SC2 removed)	63
Table 4.22. Statistics for $^{240}\text{Pu}$ concentration	65
Table 4.23. Statistics for $^{241}\text{Pu}$ concentration	67
Table 4.24. Statistics for $^{241}\text{Pu}$ concentration (KENOREST, SC2, HE2 results removed)	68
Table 4.25. Statistics for $^{242}\text{Pu}$ concentration	70
Table 4.26. Statistics for $^{241}\text{Am}$ concentration	72
Table 4.27. Statistics for $^{241}\text{Am}$ concentration (KENOREST, HE2, SC2 results removed)	73
Table 4.28. Statistics for $^{99}\text{Tc}$ concentration	75
Table 4.29. Statistics for $^{103}\text{Rh}$ concentration	77
Table 4.30. Statistics for $^{131}\text{Xe}$ concentration	78
Table 4.31. Statistics for $^{133}\text{Cs}$ concentration	80
Table 4.32. Statistics for $^{143}\text{Nd}$ concentration	81
Table 4.33. Statistics for $^{148}\text{Nd}$ concentration	83
Table 4.34. Statistics for $^{147}\text{Sm}$ concentration	86
Table 4.35. Statistics for $^{149}\text{Sm}$ concentration	88
Table 4.36. Statistics for $^{151}\text{Sm}$ concentration	90
Table 4.37. Statistics for $^{152}\text{Sm}$ concentration	92
Table 4.38. Statistics for $^{152}\text{Sm}$ concentration (KENOREST, CA1, SC2 are removed)	93
Table 4.39. Statistics for $^{155}\text{Eu}$ concentration	94
Table B.1. $K_{inf}$ results from all participants at 0% void fraction (1/4)	105
Table B.1. $K_{inf}$ results from all participants at 0% void fraction (2/4)	106
Table B.1. $K_{inf}$ results from all participants at 0% void fraction (3/4)	107
Table B.1. $K_{inf}$ results from all participants at 0% void fraction (4/4)	108
Table B.3. $K_{inf}$ results from all participants at 70% void fraction (1/4)	113
Table B.3. $K_{inf}$ results from all participants at 70% void fraction (2/4)	114
Table B.3. $K_{inf}$ results from all participants at 70% void fraction (3/4)	115
Table B.3. $K_{inf}$ results from all participants at 70% void fraction (4/4)	116
Table B.4. $^{155}\text{Gd}$ concentration results from all participants at 0% void fraction	117
Table B.5. $^{155}\text{Gd}$ concentration results from all participants at 40% void fraction	118
Table B.6. $^{155}\text{Gd}$ concentration results from all participants at 70% void fraction	119
Table B.7. $^{157}\text{Gd}$ concentration results from all participants at 0% void fraction	120
Table B.8. $^{157}\text{Gd}$ concentration results from all participants at 40% void fraction	121
Table B.9. $^{157}\text{Gd}$ concentration results from all participants at 70% void fraction	122



**List of figures**

Figure 2.1. 2D fuel assembly	15
Figure 2.2. Detail of Gd <sub>2</sub> O <sub>3</sub> rod	16
Figure 4.1. Web interface screenshot	25
Figure 4.2. Comparison of $k_{inf}$ at 0% void fraction	26
Figure 4.3. Comparison of $k_{inf}$ at 40% void fraction	26
Figure 4.4. Comparison of $k_{inf}$ at 70% void fraction	26
Figure 4.5. $k_{inf}$ at 0% void fraction reported by Monte Carlo codes	31
Figure 4.6. $k_{inf}$ at 40% void fraction reported by Monte Carlo codes	31
Figure 4.7. $k_{inf}$ at 70% void fraction reported by Monte Carlo codes	31
Figure 4.8. $k_{inf}$ at 70% void fraction reported by Monte Carlo codes using CE libraries	31
Figure 4.9. $k_{inf}$ at 0% void fraction reported by deterministic codes	35
Figure 4.10. $k_{inf}$ at 40% void fraction reported by deterministic codes	35
Figure 4.11. $k_{inf}$ at 70% void fraction reported by deterministic codes	35
Figure 4.12. $k_{inf}$ at 70% void fraction reported by deterministic codes (results with ENDF/B-V and -VI removed)	35
Figure 4.13. Rod average <sup>154</sup> Gd concentrations at 0% void fraction	38
Figure 4.14. Rod average <sup>154</sup> Gd concentration at 70% void fraction	38
Figure 4.15. Rod average <sup>155</sup> Gd concentrations at 0% void fraction	40
Figure 4.16. Rod average <sup>155</sup> Gd concentrations at 70% void fraction	40
Figure 4.17. Rod average <sup>155</sup> Gd concentrations at 0% void fraction (HE2 results removed)	40
Figure 4.18. Rod average <sup>155</sup> Gd concentrations at 70% void fraction (HE2 results removed)	40
Figure 4.19. Rod average <sup>156</sup> Gd concentrations at 0% void fraction	41
Figure 4.20. Rod average <sup>156</sup> Gd concentration at 70% void fraction	41
Figure 4.21. Rod average <sup>157</sup> Gd concentrations at 0% void fraction	43
Figure 4.22. Rod average <sup>157</sup> Gd concentrations at 70% void fraction	43
Figure 4.23. Rod average <sup>157</sup> Gd concentrations at 0% void fraction (KENOREST and HE2 results removed)	43
Figure 4.24. Rod average <sup>157</sup> Gd concentrations at 70% void fraction (KENOREST and HE2 results removed)	43
Figure 4.25. Rod average <sup>158</sup> Gd concentration at 0% void fraction	44
Figure 4.26. Rod average <sup>158</sup> Gd concentration at 70% void fraction	44
Figure 4.27. Rod average <sup>160</sup> Gd concentration at 0% void fraction	45
Figure 4.28. Rod average <sup>160</sup> Gd concentration at 70% void fraction	45
Figure 4.29. Radial change in <sup>155</sup> Gd concentration at 0% void fraction at 8 GWd/MTU	47
Figure 4.30. Radial change in <sup>155</sup> Gd concentration at 70% void fraction at 8 GWd/MTU	47
Figure 4.31. Radial change in <sup>157</sup> Gd concentration at 0% void fraction at 8 GWd/MTU	47
Figure 4.32. Radial change in <sup>157</sup> Gd concentration at 70% void fraction at 8 GWd/MTU	47
Figure 4.33. Radial <sup>155</sup> Gd concentration at 0% void fraction in ring 1	49
Figure 4.34. Radial <sup>155</sup> Gd concentration at 70% void fraction in ring 1	49
Figure 4.35. Radial <sup>157</sup> Gd concentration at 0% void fraction in ring 1	49
Figure 4.36. Radial <sup>157</sup> Gd concentration at 70% void fraction in ring 1	49
Figure 4.37. Gadolinia rod average burnup versus lattice average burnup at 0% void fraction	50
Figure 4.38. Gadolinia rod average burnup versus lattice average burnup at 70% void fraction	50
Figure 4.39. Gadolinia rod average burnup versus lattice average burnup around peak reactivity at 0% void fraction	51
Figure 4.40. Gadolinia rod average burnup versus lattice average burnup around peak reactivity at 70% void fraction	51
Figure 4.41. <sup>238</sup> U concentration at 40% void fraction	52
Figure 4.42. <sup>238</sup> U concentration at 40% void fraction in 15-20 GWd/MTU burnup interval	52
Figure 4.43. <sup>234</sup> U concentration at 40% void fraction	54
Figure 4.44. <sup>234</sup> U concentration at 40% void fraction in 15-20 GWd/MTU burnup interval	54
Figure 4.45. <sup>235</sup> U concentration at 40% void fraction	55
Figure 4.46. <sup>235</sup> U concentration at 40% void fraction in 15-20 GWd/MTU burnup interval	55
Figure 4.47. <sup>236</sup> U concentration at 40% void fraction	56
Figure 4.48. <sup>236</sup> U concentration at 40% void fraction in 15-20 GWd/MTU burnup interval	56
Figure 4.49. <sup>237</sup> Np concentration at 70% void fraction	57
Figure 4.50. <sup>237</sup> Np concentration at 70% void fraction (KENOREST results removed)	57

Figure 4.51.	<sup>238</sup> Pu concentration at 40% void fraction at discharge	59
Figure 4.52.	<sup>238</sup> Pu concentration at 40% void fraction in 17-20 GWd/MTU burnup interval	59
Figure 4.53.	<sup>238</sup> Pu concentration at 70% void fraction in 17-20 GWd/MTU burnup interval	59
Figure 4.54.	<sup>238</sup> Pu concentration at 70% void fraction after five-year decay	59
Figure 4.55.	<sup>239</sup> Pu concentration at 40% void fraction at discharge	61
Figure 4.56.	<sup>239</sup> Pu concentration at 40% void fraction after five-year decay	61
Figure 4.57.	<sup>239</sup> Pu concentration at 0% void fraction in 15-20 GWd/MTU burnup interval	61
Figure 4.58.	<sup>239</sup> Pu concentration at 70% void fraction in 17-20 GWd/MTU burnup interval	61
Figure 4.59.	<sup>240</sup> Pu concentration at 40% void fraction at discharge	64
Figure 4.60.	<sup>240</sup> Pu concentration at 40% void fraction after five-year decay (AL1 results removed)	64
Figure 4.61.	<sup>240</sup> Pu concentration at 0% void fraction in 16-20 GWd/MTU burnup interval	64
Figure 4.62.	<sup>240</sup> Pu concentration at 70% void fraction in 16-20 GWd/MTU burnup interval	64
Figure 4.63.	<sup>241</sup> Pu concentration at 40% void fraction at discharge	66
Figure 4.64.	<sup>241</sup> Pu concentration at 40% void fraction after five-year decay	66
Figure 4.65.	<sup>241</sup> Pu concentration at 0% void fraction in 16-20 GWd/MTU burnup interval	66
Figure 4.66.	<sup>241</sup> Pu concentration at 70% void fraction in 16-20 GWd/MTU burnup interval	66
Figure 4.67.	<sup>242</sup> Pu concentration at 40% void fraction at discharge	69
Figure 4.68.	<sup>242</sup> Pu concentration at 40% void fraction after five-year decay	69
Figure 4.69.	<sup>242</sup> Pu concentration at 0% void fraction in 18-20 GWd/MTU burnup interval	69
Figure 4.70.	<sup>242</sup> Pu concentration at 70% void fraction in 18-20 GWd/MTU burnup interval	69
Figure 4.71.	<sup>241</sup> Am concentration at 40% void fraction	71
Figure 4.72.	<sup>241</sup> Am concentration at 40% void fraction after five-year decay	71
Figure 4.73.	<sup>241</sup> Am concentration at 0% void fraction in 18-20 GWd/MTU burnup interval	71
Figure 4.74.	<sup>241</sup> Am concentration at 70% void fraction in 18-20 GWd/MTU burnup interval	71
Figure 4.75.	<sup>99</sup> Tc concentration at 40% void fraction at discharge	74
Figure 4.76.	<sup>99</sup> Tc concentration at 40% void fraction after five-year decay	74
Figure 4.77.	<sup>99</sup> Tc concentration at 0% void fraction in 17.5-20 GWd/MTU interval	74
Figure 4.78.	<sup>99</sup> Tc concentration at 70% void fraction in 17.5-20 GWd/MTU interval (SC1 results removed)	74
Figure 4.79.	<sup>103</sup> Rh concentration at 40% void fraction at discharge	76
Figure 4.80.	<sup>103</sup> Rh concentration at 40% void fraction after five-year decay	76
Figure 4.81.	<sup>103</sup> Rh concentration at 0% void fraction in 16.5-20 GWd/MTU interval	76
Figure 4.82.	<sup>103</sup> Rh concentration at 70% void fraction in 16.5-20 GWd/MTU interval	76
Figure 4.83.	<sup>131</sup> Xe concentration at 40% void fraction at discharge	78
Figure 4.84.	<sup>131</sup> Xe concentration at 40% void fraction in 17-20 GWd/MTU interval	78
Figure 4.85.	<sup>133</sup> Cs concentration at 40% void fraction at discharge	79
Figure 4.86.	<sup>133</sup> Cs concentration at 40% void fraction in 14-20 GWd/MTU interval	79
Figure 4.87.	<sup>143</sup> Nd concentration at 40% void fraction at discharge	81
Figure 4.88.	<sup>143</sup> Nd concentration at 40% void fraction in 18-20 GWd/MTU interval	81
Figure 4.89.	<sup>148</sup> Nd concentration at 40% void fraction at discharge	83
Figure 4.90.	<sup>148</sup> Nd concentration at 40% void fraction in 19-20 GWd/MTU interval	83
Figure 4.91.	<sup>147</sup> Sm concentration at 40% void fraction at discharge	85
Figure 4.92.	<sup>147</sup> Sm concentration at 40% void fraction with five-year decay	85
Figure 4.93.	<sup>147</sup> Sm concentration at 70% void fraction in 17-20 GWd/MTU interval	85
Figure 4.94.	<sup>147</sup> Sm concentration at 70% void fraction with five-year decay in 17-20 GWd/MTU interval	85
Figure 4.95.	<sup>149</sup> Sm concentration at 0% void fraction at discharge	87
Figure 4.96.	<sup>149</sup> Sm concentration at 0% void fraction with five-year decay	87
Figure 4.97.	<sup>149</sup> Sm concentration at 40% void fraction at discharge	87
Figure 4.98.	<sup>149</sup> Sm concentration at 40% void fraction with five-year decay	87
Figure 4.99.	<sup>149</sup> Sm concentration at 70% void fraction	88
Figure 4.100.	<sup>149</sup> Sm concentration at 70% void fraction with five-year decay	88
Figure 4.101.	<sup>151</sup> Sm concentration at 0% void fraction at discharge	89
Figure 4.102.	<sup>151</sup> Sm concentration at 0% void fraction with five-year decay	89
Figure 4.103.	<sup>151</sup> Sm concentration at 70% void fraction	89
Figure 4.104.	<sup>151</sup> Sm concentration at 70% void fraction with five-year decay	89
Figure 4.105.	<sup>152</sup> Sm concentration at 0% void fraction at discharge	91
Figure 4.106.	<sup>152</sup> Sm concentration at 70% void fraction	91
Figure 4.107.	<sup>152</sup> Sm concentration at 70% void fraction in 15-20 GWd/MTU interval	91
Figure 4.108.	<sup>152</sup> Sm concentration at 70% void fraction with five-year decay	91

---

Figure 4.109. $^{155}\text{Eu}$ concentration at 40% void fraction	94
Figure 4.110. $^{155}\text{Eu}$ concentration at 40% void fraction with five-year decay	94
Figure 4.111. SCALE $k_{inf}$ results at 0% void fraction in 6-14 GWd/MTU interval	96
Figure 4.112. Comparison SCALE $k_{inf}$ results at 70% void fraction in 5-16 GWd/MTU interval	96
Figure 4.113. Comparison of SCALE (TRITON/NEWT) $k_{inf}$ results with ENDF/B-VII.1 252g cross-section library at 0% void fraction	98
Figure 4.114. Comparison of ORNL SCALE(TRITON/NEWT) $k_{inf}$ results at 70% void fraction in 7-14 GWd/MTU interval	99
Figure 4.115. KENOREST $k_{inf}$ results at 40% void fraction	100
Figure 4.116. VESTA (predictor only) $k_{inf}$ results at 40% void fraction in 6-14 GWd/MTU interval	100

*List of abbreviations*

a/b-cm	atoms per barn-cm
BUC	Burnup credit
BWR	Boiling water reactor
CE	Continuous-Energy
EGBUC	Expert Group on Burn-up Credit Criticality (NEA)
EGUNF	Expert Group on Used Nuclear Fuel Criticality (NEA)
ENDF	Evaluated Nuclear Data File
Gd <sub>2</sub> O <sub>3</sub>	Gadolinium oxide (Gadolinia)
GRS	Global Research for Safety
ID	Identifier code
IRSN	Institute for Radiological Protection and Nuclear Safety (France)
JEFF	Joint Evaluated Fission and Fusion
JENDL	Japanese Evaluated Nuclear Data Library
MC	Monte Carlo
MG	Multigroup
MOC	Method of Characteristics
MTU	Metric Ton of Uranium
NEA	Nuclear Energy Agency
NSC	Nuclear Science Committee
OECD	Organisation for Economic Co-operation and Development
WPNCSS	Working Party on Nuclear Criticality Safety
WTI	Wissenschaftlich-Technische Ingenieurberatung GmbH

## *Executive summary*

Most modern boiling water reactor (BWR) fuel assemblies contain gadolinium oxide ( $Gd_2O_3$ , or gadolinia) as a burnable neutron absorber in some fuel rods. The gadolinium absorber depletes rapidly during the initial phase of its irradiation, causing the fuel assembly reactivity to increase initially during irradiation and reach a maximum value at an assembly average burnup typically less than 20 gigawatt days per metric ton of uranium (GWd/MTU). The reactivity then decreases for the remainder of fuel assembly irradiation. Due to the large neutron capture cross section of gadolinium isotopes, depletion calculations for gadolinia rods require special modelling to account for strong self-shielding effects and the rapid depletion of strongly absorbing gadolinium isotopes.

The Working Party on Nuclear Criticality Safety (WPNCS), under the Nuclear Energy Agency (NEA) Nuclear Science Committee (NSC), has organised several international benchmarks through its Expert Group on Burnup Credit (EGBUC) to assess variations in predicted  $k_{inf}$  and nuclide concentrations in burnup calculations by different code systems. The Phase IIIB burnup credit (BUC) benchmark provided a comparison of BWR depletion calculations based on an 8×8 STEP-2 assembly design. In addition to  $k_{inf}$  values, predicted concentrations of actinides and fission products were compared at 10 GWd/MTU intervals up to 40 GWd/MTU at different void fraction profiles. This benchmark was recently extended with the Phase IIIC based on a newer 9×9 STEP-3 assembly design. Burnup calculations up to 50 GWd/MTU with 0-15 years cooling periods were compared at 0%, 40% and 70% void fractions using different code systems and nuclear data libraries. The Phase IIIC benchmark results showed that modelling options, i.e. spatial resolution of gadolinia pins and depletion step size, can cause significant variations in predicted  $k_{inf}$  and assembly average nuclide concentrations.

The NEA Expert Group on Used Nuclear Fuel criticality (EGUNF) has thus organised a Phase IIID BUC benchmark to re-examine code and nuclear data performance for BWR lattice calculations and focus on the depletion modelling of gadolinium fuel in the burnup region near peak reactivity. Modelling of the gadolinium pins was specified in the benchmark to limit some of the modelling variations observed in the EGBUC Phase IIIC benchmark and to better isolate differences caused by code methods and nuclear data relevant to gadolinium depletion in the burnup range important to gadolinium depletion. The benchmark problem proposed here is based on the 9×9 STEP-3 assembly geometry of the Phase IIIC benchmark. The gadolinium model and depletion step sizes to be applied by all codes are specified in the benchmark, leaving the primary variables as code transport method and nuclear data library.

A uniform fuel enrichment of 4.0 wt%  $^{235}U$  for non-gadolinia fuel rods and 3.0 wt% gadolinia enrichment for gadolinia rods were used for this benchmark. Small depletion steps (0.25 GWd/MTU) until 10 GWd/MTU and 10 depletion rings for modelling gadolinia rods were requested for a detailed analysis of gadolinium burnup.

The benchmark specification was proposed and approved during the 2016 EGUNF meeting. A preliminary report was prepared and presented to participants in July 2018. The deadline for submission of the final results was August 2018 and the final report was sent in September 2018 for review.

Participants from 14 organisations in 13 countries contributed with 37 code results for this benchmark.

When all code results are considered, the maximum relative  $2\sigma$  in  $k_{inf}$  is 1.33% at 70% void fraction, at 10 GWd/MTU (burnup peak). Code results with old cross-section libraries (ENDF/B-V, ENDF/B-VI) and low fidelity calculation options are the main contributors to the large standard deviations. If these code results are eliminated, the maximum relative  $2\sigma$  decreases to 0.5% for deterministic codes and 0.61% for continuous-energy (CE) Monte Carlo (MC) codes.

Gadolinium isotope concentrations in gadolinia rods were analysed in detail. At peak reactivity, relative  $2\sigma$  standard deviations in  $^{155}\text{Gd}$  and  $^{157}\text{Gd}$  concentrations are 44% and 21%, respectively. Large sensitivity to void fraction is also observed in standard deviations.

The largest relative standard deviations among all reported nuclide concentrations are observed in  $^{155}\text{Eu}$  concentrations (26% at peak reactivity), while  $^{155}\text{Eu}$  also has the lowest concentration in all analysed fission products.

Several groupings are observed in code results for  $k_{inf}$  and nuclide concentrations. In general, these groupings are predominantly driven by the nuclear data used in calculations rather than the methods used in calculations.

## 1. Introduction

Most modern boiling water reactor (BWR) fuel assemblies contain gadolinium oxide ( $Gd_2O_3$ , or gadolinia) as a burnable neutron absorber in some fuel rods. The gadolinium absorber depletes rapidly during the initial phase of its irradiation, which causes the fuel assembly reactivity to increase initially during irradiation and reach a maximum value at an assembly average burnup typically less than 20 gigawatt days per metric ton of uranium (GWd/MTU). The reactivity then decreases for the remainder of fuel assembly irradiation. Due to the large neutron absorption cross section of gadolinium isotopes, depletion calculations for gadolinia rods require special modelling to account for strong self-shielding effects and the fast depletion of gadolinium.

The Working Party on Nuclear Criticality Safety (WPNCS), under the NEA Nuclear Science Committee (NSC), has organised several international benchmarks through its Expert Group on Burnup Credit (EGBUC) to assess variations in predicted  $k_{inf}$  and nuclide concentrations in burnup calculations by different code systems. The Phase IIIB benchmark (NEA, 2002) provided a comparison of BWR depletion calculations based on an 8×8 STEP-2 assembly design. In addition to  $k_{inf}$  values, predicted concentrations of actinides and fission products were compared at 10 GWd/MTU intervals up to 40 GWd/MTU at different void fraction profiles. This benchmark was recently extended with the Phase IIIC (NEA, 2016) based on a newer 9×9 STEP-3 assembly design. Burnup calculations up to 50 GWd/MTU with 0-15 years cooling periods were compared at 0%, 40% and 70% void fractions using different code systems and nuclear data libraries. The Phase IIIC benchmark results showed that modelling options, i.e. spatial resolution of gadolinia pins and depletion step size, can cause significant variations in predicted  $k_{inf}$  and assembly average nuclide concentrations.

The NEA Expert Group on Used Nuclear Fuel criticality (EGUNF) has thus organised a Phase IIID BUC benchmark to re-examine code and nuclear data performance for BWR lattice calculations and focus on the depletion modelling of gadolinium fuel in the burnup region near peak reactivity. Modelling of the gadolinia pins was specified in the benchmark to limit some of the modelling variations observed in the EGBUC Phase IIIC benchmark and to better isolate differences caused by code methods and nuclear data relevant to gadolinium depletion in the burnup range important to gadolinium depletion. The benchmark problem proposed here is based on the 9×9 STEP-3 assembly geometry of the Phase IIIC benchmark (NEA, 2016). The gadolinium model and depletion step sizes to be applied by all codes are specified in the benchmark, leaving the primary uncontrolled variables as code transport method and nuclear data library.

## 2. Benchmark problem

### 2.1 Geometry

The geometry of the benchmark specification from the EGBUC Phase IIIC (NEA, 2016) benchmark is retained. The problem geometry consists of a single 9×9 fuel assembly with reflective boundary conditions applied. A uniform 1.45 cm pin pitch is modelled throughout the assembly. The central region of the assembly contains a square water channel with zero-void water. Both the water and assembly channels are modelled as a square region of uniform thickness. The assembly and fuel rod geometry are shown in Figure 2.1.

The primary purpose of this benchmark is to further investigate differences in predicted gadolinium number densities in depleted boiling water reactor (BWR) fuel and their impact on criticality. This benchmark takes a prescriptive approach to gadolinium modelling to limit the variability in results caused by user modelling choices. Each gadolinia rod is modelled with ten concentric equal-area rings, as shown in Figure 2.2. Each of the ten unique regions in each gadolinia rod is to be tracked separately for depletion purposes, with the numbering scheme provided in Figure 2.2 and Table 2.1. The rings are numbered 1-10 from inside to outside. The benchmark includes eight gadolinia rods, with positions shown in Figure 2.1.

### 2.2 Materials

The enrichment zoning has been simplified to a single enrichment of 4.0 wt% <sup>235</sup>U in the non-gadolinia fuel rods. The average enrichment of these rod in the Phase IIIC benchmark is 4.05 wt% <sup>235</sup>U, so this is primarily a modelling simplification. The enrichment and gadolinium loading of the gadolinia-bearing fuel rods remain unchanged from the Phase IIIC specification. However, the number of gadolinia rods is reduced from 12 to 8 so that all gadolinia rods are symmetric and have the same nuclide composition. The number densities for fresh fuel and absorber compositions are provided in Table 2.2. The fuel temperature of 900K is maintained from the Phase IIIC specification. The cladding, water channel and channel box are all modelled as Zircaloy-2, with number densities provided in Table 2.3. The temperature of nonfuel materials is modified to 600K to be consistent with temperatures for many continuous-energy cross-section libraries. The resulting water number densities are provided for 0%, 40% and 70% void (steam) in Table 2.3, and are slightly different from the Phase IIIC values.



Figure 2.1. 2D fuel assembly

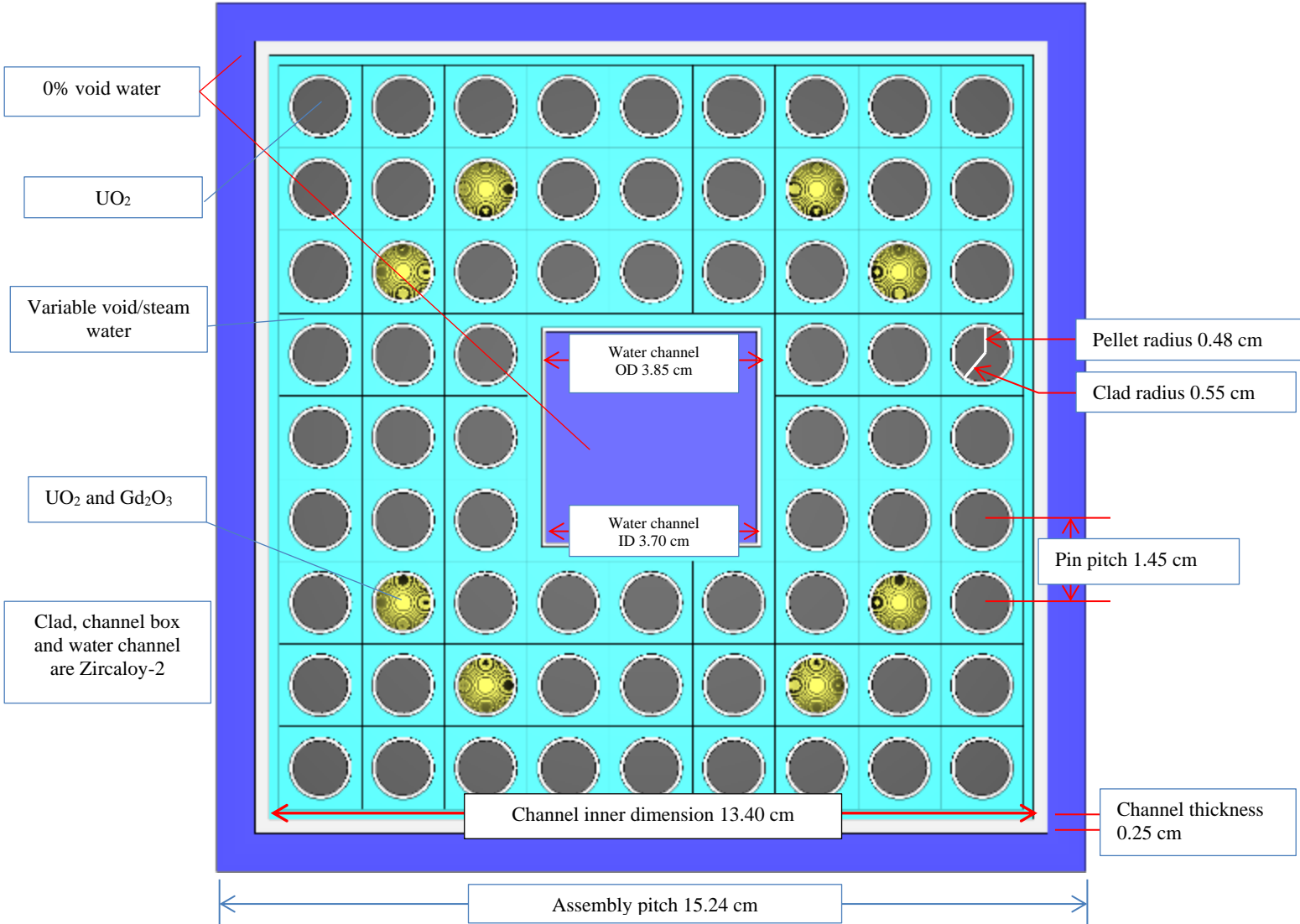


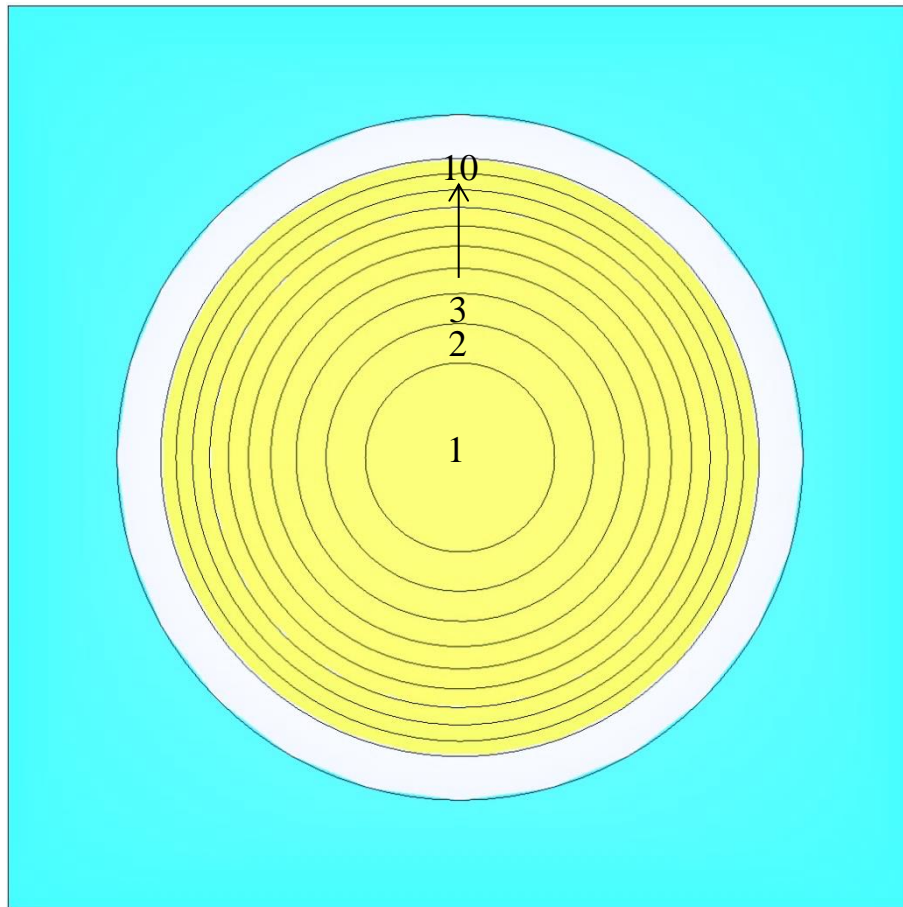
Figure 2.2. Detail of Gd<sub>2</sub>O<sub>3</sub> rod

Table 2.1. Gadolinia ring dimensions

Ring number	Outer radius (cm)
1	0.151789
2	0.214663
3	0.262907
4	0.303579
5	0.339411
6	0.371806
7	0.401597
8	0.429325
9	0.455368
10	0.48

**Table 2.2. Fuel and absorber number densities**

Composition	Nuclide or element	Number density (atoms/b-cm)
UO <sub>2</sub>	<sup>234</sup> U	$8.4700 \times 10^{-6}$
	<sup>235</sup> U	$9.4763 \times 10^{-4}$
	<sup>238</sup> U	$2.2447 \times 10^{-2}$
	O	$4.6807 \times 10^{-2}$
UO <sub>2</sub> + Gd <sub>2</sub> O <sub>3</sub>	<sup>234</sup> U	$6.8396 \times 10^{-6}$
	<sup>235</sup> U	$7.6521 \times 10^{-4}$
	<sup>238</sup> U	$2.1460 \times 10^{-2}$
	O	$4.6225 \times 10^{-2}$
	<sup>154</sup> Gd	$2.5654 \times 10^{-5}$
	<sup>155</sup> Gd	$1.7417 \times 10^{-4}$
	<sup>156</sup> Gd	$2.4089 \times 10^{-4}$
	<sup>157</sup> Gd	$1.8417 \times 10^{-4}$
	<sup>158</sup> Gd	$2.9232 \times 10^{-4}$
<sup>160</sup> Gd	$2.5725 \times 10^{-4}$	

**Table 2.3. Water and Zircaloy number densities**

Composition	Element	Number density (atoms/b-cm)
0% void water	H	$4.3417 \times 10^{-2}$
	O	$2.1708 \times 10^{-2}$
40% void water	H	$2.7998 \times 10^{-2}$
	O	$1.3999 \times 10^{-2}$
70% void water	H	$1.6434 \times 10^{-2}$
	O	$8.2170 \times 10^{-3}$
Zircaloy-2	Sn	$4.9797 \times 10^{-4}$
	Fe	$9.1782 \times 10^{-5}$
	Cr	$7.5861 \times 10^{-5}$
	Ni	$4.0314 \times 10^{-5}$
	Zr	$4.2465 \times 10^{-2}$

### 2.3 Depletion conditions

The assembly specific power is 25.0 MW/MTU (W/gU) over an exposure history defined by a single period of irradiation with no downtime, using the assembly average burnup steps provided in Table 2.4. The time steps are selected to provide (1) sufficiently accurate results for most code calculations; and (2) a precise estimate of the variation in reactivity in the burnup region where the reactivity peak occurs.

The first two steps are 0.1 and 0.15 GWd/MTU, respectively, followed by 39 steps of 0.25 GWd/MTU each to reach a burnup of 10 GWd/MTU. This is followed by a series of

20 steps that are 0.5 GWd/MTU each, reaching a final burnup of 20 GWd/MTU. Depletion calculations will be performed for void fractions of 0%, 40% and 70%, using the water densities provided in Table 2.3. The water in the central coolant channel and outside the fuel assembly channel is to be modelled as 0% void in all cases. The fuel, moderator and structural material temperatures are also assumed to be the same in all three cases. The assembly design used in this benchmark has several degrees of symmetry (half, quarter, eighth), and any of these may be used to perform the calculations.

**Table 2.4. Depletion steps**

Step #	Duration <sup>1</sup>	Cumulative exposure <sup>2</sup>	Step #	Duration <sup>1</sup>	Cumulative exposure <sup>2</sup>
1	0.10	0.10	32	0.25	7.75
2	0.15	0.25	33	0.25	8.00
3	0.25	0.50	34	0.25	8.25
4	0.25	0.75	35	0.25	8.50
5	0.25	1.00	36	0.25	8.75
6	0.25	1.25	37	0.25	9.00
7	0.25	1.50	38	0.25	9.25
8	0.25	1.75	39	0.25	9.50
9	0.25	2.00	40	0.25	9.75
10	0.25	2.25	41	0.25	10.0
11	0.25	2.50	42	0.5	10.5
12	0.25	2.75	43	0.5	11.0
13	0.25	3.00	44	0.5	11.5
14	0.25	3.25	45	0.5	12.0
15	0.25	3.50	46	0.5	12.5
16	0.25	3.75	47	0.5	13.0
17	0.25	4.00	48	0.5	13.5
18	0.25	4.25	49	0.5	14.0
19	0.25	4.50	50	0.5	14.5
20	0.25	4.75	51	0.5	15.0
21	0.25	5.00	52	0.5	15.5
22	0.25	5.25	53	0.5	16.0
23	0.25	5.50	54	0.5	16.5
24	0.25	5.75	55	0.5	17.0
25	0.25	6.00	56	0.5	17.5
26	0.25	6.25	57	0.5	18.0
27	0.25	6.50	58	0.5	18.5
28	0.25	6.75	59	0.5	19.0
29	0.25	7.00	60	0.5	19.5
30	0.25	7.25	61	0.5	20.0
31	0.25	7.50			

Note: <sup>1</sup>Durations are provided in GWd/MTU; <sup>2</sup>Cumulative exposures are assembly average and are provided in GWd/MTU.

## 2.4 Requested data

The planar  $k_{inf}$  will be reported for the fresh assembly and after each of the 61 burnup steps with no post-irradiation decay time.

Nuclide number densities will be reported in units of atoms per barn-cm (a/b-cm). The number densities for the nuclides listed in Table 2.5 will be reported every two GWd/MTU with respectively zero post-irradiation decay time and with five years of decay time. The actinide and fission product nuclides will be reported averaged over all the non-gadolinia bearing fuel rods. The gadolinium isotopes will be reported for each ring in the gadolinia bearing rod. The desired burnup and decay time combinations for reporting are listed in Table 2.6. The  $^{148}\text{Nd}$  number density will also be reported for each ring in the gadolinia rod, but only after five years of cooling time. The burnup of the gadolinia rod will also be reported at each of these ten burnup steps to assess potential differences in reported burnup caused by treatment of absorptions in gadolinium.

**Table 2.5. Nuclides to report**

<b>Actinides</b>	$^{234,235,236,238}\text{U}$ , $^{237}\text{Np}$ , $^{238,239,240,241,242}\text{Pu}$ , $^{241}\text{Am}$
<b>FP</b>	$^{99}\text{Tc}$ , $^{103}\text{Rh}$ , $^{131}\text{Xe}$ , $^{155}\text{Eu}$ , $^{133}\text{Cs}$ , $^{143,148}\text{Nd}$ , $^{147, 149,151,152}\text{Sm}$
<b>Gd</b>	$^{154,155,156,157,158,160}\text{Gd}$

**Table 2.6. Burnup and decay times for reporting**

<b>Burnup (GWd/MTU)</b>	<b>Decay time (years)</b>
2	0 and 5
4	0 and 5
6	0 and 5
8	0 and 5
10	0 and 5
12	0 and 5
14	0 and 5
16	0 and 5
18	0 and 5
20	0 and 5

### 3. Participants and codes

Participants from 13 countries contributed 40 results for the benchmark. A detailed list of the participants, affiliations and code systems are listed in Table 3.1. A list with contacts is provided in Annex A. Each benchmark participation is given an identifier code (ID) in Table 3.1 for convenient reference. As requested, several participants submitted input files for the depletion models used for their calculations. Input files provided valuable information to help identify differences in the results using similar codes.

Some 19 out of 40 results were submitted by GRS using a wide variety of codes, code options and nuclear data libraries. IRSN, AREVA-TN and WTI also provided multiple code submissions.

**Table 3.1. List of participants**

ID	Code	Cross-section library	Energy groups	Decay data library	Country	Institute
AL1	ALEPH-2.6.3	JEFF3.1.2	CE	JEFF3.1.2	Belgium	SCK/CEN
AP1	APOLLO2-A1.21.0	JEFF3.1.1	281	JEFF3.1.1	France	ORANO-TN
CA1	CASMO-4E2.10.22	JEFF2.2 <sup>c</sup>	70	-	Finland	TVO
HE1	HELIOS1.11	ENDF/B-VI	47	ENDF/B-VII	Germany	WTI
HE2 <sup>1</sup>	HELIOS1.12 <sup>1</sup>	ENDF/B-VI <sup>c</sup>	190	ENDF/B-VI-C	Germany	GRS
HE3 <sup>2</sup>	HELIOS1.12 <sup>2</sup>	ENDF/B-VI <sup>c</sup>	190	ENDF/B-VI-C	Germany	GRS
HE4 <sup>3</sup>	HELIOS1.12 <sup>3</sup>	ENDF/B-VI <sup>c</sup>	190	ENDF/B-VI-C	Germany	GRS
KE1	KENOREST1.0	ENDF/B-VII.0	84	ENDF/B-VII.0	Germany	GRS
KE2	KENOREST1.0	JEF2.2	84	JEF2.2	Germany	GRS
KE3	KENOREST1.0	JENDL/AC <sup>c</sup>	84	JENDL/AC-C	Germany	GRS
MO1	MOTIVE0.4.1	ENDF/B-VII.1	CE	ENDF/B-VII.1	Germany	GRS
SC1	SCALE6.1-KENO-VI	ENDF/B-VII.0	238	ENDF/B-VII.0	Spain	SEA
SC2	SCALE6.1.2-TRITON	ENDF/B-V	44	ENDF/B-V	Spain	ENUSA
SC3	SCALE6.1.2-TRITON	ENDF/B-VII.0	238	ENDF/B-VII.0	Germany	GRS
SC4	SCALE6.1.2-TRITON	ENDF/B-V	44	ENDF/B-V	Germany	GRS
SC5	SCALE6.1.2-TRITON	ENDF/B-V	238	ENDF/B-V	Germany	GRS
SC6	SCALE6.1.2-TRITON	ENDF/B-VI	238	ENDF/B-VI	Germany	GRS
SC7	SCALE6.1.2-TRITON	ENDF/B-VII.1	56	ENDF/B-VII.1	Germany	GRS
SC8	SCALE6.1.2-TRITON	ENDF/B-VII.0	238	ENDF/B-VII.0	Germany	GRS

**Table 3.1. List of participants (continued)**

SC9 <sup>4</sup>	SCALE6.1.2-TRITON	ENDF/B-VII.1	252	ENDF/B-VII.1	Germany	GRS
SC10	SCALE6.1.2-TRITON	ENDF/B-VII.1	252	ENDF/B-VII.1	Germany	GRS
SC11	SCALE6.1.2-TRITON	ENDF/B-VII.0	238	ENDF/B-VII.0	Germany	WTI
SC12 <sup>*</sup>	SCALE6.2-TRITON <sup>*</sup>	ENDF/B-VII.1	252	ENDF/B-VII.1	France	IRSN
SC13	SCALE6.2-TRITON	ENDF/B-VII.1	252	ENDF/B-VII.1	Switzerland	NAGRA
SC14 <sup>*</sup>	SCALE6.2.1-KENO-VI <sup>*</sup>	ENDF/B-VII.0	CE	ENDF/B-VII.0	Germany	GRS
SC15	SCALE6.2.1-Polaris	ENDF/B-VII.1	252	ENDF/B-VII.1	Germany	GRS
SC16 <sup>*</sup>	SCALE6.2.1-TRITON <sup>*</sup>	ENDF/B-VII.1	252	ENDF/B-VII.1	France	ORANO-TN
SC17	SCALE6.2.1-TRITON	ENDF/B-VII.1	252	ENDF/B-VII.1	Germany	GRS
SC18 <sup>*</sup>	SCALE6.2.1-TRITON <sup>*</sup>	ENDF/B-VII.1	252	ENDF/B-VII.1	United States	ORNL
SC19 <sup>*</sup>	SCALE6.2.3-Polaris <sup>*</sup>	ENDF/B-VII.1	56	ENDF/B-VII.1	Sweden	EMS
SC20	SCALE6.2.2-TRITON	ENDF/B-VII.1	252	ENDF/B-VII.1	Poland	NCBJ
SE1	SERPENT2.1.24	ENDF/B-VII.0	CE	ENDF/B-VII.0	Germany	GRS
SE2	SERPENT2.1.28	ENDF/B-VII.0	CE	ENDF/B-VII.0	Korea	KINS
SW1	SWAT4	JENDL-4	CE	JENDL/FPD-2000	Japan	JAEA
VE1	VESTA-MORET	JEFF3.1.1	CE	JEFF3.1.1	France	IRSN
VE2 <sup>*</sup>	VESTA-MORET	JEFF3.2	CE	JEFF3.1.1	France	IRSN
VE3 <sup>*</sup>	VESTA-MORET	ENDF/B-VII.1	CE	ENDF/B-VII.1	France	IRSN
VE3P <sup>5</sup>	VESTA-MORET	JEFF3.2	CE	JEFF3.1.1	France	IRSN
VE4P <sup>5</sup>	VESTA-MCNP	JEFF3.2	CE	JEFF3.1.1	France	IRSN
VE5P <sup>5</sup>	VESTA-MCNP	ENDF/B-VII.1	CE	ENDF/B-VII.1	France	IRSN

Note: <sup>\*</sup>Input files were received; <sup>1</sup>Simple mesh geometry, interface current coupling factor = 1; <sup>2</sup>Simple mesh geometry, interface current coupling factor = 4; <sup>3</sup>Refined mesh geometry, interface current coupling factor = 4; <sup>4</sup>No Dancoff factors; <sup>5</sup>Predictor only depletion, used for comparison and not included in the statistics; <sup>c</sup>Corrected/modified library.

### 3.1 Codes

Results from 10 different code systems were submitted. SCALE6 was the most widely used code system for this benchmark. TRITON/NEWT, TRITON/KENO-VI and Polaris sequences were used for SCALE6 lattice depletion calculations. HELIOS1, VESTA, KENOREST and SERPENT codes follow SCALE6 in number of submissions. There are single submissions using the codes SWAT4, ALEPH, APOLLO-2A and CASMO-4E. Table 3.2 lists the code systems, transport methods used for flux solution and depletion calculation coupling method. There were more submissions using Monte Carlo (MC) transport codes than deterministic transport codes. Of the eight different MC codes used in this benchmark, six used continuous-energy (CE) cross-section libraries and two used multigroup (MG) libraries.

Most codes used predictor-corrector type coupling between neutron transport and depletion calculations. VESTA results were calculated using predictor-only coupling. The choice of this approximate scheme is based on the very small depletion size (0.25 GWd/MTU) in the benchmark specifications.

As specified in Section 2.1, the benchmark lattice geometry has 1/8 symmetry. Based on code capability and code execution time, the geometry lattice was modelled differently by the participants. Most MC codes adopted the 1/8 symmetry, whereas MOTIVE and SERPENT used full lattice for calculations. Among Methods of Characteristics codes (CASMO-4E2, APOLLO-2A1, SCALE/Polaris), only the SCALE/Polaris results did not use the diagonal symmetry.

**Table 3.2. List of codes used in the benchmark**

Code name	Transport calculation	Depletion coupling	Geometry
ALEPH	Monte Carlo	Predictor Corrector	1/8
APOLLO-2A1	Method of Characteristics	Predictor Corrector	1/2
CASMO-4E2	Method of Characteristics	Predictor Corrector	1/2
HELIOS	Collision Probability	Predictor Corrector	1
KENOREST	Monte Carlo	Predictor	1
MOTIVE	Monte Carlo	Predictor Corrector	1
SCALE6-Polaris	Method of Characteristics	Predictor Corrector	1
SCALE6-TRITON/KENO-VI	Monte Carlo	Mid-Point	1/8
SCALE6-TRITON/NEWT	Slice Balance	Mid-Point	1,1/4
SERPENT	Monte Carlo	Predictor Corrector	1
SWAT4	Monte Carlo	Predictor Corrector	1/8
VESTA-MCNP6	Monte Carlo	Predictor	1/8
VESTA-MORET	Monte Carlo	Predictor	1/8
VESTA-MORET	Monte Carlo	Predictor Corrector	1/8

### 3.2 Nuclear data library

A list of nuclear data libraries is given in Table 3.3. The US ENDF/B libraries were the most commonly used for this benchmark. JEFF libraries are widely used by European institutions. JENDL-4 was only used for SWAT4 calculations performed in Japan. An earlier version of JENDL-4 (JENDL/AC) with data corrections was employed in KENOREST calculations performed in Germany. Calculations using ENDF/B-VII.1 MG libraries (252 and 238 groups) were dominant in the submissions largely because they are included in distributions of SCALE6.1 and SCALE6.2 code systems, widely used by participants. Several older libraries, ENDF/B-V, ENDF/B-VI and JEFF2.2, were also used by several participants.



**Table 3.3. List of nuclear data libraries**

Cross-section library	Energy groups	Number of results
ENDF/B-V	44	2
ENDF/B-V	238	1
ENDF/B-VI <sup>c</sup>	190	3
ENDF/B-VI	238	1
ENDF/B-VII.0	47	1
ENDF/B-VII.0	84	1
ENDF/B-VII.0	238	4
ENDF/B-VII.0	CE	3
ENDF/B-VII.1	CE	4
ENDF/B-VII.1	56	1
ENDF/B-VII.1	252	10
JEFF2.2 <sup>c</sup>	84	1
JEFF2.2	70	1
JEFF3.1.1	281	2
JEFF3.1.2	CE	1
JEFF3.2	CE	5
JENDL-4	CE	1
JENDL/AC <sup>c</sup>	84	1

Note: <sup>c</sup>Corrected, special version of the library.

## 4. Comparisons of results from participants

A statistical analysis of the results submitted by participants was performed using a similar approach as for the EGBUC Phase IIIC benchmark. Statistical definitions used in this report are as follows:

$$\bar{x} = \frac{1}{N} \sum_{i=1}^N x_i \quad (4.1)$$

$$\sigma = \sqrt{\frac{1}{N-1} \sum_{i=1}^N (x_i - \bar{x})^2} \quad (4.2)$$

$$2\sigma\% = \frac{2\sigma}{\bar{x}} \times 100 \quad (4.3)$$

where

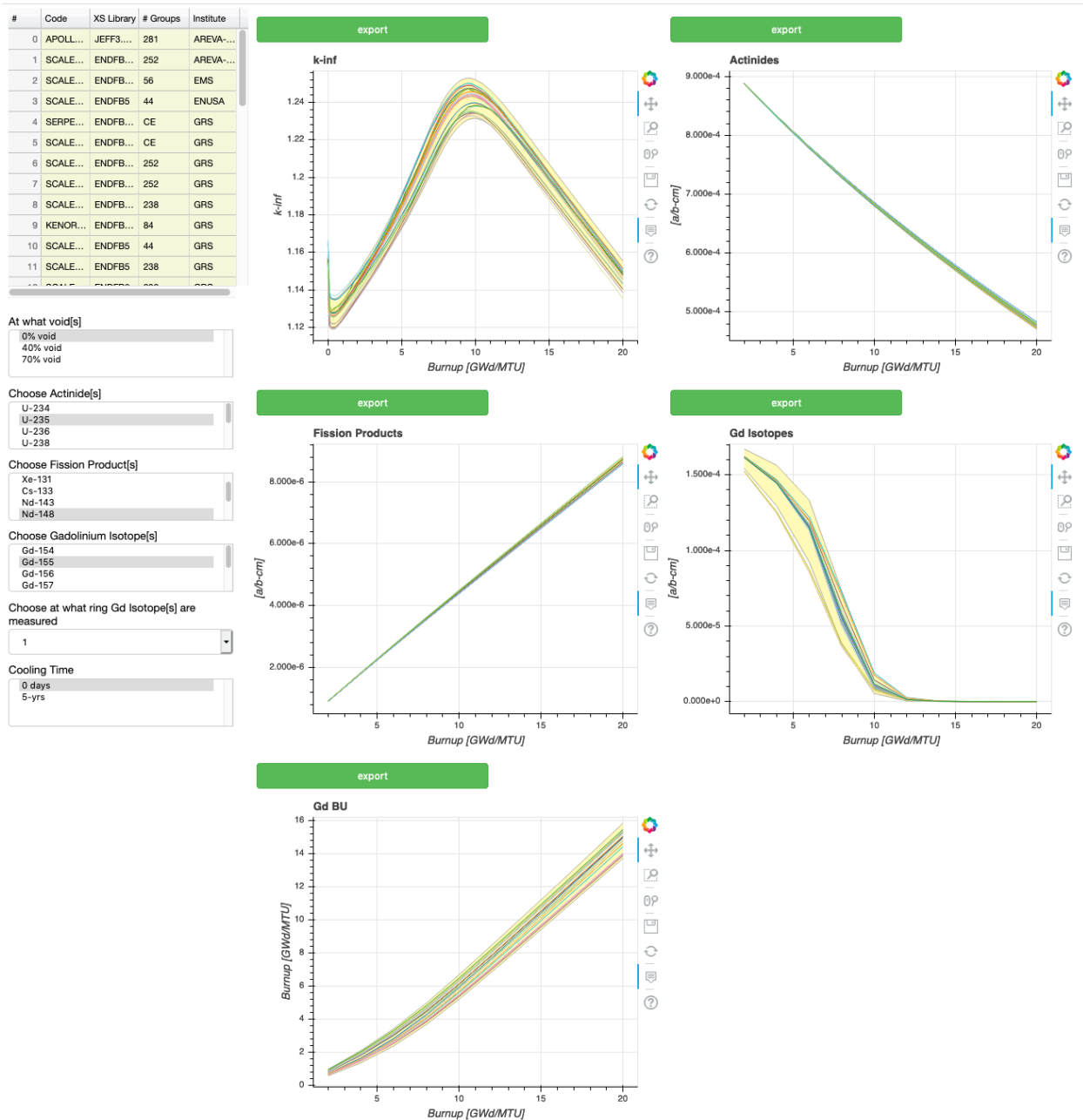
N = number of results

$x_i = k_{inf}$  or atom number density

### 4.1. Web interface

A web interface using the Python bokeh server (Bokeh, 2018) was developed to help with the review and analysis of the benchmark results. The interface allows the comparison of actinide, fission product and gadolinium number densities for selected nuclides, as well as comparisons of  $k_{inf}$  and gadolinia pin burnup for any contribution or group of contributions. Users can select the desired void fraction, nuclide, decay time and gadolinia ring (or select all rings combined) to be displayed and analysed. When multiple participant results are selected, a yellow band is displayed showing the  $\pm 2\sigma$  band. The interface also includes an option to export data for the displayed graphics. A screenshot of the interface is shown in Figure 4.1.

Figure 4.1. Web interface screenshot



## 4.2. Neutron multiplication factor, $k_{inf}$ , by all codes

Results for the infinite multiplication factor,  $k_{inf}$ , from all participants are compared at each void fraction in Figures 4.2, 4.3 and 4.4, which show that the  $2\sigma$  band widens as void fraction increases. Figure 4.4 marks the results from HE2, SC2 and KE2, which lie outside of the  $2\sigma$  band. Burnup dependent  $k_{inf}$  statistics for each void fraction are also listed in Table 4.1. Peak reactivity values and the corresponding burnup at peak reactivity are listed in Table 4.2. The burnup is given at the nearest timestep as used in the benchmark specification, i.e. to the nearest 0.25 GWd/MTU. Similar trends with respect to burnup are seen for all void fractions. Deviations in the predicted peak reactivity increase with increasing void fraction. While 0% void fraction case shows a 0.79%  $2\sigma$  deviation, the

deviation increases to 0.88% at 40% void fraction and reaches 1.33% at 70% void fraction. Similarly, the predicted burnup of peak reactivity shows larger variations as void fraction increases. The burnup of peak reactivity increases with void fraction, from 9.75 GWd/MTU, 10.00 GWd/MTU and 10.28 GWd/MTU for void fractions of 0%, 40% and 70%, respectively.

**Figure 4.2. Comparison of  $k_{inf}$  at 0% void fraction**

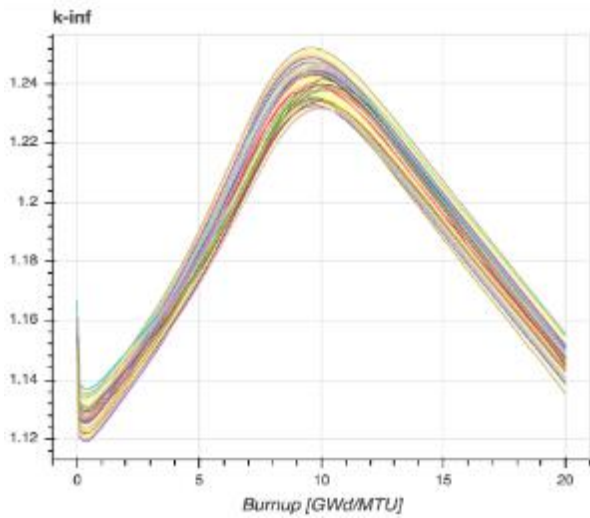


**Figure 4.3. Comparison of  $k_{inf}$  at 40% void fraction**

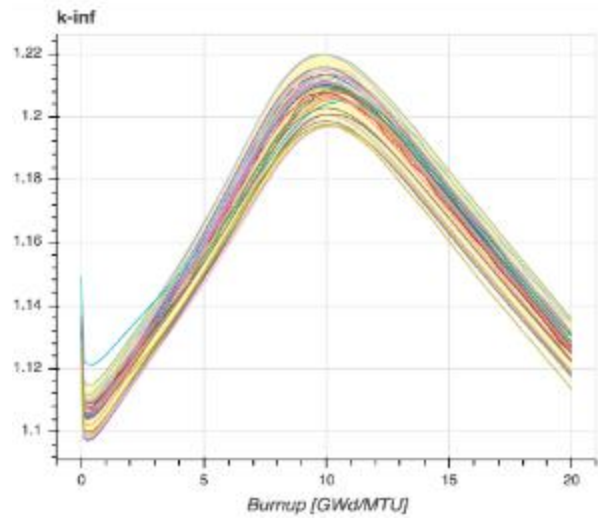


**Figure 4.4. Comparison of  $k_{inf}$  at 70% void fraction**

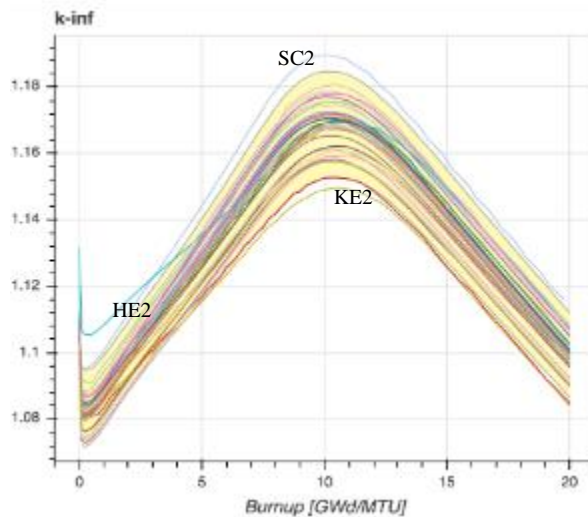


Table 4.1. Statistics for  $k_{inf}$  reported by all participants

Burnup (GWd/MTU)	Mean			$2\sigma$ (pcm)			$2\sigma\%$		
	0%	40%	70%	0%	40%	70%	0%	40%	70%
0.00	1.1565	1.1330	1.1078	830	902	1 166	0.72	0.80	1.05
0.10	1.1290	1.1073	1.0841	781	866	1 151	0.69	0.78	1.06
0.25	1.1277	1.1063	1.0834	760	844	1 131	0.67	0.76	1.04
0.50	1.1278	1.1068	1.0842	753	823	1 086	0.67	0.74	1.00
0.75	1.1294	1.1087	1.0862	725	804	1 077	0.64	0.73	0.99
1.00	1.1316	1.1112	1.0885	700	785	1 061	0.62	0.71	0.97
1.25	1.1342	1.1139	1.0912	681	767	1 041	0.60	0.69	0.95
1.50	1.1371	1.1168	1.0939	670	754	1 033	0.59	0.68	0.94
1.75	1.1398	1.1196	1.0965	659	743	1 034	0.58	0.66	0.94
2.00	1.1427	1.1225	1.0991	652	748	1 028	0.57	0.67	0.94
2.25	1.1457	1.1254	1.1017	650	741	1 031	0.57	0.66	0.94
2.50	1.1487	1.1282	1.1042	657	739	1 040	0.57	0.66	0.94
2.75	1.1516	1.1310	1.1067	659	740	1 039	0.57	0.65	0.94
3.00	1.1547	1.1339	1.1091	663	746	1 060	0.57	0.66	0.96
3.25	1.1579	1.1368	1.1116	672	751	1 059	0.58	0.66	0.95
3.50	1.1611	1.1397	1.1141	691	760	1 077	0.60	0.67	0.97
3.75	1.1644	1.1427	1.1165	711	765	1 096	0.61	0.67	0.98
4.00	1.1678	1.1456	1.1189	730	776	1 117	0.62	0.68	1.00
4.25	1.1713	1.1487	1.1213	753	796	1 128	0.64	0.69	1.01
4.50	1.1749	1.1518	1.1238	781	811	1 145	0.67	0.70	1.02
4.75	1.1785	1.1549	1.1263	814	832	1 167	0.69	0.72	1.04
5.00	1.1823	1.1581	1.1288	850	853	1 201	0.72	0.74	1.06
5.25	1.1862	1.1613	1.1313	897	878	1 219	0.76	0.76	1.08
5.50	1.1902	1.1646	1.1338	937	897	1 243	0.79	0.77	1.10
5.75	1.1943	1.1679	1.1363	972	925	1 278	0.81	0.79	1.13
6.00	1.1985	1.1713	1.1389	1017	956	1 300	0.85	0.82	1.14
6.25	1.2026	1.1748	1.1415	1053	981	1 332	0.88	0.84	1.17
6.50	1.2070	1.1782	1.1440	1089	1015	1 363	0.90	0.86	1.19
6.75	1.2113	1.1816	1.1466	1125	1041	1 396	0.93	0.88	1.22
7.00	1.2157	1.1850	1.1492	1154	1061	1 423	0.95	0.90	1.24
7.25	1.2198	1.1885	1.1517	1158	1088	1 456	0.95	0.92	1.26
7.50	1.2239	1.1917	1.1542	1166	1110	1491	0.95	0.93	1.29
7.75	1.2277	1.1948	1.1566	1165	1133	1 510	0.95	0.95	1.31

**Table 4.1. Statistics for  $k_{inf}$  reported by all participants (continued)**

8.00	1.2310	1.1977	1.1588	1152	1139	1 559	0.94	0.95	1.35
8.25	1.2341	1.2004	1.1610	1135	1142	1 580	0.92	0.95	1.36
8.50	1.2366	1.2026	1.1630	1113	1145	1 600	0.90	0.95	1.38
8.75	1.2388	1.2045	1.1647	1091	1133	1 593	0.88	0.94	1.37
9.00	1.2405	1.2062	1.1661	1072	1129	1 613	0.86	0.94	1.38
9.25	1.2417	1.2074	1.1672	1037	1120	1 605	0.84	0.93	1.38
9.50	1.2424	1.2083	1.1682	1017	1101	1 602	0.82	0.91	1.37
9.75	1.2426	1.2089	1.1689	982	1084	1 592	0.79	0.90	1.36
10.00	1.2423	1.2091	1.1693	944	1066	1 573	0.76	0.88	1.35
10.50	1.2407	1.2084	1.1694	912	1043	1 557	0.74	0.86	1.33
11.00	1.2377	1.2067	1.1686	874	1031	1 525	0.71	0.85	1.30
11.50	1.2339	1.2038	1.1669	870	992	1 483	0.70	0.82	1.27
12.00	1.2294	1.2003	1.1645	856	981	1 452	0.70	0.82	1.25
12.50	1.2245	1.1962	1.1614	846	974	1 415	0.69	0.81	1.22
13.00	1.2195	1.1918	1.1579	851	968	1 405	0.70	0.81	1.21
13.50	1.2143	1.1872	1.1541	839	960	1 369	0.69	0.81	1.19
14.00	1.2092	1.1826	1.1501	837	948	1 357	0.69	0.80	1.18
14.50	1.2040	1.1778	1.1459	830	946	1 353	0.69	0.80	1.18
15.00	1.1988	1.1731	1.1416	835	948	1 335	0.70	0.81	1.17
15.50	1.1936	1.1683	1.1373	825	945	1 326	0.69	0.81	1.17
16.00	1.1884	1.1636	1.1330	827	948	1 307	0.70	0.81	1.15
16.50	1.1833	1.1589	1.1288	830	937	1 303	0.70	0.81	1.15
17.00	1.1781	1.1542	1.1245	821	932	1 296	0.70	0.81	1.15
17.50	1.1730	1.1496	1.1203	818	922	1 282	0.70	0.80	1.14
18.00	1.1678	1.1449	1.1161	810	917	1 276	0.69	0.80	1.14
18.50	1.1627	1.1403	1.1119	811	906	1 271	0.70	0.79	1.14
19.00	1.1576	1.1357	1.1078	800	901	1 266	0.69	0.79	1.14
19.50	1.1525	1.1311	1.1036	804	896	1 240	0.70	0.79	1.12
20.00	1.1473	1.1266	1.0995	830	902	1 166	0.70	0.79	1.13

**Table 4.2. Peak  $k_{inf}$  and corresponding burnup by all participants**

ID	0%		40%		70%	
	Peak $k_{inf}$	Burnup (GWd/MTU)	Peak $k_{inf}$	Burnup (GWd/MTU)	Peak $k_{inf}$	Burnup (GWd/MTU)
AL1	1.2399	10.00	1.2079	10.50	1.1698	10.50
AP1	1.2352	9.75	1.2027	10.00	1.1654	10.50
CA1	1.2399	10.00	1.2061	10.00	1.1676	10.50
HE1	1.2318	10.00	1.1968	10.00	1.1577	10.50
HE2	1.2378	10.00	1.2048	10.50	1.1695	11.00
HE3	1.2397	10.00	1.2060	10.00	1.1687	10.50
HE4	1.2446	9.75	1.2100	10.00	1.1707	10.50
KE1	1.2492	9.50	1.2091	9.75	1.1595	11.00
KE2	1.2356	9.50	1.1976	10.00	1.1497	10.50
KE3	1.2502	9.50	1.2101	10.00	1.1609	10.50
MO1	1.2473	9.50	1.2145	9.75	1.1755	10.50
SC1	1.2469	10.00	1.2158	10.00	1.1807	10.50
SC10	1.2434	9.50	1.2098	10.00	1.1703	10.00
SC11	1.2447	9.75	1.2132	10.00	1.1781	10.50
SC12	1.2457	9.75	1.2122	10.00	1.1726	10.00
SC13	1.2401	9.75	1.2067	10.00	1.1684	10.00
SC14	1.2471	9.50	1.2133	10.00	1.1752	9.75
SC15	1.2435	9.75	1.2094	10.00	1.1683	10.00
SC16	1.2475	9.50	1.2133	10.00	1.1727	10.00
SC17	1.2434	9.50	1.2098	10.00	1.1703	10.00
SC18	1.2439	9.75	1.2110	10.00	1.1716	10.00
SC19	1.2417	9.75	1.2080	10.00	1.1687	10.00
SC2	1.2489	9.75	1.2199	10.00	1.1897	10.00
SC20	1.2489	9.50	1.2156	10.00	1.1771	10.00
SC3	1.2437	9.75	1.2106	10.00	1.1718	10.00
SC4	1.2327	9.75	1.1986	10.00	1.1582	10.50
SC5	1.2344	9.75	1.2006	10.00	1.1613	10.50
SC6	1.2341	10.00	1.2007	10.00	1.1623	10.50
SC7	1.2443	9.75	1.2105	10.00	1.1705	10.00
SC8	1.2445	9.75	1.2113	10.00	1.1721	10.00
SC9	1.2473	9.75	1.2153	10.00	1.1786	10.00

**Table 4.2. Peak  $k_{inf}$  and corresponding burnup by all participants (continued)**

SE1	1.2429	9.75	1.2102	9.75	1.1715	10.50
SE2	1.2398	10.00	1.2076	9.75	1.1528	10.50
SW1	1.2455	10.00	1.2135	10.00	1.1757	10.50
VE1	1.2450	9.75	1.2120	9.75	1.1728	9.75
VE2	1.2436	9.75	1.2104	10.00	1.1711	9.75
VE3	1.2465	9.75	1.2131	9.75	1.1739	10.50
VE3P*	1.2383	10.00	1.2060	10.5	1.1673	10
VE4P*	1.2389	10.00	1.2059	10.5	1.1674	10
Average	1.2427	9.75	1.2091	9.99	1.1695	10.28
2 $\sigma$ (pcm)	982	-	1065	-	1560	-
2 $\sigma$ (%)	0.79	3.63	0.88	3.11	1.33	6.36

### 4.3. Neutron multiplication factor by Monte Carlo codes

Neutron multiplication factors calculated by MC codes are compared in Figures 4.5, 4.6 and 4.7 at different void fractions. Except for the KE2 (JEFF2.2) results, all MC code results are closely clustered at 0% and 40% void fractions. A significant increase in standard deviation is observed at 70% void fraction, attributed primarily to the KE2 and SE2 results. As shown in Figure 4.4, KE2 results are outside the  $\pm 2\sigma$  band at 70% void fraction when all other code results are included. However, other KENOEST results (KE1 and KE3) agree well with each other. The KE2 used an older JEFF2.2 library. There is also a large difference between SE1 and SE2 results at 70% void fraction. Both results (SERPENT code) were generated using the same ENDF/B-VII.0 library. It is not clear if the large bias at 70% is due to the SERPENT versions (1.24 vs. 1.26) or differences in the modelling.

If results for the MC codes using MG libraries (SC1, KE1, KE2, KE3) are removed (Figure 4.8), the bias in SE2 results becomes evident. SE2 results increase the standard deviation of the results more than 200%. Based on this observation, the SE2 results were removed from the statistical analysis.

SC14 and MO1 results agree well at all void fractions and predict the highest values of  $k_{inf}$ . Both codes use KENO-VI as transport flux solver, but different ENDF/B-VII library versions (vers. 0 and 1) and different depletion solvers. The VESTA results (VEP1, VEP2) using two different solvers but the same JEFF3.2 library agree well but predict the lowest  $k_{inf}$  values up to peak reactivity. However, large differences in peak  $k_{inf}$  between the two other VESTA results, VE3 and VEP3 (Table 4.2), using the same library and transport solver show that the predictor-only depletion algorithm (VEP3) is not adequate for gadolinium depletion, even with depletion steps as small as 0.25 GWd/MTU. After gadolinium is depleted, all code results, except SW1, converge. SW1 results are different than most other codes and predict higher values of  $k_{inf}$  at all void fractions.

Statistics for  $k_{inf}$  results for MC codes using only CE libraries are listed in Table 4.3. Results show the maximum 2 $\sigma$ % decreases from 0.78% to 0.56% when the void fraction is increased from 0% to 70%. The decrease in standard deviation with increasing void fraction is opposite of the trend seen in Section 4.2 when all code results are evaluated. Relative standard deviation at peak reactivity also shows a small reduction at 70% (0.38%) compared to the 0% (0.40%) void fraction value.



Figure 4.5.  $k_{inf}$  at 0% void fraction reported by Monte Carlo codes

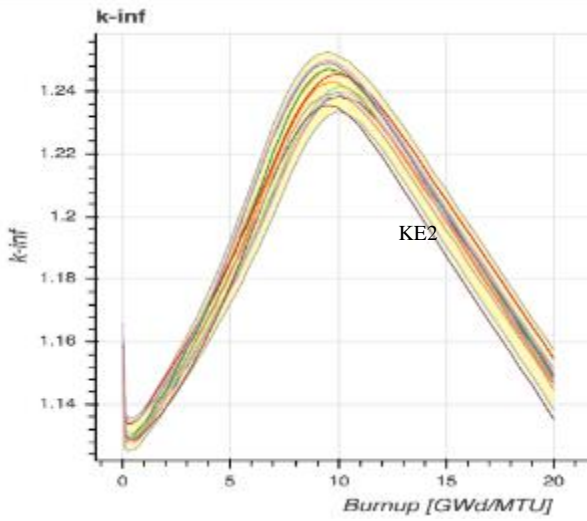


Figure 4.6.  $k_{inf}$  at 40% void fraction reported by Monte Carlo codes

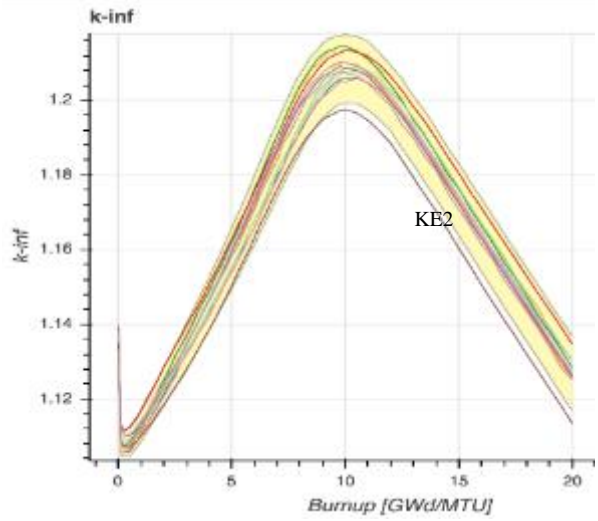


Figure 4.7.  $k_{inf}$  at 70% void fraction reported by Monte Carlo codes

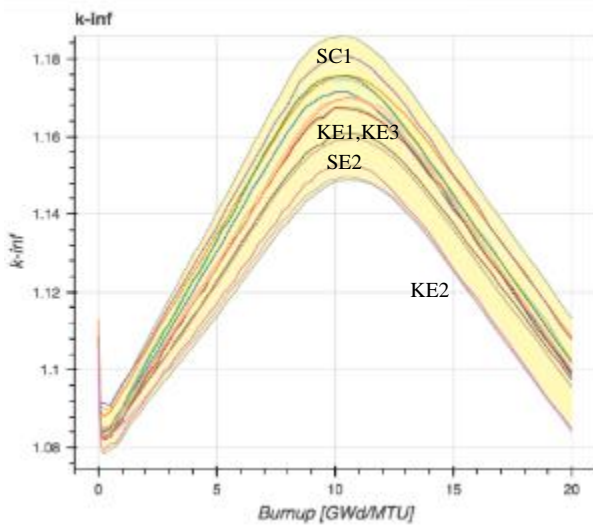


Figure 4.8.  $k_{inf}$  at 70% void fraction reported by Monte Carlo codes using CE libraries

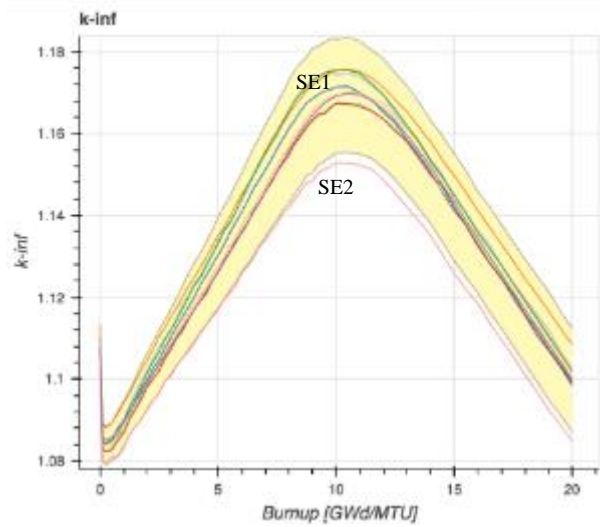


Table 4.3. Statistics for  $k_{inf}$  reported by CE MC codes

Burnup (GWd/MTU)	Mean			2 $\sigma$ (pcm)			2 $\sigma$ %		
	0%	40%	70%	0%	40%	70%	0%	40%	70%
0.00	1.1586	1.1345	1.1087	495	454	425	0.43	0.40	0.38
0.10	1.1310	1.1086	1.0849	395	374	386	0.35	0.34	0.36
0.25	1.1296	1.1076	1.0843	387	359	367	0.34	0.32	0.34
0.50	1.1302	1.1085	1.0854	376	371	329	0.33	0.34	0.30
0.75	1.1318	1.1105	1.0875	354	382	372	0.31	0.34	0.34
1.00	1.1339	1.1130	1.0899	344	377	372	0.30	0.34	0.34
1.25	1.1364	1.1159	1.0926	374	370	360	0.33	0.33	0.33
1.50	1.1395	1.1187	1.0956	362	364	355	0.32	0.33	0.32
1.75	1.1421	1.1216	1.0983	405	354	393	0.36	0.32	0.36
2.00	1.1451	1.1246	1.1010	363	382	368	0.32	0.34	0.33
2.25	1.1480	1.1276	1.1036	377	356	370	0.33	0.32	0.34
2.50	1.1510	1.1303	1.1063	388	438	427	0.34	0.39	0.39
2.75	1.1538	1.1331	1.1088	415	410	403	0.36	0.36	0.36
3.00	1.1569	1.1360	1.1112	428	423	406	0.37	0.37	0.36
3.25	1.1599	1.1389	1.1138	423	432	405	0.36	0.38	0.36
3.50	1.1632	1.1419	1.1164	469	449	457	0.40	0.39	0.41
3.75	1.1664	1.1448	1.1189	492	468	470	0.42	0.41	0.42
4.00	1.1698	1.1478	1.1214	527	479	480	0.45	0.42	0.43
4.25	1.1731	1.1509	1.1239	549	513	463	0.47	0.45	0.41
4.50	1.1766	1.1539	1.1263	562	538	495	0.48	0.47	0.44
4.75	1.1802	1.1571	1.1289	620	575	504	0.53	0.50	0.45
5.00	1.1839	1.1603	1.1317	632	575	541	0.53	0.50	0.48
5.25	1.1877	1.1637	1.1342	723	623	559	0.61	0.54	0.49
5.50	1.1919	1.1668	1.1366	744	626	517	0.62	0.54	0.45
5.75	1.1957	1.1701	1.1393	760	634	551	0.64	0.54	0.48
6.00	1.1999	1.1735	1.1420	804	681	575	0.67	0.58	0.50
6.25	1.2038	1.1771	1.1447	819	684	594	0.68	0.58	0.52
6.50	1.2082	1.1806	1.1474	853	728	611	0.71	0.62	0.53
6.75	1.2125	1.1841	1.1501	898	761	629	0.74	0.64	0.55
7.00	1.2169	1.1874	1.1526	944	756	631	0.78	0.64	0.55
7.25	1.2210	1.1909	1.1552	934	771	633	0.76	0.65	0.55
7.50	1.2250	1.1941	1.1577	937	769	631	0.76	0.64	0.54
7.75	1.2289	1.1974	1.1603	935	789	651	0.76	0.66	0.56

**Table 4.3. Statistics for  $k_{inf}$  reported by CE MC codes (continued)**

8.00	1.2323	1.2002	1.1628	895	754	637	0.73	0.63	0.55
8.25	1.2354	1.2031	1.1649	857	706	642	0.69	0.59	0.55
8.50	1.2379	1.2053	1.1670	772	706	621	0.62	0.59	0.53
8.75	1.2403	1.2071	1.1686	724	642	564	0.58	0.53	0.48
9.00	1.2422	1.2089	1.1700	684	625	570	0.55	0.52	0.49
9.25	1.2434	1.2102	1.1710	627	589	535	0.50	0.49	0.46
9.50	1.2442	1.2109	1.1720	589	496	488	0.47	0.41	0.42
9.75	1.2445	1.2115	1.1727	505	471	496	0.41	0.39	0.42
10.00	1.2441	1.2117	1.1729	446	443	439	0.36	0.37	0.37
10.50	1.2427	1.2111	1.1730	426	433	452	0.34	0.36	0.38
11.00	1.2398	1.2095	1.1722	360	441	459	0.29	0.36	0.39
11.50	1.2362	1.2064	1.1702	366	392	458	0.30	0.33	0.39
12.00	1.2316	1.2030	1.1678	407	401	427	0.33	0.33	0.37
12.50	1.2268	1.1987	1.1645	388	460	415	0.32	0.38	0.36
13.00	1.2218	1.1942	1.1609	439	417	458	0.36	0.35	0.39
13.50	1.2166	1.1897	1.1569	424	451	469	0.35	0.38	0.41
14.00	1.2113	1.1851	1.1528	442	457	494	0.36	0.39	0.43
14.50	1.2060	1.1801	1.1486	410	474	504	0.34	0.40	0.44
15.00	1.2010	1.1755	1.1441	463	500	530	0.39	0.43	0.46
15.50	1.1957	1.1707	1.1399	452	499	533	0.38	0.43	0.47
16.00	1.1906	1.1660	1.1354	470	510	540	0.39	0.44	0.48
16.50	1.1855	1.1612	1.1314	478	511	549	0.40	0.44	0.49
17.00	1.1802	1.1564	1.1270	491	521	549	0.42	0.45	0.49
17.50	1.1751	1.1518	1.1227	508	539	570	0.43	0.47	0.51
18.00	1.1697	1.1471	1.1185	524	553	574	0.45	0.48	0.51
18.50	1.1645	1.1424	1.1142	527	583	627	0.45	0.51	0.56
19.00	1.1594	1.1378	1.1101	544	566	619	0.47	0.50	0.56
19.50	1.1543	1.1331	1.1057	543	591	617	0.47	0.52	0.56
20.00	1.1491	1.1286	1.1016	530	584	625	0.46	0.01	0.01

Note: SE2 results are not included.

#### 4.4. Neutron multiplication factor by deterministic codes

Neutron multiplication factors calculated by deterministic codes are compared at different void fractions in Figures 4.9, 4.10 and 4.11. Several submitted deterministic code results are not included in the statistics in this section, as explained below:

1. HE2 results exhibit unphysical trends in  $k_{inf}$  (Figure 4.4) due to coarse current coupling approximation used in the solution.
2. SC20 results indicate likely errors in the initial fuel composition data based on the actinide results in Section 4.6.

3. SC9 results used a model without externally calculated Dancoff factors, which are known to be important BWR lattice physics calculations.
4. Although no information was provided for SC11 results regarding the use of Dancoff factors, because of their agreement with SC9 results, SC11 results were also not included.

As seen in Figures 4.9, 4.10 and 4.11, variations in the results from deterministic codes increase with increasing void fractions. SCALE code results using different cross-section libraries and solution options are the main contributors to the observed increase in the variation of results at 40% and 70% void fractions. Different cross-section processing options using the same cross-section library can calculate  $k_{inf}$  values at the opposite extremes of the  $\pm 2\sigma$  band (e.g. SC2 vs. SC4 in Figure 4.11). Possible reasons behind the variations in the SCALE results are discussed further in Section 4.8.

In general, SCALE results using ENDF/B-VII predict higher values of  $k_{inf}$ , while HE1 (ENDF/B-VI.1 47g), SC19 (ENDF/B-VII.1 56g), SC4 (ENDF/B-V 44g), SC5 (ENDF/B-V 238g) and SC6 (ENDF/B-VI 238g) consistently predict lower values of  $k_{inf}$ . Code results using older versions of ENDF/B libraries tend to predict the lowest  $k_{inf}$  values. If code results using ENDF/B-V and ENDF/B-VI are removed from comparisons, maximum standard deviation is reduced by 60% (Figure 4.12). Statistics excluding code results with the older ENDF/B-V and ENDF/B-VI libraries are provided in Table 4.4.

The maximum relative standard deviation evolves to 0.39% from 0.56% when void fraction increases from 0% to 70%. Relative standard deviation at peak reactivity are 0.5% and 0.39% at 0% and 70% void fractions, respectively. These values are similar to MC code results (0.4%, 0.38%).

**Figure 4.9.  $k_{inf}$  at 0% void fraction reported by deterministic codes**

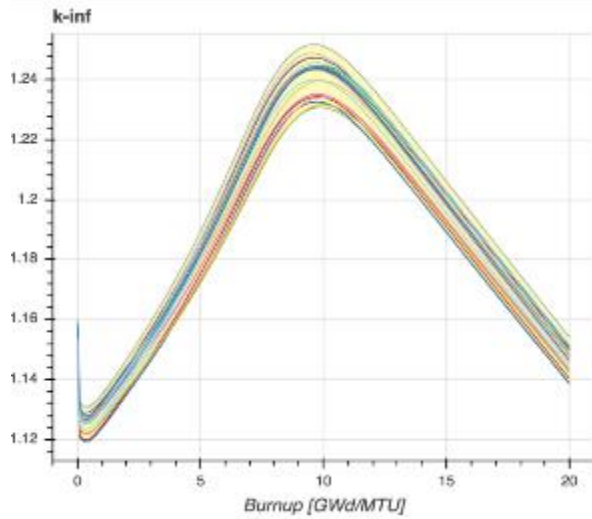


**Figure 4.10.  $k_{inf}$  at 40% void fraction reported by deterministic codes**

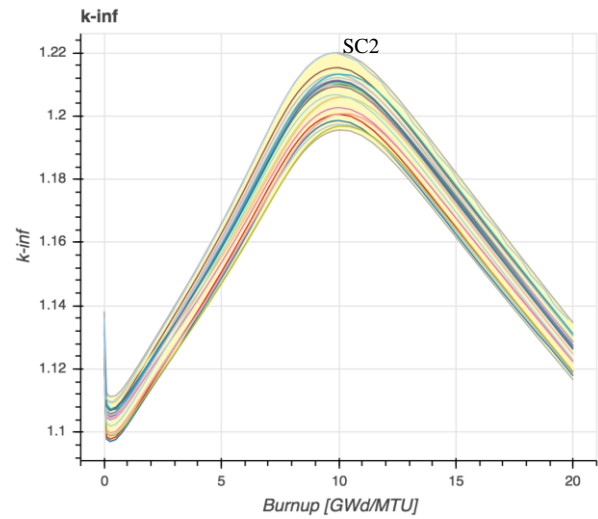


**Figure 4.11.  $k_{inf}$  at 70% void fraction reported by deterministic codes**

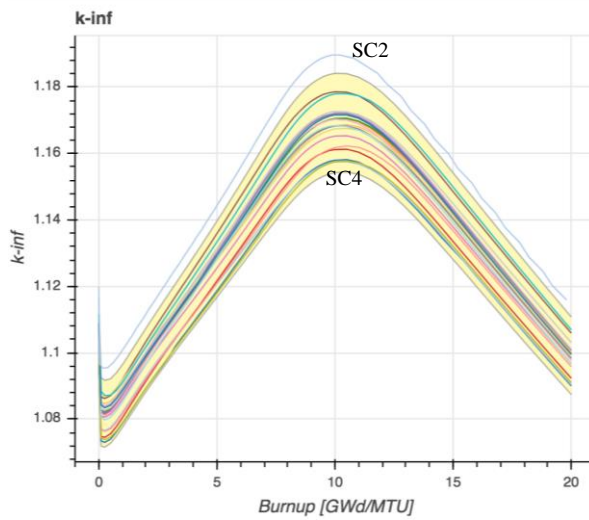


**Figure 4.12.  $k_{inf}$  at 70% void fraction reported by deterministic codes (results with ENDF/B-V and -VI removed)**

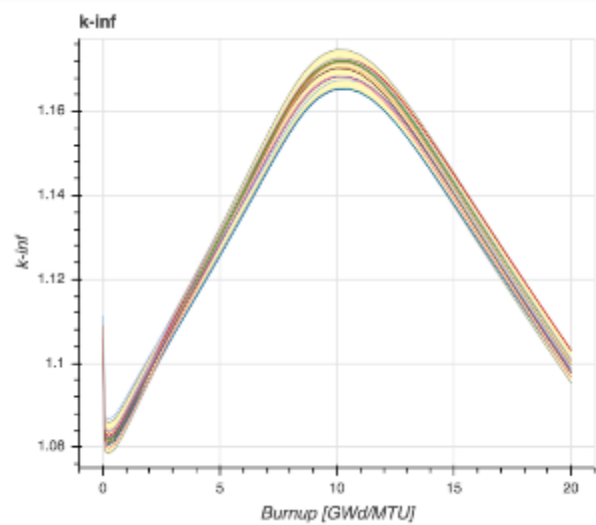


**Table 4.4. Statistics for  $k_{inf}$  reported by deterministic codes, excluding results with ENDF/B-V and ENDF/B-VI libraries**

Burnup (GWd/MTU)	Mean			$2\sigma$ (pcm)			$2\sigma\%$		
	0%	40%	70%	0%	40%	70%	0%	40%	70%
0.00	1.1556	1.1321	1.1069	381	363	359	0.33	0.32	0.32
0.10	1.1279	1.1062	1.0828	340	342	360	0.30	0.31	0.33
0.25	1.1266	1.1052	1.0822	329	334	352	0.29	0.30	0.33
0.50	1.1268	1.1058	1.0831	331	333	342	0.29	0.30	0.32
0.75	1.1285	1.1078	1.0851	328	326	335	0.29	0.29	0.31
1.00	1.1309	1.1104	1.0876	317	317	325	0.28	0.29	0.30
1.25	1.1337	1.1132	1.0904	301	303	312	0.27	0.27	0.29
1.50	1.1365	1.1161	1.0931	285	291	298	0.25	0.26	0.27
1.75	1.1395	1.1191	1.0959	269	278	282	0.24	0.25	0.26
2.00	1.1424	1.1220	1.0986	256	268	271	0.22	0.24	0.25
2.25	1.1454	1.1250	1.1012	248	260	261	0.22	0.23	0.24
2.50	1.1485	1.1279	1.1039	245	255	252	0.21	0.23	0.23
2.75	1.1516	1.1308	1.1064	248	255	247	0.22	0.23	0.22
3.00	1.1547	1.1337	1.1090	256	259	244	0.22	0.23	0.22
3.25	1.1579	1.1367	1.1115	267	267	243	0.23	0.24	0.22
3.50	1.1612	1.1397	1.1140	284	276	245	0.24	0.24	0.22
3.75	1.1646	1.1427	1.1165	304	289	247	0.26	0.25	0.22
4.00	1.1680	1.1457	1.1190	327	304	254	0.28	0.26	0.23
4.25	1.1715	1.1488	1.1215	351	321	260	0.30	0.28	0.23
4.50	1.1752	1.1519	1.1241	377	340	268	0.32	0.30	0.24
4.75	1.1789	1.1551	1.1266	405	361	279	0.34	0.31	0.25
5.00	1.1827	1.1583	1.1292	434	381	289	0.37	0.33	0.26
5.25	1.1866	1.1616	1.1317	464	401	301	0.39	0.35	0.27
5.50	1.1906	1.1649	1.1343	493	422	313	0.41	0.36	0.28
5.75	1.1947	1.1683	1.1369	521	444	327	0.44	0.38	0.29
6.00	1.1989	1.1717	1.1395	550	465	339	0.46	0.40	0.30
6.25	1.2032	1.1752	1.1422	580	485	353	0.48	0.41	0.31
6.50	1.2076	1.1787	1.1448	607	507	367	0.50	0.43	0.32
6.75	1.2119	1.1822	1.1474	632	528	380	0.52	0.45	0.33

**Table 4.4. Statistics for  $k_{inf}$  reported by deterministic codes, excluding results with ENDF/B-V and ENDF/B-VI libraries (continued)**

7.00	1.2163	1.1856	1.1500	657	546	392	0.54	0.46	0.34
7.25	1.2206	1.1891	1.1526	673	563	404	0.55	0.47	0.35
7.50	1.2246	1.1924	1.1551	682	577	416	0.56	0.48	0.36
7.75	1.2284	1.1955	1.1575	689	589	427	0.56	0.49	0.37
8.00	1.2318	1.1984	1.1598	689	595	437	0.56	0.50	0.38
8.25	1.2348	1.2010	1.1620	686	600	444	0.56	0.50	0.38
8.50	1.2373	1.2033	1.1639	679	601	450	0.55	0.50	0.39
8.75	1.2393	1.2051	1.1656	672	598	452	0.54	0.50	0.39
9.00	1.2409	1.2067	1.1670	661	596	455	0.53	0.49	0.39
9.25	1.2420	1.2079	1.1681	648	591	455	0.52	0.49	0.39
9.50	1.2427	1.2087	1.1690	632	584	454	0.51	0.48	0.39
9.75	1.2428	1.2092	1.1697	616	577	453	0.50	0.48	0.39
10.00	1.2425	1.2093	1.1700	600	568	451	0.48	0.47	0.39
10.50	1.2407	1.2086	1.1699	569	547	443	0.46	0.45	0.38
11.00	1.2376	1.2066	1.1690	544	523	431	0.44	0.43	0.37
11.50	1.2336	1.2037	1.1671	528	507	421	0.43	0.42	0.36
12.00	1.2291	1.2000	1.1646	516	493	412	0.42	0.41	0.35
12.50	1.2242	1.1959	1.1614	508	482	404	0.41	0.40	0.35
13.00	1.2192	1.1915	1.1578	501	475	397	0.41	0.40	0.34
13.50	1.2140	1.1869	1.1539	497	469	393	0.41	0.40	0.34
14.00	1.2088	1.1822	1.1498	490	463	387	0.41	0.39	0.34
14.50	1.2036	1.1774	1.1456	486	458	383	0.40	0.39	0.33
15.00	1.1984	1.1727	1.1413	483	454	381	0.40	0.39	0.33
15.50	1.1932	1.1679	1.1370	477	450	378	0.40	0.39	0.33
16.00	1.1880	1.1632	1.1327	474	447	377	0.40	0.38	0.33
16.50	1.1829	1.1584	1.1284	468	444	376	0.40	0.38	0.33
17.00	1.1777	1.1538	1.1242	467	441	376	0.40	0.38	0.33
17.50	1.1725	1.1491	1.1199	464	438	375	0.40	0.38	0.34
18.00	1.1674	1.1445	1.1157	461	435	376	0.39	0.38	0.34
18.50	1.1623	1.1398	1.1115	458	433	374	0.39	0.38	0.34
19.00	1.1572	1.1353	1.1074	455	430	375	0.39	0.38	0.34
19.50	1.1520	1.1307	1.1033	454	427	373	0.39	0.38	0.34
20.00	1.1469	1.1261	1.0992	452	426	375	0.39	0.38	0.34

Note: SC9 and SC20 results are not included.

#### 4.5. Burnup and distribution of gadolinium isotopes

Rod average concentrations of gadolinium isotopes and burnups calculated by all participants are compared for all void fractions. Radial variations in  $^{155}\text{Gd}$  and  $^{157}\text{Gd}$  concentrations are also analysed. Results outside the  $\pm 2\sigma$  band are labelled where applicable in Figures 4.13 to 4.36.

### 4.5.1. <sup>154</sup>Gd

Concentrations of <sup>154</sup>Gd at 0% and 70% void fractions are plotted in Figures 4.13 and 4.14. The concentrations predicted by codes using JEFF libraries are generally the lowest of the contributed results, while codes using ENDF/B libraries calculated the highest concentrations. Statistics for <sup>154</sup>Gd concentrations are provided in Table 4.5.

**Figure 4.13. Rod average <sup>154</sup>Gd concentrations at 0% void fraction**

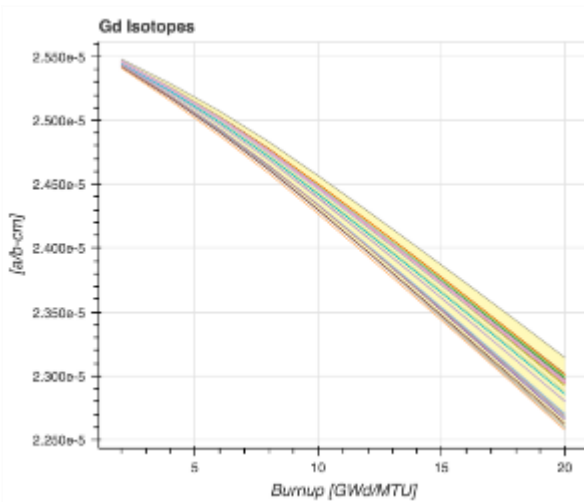


**Figure 4.14. Rod average <sup>154</sup>Gd concentration at 70% void fraction**

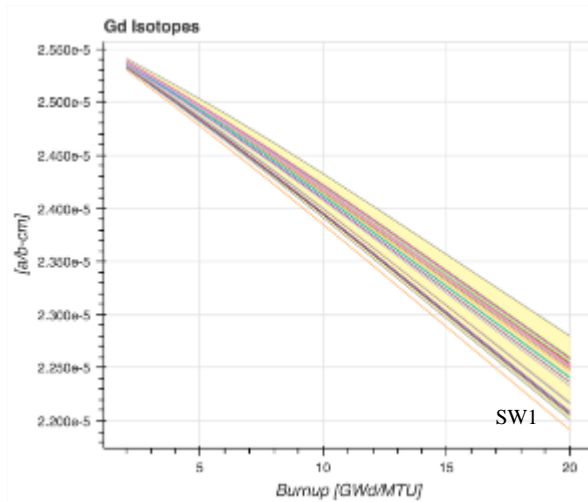


**Table 4.5. Statistics for rod average <sup>154</sup>Gd concentrations**

Burnup GWd/MTU	0% void fraction			40% void fraction			70% void fraction		
	Average	2σ	2σ%	Average	2σ	2σ%	Average	2σ	2σ%
2	2.55E-05	2.97E-08	0.12	2.54E-05	3.46E-08	0.14	2.54E-05	4.35E-08	0.17
4	2.52E-05	5.68E-08	0.23	2.52E-05	6.78E-08	0.27	2.51E-05	8.35E-08	0.33
6	2.50E-05	8.27E-08	0.33	2.49E-05	1.01E-07	0.41	2.48E-05	1.24E-07	0.50
8	2.47E-05	1.09E-07	0.44	2.46E-05	1.33E-07	0.54	2.45E-05	1.64E-07	0.67
10	2.44E-05	1.35E-07	0.55	2.43E-05	1.63E-07	0.67	2.41E-05	2.01E-07	0.83
12	2.41E-05	1.61E-07	0.67	2.40E-05	1.95E-07	0.81	2.38E-05	2.38E-07	1.00
14	2.38E-05	1.87E-07	0.79	2.36E-05	2.25E-07	0.95	2.34E-05	2.74E-07	1.17
16	2.35E-05	2.14E-07	0.91	2.33E-05	2.55E-07	1.09	2.31E-05	3.09E-07	1.34
18	2.32E-05	2.40E-07	1.03	2.30E-05	2.86E-07	1.24	2.28E-05	3.47E-07	1.52
20	2.29E-05	2.65E-07	1.16	2.27E-05	3.16E-07	1.40	2.24E-05	3.81E-07	1.70



#### 4.5.2. $^{155}\text{Gd}$

Concentrations of  $^{155}\text{Gd}$  at 0% and 70% void fractions are plotted in Figures 4.15 and 4.16. HE2 results are outside the  $2\sigma$  band throughout the depletion, increasing the standard deviation significantly. Therefore, HE2 results were removed from the statistical analysis.

Detailed plots of  $^{155}\text{Gd}$  concentrations around 8 GWd/MTU are shown in Figures 4.17 and 4.18. SCALE results are generally below the mean at all void fractions. While VESTA results from predictor-only depletion (VE3P, VE4P, VE5P) predict higher concentrations and are outside the  $2\sigma$  band, VESTA results from predictor-corrector depletion (VE1, VE2, VE3) are in line with SCALE results. If VE3P, VE4P and VE5P results are removed, the highest concentrations are predicted by AL1 at 0% and KENOREST results at 70% void fraction. The lowest concentrations are observed for the AP1, HE4, SC2 and SE1 results in general.

Statistics for  $^{155}\text{Gd}$  concentrations are provided in Table 4.6. The standard deviation in the predicted concentrations increases with void fraction. Absolute standard deviation peaks around 6 GWd/MTU and decreases afterwards at all void fractions, whereas relative standard deviation peaks around 12 GWd/MTU, reaching 52% at 70% void fraction.

Figure 4.15. Rod average <sup>155</sup>Gd concentrations at 0% void fraction

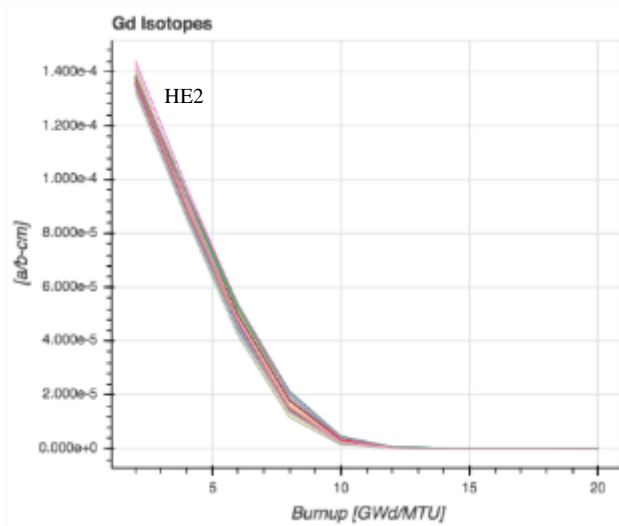


Figure 4.16. Rod average <sup>155</sup>Gd concentrations at 70% void fraction

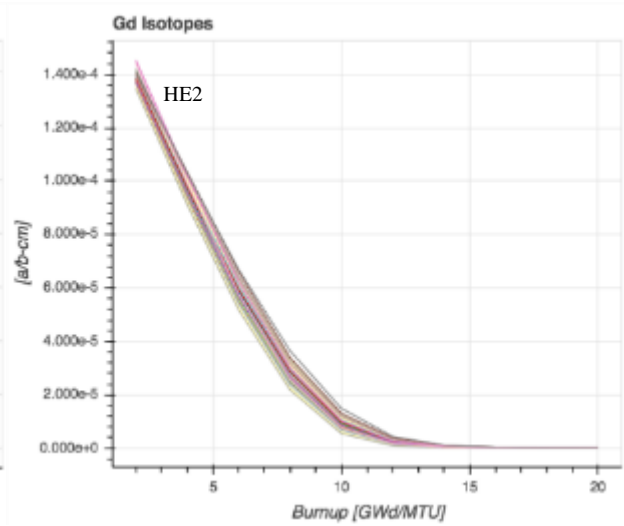


Figure 4.17. Rod average <sup>155</sup>Gd concentrations at 0% void fraction (HE2 results removed)

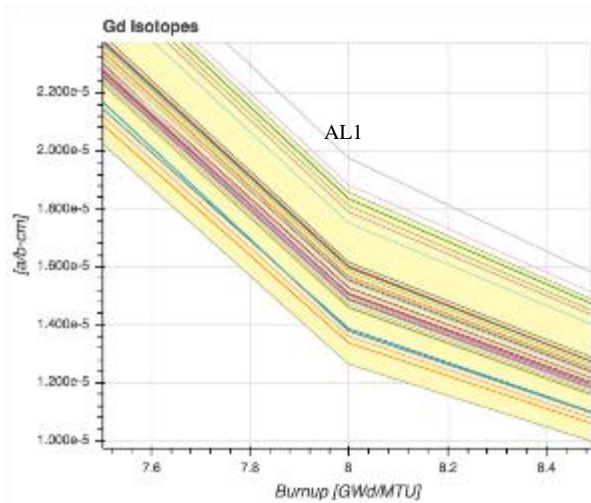
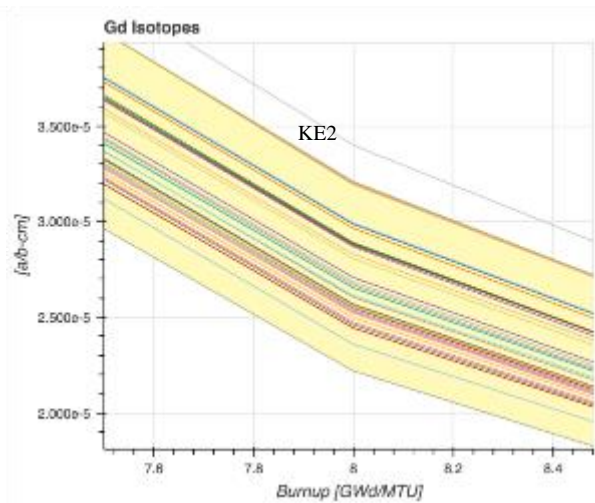


Figure 4.18. Rod average <sup>155</sup>Gd concentrations at 70% void fraction (HE2 results removed)



**Table 4.6. Statistics for rod average  $^{155}\text{Gd}$  concentrations**

Burnup	0% void fraction			40% void fraction			70% void fraction		
	Average	$2\sigma$	$2\sigma\%$	Average	$2\sigma$	$2\sigma\%$	Average	$2\sigma$	$2\sigma\%$
2	1.36E-04	1.96E-06	1.4	1.37E-04	1.69E-06	1.2	1.38E-04	1.73E-06	1.3
4	8.98E-05	3.33E-06	3.7	9.23E-05	3.61E-06	3.9	9.59E-05	4.59E-06	4.8
6	4.68E-05	3.64E-06	7.8	5.14E-05	3.57E-06	6.9	5.73E-05	5.39E-06	9.4
8	1.56E-05	2.97E-06	19.0	2.03E-05	2.85E-06	14.0	2.67E-05	4.62E-06	17.3
10	2.70E-06	8.67E-07	32.1	4.82E-06	1.23E-06	25.6	8.56E-06	2.80E-06	32.7
12	3.95E-07	1.32E-07	33.5	8.62E-07	2.87E-07	33.3	2.05E-06	1.04E-06	50.8
14	1.44E-07	2.53E-08	17.5	2.38E-07	6.02E-08	25.3	5.27E-07	2.76E-07	52.4
16	1.19E-07	1.43E-08	11.9	1.55E-07	2.36E-08	15.2	2.40E-07	7.48E-08	31.1
18	1.15E-07	1.28E-08	11.2	1.42E-07	1.83E-08	12.8	1.88E-07	3.40E-08	18.1
20	1.12E-07	1.22E-08	11.0	1.38E-07	1.71E-08	12.4	1.77E-07	2.66E-08	15.0

Note: HE2 results are not included.

#### 4.5.3. $^{156}\text{Gd}$

$^{156}\text{Gd}$  concentrations at 0% and 70% void fractions are plotted in Figures 4.19 and 4.20. The HE2 results appear to be anomalously low and were removed from the statistics. KENOREST results move from overpredicting  $^{156}\text{Gd}$  concentrations at 0% void fraction to underpredicting at 70% void fraction. KENOREST results are outside the  $2\sigma$  band at 70% void fraction. HE1 and AL1 results underpredict  $^{156}\text{Gd}$  concentrations and are outside the  $2\sigma$  band at 0% void fraction. Statistics for  $^{156}\text{Gd}$  concentrations are provided in Table 4.7.

**Figure 4.19. Rod average  $^{156}\text{Gd}$  concentrations at 0% void fraction**

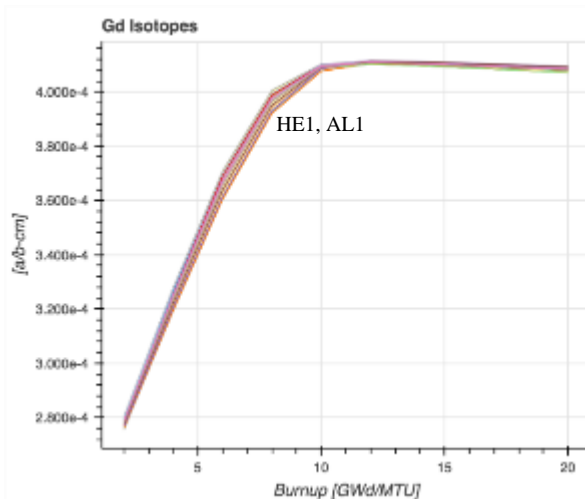


**Figure 4.20. Rod average  $^{156}\text{Gd}$  concentration at 70% void fraction**

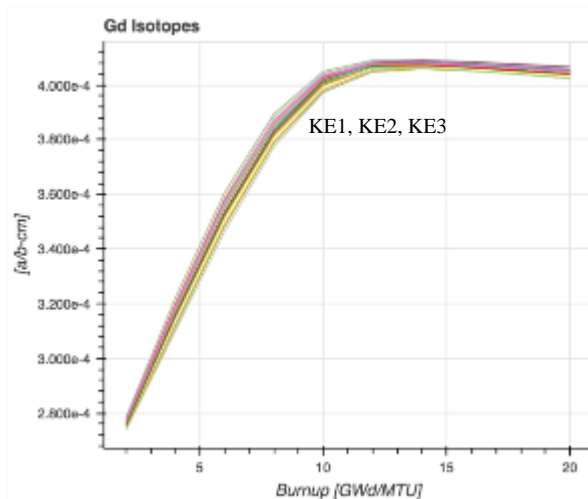


**Table 4.7. Statistics for rod average  $^{156}\text{Gd}$  concentrations**

Burnup GWd/MTU	0% void fraction			40% void fraction			70% void fraction		
	Average	2 $\sigma$	2 $\sigma\%$	Average	2 $\sigma$	2 $\sigma\%$	Average	2 $\sigma$	2 $\sigma\%$
2	2.78E-04	2.02E-06	0.72	2.78E-04	1.77E-06	0.64	2.77E-04	1.82E-06	0.66
4	3.24E-04	3.34E-06	1.03	3.21E-04	3.68E-06	1.15	3.18E-04	4.73E-06	1.49
6	3.67E-04	3.57E-06	0.97	3.62E-04	3.58E-06	0.99	3.55E-04	5.56E-06	1.56
8	3.97E-04	2.86E-06	0.72	3.92E-04	2.87E-06	0.73	3.85E-04	4.88E-06	1.27
10	4.09E-04	8.78E-07	0.21	4.06E-04	1.42E-06	0.35	4.02E-04	3.23E-06	0.80
12	4.11E-04	6.41E-07	0.16	4.09E-04	9.49E-07	0.23	4.07E-04	1.83E-06	0.45
14	4.10E-04	7.60E-07	0.19	4.09E-04	1.03E-06	0.25	4.08E-04	1.50E-06	0.37
16	4.10E-04	8.92E-07	0.22	4.08E-04	1.17E-06	0.29	4.07E-04	1.64E-06	0.40
18	4.09E-04	1.02E-06	0.25	4.07E-04	1.36E-06	0.33	4.06E-04	1.84E-06	0.45
20	4.08E-04	1.14E-06	0.28	4.07E-04	1.52E-06	0.37	4.05E-04	2.07E-06	0.51

Note: HE2 results are not included.

#### 4.5.4. $^{157}\text{Gd}$

Concentrations of  $^{157}\text{Gd}$  at 0% and 70% void fractions are plotted in Figures 4.21 and 4.22. HE2 results predict concentrations larger than the 2 $\sigma$  band at 70% void fraction, while all KENOREST results predict concentrations less than the 2 $\sigma$  band at all void fractions. The contribution of KENOREST and HE2 results to the standard deviation is significant, therefore all KENOREST and HE2 results are removed from the statistics.

The  $^{157}\text{Gd}$  concentrations at 0% and 70% void fractions, without KENOREST and HE2 results, are plotted in Figures 4.23 and 4.24 for a burnup range between 5.5 GWd/MTU and 7.5 GWd/MTU. AL1 results predict higher concentrations than the other codes and are outside the 2 $\sigma$  band at all void fractions. Statistics for  $^{157}\text{Gd}$  concentrations are provided in Table 4.8.

Unlike the results for  $^{155}\text{Gd}$ , the standard deviation decreases with increasing void fraction. Standard deviation increases with burnup and peaks around 4 GWd/MTU. The relative standard deviation peaks around 8 GWd/MTU, reaching above 60% at 0% void fraction.

**Figure 4.21. Rod average  $^{157}\text{Gd}$  concentrations at 0% void fraction** **Figure 4.22. Rod average  $^{157}\text{Gd}$  concentrations at 70% void fraction**

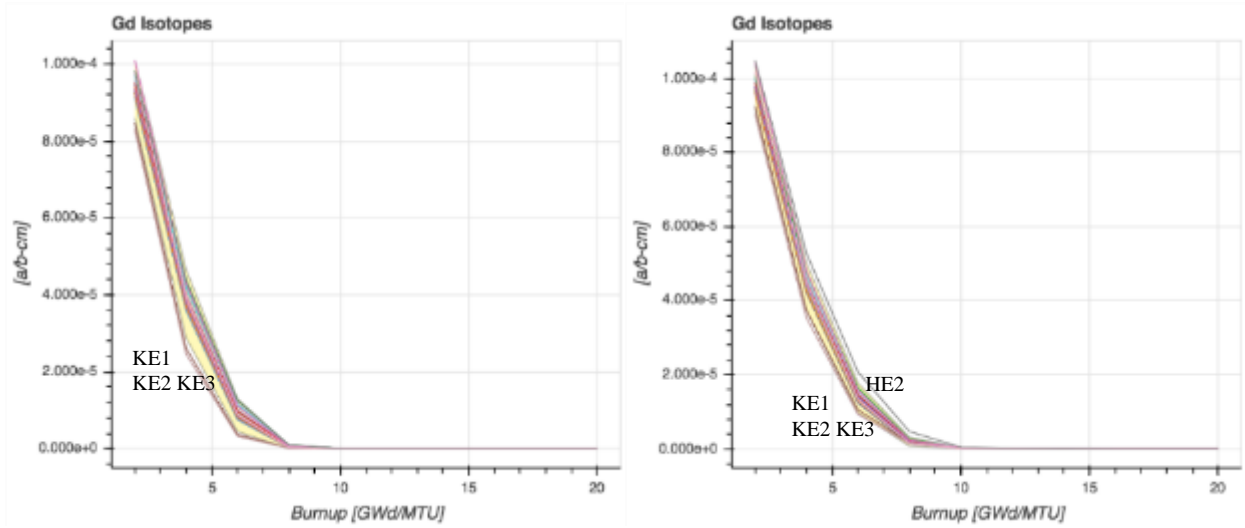


**Figure 4.23. Rod average  $^{157}\text{Gd}$  concentrations at 0% void fraction (KENOREST and HE2 results removed)** **Figure 4.24. Rod average  $^{157}\text{Gd}$  concentrations at 70% void fraction (KENOREST and HE2 results removed)**

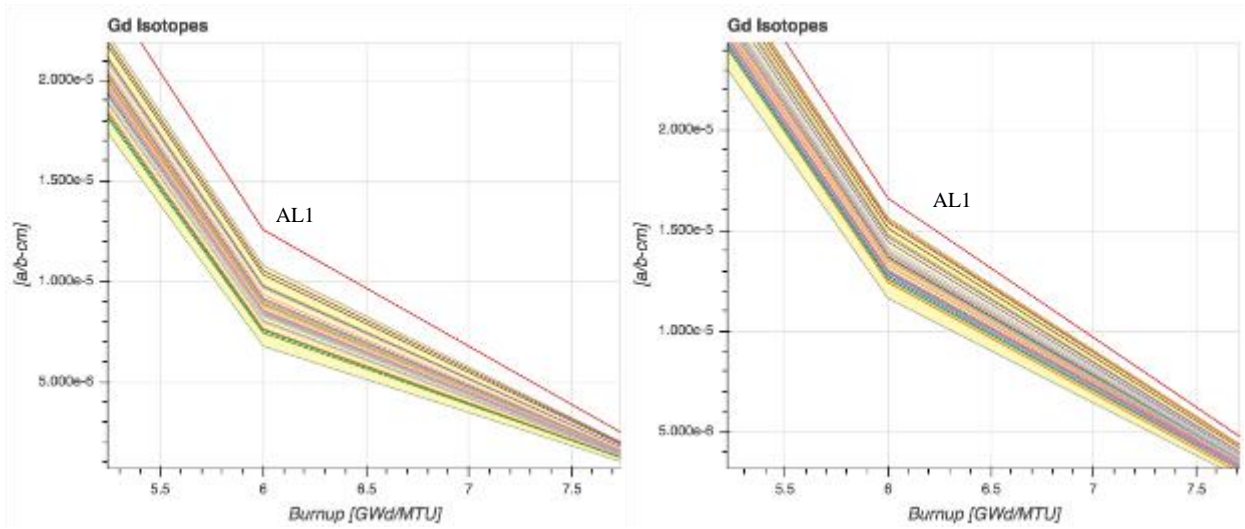


**Table 4.8. Statistics for rod average <sup>157</sup>Gd concentrations**

Burnup	0% void fraction			40% void fraction			70% void fraction		
	Average	2σ	2σ%	Average	2σ	2σ%	Average	2σ	2σ%
2	9.36E-05	2.67E-06	2.85	9.48E-05	2.52E-06	2.65	9.73E-05	2.40E-06	2.46
4	3.80E-05	3.20E-06	8.42	4.02E-05	2.92E-06	7.26	4.36E-05	2.81E-06	6.45
6	8.78E-06	2.01E-06	22.84	1.07E-05	1.93E-06	17.99	1.36E-05	2.01E-06	14.72
8	4.35E-07	2.64E-07	60.67	8.84E-07	4.01E-07	45.37	1.85E-06	6.32E-07	34.15
10	1.05E-07	1.34E-08	12.79	1.55E-07	2.36E-08	15.26	2.49E-07	4.94E-08	19.84
12	9.71E-08	1.20E-08	12.31	1.38E-07	1.93E-08	14.05	1.98E-07	3.27E-08	16.50
14	9.49E-08	1.17E-08	12.31	1.34E-07	1.86E-08	13.86	1.90E-07	3.09E-08	16.27
16	9.33E-08	1.14E-08	12.18	1.33E-07	1.84E-08	13.88	1.88E-07	3.04E-08	16.16
18	9.16E-08	1.12E-08	12.21	1.31E-07	1.80E-08	13.78	1.87E-07	3.01E-08	16.11
20	8.97E-08	1.09E-08	12.19	1.29E-07	1.78E-08	13.77	1.86E-07	3.00E-08	16.13

Note: HE2 and KENOREST results are not included.

**4.5.5. <sup>158</sup>Gd**

The concentrations of <sup>158</sup>Gd at 0% and 70% void fractions are plotted in Figures 4.25 and 4.26. While KENOREST predicts the highest concentrations, HELIOS predicts the lowest compared to other code results at all void fractions. HELIOS results are outside the 2σ band and significantly increase standard deviation, and are therefore removed from the statistics presented in Table 4.9.

**Figure 4.25. Rod average <sup>158</sup>Gd concentration at 0% void fraction**

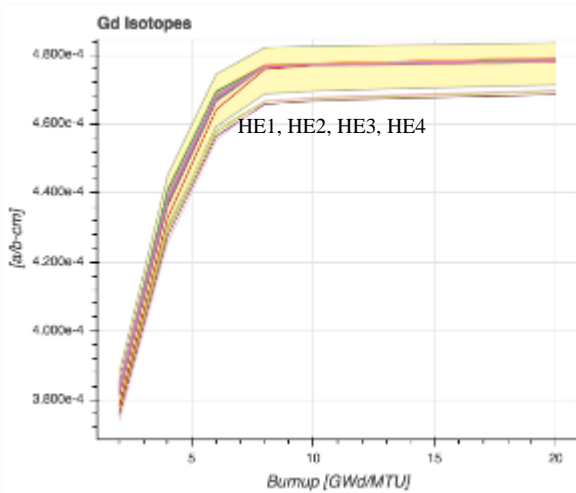


**Figure 4.26. Rod average <sup>158</sup>Gd concentration at 70% void fraction**

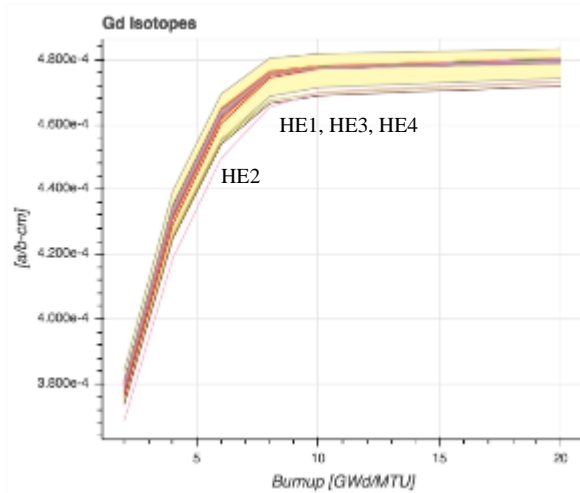


**Table 4.9. Statistics for rod average  $^{158}\text{Gd}$  concentrations**

Burnup GWd/MTU	0% void fraction			40% void fraction			70% void fraction		
	Average	$2\sigma$	$2\sigma\%$	Average	$2\sigma$	$2\sigma\%$	Average	$2\sigma$	$2\sigma\%$
2	3.84E-04	6.17E-06	1.61	3.83E-04	5.4676E-06	1.43	3.80E-04	4.11E-06	1.08
4	4.40E-04	7.89E-06	1.79	4.38E-04	6.7832E-06	1.55	4.34E-04	4.99E-06	1.15
6	4.69E-04	3.48E-06	0.74	4.67E-04	3.3587E-06	0.72	4.64E-04	2.84E-06	0.61
8	4.77E-04	3.72E-07	0.08	4.76E-04	5.02E-07	0.11	4.76E-04	7.20E-07	0.15
10	4.77E-04	3.00E-07	0.06	4.77E-04	3.48E-07	0.07	4.78E-04	4.31E-07	0.09
12	4.78E-04	3.56E-07	0.07	4.78E-04	4.27E-07	0.09	4.78E-04	5.15E-07	0.11
14	4.78E-04	4.27E-07	0.09	4.78E-04	5.06E-07	0.11	4.78E-04	6.28E-07	0.13
16	4.78E-04	4.97E-07	0.10	4.78E-04	5.95E-07	0.12	4.79E-04	7.43E-07	0.16
18	4.78E-04	5.61E-07	0.12	4.79E-04	6.88E-07	0.14	4.79E-04	8.66E-07	0.18
20	4.79E-04	6.47E-07	0.14	4.79E-04	7.96E-07	0.17	4.80E-04	9.97E-07	0.21

Note: HE1, HE2, HE3 and HE4 results are not included.

#### 4.5.6. $^{160}\text{Gd}$

$^{160}\text{Gd}$  concentrations at 0% and 70% void fractions are plotted in Figures 4.17 and 4.28. The KE2 results are below the  $2\sigma$  band. SC1 results show consistently higher  $^{160}\text{Gd}$  concentrations and are also outside the  $2\sigma$  band. SW1 results deviate from other code results and predict lower concentrations than KE2 as burnup increases. SC11 and HE1 results are excluded in comparisons due to insufficient number of digits. Statistics for  $^{160}\text{Gd}$  concentrations are provided in Table 4.10.

**Figure 4.27. Rod average  $^{160}\text{Gd}$  concentration at 0% void fraction**

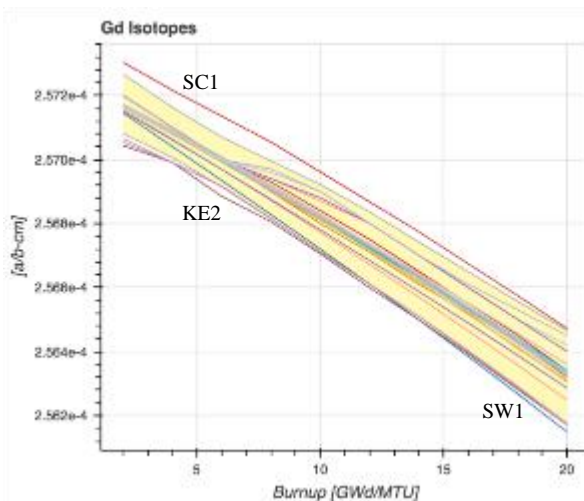


**Figure 4.28. Rod average  $^{160}\text{Gd}$  concentration at 70% void fraction**

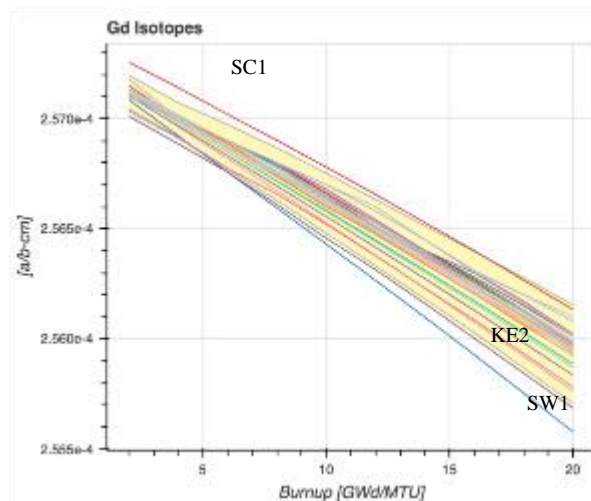


**Table 4.10. Statistics for rod average  $^{160}\text{Gd}$  concentration**

Burnup GWd/MTU	0% void fraction			40% void fraction			70% void fraction		
	Average	$2\sigma$	$2\sigma\%$	Average	$2\sigma$	$2\sigma\%$	Average	$2\sigma$	$2\sigma\%$
2	2.57E-04	9.17E-08	0.04	2.57E-04	9.03E-08	0.04	2.57E-04	8.11E-08	0.03
4	2.57E-04	7.69E-08	0.03	2.57E-04	9.52E-08	0.04	2.57E-04	8.02E-08	0.03
6	2.57E-04	7.65E-08	0.03	2.57E-04	9.31E-08	0.04	2.57E-04	9.97E-08	0.04
8	2.57E-04	8.91E-08	0.03	2.57E-04	1.03E-07	0.04	2.57E-04	1.18E-07	0.05
10	2.57E-04	1.03E-07	0.04	2.57E-04	1.14E-07	0.04	2.57E-04	1.34E-07	0.05
12	2.57E-04	1.11E-07	0.04	2.57E-04	1.26E-07	0.05	2.56E-04	1.49E-07	0.06
14	2.57E-04	1.15E-07	0.04	2.56E-04	1.37E-07	0.05	2.56E-04	1.64E-07	0.06
16	2.57E-04	1.21E-07	0.05	2.56E-04	1.49E-07	0.06	2.56E-04	1.82E-07	0.07
18	2.56E-04	1.31E-07	0.05	2.56E-04	1.63E-07	0.06	2.56E-04	2.03E-07	0.08
20	2.56E-04	1.43E-07	0.06	2.56E-04	1.74E-07	0.07	2.56E-04	2.21E-07	0.09

Note: SC11 and HE1 results are not included.

#### 4.5.7. Radial variation of $^{155}\text{Gd}$ and $^{157}\text{Gd}$ concentrations

Radial variations in  $^{155}\text{Gd}$  and  $^{157}\text{Gd}$  concentrations are analysed at 8 GWd/MTU, selected as a burnup that has the largest standard deviation of  $k_{inf}$  at all void fractions.  $^{155}\text{Gd}$  concentrations from all participants are shown in Figures 4.29 and 4.30 at 0% and 70% void fractions, respectively. Although all code results show a similar decrease in concentrations with increasing radius, there is a large variation in ring 1 (innermost) for a 0% void fraction. AL1 and HE1 predict larger concentrations than other code results in general. While AL1 predicts the largest concentrations at all void fractions, MO1 predicts the lowest concentrations. Statistics for the concentrations in each ring at 8 GWd/MTU are listed in Table 4.11.

As expected,  $^{157}\text{Gd}$  concentrations exhibit a steeper change with increasing radius (Figures 4.31 and 4.32), compared to  $^{155}\text{Gd}$  concentrations. Similar to  $^{155}\text{Gd}$ , AL1 predicts the largest concentrations of  $^{157}\text{Gd}$ , while MO1 predicts the lowest concentrations (at 70%, MO1 is the second lowest after SC16). Statistics for the concentrations in each ring at 8 GWd/MTU are listed in Table 4.12. The largest standard deviation is in ring 1, at which relative standard deviation decreases from 77% to 34% between 0% and 70% void fractions.

Since the largest variations are observed in ring 1,  $^{155}\text{Gd}$  and  $^{157}\text{Gd}$  concentrations in ring 1 as a function of burnup are plotted at 0% and 70% void fractions (Figures 4.33, 4.34, 4.35 and 4.36). KENOEST results are below the  $2\sigma$  band at all void fractions, and HE2 results are above the band at 70% void fraction.



**Figure 4.29. Radial change in  $^{155}\text{Gd}$  concentration at 0% void fraction at 8 GWd/MTU**

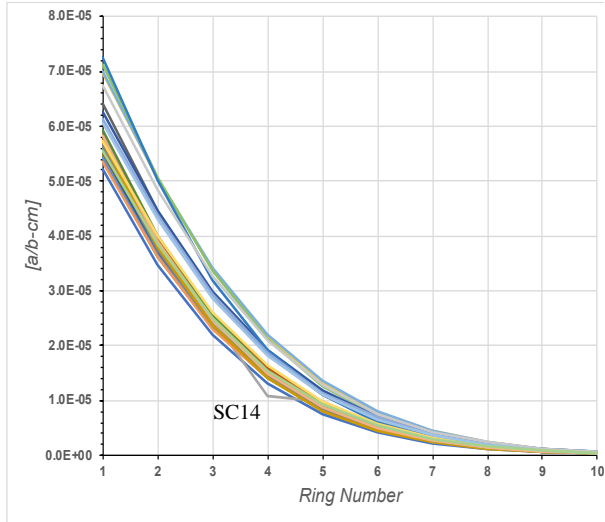


**Figure 4.30. Radial change in  $^{155}\text{Gd}$  concentration at 70% void fraction at 8 GWd/MTU**

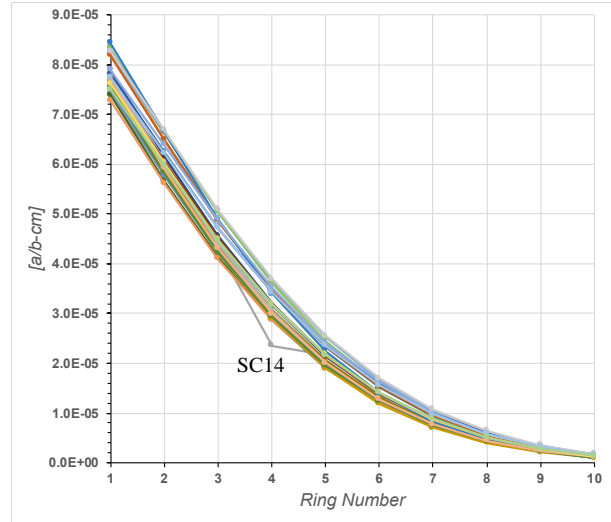


**Figure 4.31. Radial change in  $^{157}\text{Gd}$  concentration at 0% void fraction at 8 GWd/MTU**

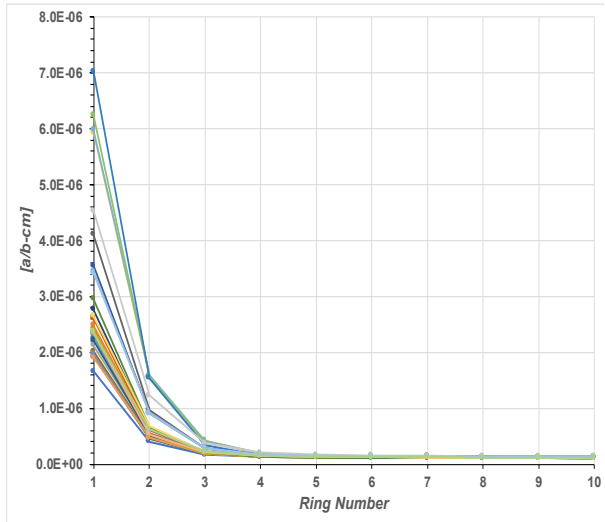


**Figure 4.32. Radial change in  $^{157}\text{Gd}$  concentration at 70% void fraction at 8 GWd/MTU**

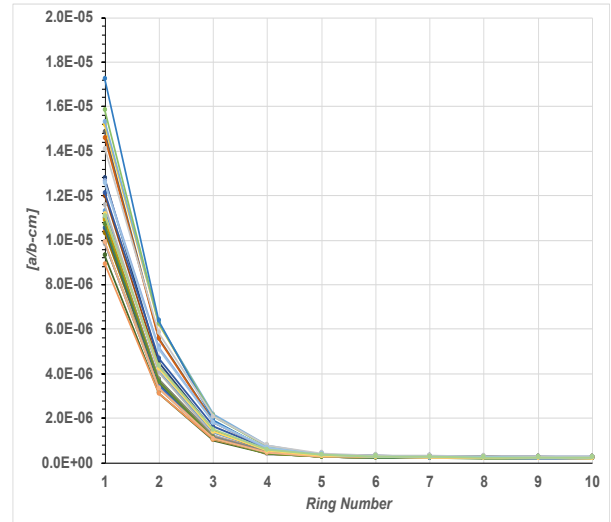


**Table 4.11. Statistics for  $^{155}\text{Gd}$  concentration at 8 GWd/MTU**

Ring number	0% void fraction			70% void fraction		
	Average	$2\sigma$	$2\sigma\%$	Average	$2\sigma$	$2\sigma\%$
1	5.73E-05	8.41E-06	14.7	7.64E-05	5.74E-06	7.5
2	3.92E-05	6.95E-06	17.7	5.97E-05	5.75E-06	9.6
3	2.54E-05	5.16E-06	20.3	4.42E-05	5.25E-06	11.9
4	1.55E-05	3.98E-06	25.6	3.09E-05	5.13E-06	16.6
5	9.36E-06	2.38E-06	25.4	2.09E-05	3.38E-06	16.1
6	5.39E-06	1.54E-06	28.6	1.35E-05	2.56E-06	19.0
7	2.98E-06	9.17E-07	30.8	8.26E-06	1.81E-06	21.9
8	1.61E-06	5.17E-07	32.2	4.83E-06	1.15E-06	23.7
9	8.34E-07	2.84E-07	34.0	2.64E-06	7.12E-07	27.0
10	4.12E-07	1.29E-07	31.3	1.29E-06	3.57E-07	27.8

Note: HE2 and KENOREST results are not included.

**Table 4.12. Statistics for  $^{157}\text{Gd}$  concentration at 8 GWd/MTU**

Ring number	0% void fraction			70% void fraction		
	Average	$2\sigma$	$2\sigma\%$	Average	$2\sigma$	$2\sigma\%$
1	2.66E-06	2.04E-06	76.8	1.12E-05	3.82E-06	34.2
2	6.43E-07	4.78E-07	74.4	4.06E-06	1.73E-06	42.6
3	2.21E-07	9.33E-08	42.2	1.33E-06	5.98E-07	45.0
4	1.46E-07	2.70E-08	18.5	5.15E-07	1.88E-07	36.4
5	1.31E-07	1.71E-08	13.1	3.18E-07	6.85E-08	21.6
6	1.25E-07	1.46E-08	11.7	2.68E-07	4.44E-08	16.6
7	1.21E-07	1.37E-08	11.3	2.50E-07	3.85E-08	15.4
8	1.19E-07	1.31E-08	11.1	2.40E-07	3.67E-08	15.2
9	1.17E-07	1.27E-08	10.9	2.33E-07	3.51E-08	15.0
10	1.16E-07	1.33E-08	11.5	2.29E-07	3.55E-08	15.5

Note: HE2 and KENOREST results are not included.

Figure 4.33. Radial  $^{155}\text{Gd}$  concentration at 0% void fraction in ring 1

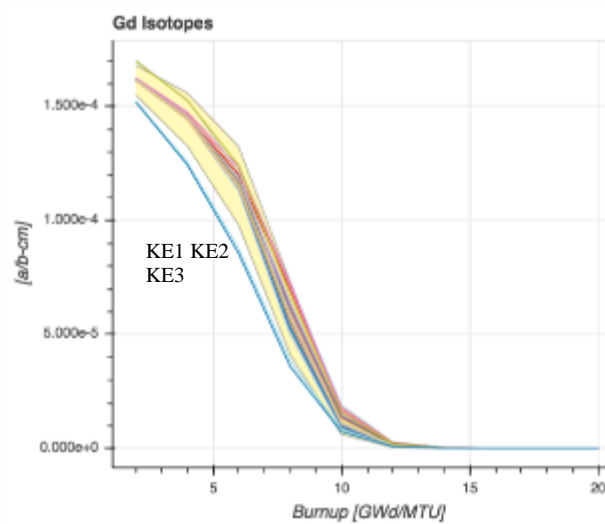


Figure 4.34. Radial  $^{155}\text{Gd}$  concentration at 70% void fraction in ring 1

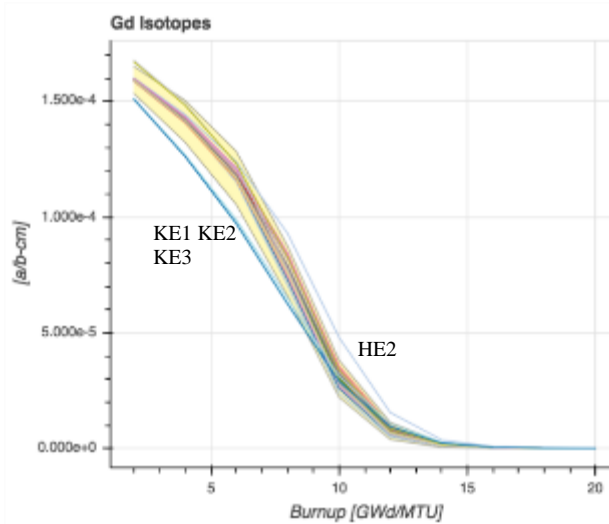


Figure 4.35. Radial  $^{157}\text{Gd}$  concentration at 0% void fraction in ring 1

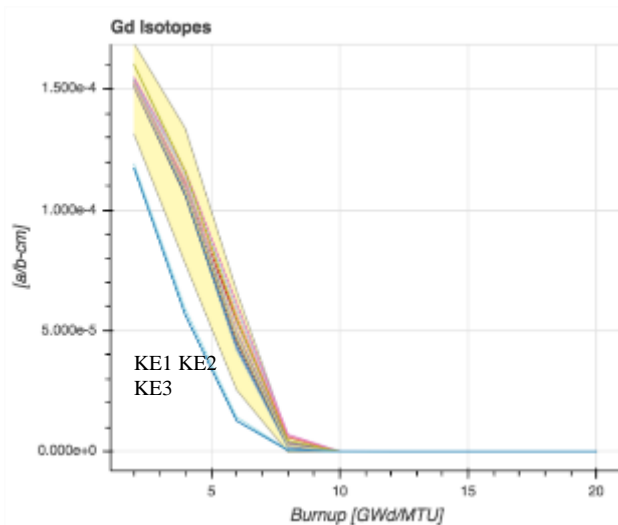
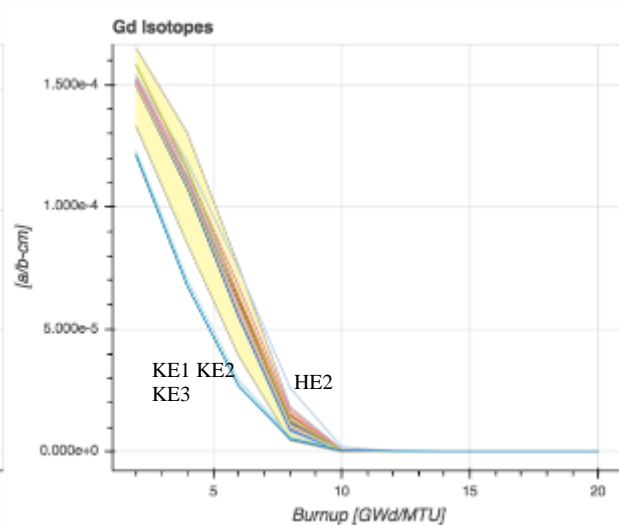


Figure 4.36. Radial  $^{157}\text{Gd}$  concentration at 70% void fraction in ring 1



#### 4.5.8. Gadolinia rod burnup

Gadolinia rod burnup versus lattice average burnup is plotted in Figures 4.37 and 4.38 at 0% and 70% void fractions, respectively. Gadolinia rod burnup exhibits a linear trend after 8 GWd/MTU, after which  $^{155}\text{Gd}$  and  $^{157}\text{Gd}$  concentrations are largely depleted. Large variations in predicted gadolinia rod burnup are observed around peak reactivity, with a relative standard deviation of 11% ( $2\sigma$  of 0.68 GWd/MTU) at an assembly burnup of 10 GWd/MTU. This variation is consistent across all void fractions. The deviation decreases to 7% at the end of depletion.

Detailed plots of gadolinia rod burnups at 0% and 70% void fractions are provided in Figures 4.39 and 4.40, respectively. AP1 predicts the largest burnups, while SCALE results

with old libraries (ENDF/B-V, ENDF/B-VI) predict the lowest burnups at all void fractions.

Statistics for the gadolinia rod burnup based on all participant results are listed in Table 4.13. The absolute  $2\sigma$  increases from 0.18 GWd/MTU to ~1 GWd/MTU at the end of depletion. Void fraction has a negligible effect on the magnitude of the standard deviation.

**Figure 4.37. Gadolinia rod average burnup versus lattice average burnup at 0% void fraction**

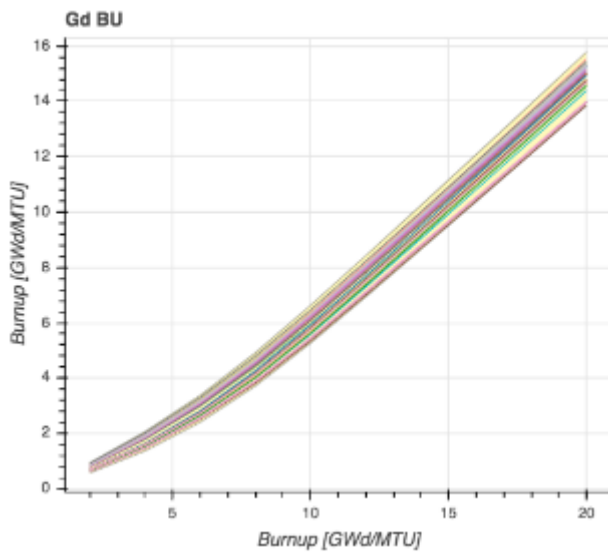


**Figure 4.38. Gadolinia rod average burnup versus lattice average burnup at 70% void fraction**

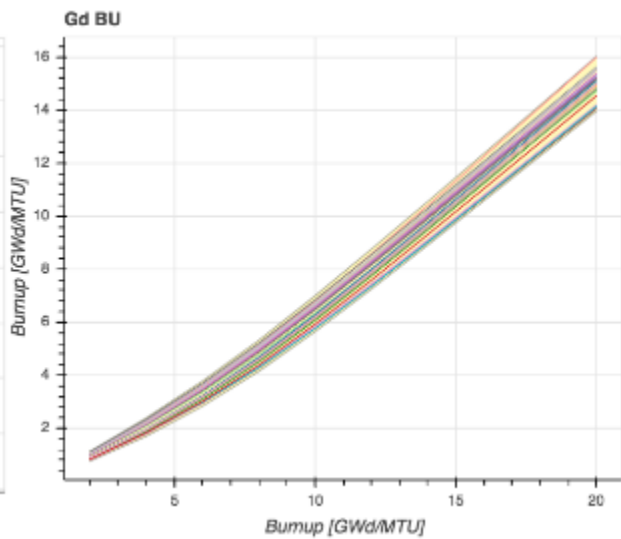


**Figure 4.39. Gadolinia rod average burnup versus lattice average burnup around peak reactivity at 0% void fraction**

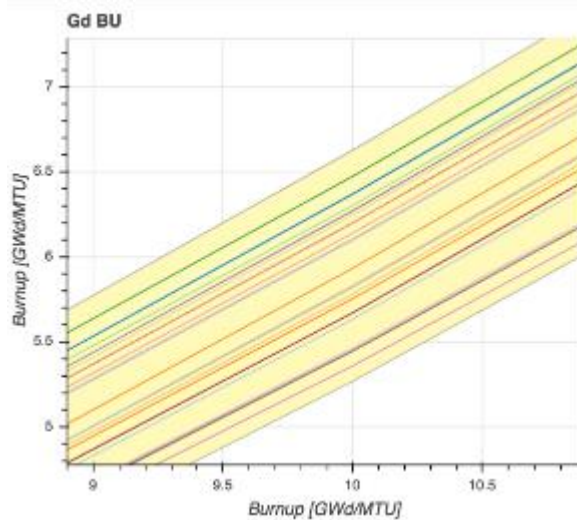


**Figure 4.40. Gadolinia rod average burnup versus lattice average burnup around peak reactivity at 70% void fraction**

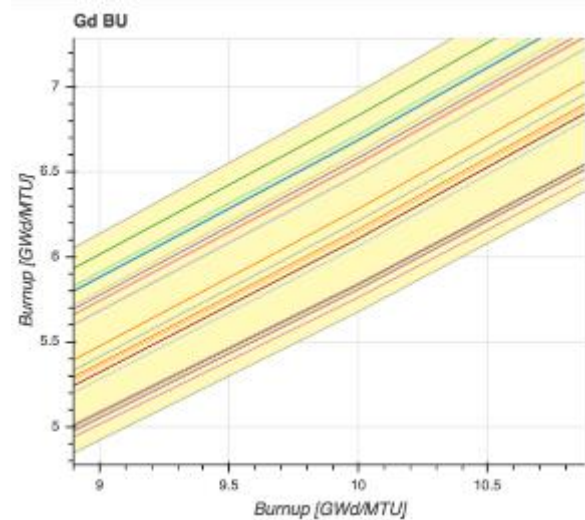


**Table 4.13. Statistics for gadolinia rod burnup**

Burnup GWd/MTU	0% void fraction			40% void fraction			70% void fraction		
	Average	2 $\sigma$	2 $\sigma$ %	Average	2 $\sigma$	2 $\sigma$	Average	2 $\sigma$	2 $\sigma$ %
2	7.68E-01	1.85E-01	24.1	8.55E-01	1.86E-01	21.7	9.41E-01	1.86E-01	19.8
4	1.73E+00	3.43E-01	19.8	1.89E+00	3.41E-01	18.1	2.04E+00	3.42E-01	16.8
6	2.91E+00	4.76E-01	16.3	3.12E+00	4.71E-01	15.1	3.31E+00	4.72E-01	14.3
8	4.34E+00	5.84E-01	13.5	4.55E+00	5.78E-01	12.7	4.74E+00	5.80E-01	12.2
10	5.97E+00	6.63E-01	11.1	6.16E+00	6.60E-01	10.7	6.33E+00	6.68E-01	10.6
12	7.71E+00	7.24E-01	9.4	7.87E+00	7.28E-01	9.3	8.01E+00	7.45E-01	9.3
14	9.47E+00	7.79E-01	8.2	9.62E+00	7.89E-01	8.2	9.74E+00	8.15E-01	8.4
16	1.12E+01	8.36E-01	7.4	1.14E+01	8.50E-01	7.5	1.15E+01	8.82E-01	7.7
18	1.30E+01	8.94E-01	6.9	1.32E+01	9.12E-01	6.9	1.33E+01	9.52E-01	7.2
20	1.48E+01	9.53E-01	6.4	1.49E+01	9.76E-01	6.5	1.50E+01	1.02E+00	6.8

#### 4.6. Actinide concentrations in UO<sub>2</sub> rods

Average actinide concentrations in UO<sub>2</sub> rods are compared in Figures 4.41 to 4.74. Only 40% void fraction results are plotted, unless a significant trend with void fraction was observed.

SC1 results did not include five-year decay results for most void fractions and were therefore not included in the statistics for decayed nuclide concentrations. SC20 actinide results indicate an error in the initial uranium isotopic concentrations and were also not

included in the analysis of actinide and fission product concentrations in the remainder of this report.

#### 4.6.1. $^{238}\text{U}$

The  $^{238}\text{U}$  results are shown in Figures 4.41. A detailed plot for the 15-20 GWd/MTU burnup interval is also provided in Figure 4.42. The lowest  $^{238}\text{U}$  concentrations are reported by KENOREST. SC11 and HE1 results were not provided with sufficient significant digits and were therefore removed from the comparisons. The oscillation of SC13 results in a  $\pm 2\sigma$  band is a possible indication of an unconverged solution. Statistics for  $^{238}\text{U}$  concentrations are provided in Table 4.14. The relative deviation is below 0.07% at all void fractions and burnups.

**Figure 4.41.  $^{238}\text{U}$  concentration at 40% void fraction**

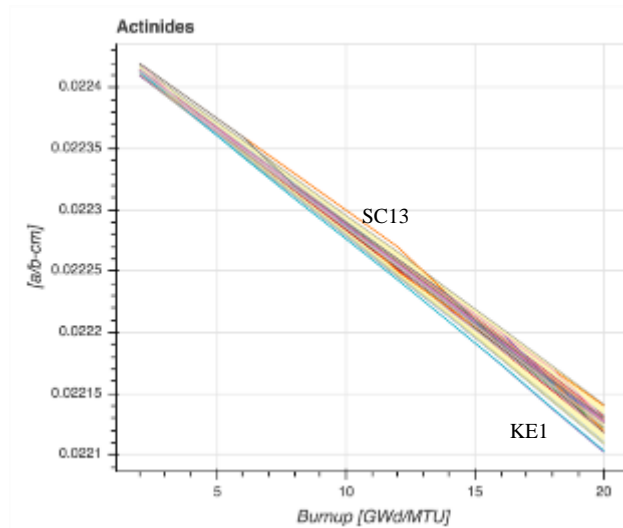


**Figure 4.42.  $^{238}\text{U}$  concentration at 40% void fraction in 15-20 GWd/MTU burnup interval**

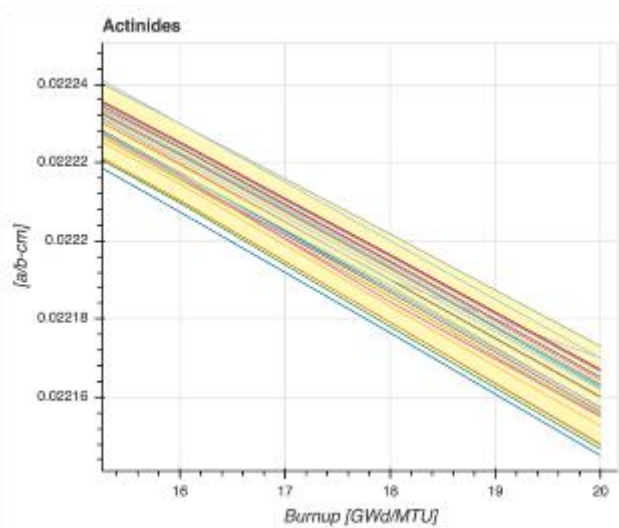


**Table 4.14. Statistics for  $^{238}\text{U}$  concentration**

Burnup GWd/MTU	0% void fraction			40% void fraction			70% void fraction		
	Mean	$2\sigma$	$2\sigma\%$	Mean	$2\sigma$	$2\sigma\%$	Mean	$2\sigma$	$2\sigma\%$
2	2.24E-02	2.43E-06	0.01	2.24E-02	2.29E-06	0.01	2.24E-02	3.39E-06	0.02
4	2.24E-02	3.06E-06	0.01	2.24E-02	2.47E-06	0.01	2.24E-02	3.87E-06	0.02
6	2.24E-02	2.67E-06	0.01	2.24E-02	3.05E-06	0.01	2.24E-02	5.53E-06	0.02
8	2.23E-02	4.57E-06	0.02	2.23E-02	4.83E-06	0.02	2.23E-02	7.23E-06	0.03
10	2.23E-02	4.79E-06	0.02	2.23E-02	6.21E-06	0.03	2.23E-02	8.30E-06	0.04
12	2.23E-02	5.65E-06	0.03	2.23E-02	6.59E-06	0.03	2.23E-02	9.96E-06	0.04
14	2.23E-02	7.08E-06	0.03	2.22E-02	8.15E-06	0.04	2.22E-02	1.03E-05	0.05
16	2.22E-02	7.16E-06	0.03	2.22E-02	8.90E-06	0.04	2.22E-02	1.21E-05	0.05
18	2.22E-02	8.10E-06	0.04	2.22E-02	1.03E-05	0.05	2.22E-02	1.38E-05	0.06
20	2.22E-02	8.95E-06	0.04	2.22E-02	1.13E-05	0.05	2.21E-02	1.57E-05	0.07

Note: SC20 results are not included.

#### 4.6.2. $^{234}\text{U}$

The  $^{234}\text{U}$  concentrations are shown in Figure 4.43. A detailed plot in 15-20 GWd/MTU burnup interval is also provided in Figure 4.44. KE2 (JEFF2.2) results are outside the  $2\sigma$  band. KE3 (JENDL/AC) results are near the upper  $2\sigma$  band while SW1 (JENDL-4) results are near the lower band. Statistics for  $^{234}\text{U}$  concentrations are provided in Table 4.15. The relative standard deviation is below 1.79%.

Figure 4.43. <sup>234</sup>U concentration at 40% void fraction

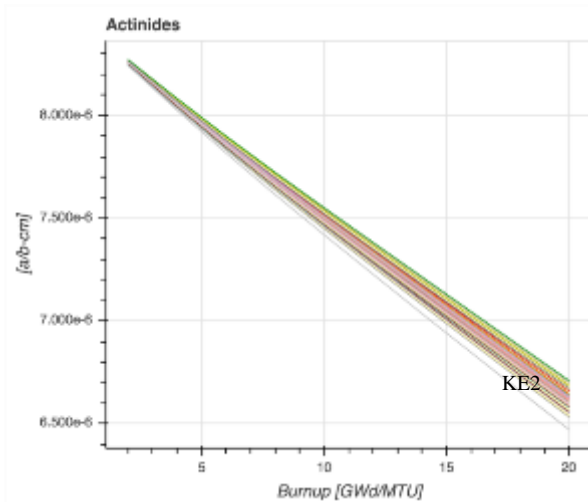


Figure 4.44. <sup>234</sup>U concentration at 40% void fraction in 15-20 GWd/MTU burnup interval

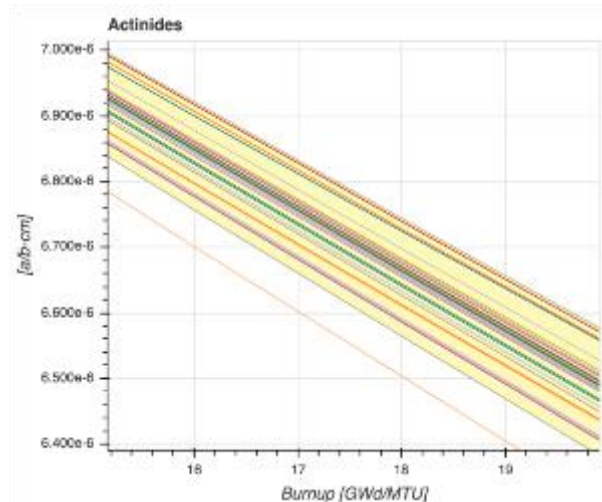


Table 4.15. Statistics for <sup>234</sup>U concentration

Burnup GWd/MTU	0% void fraction			40% void fraction			70% void fraction		
	Mean	2σ	2σ%	Mean	2σ	2σ%	Mean	2σ	2σ%
2	8.26E-06	1.22E-08	0.15	8.24E-06	1.34E-08	0.16	8.22E-06	1.56E-08	0.19
4	8.06E-06	2.28E-08	0.28	8.02E-06	2.60E-08	0.32	7.97E-06	3.03E-08	0.38
6	7.87E-06	3.25E-08	0.41	7.81E-06	3.76E-08	0.48	7.74E-06	4.36E-08	0.56
8	7.68E-06	4.26E-08	0.56	7.60E-06	4.83E-08	0.64	7.52E-06	5.62E-08	0.75
10	7.50E-06	5.09E-08	0.68	7.41E-06	5.80E-08	0.78	7.31E-06	6.68E-08	0.91
12	7.32E-06	5.90E-08	0.81	7.21E-06	6.68E-08	0.93	7.11E-06	7.75E-08	1.09
14	7.14E-06	6.69E-08	0.94	7.03E-06	7.54E-08	1.07	6.91E-06	8.73E-08	1.26
16	6.97E-06	7.43E-08	1.07	6.84E-06	8.37E-08	1.22	6.71E-06	9.68E-08	1.44
18	6.79E-06	8.13E-08	1.20	6.65E-06	9.08E-08	1.36	6.52E-06	1.05E-07	1.61
20	6.62E-06	8.80E-08	1.33	6.47E-06	9.87E-08	1.53	6.33E-06	1.13E-07	1.79

Note: SC20 results are not included.

### 4.6.3. <sup>235</sup>U

The <sup>235</sup>U concentrations are plotted in Figure 4.45. A detailed plot in 15-20 GWd/MTU burnup interval is also provided in Figure 4.46. Highest concentrations are predicted by HELIOS and CA1 codes. CA1 results are outside the 2σ band at all void fractions. AL1 and SC2 (ENDF/B-V) predict the lowest concentrations. Statistics for <sup>235</sup>U concentrations are provided in Table 4.16. The standard deviation increases with burnup and decreases with void fraction. The maximum relative standard deviation is 1.5% at 0% void fraction.



**Figure 4.45. <sup>235</sup>U concentration at 40% void fraction**

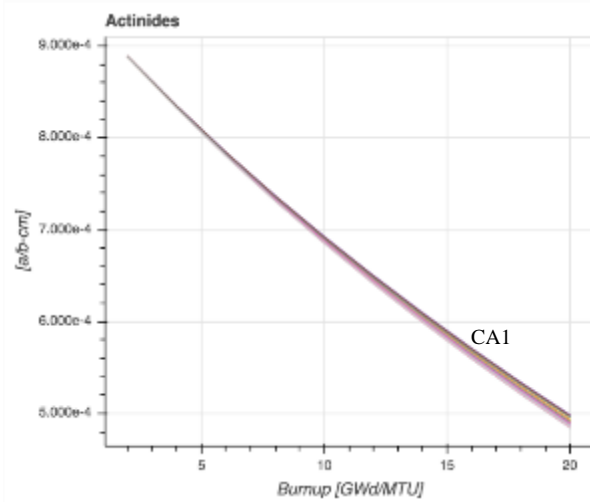


**Figure 4.46. <sup>235</sup>U concentration at 40% void fraction in 15-20 GWd/MTU burnup interval**

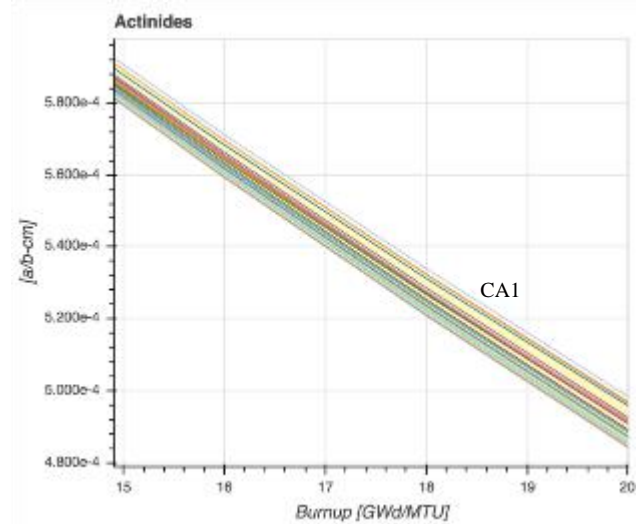


**Table 4.16. Statistics for <sup>235</sup>U concentration**

Burnup GWd/MTU	0% void fraction			40% void fraction			70% void fraction		
	Mean	2σ	2σ%	Mean	2σ	2σ%	Mean	2σ	2σ%
2	8.88E-04	8.49E-07	0.10	8.88E-04	7.26E-07	0.08	8.89E-04	7.20E-07	0.08
4	8.32E-04	1.53E-06	0.18	8.33E-04	1.44E-06	0.17	8.35E-04	1.39E-06	0.17
6	7.79E-04	2.25E-06	0.29	7.82E-04	2.08E-06	0.27	7.85E-04	1.95E-06	0.25
8	7.30E-04	3.05E-06	0.42	7.34E-04	2.78E-06	0.38	7.38E-04	2.60E-06	0.35
10	6.83E-04	3.76E-06	0.55	6.88E-04	3.46E-06	0.50	6.94E-04	3.22E-06	0.46
12	6.38E-04	4.49E-06	0.70	6.45E-04	4.09E-06	0.63	6.52E-04	3.91E-06	0.60
14	5.95E-04	5.19E-06	0.87	6.04E-04	4.77E-06	0.79	6.12E-04	4.59E-06	0.75
16	5.54E-04	5.85E-06	1.06	5.64E-04	5.37E-06	0.95	5.75E-04	5.27E-06	0.92
18	5.14E-04	6.40E-06	1.24	5.27E-04	5.92E-06	1.12	5.39E-04	5.94E-06	1.10
20	4.77E-04	6.91E-06	1.45	4.91E-04	6.49E-06	1.32	5.04E-04	6.61E-06	1.31

Note: SC20 results are not included.

**4.6.4. <sup>236</sup>U**

The <sup>236</sup>U concentrations are plotted in Figure 4.47. A detailed plot in 15-20 GWd/MTU burnup interval is also provided in Figure 4.48. As seen in Figure 4.48, all code results except KENOREST, CA1 and SC2 are tightly clustered around the mean. KE1, KE3 and SC2 predict the highest concentrations of <sup>236</sup>U, and KE2 and CA1 predict the lowest concentrations. KE1, KE2 and CA1 results are outside the 2σ band. Statistics for <sup>236</sup>U concentrations are provided in Table 4.17. Standard deviation increases with burnup and void fraction, while relative standard deviation is near constant (~2.2%).

Figure 4.47. <sup>236</sup>U concentration at 40% void fraction

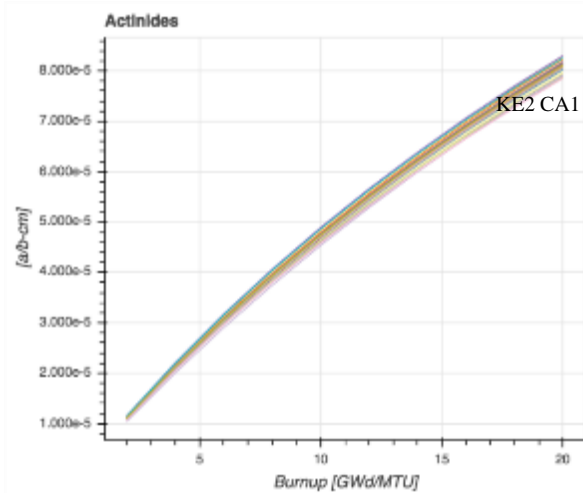


Figure 4.48. <sup>236</sup>U concentration at 40% void fraction in 15-20 GWd/MTU burnup interval

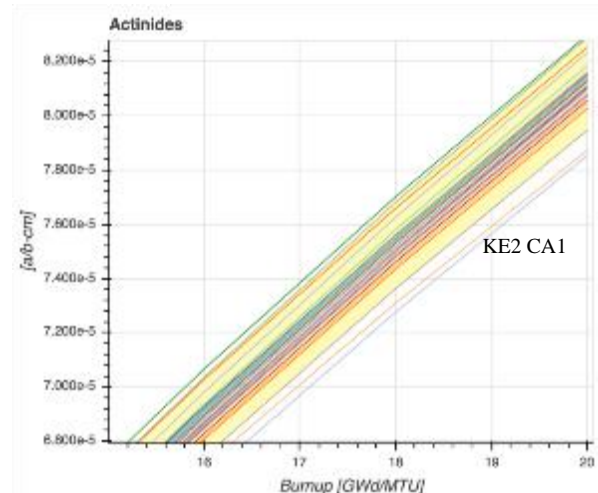


Table 4.17. Statistics for <sup>236</sup>U concentration

Burnup GWd/MTU	0% void fraction			40% void fraction			70% void fraction		
	Mean	2σ	2σ%	Mean	2σ	2σ%	Mean	2σ	2σ%
2	1.08E-05	2.49E-07	2.31	1.11E-05	2.65E-07	2.39	1.14E-05	2.96E-07	2.60
4	2.07E-05	4.76E-07	2.30	2.12E-05	4.95E-07	2.33	2.18E-05	5.44E-07	2.50
6	3.00E-05	6.74E-07	2.25	3.06E-05	6.96E-07	2.28	3.13E-05	7.55E-07	2.41
8	3.85E-05	8.53E-07	2.21	3.93E-05	8.74E-07	2.23	4.02E-05	9.37E-07	2.33
10	4.66E-05	1.02E-06	2.20	4.74E-05	1.04E-06	2.19	4.83E-05	1.10E-06	2.27
12	5.41E-05	1.18E-06	2.19	5.49E-05	1.19E-06	2.17	5.60E-05	1.24E-06	2.22
14	6.13E-05	1.33E-06	2.17	6.21E-05	1.33E-06	2.14	6.31E-05	1.37E-06	2.18
16	6.81E-05	1.47E-06	2.16	6.88E-05	1.45E-06	2.11	6.99E-05	1.49E-06	2.14
18	7.45E-05	1.60E-06	2.14	7.52E-05	1.57E-06	2.09	7.62E-05	1.61E-06	2.11
20	8.06E-05	1.71E-06	2.12	8.12E-05	1.68E-06	2.07	8.21E-05	1.73E-06	2.11

Note: SC20 results are not included.

#### 4.6.5. <sup>237</sup>Np

The <sup>237</sup>Np concentrations are shown in Figure 4.49. All code results are tightly clustered around the mean, with the exception of KENOREST results (KE1, KE2, KE3) and SE2. All KENOREST results have a large bias compared to other code results. KENOREST results increase the standard deviation threefold. Therefore, the KENOREST results are removed from statistics (Figure 4.50). The lowest concentrations are predicted by SE and are below the 2σ band. Statistics for <sup>237</sup>Np concentrations at discharge and five-year decay are provided in Table 4.18. The standard deviation decreases with burnup and void fraction at discharge. After five-year decay, the standard deviation does not change significantly. The lowest standard deviations are observed at 40% void fraction.

Figure 4.49.  $^{237}\text{Np}$  concentration at 70% void fraction

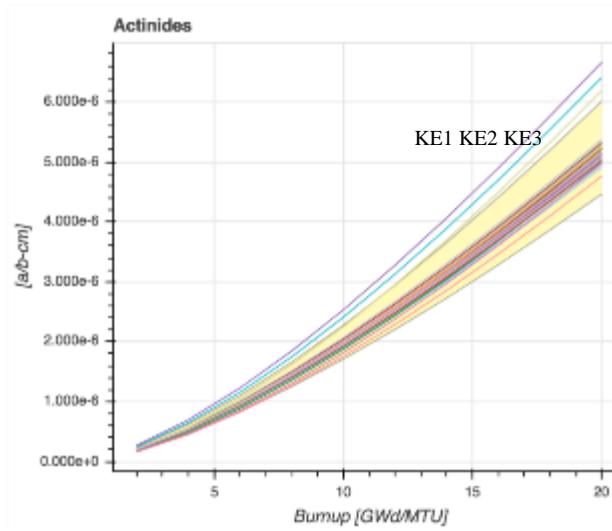


Figure 4.50.  $^{237}\text{Np}$  concentration at 70% void fraction (KENOREST results removed)

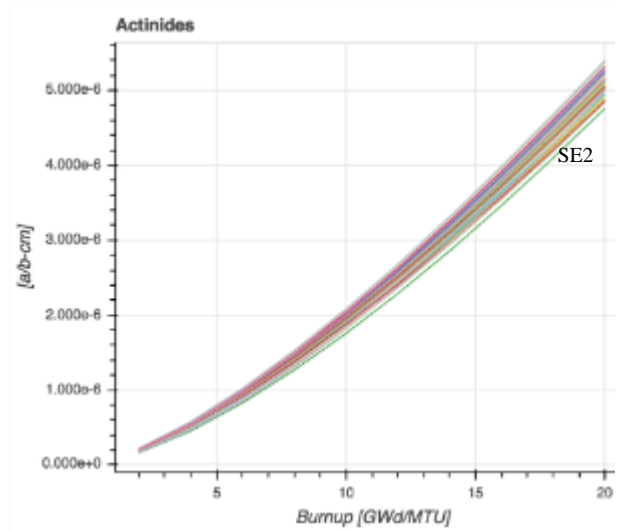


Table 4.18. Statistics for  $^{237}\text{Np}$  concentration

0-years									
Burnup GWd/MTU	0% void fraction			40% void fraction			70% void fraction		
	Mean	2 $\sigma$	2 $\sigma$ %	Mean	2 $\sigma$	2 $\sigma$ %	Mean	2 $\sigma$	2 $\sigma$ %
2	1.49E-07	1.16E-08	7.77	1.74E-07	1.32E-08	7.58	1.98E-07	1.98E-08	9.99
4	3.96E-07	2.50E-08	6.31	4.64E-07	2.88E-08	6.22	5.31E-07	4.36E-08	8.22
6	7.05E-07	4.00E-08	5.67	8.27E-07	4.61E-08	5.57	9.49E-07	6.89E-08	7.26
8	1.06E-06	5.59E-08	5.26	1.25E-06	6.39E-08	5.13	1.43E-06	9.31E-08	6.51
10	1.45E-06	7.17E-08	4.93	1.71E-06	8.04E-08	4.72	1.96E-06	1.16E-07	5.91
12	1.88E-06	8.82E-08	4.68	2.21E-06	9.71E-08	4.40	2.53E-06	1.40E-07	5.54
14	2.35E-06	1.05E-07	4.47	2.74E-06	1.15E-07	4.20	3.13E-06	1.65E-07	5.27
16	2.84E-06	1.21E-07	4.27	3.31E-06	1.34E-07	4.04	3.77E-06	1.92E-07	5.10
18	3.37E-06	1.40E-07	4.14	3.91E-06	1.55E-07	3.97	4.44E-06	2.20E-07	4.95
20	3.92E-06	1.58E-07	4.03	4.53E-06	1.77E-07	3.91	5.13E-06	2.47E-07	4.82
5-years									
Burnup GWd/MTU	0% void fraction			40% void fraction			70% void fraction		
	Mean	2 $\sigma$	2 $\sigma$ %	Mean	2 $\sigma$	2 $\sigma$ %	Mean	2 $\sigma$	2 $\sigma$ %
2	1.76E-07	1.27E-08	7.23	2.05E-07	1.44E-08	7.01	2.34E-07	2.23E-08	9.54
4	4.32E-07	2.65E-08	6.14	5.07E-07	3.05E-08	6.03	5.81E-07	4.71E-08	8.11
6	7.50E-07	4.23E-08	5.63	8.81E-07	4.87E-08	5.52	1.01E-06	7.31E-08	7.23
8	1.11E-06	5.93E-08	5.33	1.31E-06	6.67E-08	5.10	1.50E-06	9.81E-08	6.53
10	1.51E-06	7.66E-08	5.06	1.78E-06	8.46E-08	4.76	2.04E-06	1.22E-07	5.97
12	1.95E-06	9.33E-08	4.78	2.28E-06	1.00E-07	4.39	2.62E-06	1.48E-07	5.63
14	2.42E-06	1.11E-07	4.58	2.83E-06	1.19E-07	4.19	3.24E-06	1.74E-07	5.38
16	2.93E-06	1.29E-07	4.41	3.41E-06	1.37E-07	4.03	3.89E-06	2.03E-07	5.22
18	3.46E-06	1.48E-07	4.26	4.02E-06	1.59E-07	3.96	4.57E-06	2.32E-07	5.08
20	4.02E-06	1.68E-07	4.18	4.65E-06	1.90E-07	4.08	5.27E-06	2.60E-07	4.94

Note: SC20 and KENOREST results are not included.

#### 4.6.6. $^{238}\text{Pu}$

The  $^{238}\text{Pu}$  concentrations are shown in Figures 4.51, 4.52, 4.53 and 4.54. SC1 results do not include  $^{238}\text{Pu}$  concentrations; therefore, five-year decay concentrations for any Pu isotope are not included in the comparisons. Figure 4.51 shows the general trend in the  $^{238}\text{Pu}$  concentration.  $^{238}\text{Pu}$  concentrations in 17-20 GWd/MTU burnup interval are shown in Figures 4.52 and 4.53. A bias between KENOREST is evident in Figures 4.52 and 4.53, with KENOREST predicting higher concentrations than other code results. CA1 predict the lowest concentrations, except at 70% void fraction. SE2 and SE1 results are separated with a bias at 70% void fraction, and SE2 results are outside the 2 $\sigma$  band.

After five-year decay (Figure 4.54), the trend in  $^{238}\text{Pu}$  concentrations stays the same. Statistics for  $^{238}\text{Pu}$  concentrations are provided in Table 4.19. Standard deviation in the discharge results increases with increasing burnup and void fraction. The relative standard

deviation is around 10-13% at peak reactivity until the end of depletion. The relative standard deviation doesn't change significantly after five-year decay.

**Figure 4.51.  $^{238}\text{Pu}$  concentration at 40% void fraction at discharge**

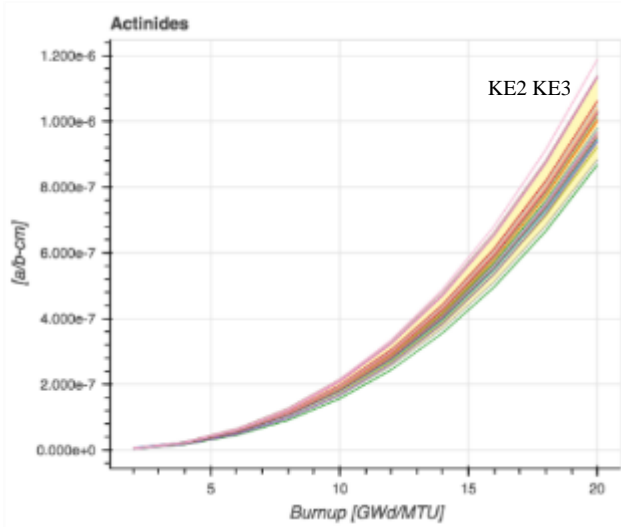


**Figure 4.52.  $^{238}\text{Pu}$  concentration at 40% void fraction in 17-20 GWd/MTU burnup interval**

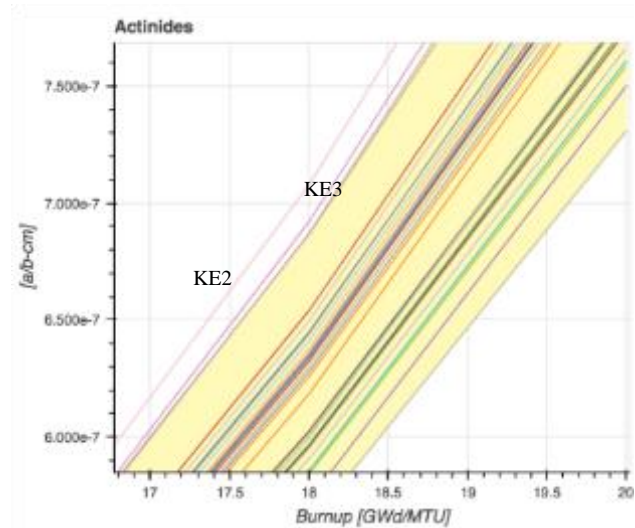


**Figure 4.53.  $^{238}\text{Pu}$  concentration at 70% void fraction in 17-20 GWd/MTU burnup interval**

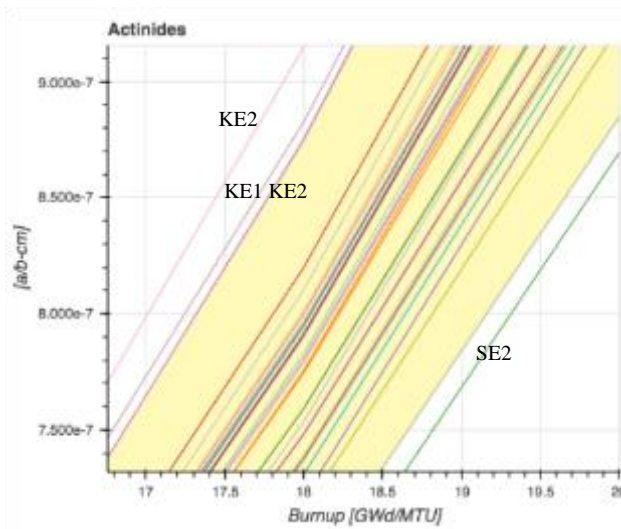


**Figure 4.54.  $^{238}\text{Pu}$  concentration at 70% void fraction after five-year decay**

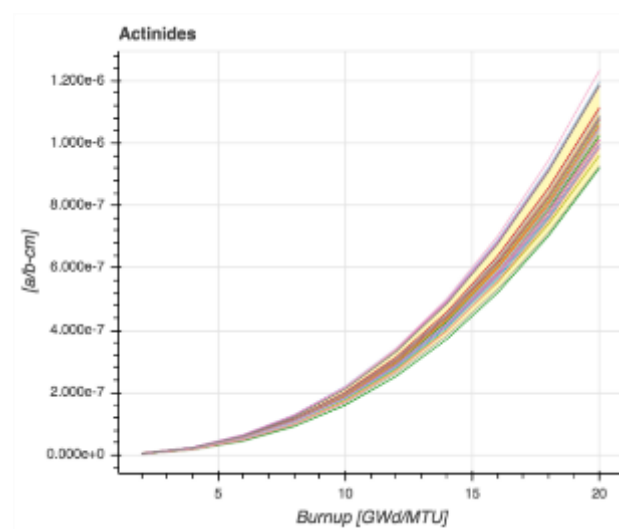


**Table 4.19. Statistics for  $^{238}\text{Pu}$  concentration**

0-years									
Burnup GWd/MTU	0% void fraction			40% void fraction			70% void fraction		
	Mean	2 $\sigma$	2 $\sigma$ %	Mean	2 $\sigma$	2 $\sigma$ %	Mean	2 $\sigma$	2 $\sigma$ %
2	2.40E-09	9.02E-10	37.60	3.07E-09	9.26E-10	30.15	3.84E-09	1.03E-09	26.91
4	1.28E-08	1.48E-09	11.55	1.65E-08	1.83E-09	11.03	2.08E-08	2.87E-09	13.80
6	3.40E-08	3.12E-09	9.17	4.40E-08	4.14E-09	9.43	5.55E-08	6.91E-09	12.46
8	6.76E-08	5.93E-09	8.77	8.76E-08	8.04E-09	9.19	1.11E-07	1.34E-08	12.08
10	1.15E-07	1.02E-08	8.84	1.49E-07	1.39E-08	9.29	1.89E-07	2.26E-08	12.00
12	1.79E-07	1.62E-08	9.02	2.31E-07	2.20E-08	9.52	2.92E-07	3.52E-08	12.04
14	2.62E-07	2.42E-08	9.25	3.37E-07	3.27E-08	9.72	4.23E-07	5.14E-08	12.14
16	3.65E-07	3.45E-08	9.45	4.68E-07	4.64E-08	9.92	5.86E-07	7.17E-08	12.24
18	4.92E-07	4.75E-08	9.67	6.27E-07	6.33E-08	10.09	7.82E-07	9.64E-08	12.33
20	6.44E-07	6.36E-08	9.88	8.17E-07	8.43E-08	10.32	1.01E-06	1.26E-07	12.42

**Table 4.19. Statistics for  $^{238}\text{Pu}$  concentration (continued)**

5-years									
Burnup GWd/MTU	0% void fraction			40% void fraction			70% void fraction		
	Mean	2 $\sigma$	2 $\sigma$ %	Mean	2 $\sigma$	2 $\sigma$ %	Mean	2 $\sigma$	2 $\sigma$ %
2	2.53E-09	8.75E-10	34.63	3.24E-09	9.02E-10	27.88	4.04E-09	1.02E-09	25.25
4	1.30E-08	1.47E-09	11.30	1.68E-08	1.83E-09	10.87	2.11E-08	2.89E-09	13.65
6	3.43E-08	3.12E-09	9.11	4.44E-08	4.15E-09	9.36	5.60E-08	6.91E-09	12.33
8	6.85E-08	5.98E-09	8.73	8.87E-08	8.09E-09	9.12	1.12E-07	1.34E-08	11.92
10	1.18E-07	1.03E-08	8.79	1.52E-07	1.40E-08	9.20	1.92E-07	2.27E-08	11.80
12	1.84E-07	1.65E-08	8.97	2.37E-07	2.26E-08	9.54	2.99E-07	3.54E-08	11.83
14	2.72E-07	2.49E-08	9.18	3.48E-07	3.37E-08	9.68	4.37E-07	5.20E-08	11.90
16	3.82E-07	3.58E-08	9.38	4.87E-07	4.80E-08	9.87	6.08E-07	7.28E-08	11.97
18	5.17E-07	4.94E-08	9.56	6.56E-07	6.57E-08	10.01	8.15E-07	9.83E-08	12.05
20	6.80E-07	6.64E-08	9.76	8.59E-07	8.74E-08	10.17	1.06E-06	1.29E-07	12.12

Note: SC20 and SC1 results are not included.

#### 4.6.7. $^{239}\text{Pu}$

The  $^{239}\text{Pu}$  concentrations at discharge and after five-year decay are compared in Figures 4.55 and 4.56. Concentrations in the range of 15-20 GWd/MTU interval are plotted in Figures 4.57 and 4.58 at 0% and 70% void fractions, respectively. KENOREST results predict higher concentrations than other code results in general. As void fraction increases, more KENOREST results move outside the 2 $\sigma$  band. The lowest concentrations are predicted by VESTA results at 0% and 40% void fractions. Statistics for  $^{239}\text{Pu}$  concentrations at discharge and after five-year decay are provided in Table 4.20.

At 70% void fraction, SC2 predicts the lowest  $^{239}\text{Pu}$  concentrations. The KENOEST and SC2 results increase the standard deviation by more than 50%. Statistics where KENOEST and SC2 results are removed are provided in Table 4.21. Standard deviation increases with burnup and void fraction. Standard deviation at 70% void fraction is twice as large as 0% void fraction values. Overall relative  $2\sigma$  is in the range of 3-4%.

**Figure 4.55.  $^{239}\text{Pu}$  concentration at 40% void fraction at discharge**

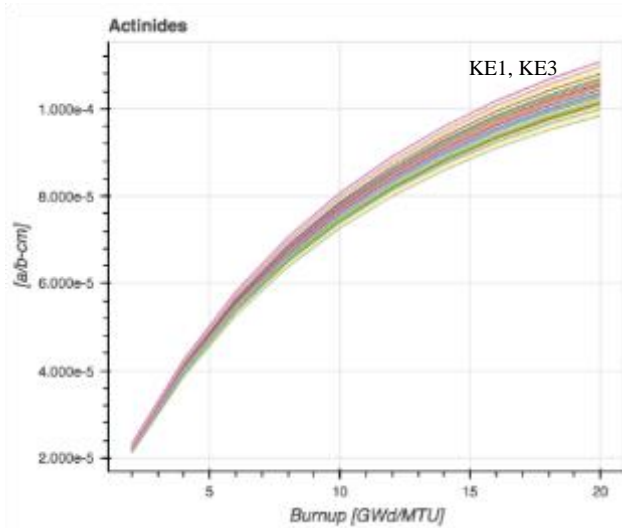


**Figure 4.56.  $^{239}\text{Pu}$  concentration at 40% void fraction after five-year decay**

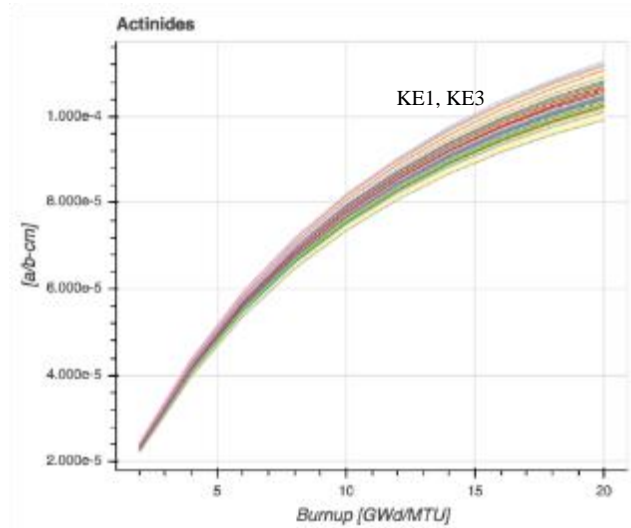


**Figure 4.57.  $^{239}\text{Pu}$  concentration at 0% void fraction in 15-20 GWd/MTU burnup interval**

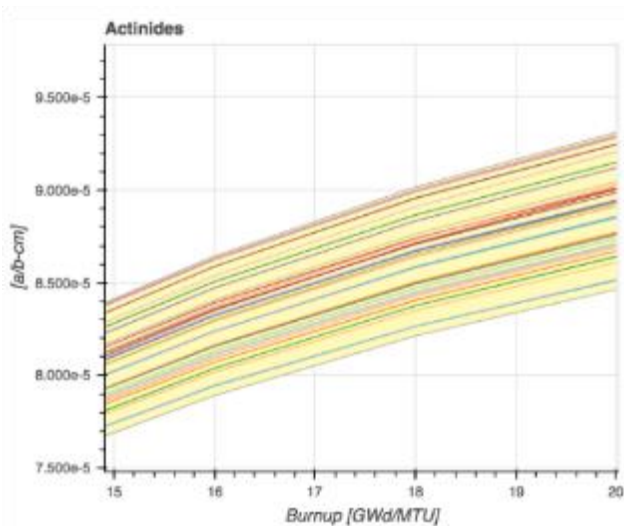


**Figure 4.58.  $^{239}\text{Pu}$  concentration at 70% void fraction in 17-20 GWd/MTU burnup interval**

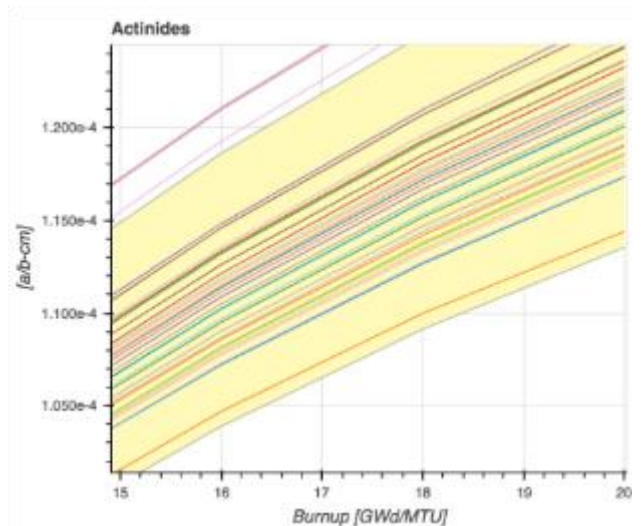


**Table 4.20. Statistics for <sup>239</sup>Pu concentration**

0-years <sup>1</sup>									
Burnup GWd/MTU	0% void fraction			40% void fraction			70% void fraction		
	Mean	2σ	2σ%	Mean	2σ	2σ%	Mean	2σ	2σ%
2	1.94E-05	6.80E-07	3.51	2.20E-05	8.64E-07	3.93	2.47E-05	1.26E-06	5.10
4	3.56E-05	1.29E-06	3.62	4.04E-05	1.64E-06	4.07	4.55E-05	2.40E-06	5.27
6	4.84E-05	1.82E-06	3.77	5.51E-05	2.34E-06	4.24	6.23E-05	3.42E-06	5.49
8	5.85E-05	2.31E-06	3.94	6.68E-05	2.96E-06	4.44	7.59E-05	4.35E-06	5.73
10	6.66E-05	2.75E-06	4.13	7.63E-05	3.55E-06	4.65	8.71E-05	5.20E-06	5.97
12	7.31E-05	3.13E-06	4.29	8.41E-05	4.06E-06	4.83	9.65E-05	5.96E-06	6.18
14	7.84E-05	3.48E-06	4.43	9.05E-05	4.51E-06	4.99	1.04E-04	6.62E-06	6.34
16	8.27E-05	3.77E-06	4.56	9.59E-05	4.92E-06	5.13	1.11E-04	7.26E-06	6.53
18	8.62E-05	4.02E-06	4.66	1.00E-04	5.26E-06	5.24	1.17E-04	7.86E-06	6.72
20	8.89E-05	4.24E-06	4.77	1.04E-04	5.62E-06	5.40	1.22E-04	8.40E-06	6.89
5-years <sup>2</sup>									
Burnup GWd/MTU	0% void fraction			40% void fraction			70% void fraction		
	Mean	2σ	2σ%	Mean	2σ	2σ%	Mean	2σ	2σ%
2	2.03E-05	7.20E-07	3.54	2.31E-05	9.19E-07	3.98	2.60E-05	1.34E-06	5.15
4	3.65E-05	1.33E-06	3.66	4.15E-05	1.70E-06	4.11	4.67E-05	2.48E-06	5.32
6	4.93E-05	1.88E-06	3.81	5.61E-05	2.40E-06	4.28	6.35E-05	3.51E-06	5.53
8	5.94E-05	2.37E-06	3.99	6.79E-05	3.04E-06	4.48	7.71E-05	4.45E-06	5.77
10	6.75E-05	2.82E-06	4.19	7.74E-05	3.63E-06	4.70	8.84E-05	5.31E-06	6.01
12	7.40E-05	3.22E-06	4.36	8.51E-05	4.16E-06	4.88	9.77E-05	6.05E-06	6.19
14	7.93E-05	3.55E-06	4.48	9.16E-05	4.60E-06	5.02	1.06E-04	6.77E-06	6.41
16	8.37E-05	3.85E-06	4.60	9.71E-05	5.05E-06	5.20	1.13E-04	7.37E-06	6.55
18	8.72E-05	4.10E-06	4.70	1.02E-04	5.34E-06	5.25	1.18E-04	7.93E-06	6.70
20	8.99E-05	4.32E-06	4.81	1.05E-04	5.71E-06	5.42	1.23E-04	8.50E-06	6.89

Note: <sup>1</sup>SC20 results are not included; <sup>2</sup>SC20 and SC1 results are not included.



**Table 4.21. Statistics for  $^{239}\text{Pu}$  concentration (KENOREST and SC2 removed)**

0-years									
Burnup GWd/MTU	0% void fraction			40% void fraction			70% void fraction		
	Mean	$2\sigma$	$2\sigma\%$	Mean	$2\sigma$	$2\sigma\%$	Mean	$2\sigma$	$2\sigma\%$
2	1.93E-05	5.75E-07	2.98	2.19E-05	6.24E-07	2.85	2.46E-05	7.57E-07	3.07
4	3.54E-05	1.09E-06	3.08	4.02E-05	1.19E-06	2.95	4.53E-05	1.41E-06	3.12
6	4.82E-05	1.56E-06	3.24	5.49E-05	1.70E-06	3.09	6.19E-05	1.99E-06	3.21
8	5.83E-05	2.01E-06	3.44	6.66E-05	2.17E-06	3.26	7.55E-05	2.53E-06	3.35
10	6.64E-05	2.42E-06	3.65	7.60E-05	2.63E-06	3.47	8.66E-05	3.04E-06	3.51
12	7.28E-05	2.78E-06	3.82	8.37E-05	3.05E-06	3.64	9.59E-05	3.50E-06	3.65
14	7.81E-05	3.10E-06	3.97	9.01E-05	3.41E-06	3.78	1.04E-04	3.90E-06	3.76
16	8.24E-05	3.37E-06	4.09	9.55E-05	3.72E-06	3.90	1.11E-04	4.37E-06	3.95
18	8.59E-05	3.59E-06	4.18	1.00E-04	3.98E-06	3.98	1.16E-04	4.75E-06	4.08
20	8.86E-05	3.78E-06	4.26	1.04E-04	4.23E-06	4.08	1.21E-04	5.03E-06	4.15

Note: KENOREST and SC2 results are not included.

#### 4.6.8. $^{240}\text{Pu}$

General trends in concentrations of  $^{240}\text{Pu}$  at discharge and after five-year decay are compared in Figures 4.59 and 4.60. Due to large bias in AL1 five-year decay results at 40% and 70% void fractions, AL1 results were eliminated from comparison. Concentrations in the range of 16-20 GWd/MTU interval are plotted in Figures 4.61 and 4.62 at 0% and 70% void fractions, respectively. The highest concentrations are predicted by KENOREST, SC14 (ENDF/B-VII.0 CE) and SCALE codes using ENDF/B-V libraries (SC4, SC5). The lowest concentrations are predicted by CA1, AL1 and HELIOS codes. SC14 results are outside the  $2\sigma$  band at all void fractions. Statistics for  $^{240}\text{Pu}$  concentrations are provided in Table 4.22. Standard deviation increases with burnup and void fraction. In general, relative standard deviation stays in the 4-5% range. A small increase in the standard deviation is observed after five-year decay.

**Figure 4.59.**  $^{240}\text{Pu}$  concentration at 40% void fraction at discharge

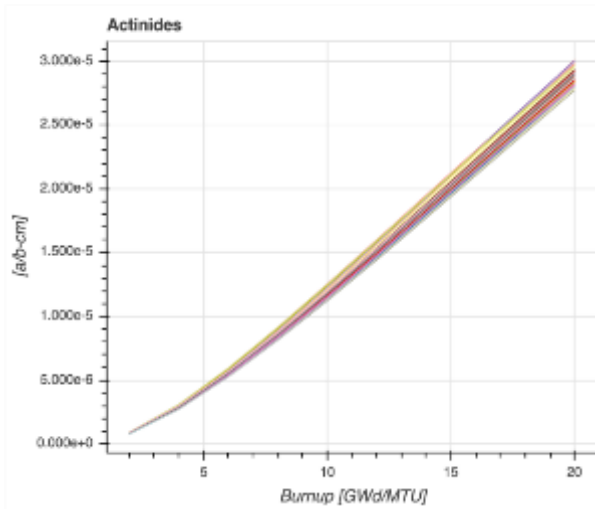


**Figure 4.60.**  $^{240}\text{Pu}$  concentration at 40% void fraction after five-year decay (AL1 results removed)

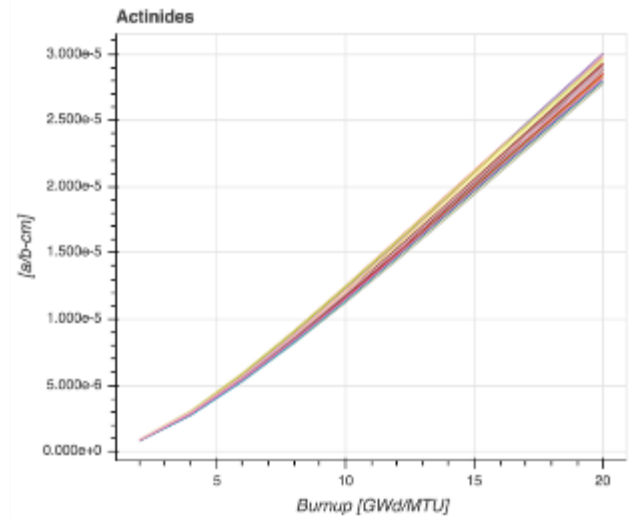


**Figure 4.61.**  $^{240}\text{Pu}$  concentration at 0% void fraction in 16-20  $\text{GWd/MTU}$  burnup interval

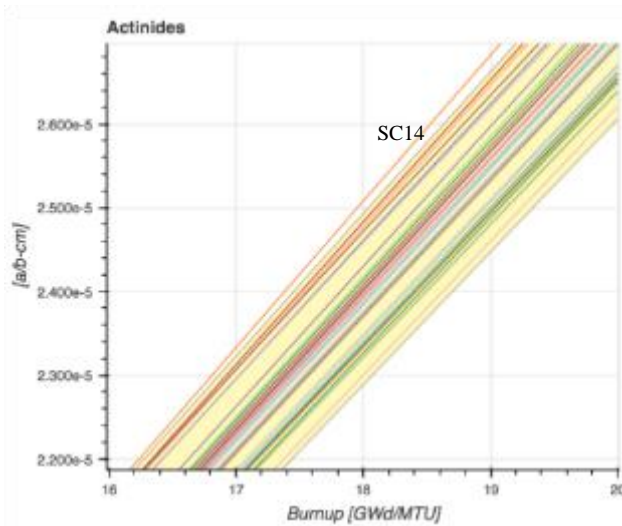


**Figure 4.62.**  $^{240}\text{Pu}$  concentration at 70% void fraction in 16-20  $\text{GWd/MTU}$  burnup interval

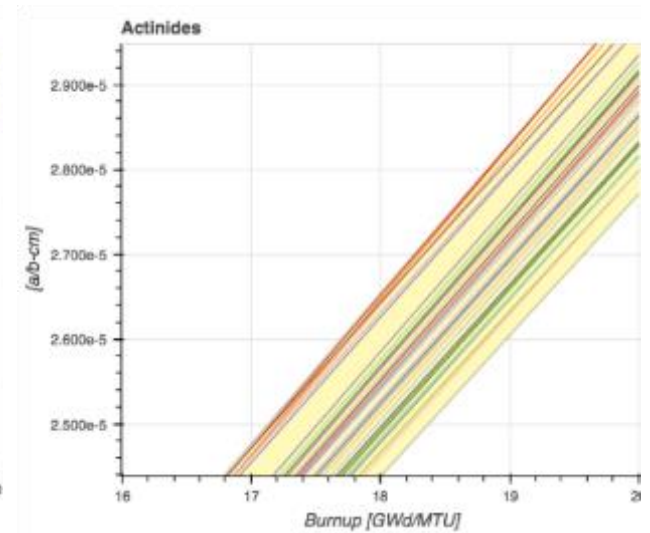


Table 4.22. Statistics for  $^{240}\text{Pu}$  concentration

0-years <sup>1</sup>									
Burnup GWd/MTU	0% void fraction			40% void fraction			70% void fraction		
	Mean	2 $\sigma$	2 $\sigma$ %	Mean	2 $\sigma$	2 $\sigma$ %	Mean	2 $\sigma$	2 $\sigma$ %
2	7.45E-07	4.20E-08	5.64	8.44E-07	5.33E-08	6.32	9.37E-07	7.18E-08	7.66
4	2.59E-06	1.32E-07	5.08	2.88E-06	1.62E-07	5.61	3.14E-06	2.12E-07	6.77
6	5.07E-06	2.51E-07	4.96	5.55E-06	3.00E-07	5.40	5.98E-06	3.82E-07	6.39
8	7.89E-06	3.82E-07	4.84	8.57E-06	4.47E-07	5.22	9.18E-06	5.56E-07	6.06
10	1.09E-05	5.18E-07	4.74	1.18E-05	5.93E-07	5.03	1.26E-05	7.22E-07	5.73
12	1.41E-05	6.51E-07	4.62	1.51E-05	7.32E-07	4.84	1.61E-05	8.70E-07	5.40
14	1.73E-05	7.78E-07	4.49	1.86E-05	8.57E-07	4.62	1.97E-05	9.96E-07	5.05
16	2.06E-05	8.97E-07	4.35	2.20E-05	9.68E-07	4.40	2.33E-05	1.11E-06	4.74
18	2.39E-05	1.01E-06	4.21	2.55E-05	1.07E-06	4.20	2.70E-05	1.20E-06	4.46
20	2.72E-05	1.11E-06	4.08	2.89E-05	1.17E-06	4.03	3.06E-05	1.29E-06	4.21
5-years <sup>2</sup>									
Burnup GWd/MTU	0% void fraction			40% void fraction			70% void fraction		
	Mean	2 $\sigma$	2 $\sigma$ %	Mean	2 $\sigma$	2 $\sigma$ %	Mean	2 $\sigma$	2 $\sigma$ %
2	7.45E-07	4.26E-08	5.72	8.44E-07	5.41E-08	6.41	9.37E-07	7.26E-08	7.74
4	2.59E-06	1.33E-07	5.14	2.88E-06	1.64E-07	5.68	3.14E-06	2.15E-07	6.84
6	5.06E-06	2.54E-07	5.01	5.55E-06	3.04E-07	5.47	5.98E-06	3.87E-07	6.46
8	7.89E-06	3.87E-07	4.91	8.57E-06	4.53E-07	5.29	9.18E-06	5.63E-07	6.13
10	1.09E-05	5.24E-07	4.80	1.18E-05	6.04E-07	5.12	1.26E-05	7.29E-07	5.79
12	1.41E-05	6.59E-07	4.68	1.51E-05	7.89E-07	5.22	1.61E-05	8.80E-07	5.46
14	1.73E-05	7.86E-07	4.54	1.85E-05	9.13E-07	4.93	1.97E-05	1.01E-06	5.11
16	2.06E-05	9.06E-07	4.40	2.20E-05	1.02E-06	4.66	2.33E-05	1.12E-06	4.80
18	2.39E-05	1.02E-06	4.26	2.54E-05	1.12E-06	4.42	2.70E-05	1.22E-06	4.52
20	2.72E-05	1.12E-06	4.13	2.89E-05	1.18E-06	4.09	3.06E-05	1.31E-06	4.28

Note: <sup>1</sup>SC20 results are not included; <sup>2</sup>SC20 and SC1 results are not included.

#### 4.6.9. $^{241}\text{Pu}$

General trends in concentrations of  $^{241}\text{Pu}$  at discharge and after five-year decay are compared in Figures 4.63 and 4.64. Concentrations in the range of 16-20 GWd/MTU interval are plotted in Figures 4.65 and 4.66 at 0% and 70% void fractions, respectively. All KENOREST, SC2 and HE2 results are separated with large biases from the rest of code results. While KENOREST codes predict the highest concentrations, SC2 and HE2 predict the lowest concentrations. All KENOREST results are above the 2 $\sigma$  band at all void fractions.

Statistics for  $^{241}\text{Pu}$  concentrations are provided in Table 4.23. Standard deviation increases with void fraction and burnup. Relative standard deviation is around the 4-9% range at all void fractions. KENOREST, SC2 and HE2 results increase standard deviation in the results by a factor of three to five. Statistics excluding KENOREST, SC2 and HE2 results are also

provided in Table 2.24. Relative standard deviation is reduced to 3% around peak reactivity and 2% at the end of depletion.

**Figure 4.63.**  $^{241}\text{Pu}$  concentration at 40% void fraction at discharge

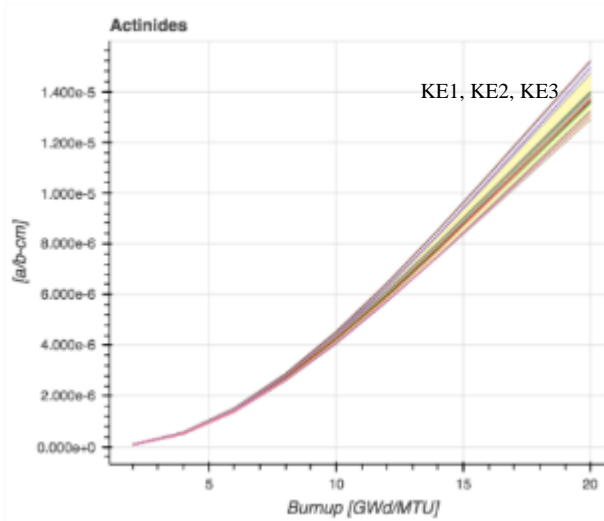


**Figure 4.64.**  $^{241}\text{Pu}$  concentration at 40% void fraction after five-year decay

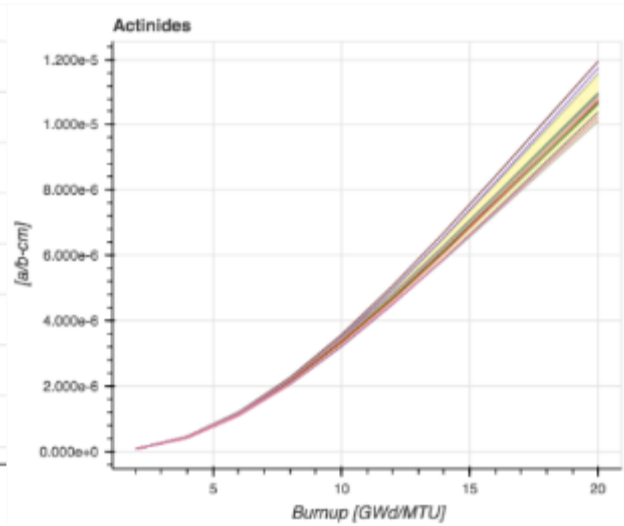


**Figure 4.65.**  $^{241}\text{Pu}$  concentration at 0% void fraction in 16-20 GWd/MTU burnup interval

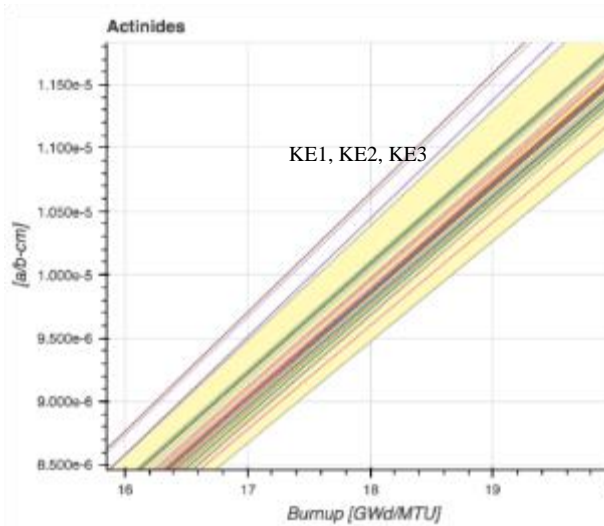


**Figure 4.66.**  $^{241}\text{Pu}$  concentration at 70% void fraction in 16-20 GWd/MTU burnup interval

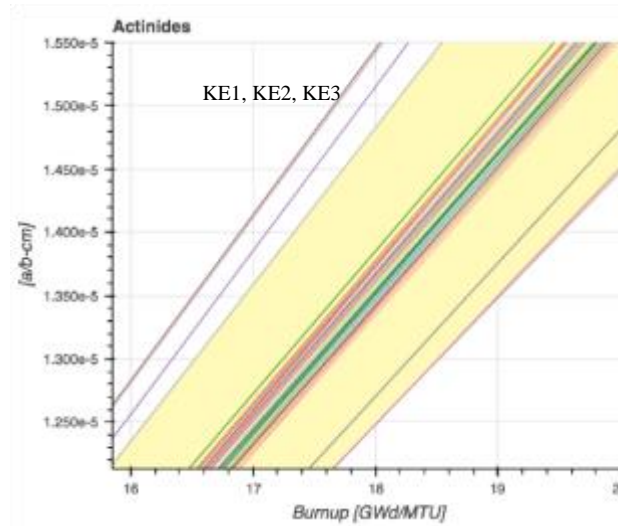


**Table 4.23. Statistics for <sup>241</sup>Pu concentration**

0-years <sup>1</sup>									
Burnup GWd/MTU	0% void fraction			40% void fraction			70% void fraction		
	Mean	2σ	2σ%	Mean	2σ	2σ%	Mean	2σ	2σ%
2	6.47E-08	5.00E-09	7.73	8.57E-08	7.27E-09	8.48	1.09E-07	1.05E-08	9.63
4	4.30E-07	2.36E-08	5.48	5.54E-07	3.26E-08	5.89	6.88E-07	4.78E-08	6.95
6	1.17E-06	4.98E-08	4.27	1.47E-06	6.97E-08	4.73	1.79E-06	1.09E-07	6.09
8	2.22E-06	8.06E-08	3.64	2.76E-06	1.19E-07	4.32	3.30E-06	2.00E-07	6.05
10	3.50E-06	1.23E-07	3.52	4.30E-06	1.93E-07	4.48	5.10E-06	3.31E-07	6.48
12	4.96E-06	1.88E-07	3.78	6.03E-06	2.97E-07	4.92	7.09E-06	5.02E-07	7.09
14	6.55E-06	2.70E-07	4.12	7.89E-06	4.24E-07	5.38	9.21E-06	7.05E-07	7.66
16	8.22E-06	3.66E-07	4.45	9.84E-06	5.71E-07	5.81	1.14E-05	9.30E-07	8.15
18	9.93E-06	4.74E-07	4.77	1.18E-05	7.30E-07	6.18	1.37E-05	1.16E-06	8.53
20	1.16E-05	5.88E-07	5.05	1.38E-05	8.98E-07	6.50	1.59E-05	1.41E-06	8.87

**Table 4.23. Statistics for <sup>241</sup>Pu concentration (continued)**

5-years <sup>2</sup>									
Burnup GWd/MTU	0% void fraction			40% void fraction			70% void fraction		
	Mean	2σ	2σ%	Mean	2σ	2σ%	Mean	2σ	2σ%
2	5.08E-08	3.95E-09	7.77	6.73E-08	5.75E-09	8.55	8.58E-08	8.35E-09	9.73
4	3.38E-07	1.83E-08	5.43	4.35E-07	2.59E-08	5.95	5.40E-07	3.78E-08	7.00
6	9.16E-07	3.84E-08	4.19	1.16E-06	5.44E-08	4.71	1.41E-06	8.58E-08	6.10
8	1.74E-06	6.23E-08	3.58	2.16E-06	9.54E-08	4.41	2.59E-06	1.60E-07	6.15
10	2.75E-06	9.68E-08	3.52	3.38E-06	1.53E-07	4.54	4.00E-06	2.64E-07	6.59
12	3.89E-06	1.49E-07	3.81	4.73E-06	2.59E-07	5.49	5.56E-06	4.01E-07	7.21
14	5.14E-06	2.15E-07	4.18	6.19E-06	3.60E-07	5.82	7.23E-06	5.63E-07	7.79
16	6.46E-06	2.93E-07	4.54	7.72E-06	4.76E-07	6.17	8.96E-06	7.41E-07	8.27
18	7.80E-06	3.79E-07	4.87	9.27E-06	6.01E-07	6.48	1.07E-05	9.31E-07	8.68
20	9.14E-06	4.71E-07	5.16	1.08E-05	7.18E-07	6.63	1.25E-05	1.13E-06	9.01

Note: <sup>1</sup>SC20 results are not included; <sup>2</sup>SC20 and SC1 results are not included.

**Table 4.24. Statistics for  $^{241}\text{Pu}$  concentration (KENOREST, SC2, HE2 results removed)**

0-years									
Burnup Gwd/MTU	0% void fraction			40% void fraction			70% void fraction		
	Mean	$2\sigma$	$2\sigma\%$	Mean	$2\sigma$	$2\sigma\%$	Mean	$2\sigma$	$2\sigma\%$
2	6.51E-08	4.67E-09	7.17	8.63E-08	6.63E-09	7.68	1.10E-07	9.41E-09	8.54
4	4.32E-07	2.20E-08	5.10	5.56E-07	2.91E-08	5.23	6.90E-07	3.96E-08	5.74
6	1.17E-06	4.67E-08	3.99	1.48E-06	5.89E-08	3.99	1.79E-06	7.85E-08	4.38
8	2.22E-06	7.37E-08	3.32	2.76E-06	8.88E-08	3.22	3.30E-06	1.16E-07	3.52
10	3.50E-06	1.02E-07	2.93	4.29E-06	1.19E-07	2.78	5.09E-06	1.52E-07	2.99
12	4.95E-06	1.37E-07	2.77	6.01E-06	1.51E-07	2.51	7.06E-06	1.86E-07	2.64
14	6.53E-06	1.75E-07	2.68	7.86E-06	1.86E-07	2.36	9.16E-06	2.28E-07	2.48
16	8.19E-06	2.16E-07	2.63	9.79E-06	2.25E-07	2.30	1.13E-05	2.74E-07	2.42
18	9.89E-06	2.61E-07	2.64	1.18E-05	2.71E-07	2.31	1.36E-05	3.18E-07	2.34
20	1.16E-05	3.08E-07	2.66	1.37E-05	3.21E-07	2.34	1.58E-05	3.72E-07	2.36

Note: SC20, KENOREST, SC2 and HE2 results are not included.

#### 4.6.10. $^{242}\text{Pu}$

General trends in concentrations of  $^{242}\text{Pu}$  at discharge and after five-year decay are compared in Figures 4.67 and 4.68. AL1 five-year decay results at 40% have erroneous data at 8 Gwd/MTU and are therefore not included in comparisons at 8 Gwd/MTU. Concentrations in the range of 18-20 Gwd/MTU interval are plotted in Figures 4.69 and 4.70 at 0% and 70% void fractions, respectively. The highest concentrations are observed in KE1 and KE3 results at all void fractions. KE3 results are placed outside the  $2\sigma$  band at 70% void fraction. HE1 and HE2 codes predict the lowest concentrations. H1 and HE2 results also lay outside the  $2\sigma$  band at all void fractions.

Statistics for  $^{242}\text{Pu}$  concentrations are provided in Table 4.25. Standard deviation increases with void fraction and burnup. Relative standard deviation is around 10-12% and shows negligible increase with five-year decay.

**Figure 4.67.**  $^{242}\text{Pu}$  concentration at 40% void fraction at discharge

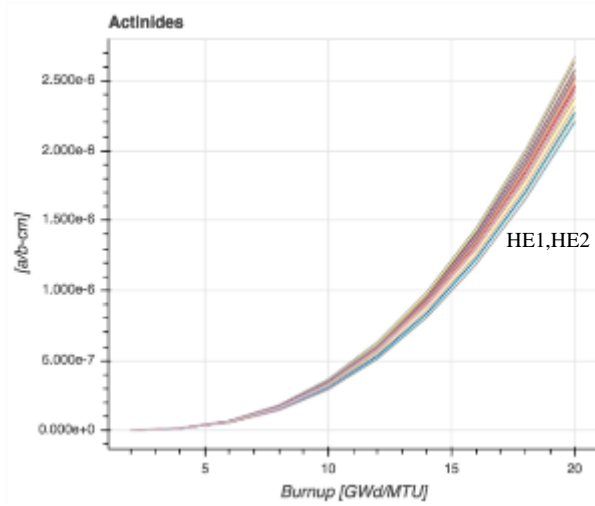


**Figure 4.68.**  $^{242}\text{Pu}$  concentration at 40% void fraction after five-year decay

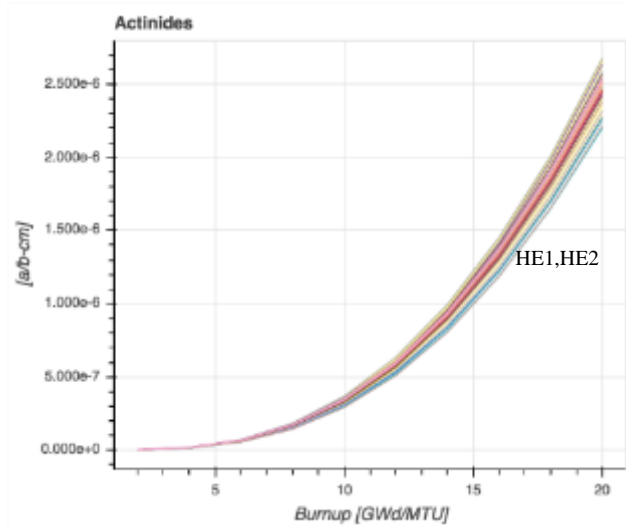


**Figure 4.69.**  $^{242}\text{Pu}$  concentration at 0% void fraction in 18-20 GWd/MTU burnup interval

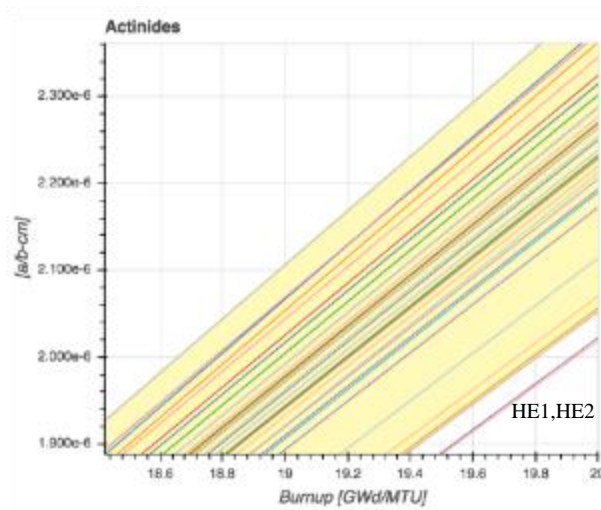


**Figure 4.70.**  $^{242}\text{Pu}$  concentration at 70% void fraction in 18-20 GWd/MTU burnup interval

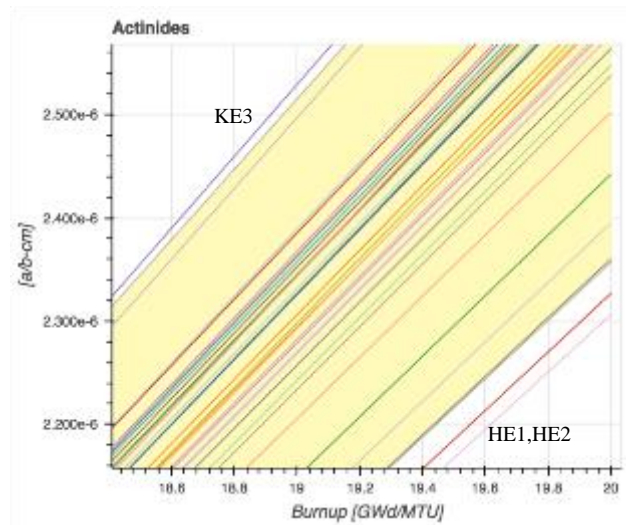


**Table 4.25. Statistics for <sup>242</sup>Pu concentration**

0-years <sup>1</sup>									
Burnup GWd/MTU	0% void fraction			40% void fraction			70% void fraction		
	Mean	2σ	2σ%	Mean	2σ	2σ%	Mean	2σ	2σ%
2	9.51E-10	9.06E-10	95.31	1.22E-09	9.10E-10	74.48	1.51E-09	9.17E-10	60.59
4	1.23E-08	1.73E-09	14.11	1.56E-08	2.12E-09	13.61	1.89E-08	2.62E-09	13.85
6	5.20E-08	5.38E-09	10.36	6.42E-08	6.88E-09	10.71	7.60E-08	8.69E-09	11.44
8	1.37E-07	1.28E-08	9.34	1.66E-07	1.61E-08	9.70	1.92E-07	2.01E-08	10.47
10	2.81E-07	2.45E-08	8.70	3.35E-07	3.04E-08	9.10	3.81E-07	3.81E-08	10.02
12	4.96E-07	4.15E-08	8.38	5.80E-07	5.11E-08	8.81	6.49E-07	6.34E-08	9.76
14	7.91E-07	6.44E-08	8.15	9.10E-07	7.85E-08	8.63	1.00E-06	9.67E-08	9.63
16	1.17E-06	9.33E-08	7.94	1.33E-06	1.13E-07	8.47	1.45E-06	1.38E-07	9.52
18	1.65E-06	1.30E-07	7.89	1.85E-06	1.55E-07	8.38	1.98E-06	1.88E-07	9.49
20	2.23E-06	1.74E-07	7.79	2.46E-06	2.04E-07	8.31	2.61E-06	2.46E-07	9.42

**Table 4.25. Statistics for <sup>242</sup>Pu concentration (continued)**

5-years <sup>2</sup>									
Burnup GWd/MTU	0% void fraction			40% void fraction			70% void fraction		
	Mean	2σ	2σ%	Mean	2σ	2σ%	Mean	2σ	2σ%
2	9.53E-10	9.19E-10	96.40	1.22E-09	9.23E-10	75.37	1.52E-09	9.30E-10	61.32
4	1.23E-08	1.75E-09	14.26	1.56E-08	2.15E-09	13.79	1.89E-08	2.65E-09	14.02
6	5.20E-08	5.44E-09	10.46	6.43E-08	6.98E-09	10.86	7.60E-08	8.80E-09	11.58
8	1.37E-07	1.29E-08	9.44	1.66E-07	1.63E-08	9.83	1.92E-07	2.04E-08	10.61
10	2.81E-07	2.47E-08	8.78	3.35E-07	3.09E-08	9.23	3.81E-07	3.87E-08	10.15
12	4.96E-07	4.19E-08	8.46	5.79E-07	5.49E-08	9.48	6.50E-07	6.42E-08	9.89
14	7.91E-07	6.51E-08	8.23	9.09E-07	8.34E-08	9.18	1.00E-06	9.80E-08	9.76
16	1.17E-06	9.43E-08	8.03	1.33E-06	1.19E-07	8.93	1.45E-06	1.40E-07	9.64
18	1.65E-06	1.32E-07	7.98	1.85E-06	1.62E-07	8.77	1.98E-06	1.91E-07	9.61
20	2.23E-06	1.76E-07	7.88	2.46E-06	2.07E-07	8.42	2.61E-06	2.49E-07	9.54

Note: <sup>1</sup>SC20 results are not included; <sup>2</sup>SC20 and SC1 results are not included.



#### 4.6.11. $^{241}\text{Am}$

General trends in concentrations of  $^{241}\text{Am}$  at discharge and after five-year decay are compared in Figures 4.71 and 4.72. Concentrations in the range of 18-20 GWd/MTU interval are plotted in Figures 4.73 and 4.74 at 0% and 70% void fractions, respectively. While all KENOEST codes predict the highest concentrations, VE2(JEFF3.2), VE1(JEFF3.1.1) and AL1(JEFF3.3) predict the lowest concentrations of  $^{241}\text{Am}$ . After five-year decay, the highest concentrations are still observed in KENOEST results, and the lowest concentrations are predicted by HE2 and SC2 results.

KENOEST, HE2 and SC2 results increase standard deviation significantly in five-year decay results. Statistics for  $^{241}\text{Am}$  concentrations are provided in Table 4.26. Standard deviation increases with burnup and void fraction. Standard deviation at 70% void fraction is twice as large as standard deviation at 0% void fraction.

If KENOEST, HE2 and SC2 results are removed, standard deviation in five-year decay results (Table 4.27) decreases by 50% at 70% void fraction around peak reactivity. The relative standard deviation is below 3% after peak reactivity at all void fractions.

**Figure 4.71.  $^{241}\text{Am}$  concentration at 40% void fraction**

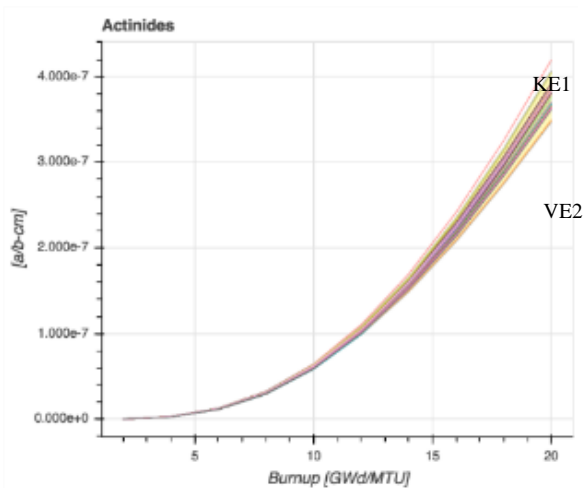


**Figure 4.72.  $^{241}\text{Am}$  concentration at 40% void fraction after five-year decay**

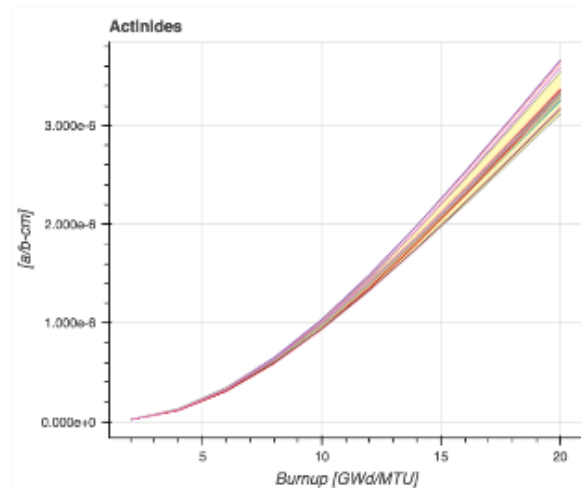


**Figure 4.73.  $^{241}\text{Am}$  concentration at 0% void fraction in 18-20 GWd/MTU burnup interval**

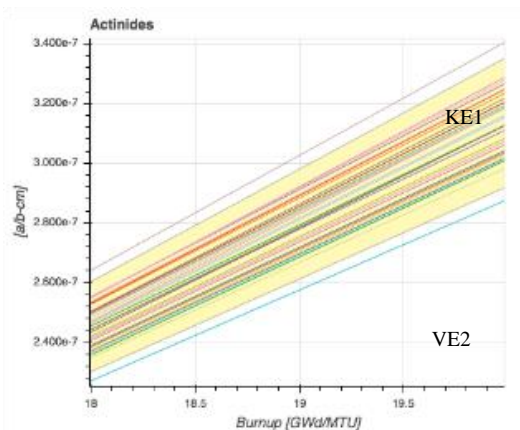


**Figure 4.74.  $^{241}\text{Am}$  concentration at 70% void fraction in 18-20 GWd/MTU burnup interval**

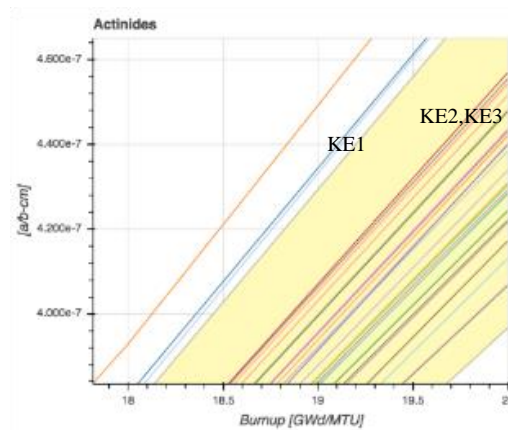


Table 4.26. Statistics for <sup>241</sup>Am concentration

0-years <sup>1</sup>									
Burnup GWd/MTU	0% void fraction			40% void fraction			70% void fraction		
	Mean	2σ	2σ%	Mean	2σ	2σ%	Mean	2σ	2σ%
2	1.70E-10	1.72E-11	10.16	2.25E-10	2.34E-11	10.39	2.89E-10	3.26E-11	11.29
4	2.32E-09	1.42E-10	6.14	3.01E-09	2.00E-10	6.66	3.76E-09	2.87E-10	7.62
6	9.64E-09	4.58E-10	4.75	1.23E-08	6.22E-10	5.06	1.51E-08	9.34E-10	6.20
8	2.49E-08	1.01E-09	4.04	3.12E-08	1.39E-09	4.46	3.77E-08	2.18E-09	5.76
10	4.96E-08	1.93E-09	3.90	6.15E-08	2.72E-09	4.42	7.36E-08	4.39E-09	5.97
12	8.43E-08	3.50E-09	4.15	1.04E-07	4.96E-09	4.78	1.23E-07	8.03E-09	6.53
14	1.29E-07	6.07E-09	4.70	1.57E-07	8.56E-09	5.44	1.85E-07	1.34E-08	7.24
16	1.83E-07	9.85E-09	5.38	2.22E-07	1.37E-08	6.17	2.60E-07	2.08E-08	8.00
18	2.45E-07	1.50E-08	6.09	2.96E-07	2.04E-08	6.91	3.46E-07	3.03E-08	8.77
20	3.14E-07	2.15E-08	6.85	3.77E-07	2.90E-08	7.68	4.40E-07	4.19E-08	9.52
5-years <sup>2</sup>									
Burnup GWd/MTU	0% void fraction			40% void fraction			70% void fraction		
	Mean	2σ	2σ%	Mean	2σ	2σ%	Mean	2σ	2σ%
2	1.40E-08	1.12E-09	7.97	1.86E-08	1.63E-09	8.77	2.37E-08	2.35E-09	9.93
4	9.44E-08	5.32E-09	5.63	1.22E-07	7.41E-09	6.09	1.51E-07	1.08E-08	7.14
6	2.59E-07	1.11E-08	4.28	3.28E-07	1.60E-08	4.88	3.99E-07	2.47E-08	6.19
8	5.00E-07	1.80E-08	3.61	6.21E-07	2.67E-08	4.30	7.45E-07	4.53E-08	6.08
10	7.99E-07	2.75E-08	3.44	9.82E-07	4.36E-08	4.44	1.17E-06	7.49E-08	6.43
12	1.15E-06	4.17E-08	3.64	1.39E-06	7.46E-08	5.36	1.64E-06	1.15E-07	6.99
14	1.53E-06	6.07E-08	3.97	1.84E-06	1.04E-07	5.63	2.16E-06	1.63E-07	7.55
16	1.94E-06	8.37E-08	4.31	2.32E-06	1.39E-07	5.98	2.70E-06	2.17E-07	8.02
18	2.37E-06	1.10E-07	4.66	2.82E-06	1.77E-07	6.28	3.27E-06	2.76E-07	8.44
20	2.80E-06	1.39E-07	4.97	3.33E-06	2.13E-07	6.41	3.84E-06	3.38E-07	8.80

Note: <sup>1</sup>SC20 results are not included; <sup>2</sup>SC20 and SC1 results are not included.

**Table 4.27. Statistics for <sup>241</sup>Am concentration (KENOREST, HE2, SC2 results removed)**

5-years									
Burnup GWd/MTU	0% void fraction			40% void fraction			70% void fraction		
	Mean	2σ	2σ%	Mean	2σ	2σ%	Mean	2σ	2σ%
2	1.41E-08	1.04E-09	7.34	1.87E-08	1.48E-09	7.91	2.39E-08	2.10E-09	8.80
4	9.48E-08	4.91E-09	5.17	1.22E-07	6.58E-09	5.39	1.52E-07	8.99E-09	5.93
6	2.60E-07	1.02E-08	3.93	3.28E-07	1.37E-08	4.16	3.99E-07	1.81E-08	4.53
8	5.00E-07	1.64E-08	3.28	6.21E-07	2.01E-08	3.24	7.45E-07	2.73E-08	3.66
10	7.99E-07	2.33E-08	2.91	9.81E-07	2.81E-08	2.87	1.16E-06	3.62E-08	3.11
12	1.14E-06	3.13E-08	2.74	1.39E-06	4.97E-08	3.58	1.63E-06	4.48E-08	2.74
14	1.53E-06	4.09E-08	2.68	1.84E-06	5.93E-08	3.23	2.15E-06	5.60E-08	2.61
16	1.94E-06	5.20E-08	2.68	2.31E-06	7.09E-08	3.07	2.69E-06	6.78E-08	2.52
18	2.36E-06	6.49E-08	2.75	2.81E-06	8.37E-08	2.98	3.25E-06	8.25E-08	2.54
20	2.79E-06	7.93E-08	2.84	3.31E-06	8.43E-08	2.55	3.81E-06	9.91E-08	2.60

Note: SC20, SC1, SC2, HE2 and KENOREST results are not included.

#### 4.7. Fission product distribution in UO<sub>2</sub> rods

Average fission product concentrations are compared in Figures 4.75 to 4.110. Results from three participants include repeated erroneous or missing data at certain burnup values and void fractions. Erroneous data were identified based on the sudden increase or reduction in smoothly varying data and more than 4σ bias with respect to other code results. The sources of the errors were tracked to misplaced or intermittently overwritten data, or likely errors in material compositions.

The following data points were ignored in the comparison of concentrations:

- SC1: five-year decay for nuclides at 16, 18, 20 GWd/MTU at 40% void fraction;
- SC1: five-year decay for all nuclides 2, 4, 6, 8, 10, 12, 14, 16, 18 at 0% and 70% void fractions;
- SC1: <sup>103</sup>Rh and <sup>131</sup>Xe at 70% void fraction (two series seem to be exchanged);
- SC1: missing <sup>147</sup>Sm, <sup>152</sup>Sm, <sup>155</sup>Eu;
- SC1: 20% higher concentrations of <sup>99</sup>Tc at 70% void fractions.

Figures 4.75 to 4.110 compare fission product concentrations. Only 40% void fraction results are plotted, unless a significant trend with void fraction was observed. Statistics for all fission products are listed in Tables 4.28 to 4.39.

##### 4.7.1. <sup>99</sup>Tc

<sup>99</sup>Tc concentration increases linearly with burnup at all void fractions (Figures 4.75 to 4.78). Relative variation in the results is around 2.5% across all burnups and void fractions. SC1 and SW1 predict the highest concentrations, and HELIOS and SERPENT codes predict the lowest concentrations (Figures 4.77 and 4.78). As void fraction increases, biases in SC1 and SW1 results with respect to other codes also increase (Figure 4.78). Statistics for <sup>99</sup>Tc concentrations are provided in Table 4.28.

**Figure 4.75. <sup>99</sup>Tc concentration at 40% void fraction at discharge**

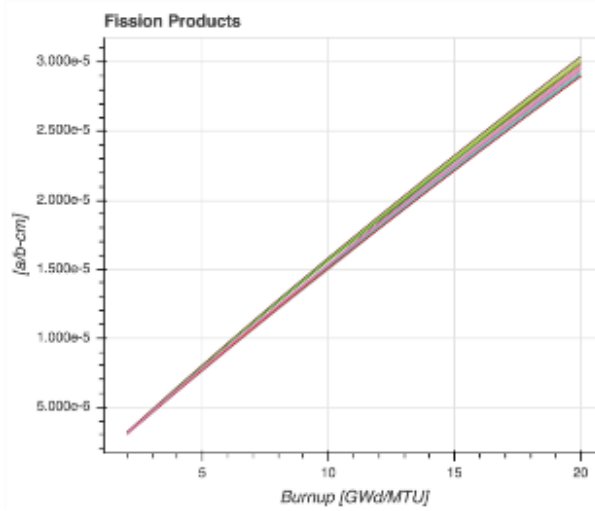


**Figure 4.76. <sup>99</sup>Tc concentration at 40% void fraction after five-year decay**

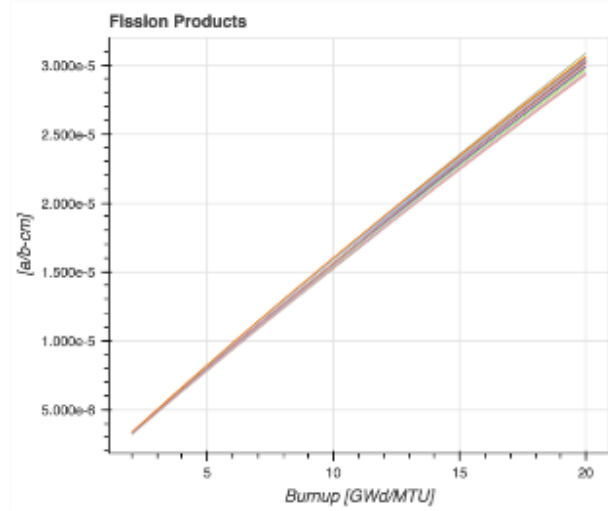


**Figure 4.77. <sup>99</sup>Tc concentration at 0% void fraction in 17.5-20 GWd/MTU interval**

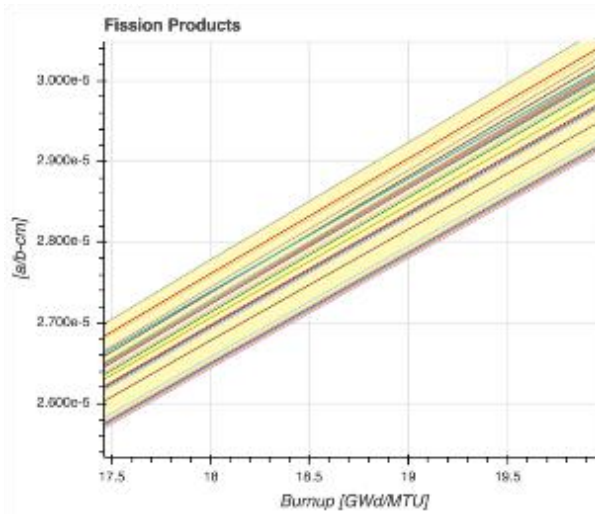


**Figure 4.78. <sup>99</sup>Tc concentration at 70% void fraction in 17.5-20 GWd/MTU interval (SC1 results removed)**

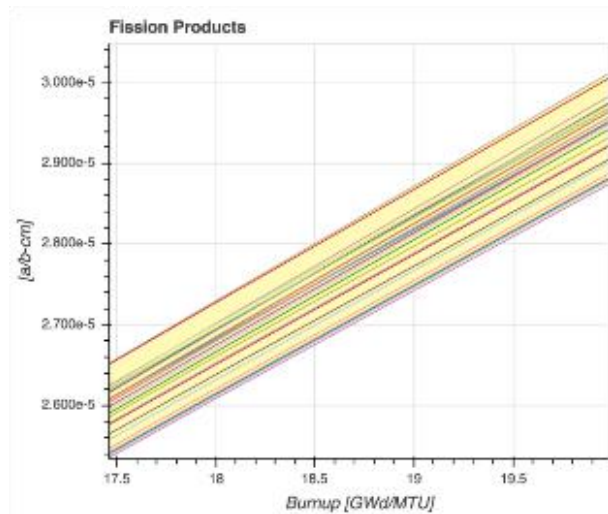


Table 4.28. Statistics for  $^{99}\text{Tc}$  concentration

0-years <sup>1</sup>									
Burnup GWd/MTU	0% void fraction			40% void fraction			70% void fraction <sup>2</sup>		
	Mean	2 $\sigma$	2 $\sigma$ %	Mean	2 $\sigma$	2 $\sigma$ %	Mean	2 $\sigma$	2 $\sigma$ %
2	3.10E-06	7.91E-08	2.55	3.08E-06	7.95E-08	2.58	3.06E-06	7.85E-08	2.57
4	6.30E-06	1.61E-07	2.55	6.26E-06	1.60E-07	2.56	6.21E-06	1.58E-07	2.54
6	9.43E-06	2.40E-07	2.54	9.36E-06	2.38E-07	2.54	9.30E-06	2.34E-07	2.52
8	1.25E-05	3.13E-07	2.51	1.24E-05	3.14E-07	2.53	1.23E-05	3.07E-07	2.49
10	1.55E-05	3.90E-07	2.52	1.54E-05	3.87E-07	2.52	1.53E-05	3.77E-07	2.47
12	1.84E-05	4.43E-07	2.40	1.83E-05	4.33E-07	2.36	1.82E-05	4.23E-07	2.33
14	2.14E-05	5.18E-07	2.43	2.12E-05	5.01E-07	2.36	2.11E-05	4.81E-07	2.28
16	2.43E-05	6.00E-07	2.47	2.41E-05	5.83E-07	2.42	2.39E-05	5.46E-07	2.28
18	2.71E-05	6.81E-07	2.51	2.69E-05	6.56E-07	2.44	2.67E-05	6.23E-07	2.33
20	2.99E-05	7.69E-07	2.57	2.97E-05	7.42E-07	2.50	2.95E-05	7.01E-07	2.38
5-years <sup>2</sup>									
Burnup GWd/MTU	0% void fraction			40% void fraction			70% void fraction		
	Mean	2 $\sigma$	2 $\sigma$ %	Mean	2 $\sigma$	2 $\sigma$ %	Mean	2 $\sigma$	2 $\sigma$ %
2	3.06E-06	7.85E-08	2.57	3.25E-06	7.87E-08	2.42	3.23E-06	7.76E-08	2.40
4	6.21E-06	1.58E-07	2.54	6.42E-06	1.54E-07	2.39	6.38E-06	1.51E-07	2.36
6	9.30E-06	2.34E-07	2.52	9.52E-06	2.25E-07	2.36	9.45E-06	2.21E-07	2.33
8	1.23E-05	3.07E-07	2.49	1.25E-05	2.98E-07	2.38	1.25E-05	2.86E-07	2.29
10	1.53E-05	3.77E-07	2.47	1.55E-05	3.57E-07	2.30	1.54E-05	3.49E-07	2.26
12	1.82E-05	4.23E-07	2.33	1.84E-05	4.28E-07	2.32	1.83E-05	3.92E-07	2.14
14	2.11E-05	4.81E-07	2.28	2.13E-05	4.95E-07	2.32	2.12E-05	4.49E-07	2.12
16	2.39E-05	5.46E-07	2.28	2.42E-05	5.67E-07	2.34	2.40E-05	5.24E-07	2.18
18	2.67E-05	6.23E-07	2.33	2.70E-05	6.54E-07	2.42	2.68E-05	6.05E-07	2.25
20	2.95E-05	7.01E-07	2.38	2.98E-05	7.22E-07	2.42	2.96E-05	6.85E-07	2.31

Note: <sup>1</sup>SC20 results are not included; <sup>2</sup>SC20 and SC1 results are not included.

#### 4.7.2. $^{103}\text{Rh}$

Similarly to  $^{99}\text{Tc}$ ,  $^{103}\text{Rh}$  concentrations increase linearly with lattice burnup (Figure 4.79 and 4.80). As  $^{103}\text{Rh}$  concentration increases with increasing void fraction and decay time, the trend with burnup does not change. Detailed comparisons of  $^{103}\text{Rh}$  concentrations are shown in Figure 4.81 and 4.82 at 0% and 70% void fractions. CA1 results have the lowest concentrations and are located below the 2 $\sigma$  band. The lowest concentrations are predicted by SC15, KE1 and KE3, in general.

Statistics for  $^{103}\text{Rh}$  concentrations are provided in Table 4.29. Relative standard deviation is around 2% and shows small variations with burnup and void fraction.

**Figure 4.79.**  $^{103}\text{Rh}$  concentration at 40% void fraction at discharge

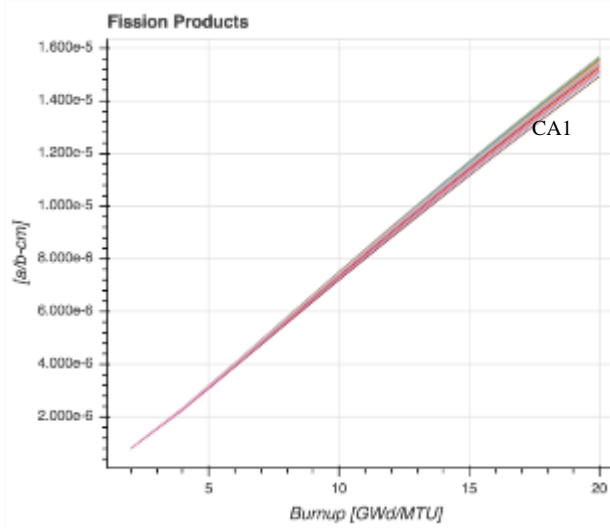


**Figure 4.80.**  $^{103}\text{Rh}$  concentration at 40% void fraction after five-year decay

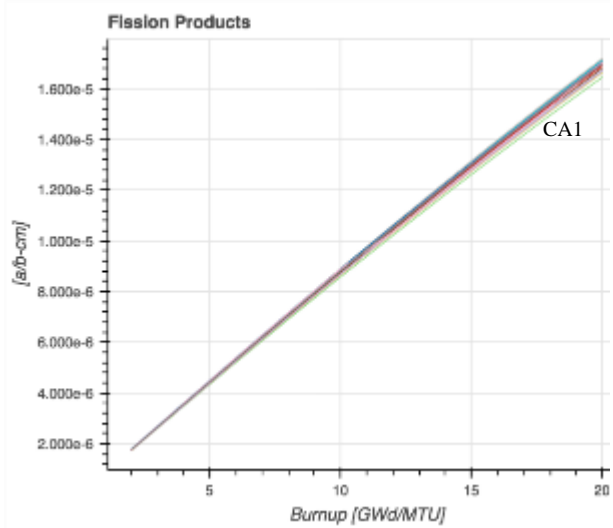


**Figure 4.81.**  $^{103}\text{Rh}$  concentration at 0% void fraction in 16.5-20 GWd/MTU interval

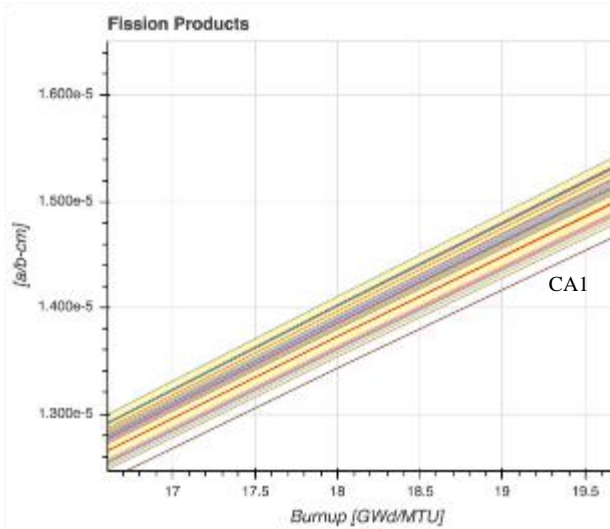


**Figure 4.82.**  $^{103}\text{Rh}$  concentration at 70% void fraction in 16.5-20 GWd/MTU interval

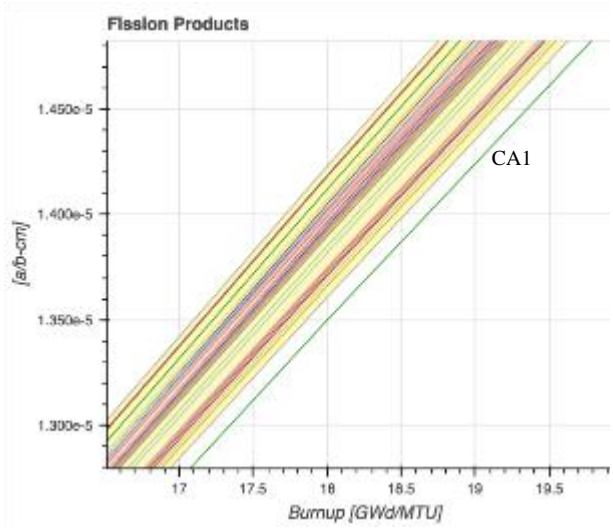


**Table 4.29. Statistics for  $^{103}\text{Rh}$  concentration**

0-years <sup>1</sup>									
Burnup GWd/MTU	0% void fraction			40% void fraction			70% void fraction <sup>2</sup>		
	Mean	2 $\sigma$	2 $\sigma$ %	Mean	2 $\sigma$	2 $\sigma$ %	Mean	2 $\sigma$	2 $\sigma$ %
2	7.98E-07	1.22E-08	1.53	8.01E-07	1.19E-08	1.48	8.05E-07	1.19E-08	1.48
4	2.30E-06	3.70E-08	1.61	2.31E-06	3.65E-08	1.58	2.32E-06	3.73E-08	1.61
6	3.96E-06	6.68E-08	1.68	3.99E-06	6.66E-08	1.67	4.01E-06	6.78E-08	1.69
8	5.65E-06	9.90E-08	1.75	5.69E-06	9.89E-08	1.74	5.73E-06	1.03E-07	1.79
10	7.32E-06	1.32E-07	1.80	7.38E-06	1.34E-07	1.81	7.43E-06	1.40E-07	1.89
12	8.96E-06	1.68E-07	1.87	9.04E-06	1.70E-07	1.88	9.10E-06	1.80E-07	1.98
14	1.06E-05	2.05E-07	1.94	1.07E-05	2.08E-07	1.95	1.07E-05	2.20E-07	2.05
16	1.22E-05	2.37E-07	1.95	1.23E-05	2.44E-07	1.99	1.23E-05	2.60E-07	2.11
18	1.37E-05	2.75E-07	2.01	1.38E-05	2.85E-07	2.06	1.39E-05	3.06E-07	2.20
20	1.52E-05	3.10E-07	2.04	1.54E-05	3.24E-07	2.11	1.55E-05	3.50E-07	2.27
5-years <sup>2</sup>									
Burnup GWd/MTU	0% void fraction			40% void fraction			70% void fraction		
	Mean	2 $\sigma$	2 $\sigma$ %	Mean	2 $\sigma$	2 $\sigma$ %	Mean	2 $\sigma$	2 $\sigma$ %
2	1.75E-06	2.75E-08	1.58	1.86E-08	1.63E-09	8.77	1.77E-06	2.63E-08	1.49
4	3.52E-06	5.69E-08	1.62	1.22E-07	7.41E-09	6.09	3.57E-06	5.66E-08	1.58
6	5.28E-06	8.78E-08	1.66	3.28E-07	1.60E-08	4.88	5.37E-06	9.02E-08	1.68
8	7.01E-06	1.22E-07	1.73	6.21E-07	2.67E-08	4.30	7.15E-06	1.26E-07	1.77
10	8.71E-06	1.56E-07	1.79	9.82E-07	4.36E-08	4.44	8.89E-06	1.65E-07	1.86
12	1.04E-05	1.96E-07	1.88	1.39E-06	7.46E-08	5.36	1.06E-05	2.10E-07	1.98
14	1.20E-05	2.24E-07	1.86	1.84E-06	1.04E-07	5.63	1.23E-05	2.48E-07	2.02
16	1.36E-05	2.69E-07	1.97	2.32E-06	1.39E-07	5.98	1.39E-05	2.90E-07	2.09
18	1.52E-05	2.99E-07	1.97	2.82E-06	1.77E-07	6.28	1.55E-05	3.31E-07	2.13
20	1.68E-05	3.36E-07	2.00	3.33E-06	2.13E-07	6.41	1.71E-05	3.78E-07	2.21

Note: <sup>1</sup>SC20 results are not included; <sup>2</sup>SC20 and SC1 results are not included.

#### 4.7.3. $^{131}\text{Xe}$

The general trend in concentrations of  $^{131}\text{Xe}$  with lattice burnup is shown in Figure 4.83. A detailed plot for the 17-20 GWd/MTU burnup interval is also provided in Figure 4.84. AP1 results are outside the 2 $\sigma$  band with a bias compared to other code results. SCALE codes with ENDF/B-VI and ENDF/B-VII libraries predict the highest concentrations, while HELIOS codes predict the lowest concentrations.  $^{131}\text{Xe}$  concentration increases with decay and decreases with void fraction; however, the trend with burnup stays the same. SC1 (ENDF/B-VII.0) exhibits an increasing bias with the rest of the code results at 70% void fraction and therefore not included in the statistics.

Statistics for  $^{131}\text{Xe}$  concentrations are provided in Table 4.30. Standard deviation in the results increases with burnup and decreases with void fraction. The maximum relative standard deviation is 2.7% at the end of depletion at 70% void fraction.

**Figure 4.83. <sup>131</sup>Xe concentration at 40% void fraction at discharge**

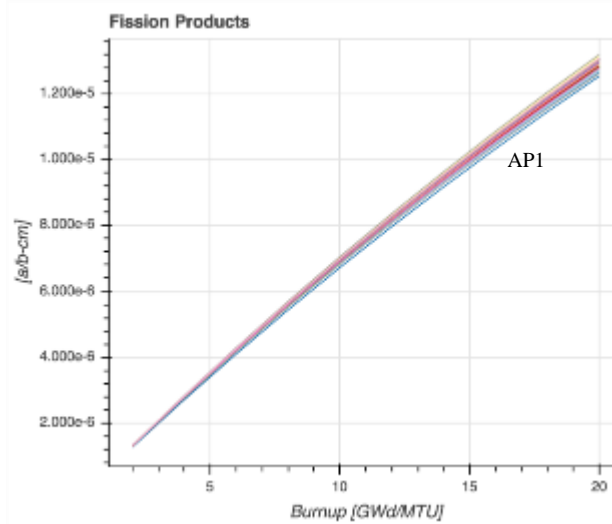


**Figure 4.84. <sup>131</sup>Xe concentration at 40% void fraction in 17-20 GWd/MTU interval**

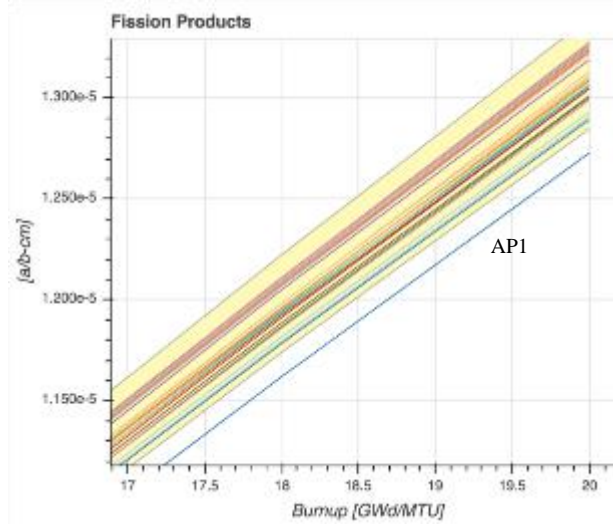


**Table 4.30. Statistics for <sup>131</sup>Xe concentration**

0-years <sup>1</sup>									
Burnup GWd/MTU	0% void fraction			40% void fraction			70% void fraction <sup>2</sup>		
	Mean	2σ	2σ%	Mean	2σ	2σ%	Mean	2σ	2σ%
2	1.31E-06	1.70E-08	1.30	1.30E-06	1.59E-08	1.22	1.30E-06	1.50E-08	1.16
4	2.81E-06	4.05E-08	1.44	2.79E-06	3.78E-08	1.35	2.77E-06	3.59E-08	1.30
6	4.26E-06	6.61E-08	1.55	4.23E-06	6.23E-08	1.47	4.19E-06	5.99E-08	1.43
8	5.66E-06	9.33E-08	1.65	5.61E-06	8.91E-08	1.59	5.56E-06	8.63E-08	1.55
10	7.01E-06	1.21E-07	1.73	6.94E-06	1.18E-07	1.70	6.87E-06	1.16E-07	1.69
12	8.31E-06	1.50E-07	1.81	8.22E-06	1.47E-07	1.79	8.13E-06	1.46E-07	1.80
14	9.58E-06	1.80E-07	1.88	9.46E-06	1.78E-07	1.88	9.34E-06	1.81E-07	1.94
16	1.08E-05	2.11E-07	1.96	1.07E-05	2.08E-07	1.95	1.05E-05	2.20E-07	2.09
18	1.20E-05	2.40E-07	2.01	1.18E-05	2.46E-07	2.08	1.16E-05	2.59E-07	2.23
20	1.31E-05	2.72E-07	2.07	1.29E-05	2.82E-07	2.18	1.27E-05	3.02E-07	2.38



**Table 4.30. Statistics for  $^{131}\text{Xe}$  concentration (continued)**

5-years <sup>2</sup>									
Burnup GWd/MTU	0% void fraction			40% void fraction			70% void fraction		
	Mean	2 $\sigma$	2 $\sigma\%$	Mean	2 $\sigma$	2 $\sigma\%$	Mean	2 $\sigma$	2 $\sigma\%$
2	1.55E-06	2.39E-08	1.55	1.54E-06	2.22E-08	1.44	1.53E-06	2.08E-08	1.36
4	3.05E-06	4.88E-08	1.60	3.03E-06	4.56E-08	1.51	3.01E-06	4.29E-08	1.43
6	4.50E-06	7.53E-08	1.68	4.46E-06	7.07E-08	1.59	4.43E-06	6.74E-08	1.52
8	5.89E-06	1.02E-07	1.73	5.84E-06	9.71E-08	1.66	5.79E-06	9.41E-08	1.63
10	7.24E-06	1.31E-07	1.81	7.17E-06	1.26E-07	1.76	7.10E-06	1.23E-07	1.73
12	8.54E-06	1.60E-07	1.88	8.45E-06	1.63E-07	1.93	8.36E-06	1.55E-07	1.85
14	9.81E-06	1.91E-07	1.94	9.69E-06	1.92E-07	1.98	9.58E-06	1.89E-07	1.97
16	1.10E-05	2.22E-07	2.01	1.09E-05	2.24E-07	2.05	1.07E-05	2.27E-07	2.12
18	1.22E-05	2.50E-07	2.04	1.20E-05	2.62E-07	2.17	1.19E-05	2.71E-07	2.28
20	1.34E-05	2.85E-07	2.14	1.32E-05	2.93E-07	2.23	1.29E-05	3.13E-07	2.42

Note: <sup>1</sup>SC20 results are not included; <sup>2</sup>SC20 and SC1 results are not included.

#### 4.7.4. $^{133}\text{Cs}$

The general trend in concentrations of  $^{133}\text{Cs}$  with lattice burnup is shown in Figure 4.85.  $^{133}\text{Cs}$  concentrations also exhibit a linear trend with burnup. A detailed plot for the 14–20 GWd/MTU burnup interval is also provided in Figure 4.86. As KE1 and KE3 results agree, the largest concentrations are observed in KE1, KE2 and VE3 results. CA1 and AP1 codes predict the lowest concentrations at all void fractions. KE1 and CA1 results are placed outside the 2 $\sigma$  band.

Statistics for  $^{133}\text{Cs}$  concentrations are provided in Table 4.31. While relative standard deviation of the results decreases with burnup and void fraction, standard deviation increases with burnup. Relative standard deviation is less than 2.20% at peak reactivity and around 2% at the end of depletion.

**Figure 4.85.  $^{133}\text{Cs}$  concentration at 40% void fraction at discharge**

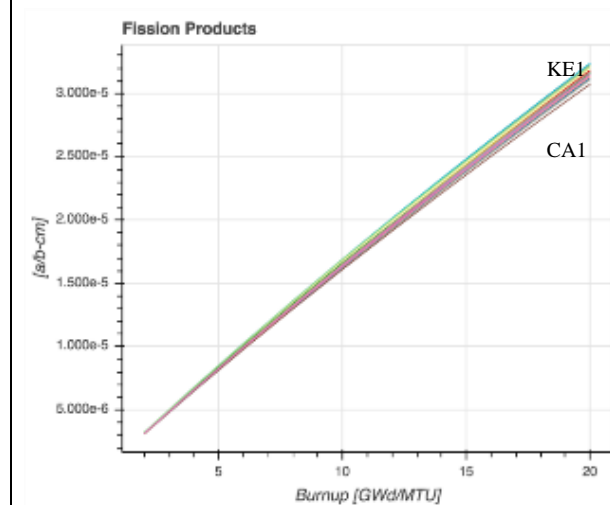


**Figure 4.86.  $^{133}\text{Cs}$  concentration at 40% void fraction in 14–20 GWd/MTU interval**

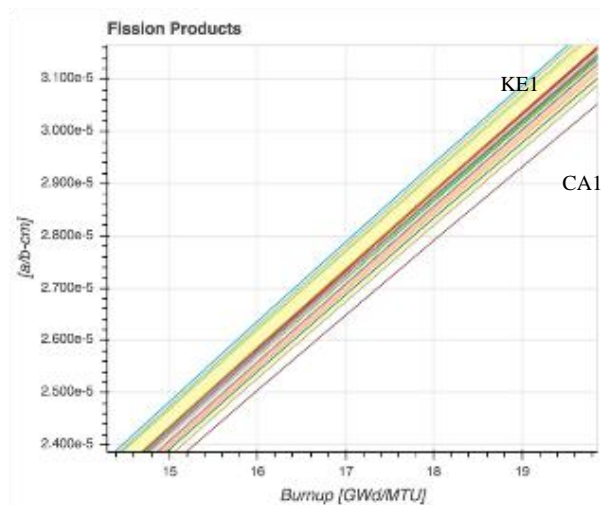


**Table 4.31. Statistics for <sup>133</sup>Cs concentration**

0-years <sup>1</sup>									
Burnup GWd/MTU	0% void fraction			40% void fraction			70% void fraction <sup>2</sup>		
	Mean	2σ	2σ%	Mean	2σ	2σ%	Mean	2σ	2σ%
2	3.18E-06	6.79E-08	2.13	3.16E-06	6.68E-08	2.11	3.14E-06	6.57E-08	2.09
4	6.67E-06	1.41E-07	2.12	6.62E-06	1.37E-07	2.07	6.58E-06	1.33E-07	2.02
6	1.01E-05	2.15E-07	2.14	1.00E-05	2.08E-07	2.08	9.93E-06	2.01E-07	2.02
8	1.34E-05	2.85E-07	2.13	1.33E-05	2.76E-07	2.08	1.32E-05	2.66E-07	2.02
10	1.66E-05	3.55E-07	2.14	1.65E-05	3.41E-07	2.07	1.64E-05	3.26E-07	1.99
12	1.98E-05	4.14E-07	2.09	1.96E-05	3.94E-07	2.00	1.95E-05	3.71E-07	1.90
14	2.29E-05	4.74E-07	2.07	2.27E-05	4.45E-07	1.96	2.26E-05	4.19E-07	1.86
16	2.60E-05	5.28E-07	2.03	2.58E-05	4.97E-07	1.93	2.56E-05	4.64E-07	1.82
18	2.90E-05	5.84E-07	2.01	2.88E-05	5.46E-07	1.90	2.85E-05	5.13E-07	1.80
20	3.20E-05	6.38E-07	1.99	3.17E-05	5.96E-07	1.88	3.14E-05	5.60E-07	1.79

**Table 4.31. Statistics for <sup>133</sup>Cs concentration (continued)**

5-years <sup>2</sup>									
Burnup GWd/MTU	0% void fraction			40% void fraction			70% void fraction		
	Mean	2σ	2σ%	Mean	2σ	2σ%	Mean	2σ	2σ%
2	3.56E-06	8.41E-08	2.36	3.54E-06	8.05E-08	2.27	3.52E-06	7.66E-08	2.18
4	7.05E-06	1.64E-07	2.33	7.00E-06	1.57E-07	2.25	6.95E-06	1.50E-07	2.17
6	1.04E-05	2.42E-07	2.32	1.04E-05	2.28E-07	2.20	1.03E-05	2.20E-07	2.13
8	1.38E-05	3.13E-07	2.27	1.37E-05	3.01E-07	2.20	1.36E-05	2.89E-07	2.13
10	1.70E-05	3.83E-07	2.25	1.69E-05	3.66E-07	2.17	1.67E-05	3.49E-07	2.08
12	2.02E-05	4.46E-07	2.21	2.00E-05	4.69E-07	2.35	1.99E-05	3.95E-07	1.99
14	2.33E-05	5.06E-07	2.18	2.31E-05	5.18E-07	2.24	2.29E-05	4.44E-07	1.94
16	2.63E-05	5.61E-07	2.13	2.61E-05	5.69E-07	2.18	2.59E-05	4.91E-07	1.90
18	2.94E-05	6.17E-07	2.10	2.91E-05	6.17E-07	2.12	2.89E-05	5.36E-07	1.86
20	3.23E-05	6.72E-07	2.08	3.20E-05	6.27E-07	1.96	3.17E-05	5.84E-07	1.84

Note: <sup>1</sup>SC20 results are not included; <sup>2</sup>SC20 and SC1 results are not included.

#### 4.7.5. <sup>143</sup>Nd

The <sup>143</sup>Nd results are shown in Figure 4.87. <sup>143</sup>Nd concentrations exhibit the same trend with respect to lattice burnup at all void fractions and five-year decay. A detailed plot for the 18-20 GWd/MTU burnup interval is also provided in Figure 4.88. KE2 (JEFF2.2) predicts the highest concentrations, while HELIOS and SERPENT codes predict the lowest concentrations. HE4 results are below the 2σ band at all void fractions, and all HELIOS results are below the 2σ band at 70% void fraction.

Statistics for <sup>143</sup>Nd concentrations are provided in Table 4.32. Standard deviation in the results are small. Relative standard deviation is below 1.2% at peak reactivity and less than 1% at the end of depletion.

**Figure 4.87. <sup>143</sup>Nd concentration at 40% void fraction at discharge**

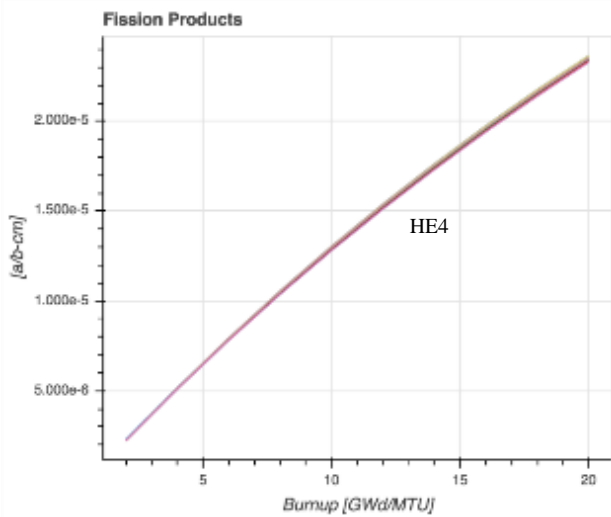


**Figure 4.88. <sup>143</sup>Nd concentration at 40% void fraction in 18-20 GWd/MTU interval**

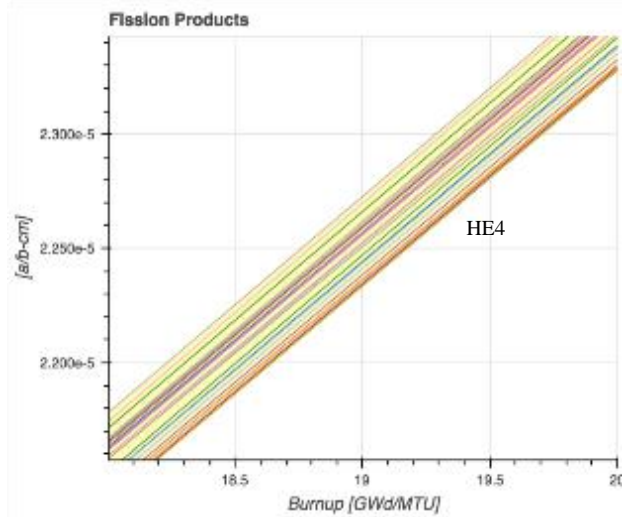


**Table 4.32. Statistics for <sup>143</sup>Nd concentration**

0-years <sup>1</sup>									
Burnup GWd/MTU	0% void fraction			40% void fraction			70% void fraction		
	Mean	2σ	2σ%	Mean	2σ	2σ%	Mean	2σ	2σ%
2	2.27E-06	3.38E-08	1.49	2.25E-06	3.18E-08	1.41	2.23E-06	2.94E-08	1.32
4	5.19E-06	6.30E-08	1.21	5.15E-06	5.74E-08	1.11	5.10E-06	5.02E-08	0.98
6	7.96E-06	9.45E-08	1.19	7.89E-06	8.52E-08	1.08	7.83E-06	7.51E-08	0.96
8	1.06E-05	1.22E-07	1.16	1.05E-05	1.10E-07	1.05	1.04E-05	9.79E-08	0.94
10	1.30E-05	1.56E-07	1.20	1.29E-05	1.41E-07	1.09	1.29E-05	1.25E-07	0.97
12	1.54E-05	1.71E-07	1.11	1.53E-05	1.56E-07	1.02	1.52E-05	1.44E-07	0.95
14	1.76E-05	1.86E-07	1.06	1.75E-05	1.75E-07	1.00	1.74E-05	1.44E-07	0.83
16	1.96E-05	1.98E-07	1.01	1.96E-05	1.86E-07	0.95	1.96E-05	1.56E-07	0.80
18	2.16E-05	2.13E-07	0.99	2.16E-05	1.95E-07	0.90	2.16E-05	1.69E-07	0.78
20	2.35E-05	2.13E-07	0.91	2.35E-05	2.02E-07	0.86	2.35E-05	1.86E-07	0.79

**Table 4.32. Statistics for  $^{143}\text{Nd}$  concentration (continued)**

5-years <sup>2</sup>									
Burnup GWd/MTU	0% void fraction			40% void fraction			70% void fraction		
	Mean	2 $\sigma$	2 $\sigma$ %	Mean	2 $\sigma$	2 $\sigma$ %	Mean	2 $\sigma$	2 $\sigma$ %
2	3.09E-06	3.79E-08	1.23	3.06E-06	3.28E-08	1.07	3.03E-06	2.90E-08	0.96
4	6.00E-06	7.25E-08	1.21	5.95E-06	6.47E-08	1.09	5.89E-06	5.62E-08	0.95
6	8.75E-06	1.07E-07	1.22	8.67E-06	9.39E-08	1.08	8.60E-06	8.16E-08	0.95
8	1.13E-05	1.40E-07	1.24	1.13E-05	1.25E-07	1.12	1.12E-05	9.99E-08	0.89
10	1.38E-05	1.72E-07	1.24	1.37E-05	1.47E-07	1.07	1.36E-05	1.28E-07	0.94
12	1.61E-05	1.94E-07	1.21	1.60E-05	1.92E-07	1.20	1.59E-05	1.41E-07	0.88
14	1.83E-05	2.08E-07	1.14	1.82E-05	2.03E-07	1.11	1.81E-05	1.53E-07	0.84
16	2.04E-05	2.18E-07	1.07	2.03E-05	2.13E-07	1.05	2.03E-05	1.64E-07	0.81
18	2.23E-05	2.28E-07	1.02	2.23E-05	2.20E-07	0.99	2.23E-05	1.75E-07	0.79
20	2.42E-05	2.30E-07	0.95	2.42E-05	2.08E-07	0.86	2.42E-05	1.90E-07	0.78

Note: <sup>1</sup>SC20 results are not included; <sup>2</sup>SC20 and SC1 results are not included.

#### 4.7.6. $^{148}\text{Nd}$

$^{148}\text{Nd}$  concentrations show a linear trend with burnup (Figure 4.89). The same trend is observed at all void fractions and five-year decay. A detailed plot for the 19-20 GWd/MTU burnup interval is provided in Figure 4.90. As the highest concentrations are observed in AL1 and AP1 results, AP1 results are above the 2 $\sigma$  band. HELIOS codes predict the lowest concentrations at all void fractions.

Statistics for  $^{148}\text{Nd}$  concentrations are provided in Table 4.33. Standard deviation of the results is small, although it increases with burnup and decreases with void fraction. Relative standard deviation at peak power is less than 1.35% and increases to 1.40% at the end of depletion.

**Figure 4.89. <sup>148</sup>Nd concentration at 40% void fraction at discharge**

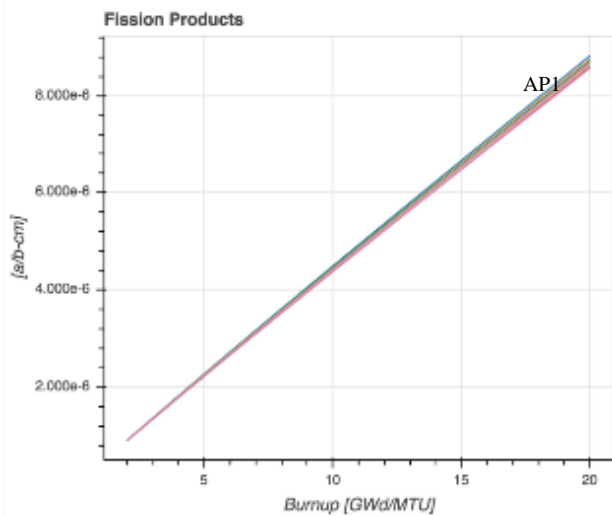


**Figure 4.90. <sup>148</sup>Nd concentration at 40% void fraction in 19-20 GWd/MTU interval**

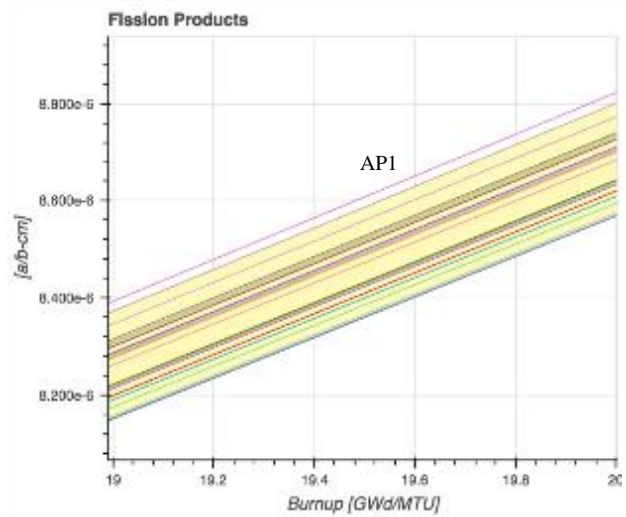


**Table 4.33. Statistics for <sup>148</sup>Nd concentration**

0-years <sup>1</sup>									
Burnup GWd/MTU	0% void fraction			40% void fraction			70% void fraction		
	Mean	2σ	2σ%	Mean	2σ	2σ%	Mean	2σ	2σ%
2	9.14E-07	1.07E-08	1.18	9.11E-07	1.05E-08	1.15	9.08E-07	1.05E-08	1.15
4	1.82E-06	2.17E-08	1.20	1.81E-06	2.16E-08	1.19	1.81E-06	2.08E-08	1.15
6	2.71E-06	3.37E-08	1.25	2.70E-06	3.26E-08	1.21	2.69E-06	3.22E-08	1.20
8	3.58E-06	4.62E-08	1.29	3.57E-06	4.44E-08	1.24	3.56E-06	4.35E-08	1.22
10	4.44E-06	5.95E-08	1.34	4.43E-06	5.68E-08	1.28	4.43E-06	5.54E-08	1.25
12	5.30E-06	7.30E-08	1.38	5.29E-06	6.92E-08	1.31	5.28E-06	6.61E-08	1.25
14	6.15E-06	8.56E-08	1.39	6.14E-06	8.13E-08	1.32	6.14E-06	7.76E-08	1.26
16	7.00E-06	9.76E-08	1.39	6.99E-06	9.24E-08	1.32	6.99E-06	8.86E-08	1.27
18	7.85E-06	1.10E-07	1.40	7.84E-06	1.03E-07	1.31	7.83E-06	1.00E-07	1.28
20	8.69E-06	1.21E-07	1.39	8.69E-06	1.14E-07	1.32	8.68E-06	1.10E-07	1.27

Table 4.33. Statistics for  $^{148}\text{Nd}$  concentration (continued)

5-years <sup>2</sup>									
Burnup GWd/MTU	0% void fraction			40% void fraction			70% void fraction		
	Mean	2 $\sigma$	2 $\sigma$ %	Mean	2 $\sigma$	2 $\sigma$ %	Mean	2 $\sigma$	2 $\sigma$ %
2	9.14E-07	1.08E-08	1.19	9.11E-07	1.05E-08	1.15	9.08E-07	1.05E-08	1.16
4	1.82E-06	2.19E-08	1.21	1.81E-06	2.17E-08	1.20	1.81E-06	2.09E-08	1.16
6	2.71E-06	3.40E-08	1.26	2.70E-06	3.26E-08	1.21	2.69E-06	3.24E-08	1.20
8	3.58E-06	4.66E-08	1.30	3.57E-06	4.44E-08	1.24	3.56E-06	4.37E-08	1.23
10	4.44E-06	5.99E-08	1.35	4.43E-06	5.69E-08	1.28	4.43E-06	5.56E-08	1.26
12	5.30E-06	7.35E-08	1.39	5.29E-06	6.86E-08	1.30	5.28E-06	6.64E-08	1.26
14	6.15E-06	8.62E-08	1.40	6.14E-06	7.93E-08	1.29	6.14E-06	7.80E-08	1.27
16	7.00E-06	9.83E-08	1.40	6.99E-06	8.96E-08	1.28	6.99E-06	8.90E-08	1.27
18	7.85E-06	1.11E-07	1.41	7.84E-06	9.95E-08	1.27	7.83E-06	1.01E-07	1.28
20	8.69E-06	1.21E-07	1.40	8.68E-06	1.14E-07	1.32	8.68E-06	1.10E-07	1.27

Note: <sup>1</sup>SC20 results are not included; <sup>2</sup>SC20 and SC1 results are not included.

#### 4.7.7. $^{147}\text{Sm}$

Concentrations of  $^{147}\text{Sm}$  at discharge and after five-year decay are displayed in Figures 4.91 and 4.92, respectively. A detailed plot for the 17-20 GWd/MTU burnup interval is also provided in Figure 4.93 at discharge and Figure 4.94 after five-years decay. While the lowest concentrations are predicted by KENOREST, CA1 and SC2 (ENDF/B-V), KENOREST results exhibit a bias compared to other code results. Among KENOREST results, KE2 (JEFF2.2) results are separated from other KENOREST results with a large negative bias. All KENOREST results are below the 2 $\sigma$  band at all void fractions.

Statistics for  $^{147}\text{Sm}$  concentrations are provided in Table 4.34. Standard deviation increases with burnup, void fraction and five-year decay. Maximum relative standard deviation is 1.2% at peak reactivity, increasing to 2.64% at the end of depletion.

**Figure 4.91.  $^{147}\text{Sm}$  concentration at 40% void fraction at discharge**

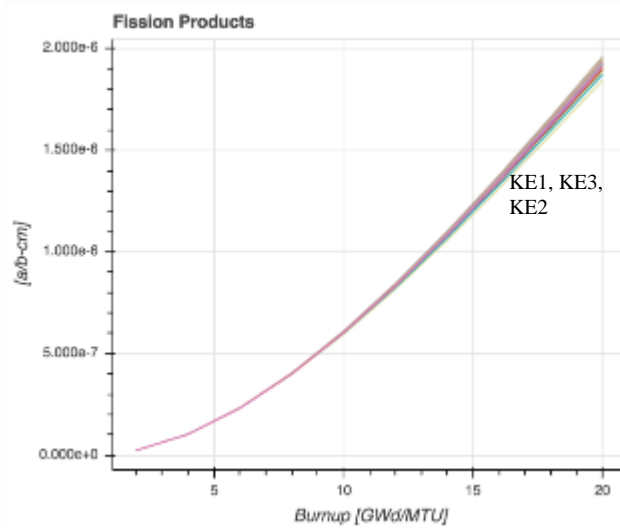


**Figure 4.92.  $^{147}\text{Sm}$  concentration at 40% void fraction with five-year decay**

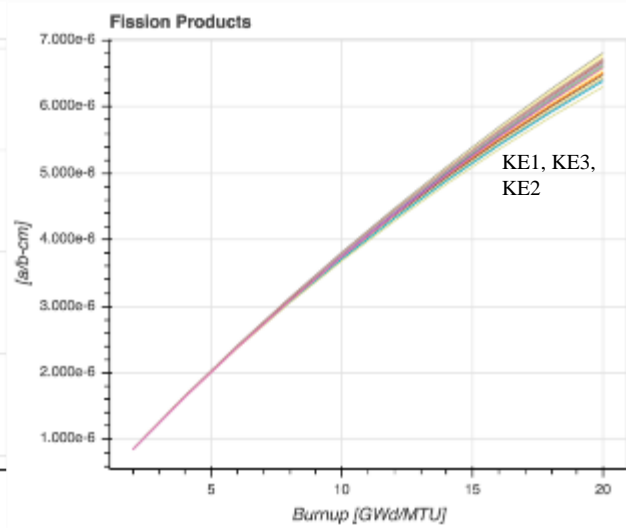


**Figure 4.93.  $^{147}\text{Sm}$  concentration at 70% void fraction in 17-20 GWd/MTU interval**

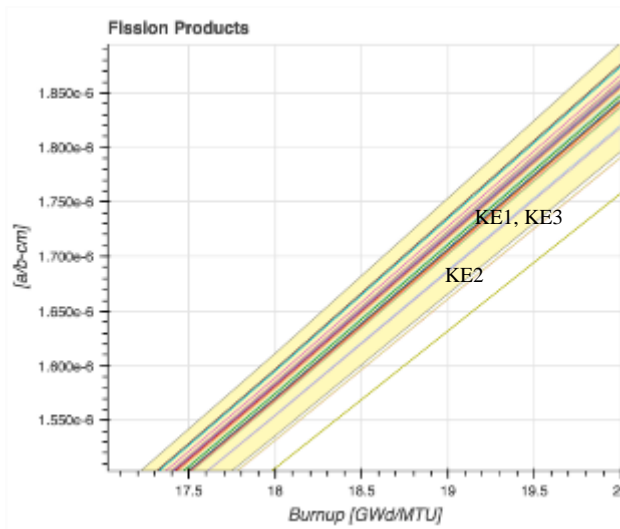


**Figure 4.94.  $^{147}\text{Sm}$  concentration at 70% void fraction with five-year decay in 17-20 GWd/MTU interval**

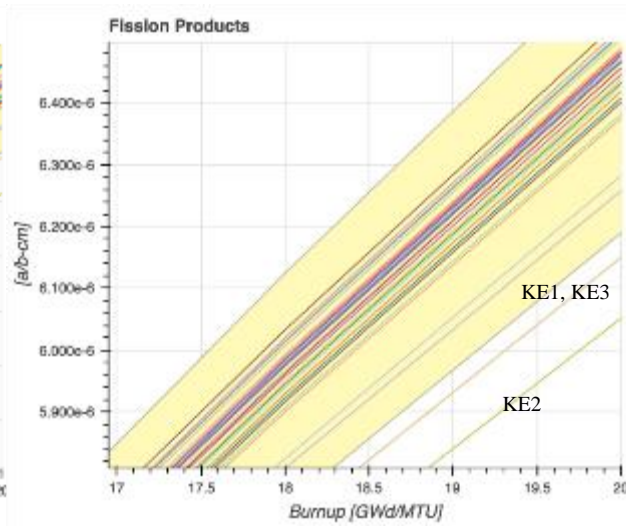


Table 4.34. Statistics for  $^{147}\text{Sm}$  concentration

0-years <sup>1</sup>									
Burnup GWd/MTU	0% void fraction			40% void fraction			70% void fraction		
	Mean	2 $\sigma$	2 $\sigma$ %	Mean	2 $\sigma$	2 $\sigma$ %	Mean	2 $\sigma$	2 $\sigma$ %
2	2.27E-08	2.30E-10	1.01	2.24E-08	1.94E-10	0.86	2.22E-08	1.65E-10	0.74
4	1.03E-07	9.72E-10	0.94	1.02E-07	8.55E-10	0.84	1.01E-07	7.20E-10	0.72
6	2.35E-07	2.23E-09	0.95	2.31E-07	1.98E-09	0.86	2.27E-07	1.79E-09	0.79
8	4.09E-07	4.02E-09	0.98	4.01E-07	3.76E-09	0.94	3.92E-07	3.79E-09	0.97
10	6.19E-07	6.60E-09	1.07	6.04E-07	6.45E-09	1.07	5.89E-07	7.03E-09	1.19
12	8.58E-07	1.02E-08	1.19	8.34E-07	1.05E-08	1.26	8.11E-07	1.18E-08	1.46
14	1.12E-06	1.52E-08	1.36	1.09E-06	1.58E-08	1.46	1.05E-06	1.83E-08	1.74
16	1.40E-06	2.09E-08	1.49	1.35E-06	2.32E-08	1.71	1.31E-06	2.68E-08	2.05
18	1.70E-06	2.81E-08	1.66	1.63E-06	3.14E-08	1.92	1.57E-06	3.67E-08	2.33
20	2.00E-06	3.71E-08	1.85	1.92E-06	4.15E-08	2.16	1.85E-06	4.87E-08	2.64
5-years <sup>2</sup>									
Burnup GWd/MTU	0% void fraction			40% void fraction			70% void fraction		
	Mean	2 $\sigma$	2 $\sigma$ %	Mean	2 $\sigma$	2 $\sigma$ %	Mean	2 $\sigma$	2 $\sigma$ %
2	8.62E-07	8.72E-09	1.01	8.55E-07	7.47E-09	0.87	8.47E-07	6.53E-09	0.77
4	1.67E-06	1.52E-08	0.91	1.65E-06	1.30E-08	0.79	1.63E-06	1.17E-08	0.71
6	2.44E-06	2.27E-08	0.93	2.40E-06	2.11E-08	0.88	2.36E-06	2.03E-08	0.86
8	3.16E-06	3.33E-08	1.06	3.10E-06	3.66E-08	1.18	3.05E-06	3.63E-08	1.19
10	3.85E-06	4.73E-08	1.23	3.77E-06	4.99E-08	1.33	3.69E-06	5.70E-08	1.54
12	4.50E-06	6.53E-08	1.45	4.40E-06	7.27E-08	1.65	4.30E-06	8.36E-08	1.94
14	5.13E-06	8.55E-08	1.67	5.00E-06	9.67E-08	1.94	4.88E-06	1.14E-07	2.34
16	5.72E-06	1.09E-07	1.90	5.57E-06	1.24E-07	2.24	5.42E-06	1.48E-07	2.73
18	6.29E-06	1.35E-07	2.14	6.11E-06	1.56E-07	2.55	5.94E-06	1.84E-07	3.10
20	6.83E-06	1.64E-07	2.39	6.62E-06	1.90E-07	2.88	6.42E-06	2.23E-07	3.47

Note: <sup>1</sup>SC20 results are not included; <sup>2</sup>SC20 and SC1 results are not included.

#### 4.7.8. $^{149}\text{Sm}$

$^{149}\text{Sm}$  concentrations at different void fractions and with five-year decay are shown in Figures 4.95 to 4.100. Comparisons of  $^{149}\text{Sm}$  results show a large spread at all void fractions. VE1, VE2, AP1 and AL1 codes predict the lowest concentrations of  $^{149}\text{Sm}$ , and most of the results in this group are outside the 2 $\sigma$  band. Although VE1, VE2 AP1 and AL1 have different MC and deterministic transport solvers, they all use JEFF3 (JEFF3.1 and JEFF3.2) libraries. VE1, VE2 and AP1 results are outside the 2 $\sigma$  band. KE2 (JEFF2.2) code predicts the highest concentrations at all void fractions. Although a bias exists between KE2 and CA1 results, they exhibit a different trend with lattice burnup compared to other codes (Figures 4.95 and 4.96). Considering that KE2 and CA1 codes use different transport solvers (MC, deterministic) and different depletion algorithms, the common trend can be attributed to the common JEFF2.2 library.



Statistics for  $^{149}\text{Sm}$  concentrations are provided in Table 4.35. Standard deviation in the results increases with increasing burnup, void fraction and after five-year decay. Although, average concentrations stay almost constant, standard deviation increases with burnup. The largest increase in standard deviation is observed with respect to void fraction. At peak reactivity, the standard deviation at 70% void fraction is 60% higher than the standard deviation at 0% void fraction. The largest relative standard deviation is 10.1% at peak reactivity and increases to 13.3% at the end of depletion. Decay time also increases standard deviations: after five-year decay, standard deviations increase by 20% to 50% at 0% and 70% void fractions, respectively.

**Figure 4.95.  $^{149}\text{Sm}$  concentration at 0% void fraction at discharge**

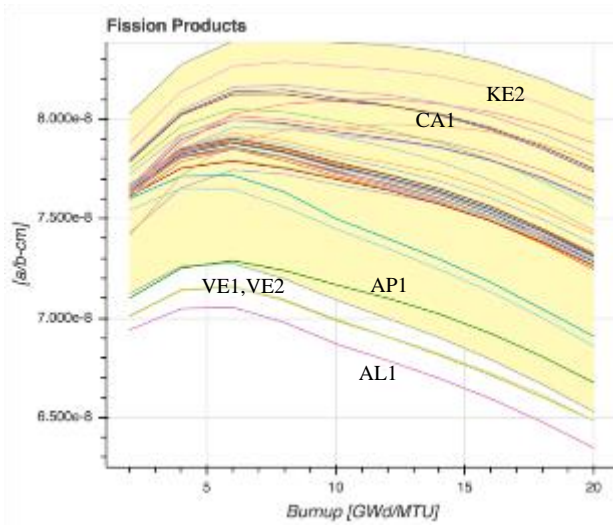


**Figure 4.96.  $^{149}\text{Sm}$  concentration at 0% void fraction with five-year decay**

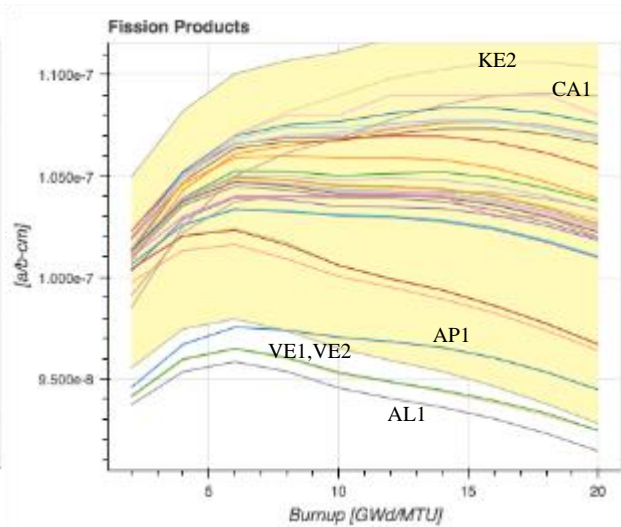


**Figure 4.97.  $^{149}\text{Sm}$  concentration at 40% void fraction at discharge**

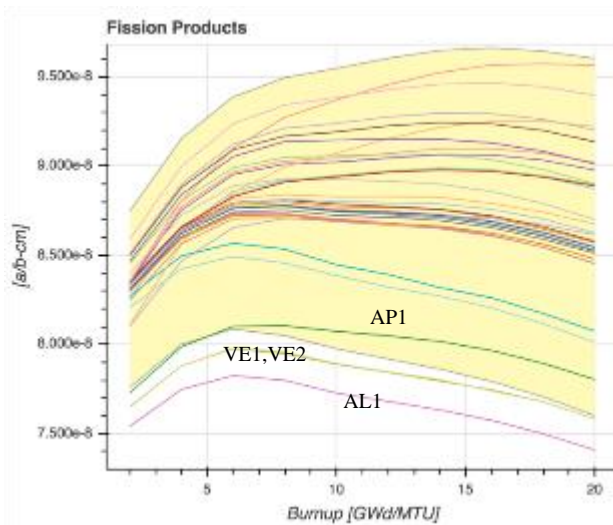


**Figure 4.98.  $^{149}\text{Sm}$  concentration at 40% void fraction with five-year decay**

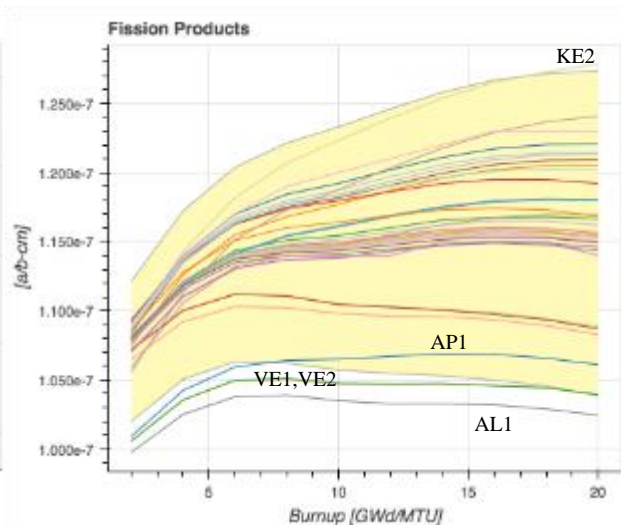


Figure 4.99. <sup>149</sup>Sm concentration at 70% void fraction

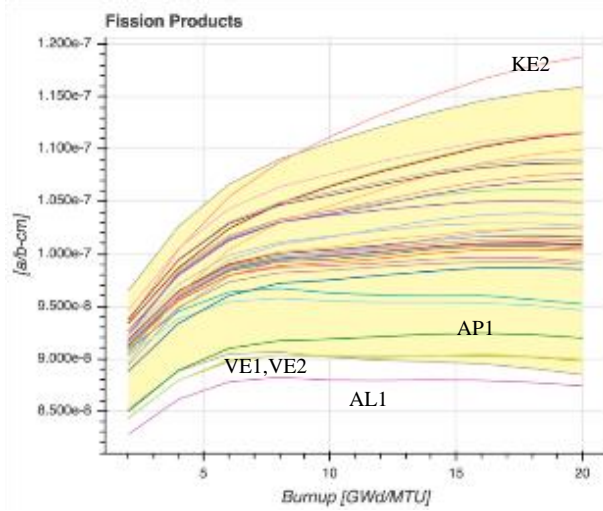


Figure 4.100. <sup>149</sup>Sm concentration at 70% void fraction with five-year decay

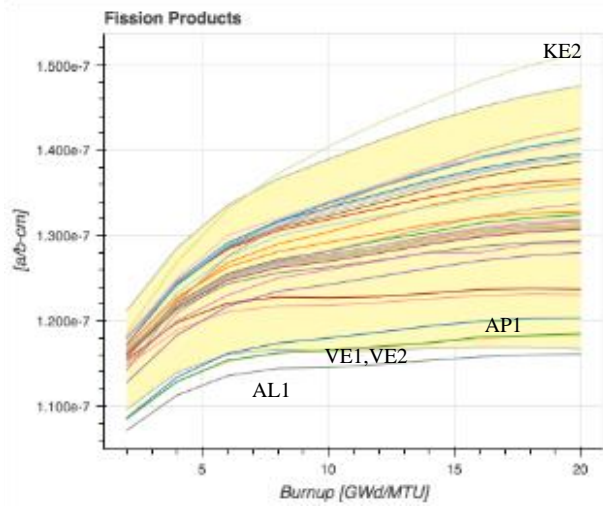


Table 4.35. Statistics for <sup>149</sup>Sm concentration

0-years <sup>1</sup>									
Burnup GWd/MTU	0% void fraction			40% void fraction			70% void fraction		
	Mean	2σ	2σ%	Mean	2σ	2σ%	Mean	2σ	2σ%
2	7.58E-08	4.49E-09	5.92	8.26E-08	4.89E-09	5.93	9.08E-08	5.58E-09	6.15
4	7.77E-08	5.06E-09	6.51	8.58E-08	5.73E-09	6.68	9.57E-08	6.86E-09	7.17
6	7.84E-08	5.59E-09	7.13	8.74E-08	6.51E-09	7.45	9.85E-08	8.02E-09	8.14
8	7.80E-08	6.06E-09	7.76	8.77E-08	7.22E-09	8.23	9.98E-08	9.12E-09	9.14
10	7.74E-08	6.46E-09	8.35	8.77E-08	7.80E-09	8.90	1.00E-07	1.02E-08	10.14
12	7.69E-08	6.82E-09	8.87	8.77E-08	8.34E-09	9.52	1.01E-07	1.10E-08	10.91
14	7.63E-08	7.13E-09	9.35	8.76E-08	8.80E-09	10.05	1.02E-07	1.17E-08	11.52
16	7.54E-08	7.39E-09	9.80	8.73E-08	9.21E-09	10.54	1.02E-07	1.24E-08	12.12
18	7.44E-08	7.59E-09	10.21	8.68E-08	9.56E-09	11.02	1.02E-07	1.29E-08	12.64
20	7.32E-08	7.77E-09	10.62	8.61E-08	9.85E-09	11.44	1.02E-07	1.35E-08	13.21
5-years <sup>2</sup>									
Burnup GWd/MTU	0% void fraction			40% void fraction			70% void fraction		
	Mean	2σ	2σ%	Mean	2σ	2σ%	Mean	2σ	2σ%
2	1.00E-07	4.82E-09	4.81	1.07E-07	5.19E-09	4.85	1.15E-07	5.91E-09	5.12
4	1.03E-07	5.53E-09	5.37	1.11E-07	6.23E-09	5.61	1.21E-07	7.41E-09	6.10
6	1.04E-07	6.23E-09	5.98	1.13E-07	7.20E-09	6.35	1.25E-07	8.89E-09	7.11
8	1.04E-07	6.87E-09	6.60	1.14E-07	8.10E-09	7.09	1.27E-07	1.01E-08	7.99
10	1.04E-07	7.42E-09	7.14	1.15E-07	8.88E-09	7.74	1.28E-07	1.13E-08	8.85
12	1.04E-07	7.99E-09	7.68	1.15E-07	9.59E-09	8.33	1.29E-07	1.23E-08	9.54
14	1.04E-07	8.43E-09	8.10	1.16E-07	1.02E-08	8.81	1.30E-07	1.32E-08	10.11
16	1.04E-07	8.84E-09	8.53	1.16E-07	1.08E-08	9.27	1.31E-07	1.39E-08	10.62
18	1.03E-07	9.19E-09	8.90	1.16E-07	1.12E-08	9.67	1.32E-07	1.46E-08	11.07
20	1.03E-07	9.45E-09	9.22	1.16E-07	1.16E-08	10.03	1.32E-07	1.52E-08	11.51

Note: <sup>1</sup>SC20 results are not included; <sup>2</sup>SC20 and SC1 results are not included.

#### 4.7.9. $^{151}\text{Sm}$

Concentrations of  $^{151}\text{Sm}$  at different void fractions and after five-year decay are compared in Figures 4.101 to 4.104. The largest concentrations are predicted by SCALE codes using ENDF/B-V libraries (SC2, SC4, SC5). SC2, SC4 and SC5 results are placed outside the  $2\sigma$  band at all void fractions and exhibit a large bias compared to other code results. CA1, KENOREST and HELIOS codes also predict high concentrations, and are grouped together.

Statistics for  $^{151}\text{Sm}$  concentrations are provided in Table 4.36. Standard deviation in the results increases with burnup and void fraction, but is not significantly affected by decay time. The maximum relative standard deviation is 10.5% at peak reactivity and increases to 15% at the end of depletion.

**Figure 4.101.  $^{151}\text{Sm}$  concentration at 0% void fraction at discharge**

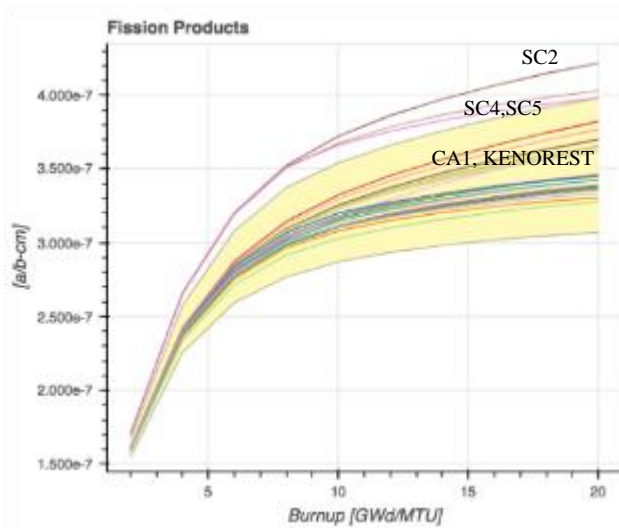


**Figure 4.102.  $^{151}\text{Sm}$  concentration at 0% void fraction with five-year decay**

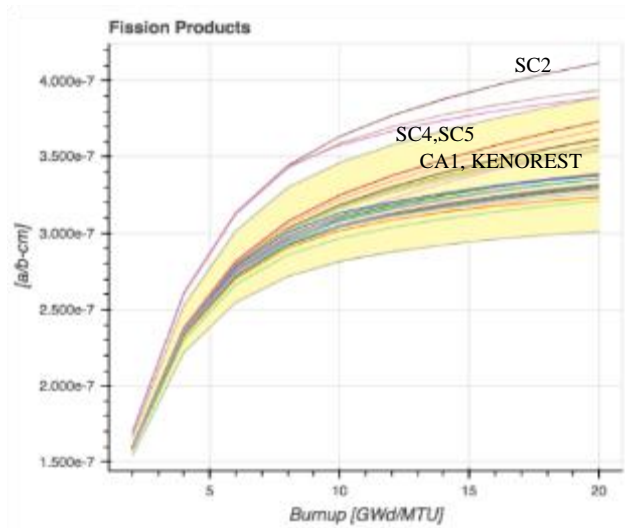


**Figure 4.103.  $^{151}\text{Sm}$  concentration at 70% void fraction**

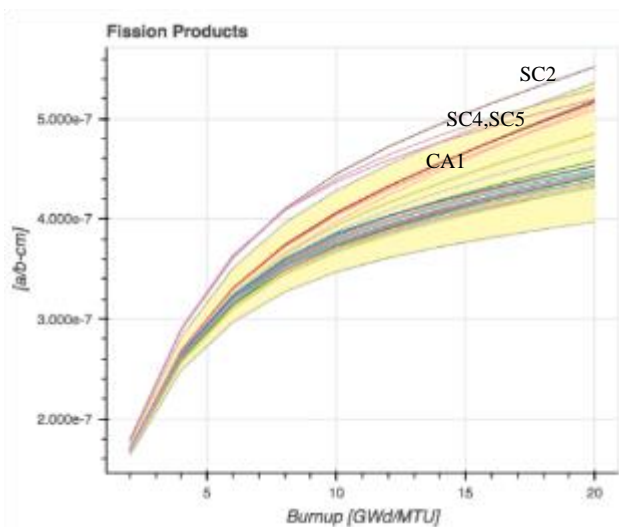


**Figure 4.104.  $^{151}\text{Sm}$  concentration at 70% void fraction with five-year decay**

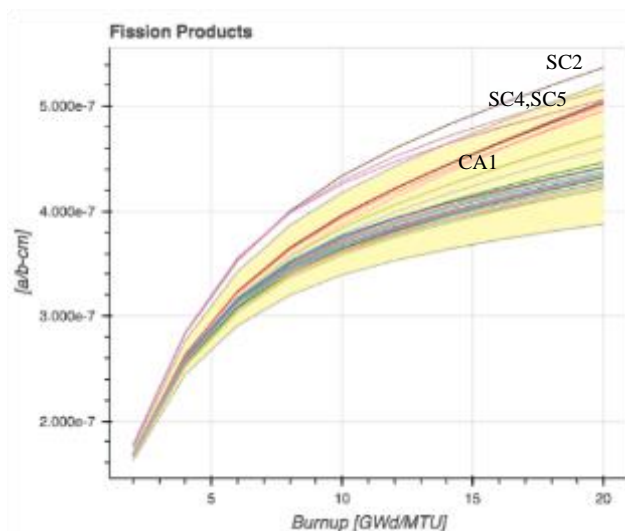


Table 4.36. Statistics for  $^{151}\text{Sm}$  concentration

0-years <sup>1</sup>									
Burnup GWd/MTU	0% void fraction			40% void fraction			70% void fraction		
	Mean	2 $\sigma$	2 $\sigma$ %	Mean	2 $\sigma$	2 $\sigma$ %	Mean	2 $\sigma$	2 $\sigma$ %
2	1.61E-07	6.04E-09	3.76	1.65E-07	5.97E-09	3.62	1.69E-07	5.91E-09	3.49
4	2.41E-07	1.55E-08	6.42	2.53E-07	1.58E-08	6.24	2.65E-07	1.61E-08	6.07
6	2.83E-07	2.36E-08	8.34	3.02E-07	2.48E-08	8.21	3.23E-07	2.61E-08	8.08
8	3.06E-07	2.95E-08	9.64	3.32E-07	3.15E-08	9.48	3.61E-07	3.37E-08	9.35
10	3.20E-07	3.28E-08	10.26	3.51E-07	3.60E-08	10.26	3.87E-07	3.99E-08	10.32
12	3.29E-07	3.56E-08	10.83	3.65E-07	4.02E-08	11.03	4.06E-07	4.58E-08	11.28
14	3.36E-07	3.81E-08	11.35	3.76E-07	4.41E-08	11.71	4.23E-07	5.15E-08	12.19
16	3.42E-07	4.05E-08	11.84	3.86E-07	4.78E-08	12.38	4.38E-07	5.72E-08	13.06
18	3.47E-07	4.27E-08	12.30	3.95E-07	5.15E-08	13.03	4.52E-07	6.28E-08	13.91
20	3.51E-07	4.49E-08	12.78	4.03E-07	5.51E-08	13.67	4.64E-07	6.85E-08	14.76
5-years <sup>2</sup>									
Burnup GWd/MTU	0% void fraction			40% void fraction			70% void fraction		
	Mean	2 $\sigma$	2 $\sigma$ %	Mean	2 $\sigma$	2 $\sigma$ %	Mean	2 $\sigma$	2 $\sigma$ %
2	1.60E-07	5.91E-09	3.70	1.64E-07	5.83E-09	3.57	1.68E-07	5.79E-09	3.45
4	2.37E-07	1.51E-08	6.37	2.48E-07	1.54E-08	6.20	2.60E-07	1.57E-08	6.03
6	2.78E-07	2.30E-08	8.29	2.96E-07	2.42E-08	8.16	3.16E-07	2.54E-08	8.03
8	3.00E-07	2.87E-08	9.58	3.25E-07	3.06E-08	9.42	3.53E-07	3.27E-08	9.28
10	3.13E-07	3.19E-08	10.18	3.43E-07	3.50E-08	10.19	3.78E-07	3.87E-08	10.23
12	3.22E-07	3.46E-08	10.73	3.57E-07	3.91E-08	10.95	3.97E-07	4.43E-08	11.16
14	3.29E-07	3.69E-08	11.23	3.68E-07	4.27E-08	11.62	4.13E-07	4.98E-08	12.06
16	3.35E-07	3.92E-08	11.71	3.78E-07	4.63E-08	12.27	4.28E-07	5.52E-08	12.90
18	3.40E-07	4.13E-08	12.16	3.86E-07	4.99E-08	12.91	4.41E-07	6.06E-08	13.75
20	3.44E-07	4.35E-08	12.63	3.94E-07	5.33E-08	13.53	4.54E-07	6.62E-08	14.59

Note: <sup>1</sup>SC20 results are not included; <sup>2</sup>SC20 and SC1 results are not included.

#### 4.7.10. $^{152}\text{Sm}$

Comparisons of  $^{152}\text{Sm}$  concentrations at different void fractions and after five-year decay are shown in Figures 4.105 to 4.108. A detailed plot for the 15-20 GWd/MTU burnup interval is also provided in Figure 4.107 at 70% void fraction.

In general, KENOEST, SC2 (ENDF/B-V) and CA1 results are grouped together and predict the largest concentrations. Except for CA1, the results of these codes lay outside the 2 $\sigma$  band.

Statistics for  $^{152}\text{Sm}$  concentrations are provided in Table 4.37. Standard deviation in the results increases with increasing void fraction and burnup. Decay time does not change standard deviations significantly. The maximum relative standard deviation is 4.5% at peak reactivity and increases to 8.6% at the end of depletion. If KENOEST, SC2 and CA1 results are removed from the statistics, standard deviation drops by 50% (Table 4.38).

**Figure 4.105.**  $^{152}\text{Sm}$  concentration at 0% void fraction at discharge

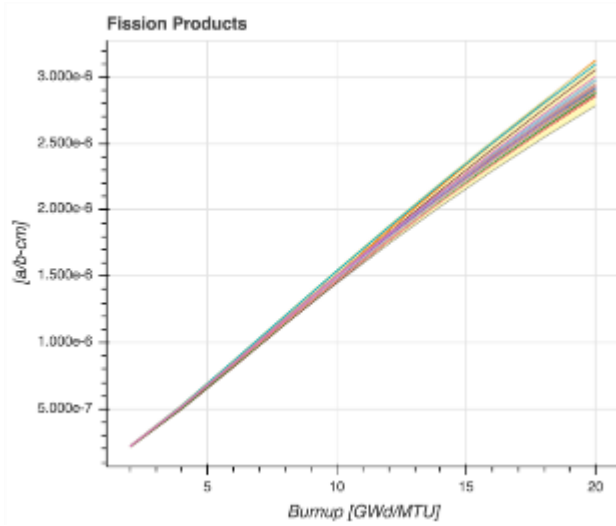


**Figure 4.106.**  $^{152}\text{Sm}$  concentration at 70% void fraction

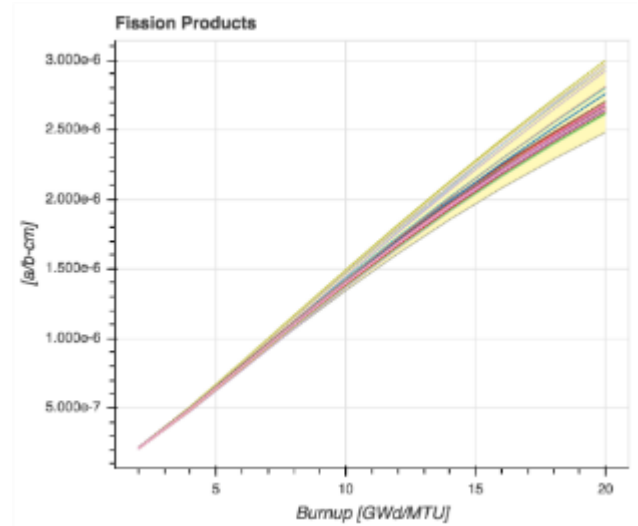


**Figure 4.107.**  $^{152}\text{Sm}$  concentration at 70% void fraction in 15-20 GWd/MTU interval

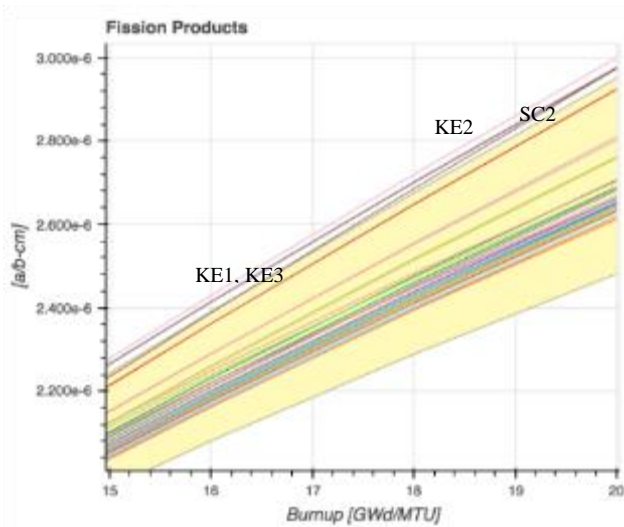


**Figure 4.108.**  $^{152}\text{Sm}$  concentration at 70% void fraction with five-year decay

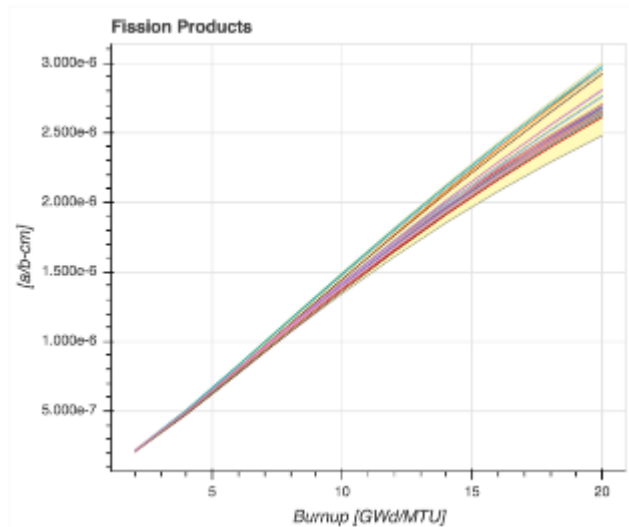


Table 4.37. Statistics for  $^{152}\text{Sm}$  concentration

0-years <sup>1</sup>									
Burnup GWd/MTU	0% void fraction			40% void fraction			70% void fraction		
	Mean	2 $\sigma$	2 $\sigma$ %	Mean	2 $\sigma$	2 $\sigma$ %	Mean	2 $\sigma$	2 $\sigma$ %
2	2.19E-07	6.35E-09	2.90	2.16E-07	5.86E-09	2.72	2.12E-07	5.39E-09	2.54
4	5.18E-07	1.44E-08	2.78	5.07E-07	1.39E-08	2.74	4.96E-07	1.36E-08	2.75
6	8.42E-07	2.21E-08	2.63	8.22E-07	2.32E-08	2.82	8.01E-07	2.52E-08	3.14
8	1.17E-06	3.11E-08	2.66	1.14E-06	3.56E-08	3.12	1.11E-06	4.17E-08	3.76
10	1.49E-06	4.37E-08	2.93	1.45E-06	5.24E-08	3.61	1.41E-06	6.31E-08	4.47
12	1.80E-06	5.91E-08	3.28	1.75E-06	7.28E-08	4.15	1.70E-06	8.92E-08	5.25
14	2.10E-06	7.83E-08	3.72	2.04E-06	9.75E-08	4.77	1.97E-06	1.19E-07	6.03
16	2.39E-06	9.99E-08	4.17	2.32E-06	1.25E-07	5.39	2.23E-06	1.53E-07	6.86
18	2.67E-06	1.24E-07	4.66	2.58E-06	1.56E-07	6.05	2.48E-06	1.91E-07	7.71
20	2.94E-06	1.52E-07	5.18	2.83E-06	1.90E-07	6.73	2.71E-06	2.32E-07	8.54
5-years <sup>2</sup>									
Burnup GWd/MTU	0% void fraction			40% void fraction			70% void fraction		
	Mean	2 $\sigma$	2 $\sigma$ %	Mean	2 $\sigma$	2 $\sigma$ %	Mean	2 $\sigma$	2 $\sigma$ %
2	2.19E-07	6.35E-09	2.90	2.16E-07	5.87E-09	2.72	2.12E-07	5.39E-09	2.54
4	5.18E-07	1.44E-08	2.78	5.07E-07	1.39E-08	2.73	4.96E-07	1.36E-08	2.75
6	8.42E-07	2.21E-08	2.63	8.22E-07	2.32E-08	2.82	8.02E-07	2.52E-08	3.14
8	1.17E-06	3.11E-08	2.66	1.14E-06	3.56E-08	3.12	1.11E-06	4.17E-08	3.76
10	1.49E-06	4.37E-08	2.93	1.45E-06	5.23E-08	3.60	1.41E-06	6.30E-08	4.47
12	1.80E-06	5.91E-08	3.27	1.75E-06	7.47E-08	4.26	1.70E-06	8.92E-08	5.25
14	2.11E-06	7.84E-08	3.72	2.04E-06	9.91E-08	4.85	1.97E-06	1.19E-07	6.03
16	2.39E-06	9.99E-08	4.17	2.32E-06	1.26E-07	5.46	2.23E-06	1.53E-07	6.85
18	2.67E-06	1.24E-07	4.66	2.58E-06	1.57E-07	6.10	2.48E-06	1.91E-07	7.71
20	2.94E-06	1.52E-07	5.17	2.83E-06	1.90E-07	6.73	2.71E-06	2.32E-07	8.54

Note: <sup>1</sup>SC20 results are not included; <sup>2</sup>SC20 and SC1 results are not included.

**Table 4.38. Statistics for  $^{152}\text{Sm}$  concentration (KENOREST, CA1, SC2 are removed)**

0-years									
Burnup GWd/MTU	0% void fraction			40% void fraction			70% void fraction		
	Mean	$2\sigma$	$2\sigma\%$	Mean	$2\sigma$	$2\sigma\%$	Mean	$2\sigma$	$2\sigma\%$
2	2.19E-07	6.04E-09	2.75	2.16E-07	5.58E-09	2.59	2.12E-07	5.13E-09	2.42
4	5.17E-07	1.31E-08	2.53	5.06E-07	1.21E-08	2.40	4.95E-07	1.14E-08	2.30
6	8.40E-07	1.86E-08	2.21	8.20E-07	1.78E-08	2.17	7.98E-07	1.74E-08	2.18
8	1.17E-06	2.31E-08	1.98	1.14E-06	2.35E-08	2.07	1.10E-06	2.46E-08	2.23
10	1.49E-06	2.96E-08	1.99	1.44E-06	3.08E-08	2.13	1.40E-06	3.28E-08	2.34
12	1.79E-06	3.61E-08	2.01	1.74E-06	3.95E-08	2.27	1.68E-06	4.50E-08	2.67
14	2.09E-06	4.56E-08	2.18	2.02E-06	5.08E-08	2.51	1.95E-06	5.65E-08	2.89
16	2.38E-06	5.39E-08	2.27	2.29E-06	6.09E-08	2.65	2.21E-06	6.92E-08	3.14
18	2.65E-06	6.32E-08	2.38	2.55E-06	7.33E-08	2.87	2.45E-06	8.48E-08	3.47
20	2.91E-06	7.59E-08	2.61	2.79E-06	8.81E-08	3.15	2.67E-06	1.01E-07	3.78

Note: SC20, SC2, KENOREST, CA1 results are not included.

#### 4.7.11. $^{155}\text{Eu}$

Concentrations of  $^{155}\text{Eu}$  at different void fractions and after five-year decay are compared in Figures 4.109 and 4.110. Groupings in the code results are clearly observed in the figures. HELIOS, CA1 and SCALE codes using ENDFB-V library (SC2, SC4, SC5) are grouped together and predict the lower concentrations with a large negative bias compared to other code results. While the lowest concentrations are predicted by SC2, the largest concentrations are predicted by KE2 (JEFF2.2). Similar trends in  $^{155}\text{Eu}$  concentrations are observed at all void fractions and after five-year decay. However, CA1 results exhibit a bias with respect to results located in the bottom group after five-year decay.

Statistics for  $^{155}\text{Eu}$  concentrations are provided in Table 4.39. Because of the large differences in the predicted concentrations between the two groups of results,  $^{155}\text{Eu}$  concentrations have the largest standard deviations in all fission product nuclides investigated in this benchmark. Standard deviations in the results increase with burnup and void fraction and decrease by 50% after five-year decay. The largest relative standard deviation is 26% at peak reactivity. This value increases to 28% at the end of depletion.

**Figure 4.109. <sup>155</sup>Eu concentration at 40% void fraction**

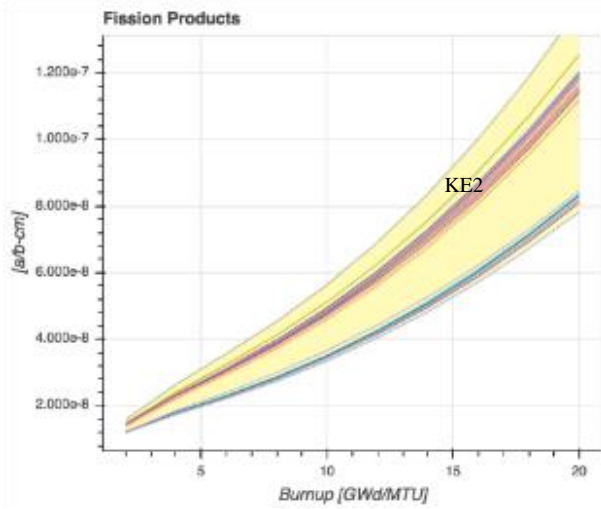


**Figure 4.110. <sup>155</sup>Eu concentration at 40% void fraction with five-year decay**

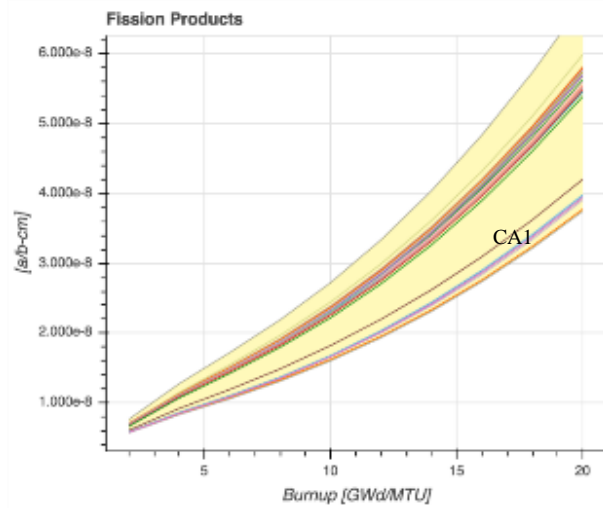


**Table 4.39. Statistics for <sup>155</sup>Eu concentration**

0-years <sup>1</sup>									
Burnup GWd/MTU	0% void fraction			40% void fraction			70% void fraction		
	Mean	2σ	2σ%	Mean	2σ	2σ%	Mean	2σ	2σ%
2	1.39E-08	1.80E-09	12.92	1.39E-08	1.95E-09	14.04	1.39E-08	2.09E-09	15.05
4	2.20E-08	4.24E-09	19.25	2.19E-08	4.48E-09	20.42	2.19E-08	4.71E-09	21.51
6	2.89E-08	6.41E-09	22.19	2.89E-08	6.71E-09	23.18	2.90E-08	7.01E-09	24.13
8	3.61E-08	8.52E-09	23.61	3.64E-08	8.93E-09	24.49	3.69E-08	9.34E-09	25.32
10	4.42E-08	1.08E-08	24.53	4.50E-08	1.14E-08	25.29	4.60E-08	1.20E-08	26.02
12	5.34E-08	1.35E-08	25.29	5.49E-08	1.43E-08	25.98	5.65E-08	1.50E-08	26.63
14	6.39E-08	1.66E-08	25.99	6.62E-08	1.76E-08	26.59	6.85E-08	1.86E-08	27.19
16	7.59E-08	2.02E-08	26.59	7.90E-08	2.14E-08	27.14	8.21E-08	2.27E-08	27.68
18	8.94E-08	2.42E-08	27.06	9.33E-08	2.57E-08	27.56	9.73E-08	2.73E-08	28.06
20	1.04E-07	2.87E-08	27.46	1.09E-07	3.05E-08	27.90	1.14E-07	3.24E-08	28.35



**Table 4.39. Statistics for <sup>155</sup>Eu concentration (continued)**

5-years <sup>2</sup>									
Burnup GWd/MTU	0% void fraction			40% void fraction			70% void fraction		
	Mean	2σ	2σ%	Mean	2σ	2σ%	Mean	2σ	2σ%
2	6.71E-09	8.68E-10	12.95	6.70E-09	9.38E-10	14.00	6.71E-09	1.01E-09	14.98
4	1.06E-08	2.04E-09	19.20	1.06E-08	2.15E-09	20.37	1.06E-08	2.26E-09	21.44
6	1.39E-08	3.08E-09	22.12	1.39E-08	3.22E-09	23.11	1.40E-08	3.37E-09	24.07
8	1.74E-08	4.10E-09	23.59	1.76E-08	4.31E-09	24.52	1.78E-08	4.48E-09	25.22
10	2.13E-08	5.22E-09	24.50	2.17E-08	5.48E-09	25.25	2.22E-08	5.76E-09	25.99
12	2.57E-08	6.51E-09	25.28	2.64E-08	6.86E-09	25.93	2.72E-08	7.24E-09	26.59
14	3.08E-08	8.00E-09	25.95	3.19E-08	8.45E-09	26.52	3.30E-08	8.96E-09	27.14
16	3.66E-08	9.72E-09	26.56	3.80E-08	1.03E-08	27.08	3.96E-08	1.09E-08	27.65
18	4.31E-08	1.17E-08	27.05	4.49E-08	1.24E-08	27.51	4.69E-08	1.31E-08	28.02
20	5.03E-08	1.38E-08	27.41	5.26E-08	1.47E-08	27.88	5.50E-08	1.56E-08	28.32

Note: <sup>1</sup>SC20 results are not included; <sup>2</sup>SC20 and SC1 results are not included.

#### 4.8. Comparison of SCALE code results

More than half of the submitted results in this benchmark were obtained using SCALE codes. SCALE code results exhibit a large spread in  $k_{inf}$  and nuclide concentrations. Comparisons of  $k_{inf}$  results by SCALE codes are shown in Figures 4.111 and 4.112 at 0% and 70% void fraction for the peak reactivity region. Groups in the results are observed in the figures, attributed largely to the different cross-section library used in the calculations. SCALE offers different transport solvers and cross-section libraries for lattice physics problems. SCALE sequences and cross-section libraries used by the participants include:

- TRITON/CE KENO-VI (MC transport solver with continuous-energy library)
  - ENDF/B-VII.0
- TRITON/MG KENO-VI (MC transport solver with multigroup energy library)
  - ENDF/B-VII.0 238 group
- TRITON/NEWT (deterministic slice balance transport solver with multigroup energy library)
  - ENDF/B-V 44 group
  - ENDF/B-V 238 group
  - ENDF/B-VI 238 group
  - ENDF/B-VII.0 238 group
  - ENDF/B-VII.1 252 group
  - ENDF/B-VII.1 56 group
- Polaris (deterministic Methods of Characteristics (MOC) transport solver with multigroup energy library)
  - ENDF/B-VII.1 252 group
  - ENDF/B-VII.1 56 group

**Figure 4.111. SCALE  $k_{inf}$  results at 0% void fraction in 6-14 GWd/MTU interval**

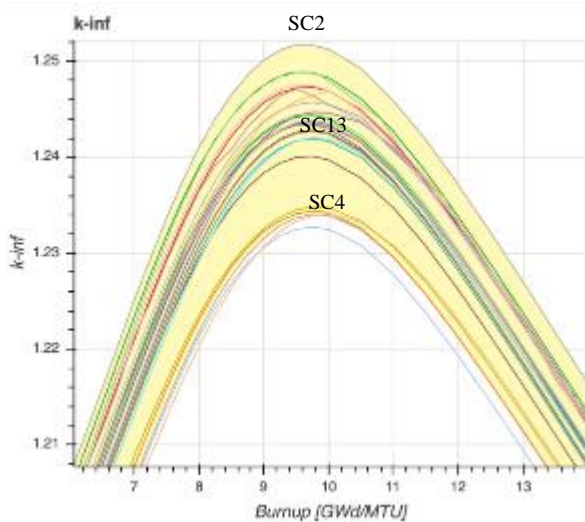
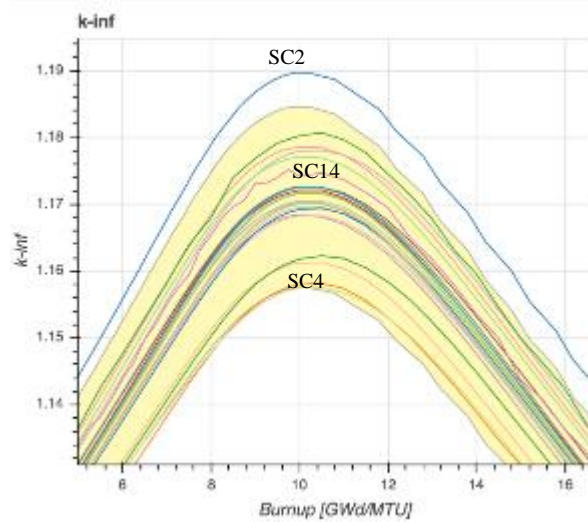


**Figure 4.112. Comparison SCALE  $k_{inf}$  results at 70% void fraction in 5-16 GWd/MTU interval**



A potential significant source of variation in the SCALE results is attributed to the treatment of Dancoff factors for cross-section processing. Dancoff factors are important in the processing of multigroup cross sections, especially for BWR lattice problems. TRITON does not offer an option for automated Dancoff factor calculations for heterogeneous lattice geometries (the default is to apply factors for an infinite pin cell lattice). Improved pin-specific Dancoff factors can be calculated externally using the SCALE/MCDANCOFF sequence, which requires another input model.

At least one SCALE code result (SC9) did not include externally calculated Dancoff factors for the benchmark calculations. Very similar results were observed for the results of SC1 and SC11; however, it is not known if these contributions applied external Dancoff factors.

The lowest  $k_{inf}$  results are attributed to the codes using ENDF/B-V and ENDF/B-VI libraries. There is also a clear separation in results of the codes using ENDF/B-VII.0 and ENDF/B-VII.1 libraries at 70% void fraction (Figure 4.112). SC14 (KENO-VI using CE ENDF/B-VII.0 library) results are near the average  $k_{inf}$  (Figure 4.112). The oscillations in SC14 results indicate a potential convergence problem (i.e. inadequate number of cycles/generations for MC calculations).

SC2 results predict the highest  $k_{inf}$  at all void fractions and are separated from all other SCALE code results at 70% void fraction. Considering that SC2 and SC4 results were calculated using the same cross-section library (ENDF/B-V 44 group), the bias observed in SC2 results at high void fraction may again be due to the Dancoff factor treatment. The highest  $k_{inf}$  values inside the  $2\sigma$  band are calculated by SC1 (ENDF/B-VII.0 238 group), SC11 (ENDF/B-VII.0 238 group) and SC9 (ENDF/B-VII.1 252 group).

#### 4.8.1. TRITON/NEWT results using only ENDF/B-VII.1 252g library

To reduce differences due to different transport solvers and cross-section libraries, the results of SCALE codes using the TRITON/NEWT sequence using only the ENDF/B-VII.1 252 group library are compared around the peak reactivity region in Figure 4.113. SE1 results (SERPENT with ENDF/B-VII.0) are also included to provide a comparison with an

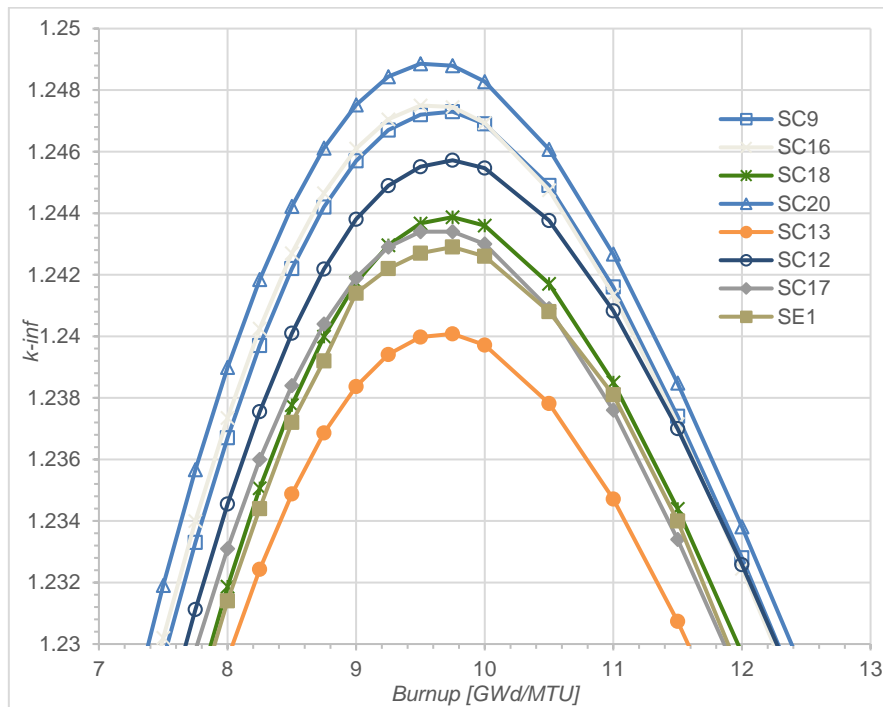
MC code using a modern data library. Considering that the same cross-section library and SCALE versions were used, the variation in the calculated  $k_{inf}$  (~800 pcm) is likely to be largely attributed to selected cross-section processing treatment and transport solution options.

In addition to different transport code options and cross-section libraries used in the benchmark, participants also used several different solution and modelling options. Based on input files submitted by several participants, and information provided with each submission, SCALE users selected different strategies in their models. For example, while some participants applied high fidelity calculations by increasing angular mesh quadrature order (e.g. Sn=16 instead of default Sn=6) and increasing convergence criteria and spatial mesh size in the deterministic solutions, other participants applied faster, low fidelity depletion solutions by increasing convergence criteria. Several participants used an approximate cross-section collapse option (*weight*) that collapses a fine group library to a broad group library. A critical spectrum option was also used by some participants.

The largest  $k_{inf}$  values are calculated by SC20. However, as discussed in Section 4.6, the actinide concentrations predicted by SC20 suggest a possible anomaly in the initial uranium fuel specification in the SC20 input model. If SC20 is removed from consideration, the highest  $k_{inf}$  values are calculated by SC16 and SC9. The SC9 model does not include external Dancoff factors, and higher  $k_{inf}$  values are expected. The SC16 model includes external Dancoff factors; however, this model also uses the “weight” option for the transport calculations. The weight option collapses multigroup cross sections to a smaller energy group set using the initial flux spectrum calculation, and applies this collapsed library for the remainder of the depletion calculation. While this option provides fast depletion calculations and generally acceptable results in many cases, larger differences can be expected when the initial flux spectrum (initial fuel composition with full gadolinium inventory) is not representative of the statepoint of interest (i.e. peak reactivity with near fully depleted gadolinium inventory).

The lowest  $k_{inf}$  values are calculated by SC13. However, details of the input model were not available. SC17, SC18 and SE1 results show good agreement at all void fractions. The largest difference in  $k_{inf}$  values calculated by SC17 and SC18 is less than 300 pcm at all void fractions. Based on the declared information with submitted results, the difference is expected to be due to the use of critical spectrum in SC17 results and of higher order quadrature (Sn=16) and a finer spatial mesh (8x8) used in SC18.

**Figure 4.113. Comparison of SCALE (TRITON/NEWT)  $k_{inf}$  results with ENDF/B-VII.1 252g cross-section library at 0% void fraction**



#### 4.8.2. Additional analysis of modelling and solution options in TRITON/NEWT

The TRITON depletion sequence uses a mid-point depletion scheme. Therefore, transport calculations are only executed at the mid-exposure point of each depletion step. Since  $k_{inf}$  results at each depletion step were requested, the  $k_{inf}$  should be interpolated to the requested time step or separate transport calculations performed at the requested time steps. The second option is more rigorous; however, this requires either adding a very small time step at each point (doubling the number of transport calculations) or extracting nuclide concentrations at each depletion step and executing a separate set of NEWT calculations.

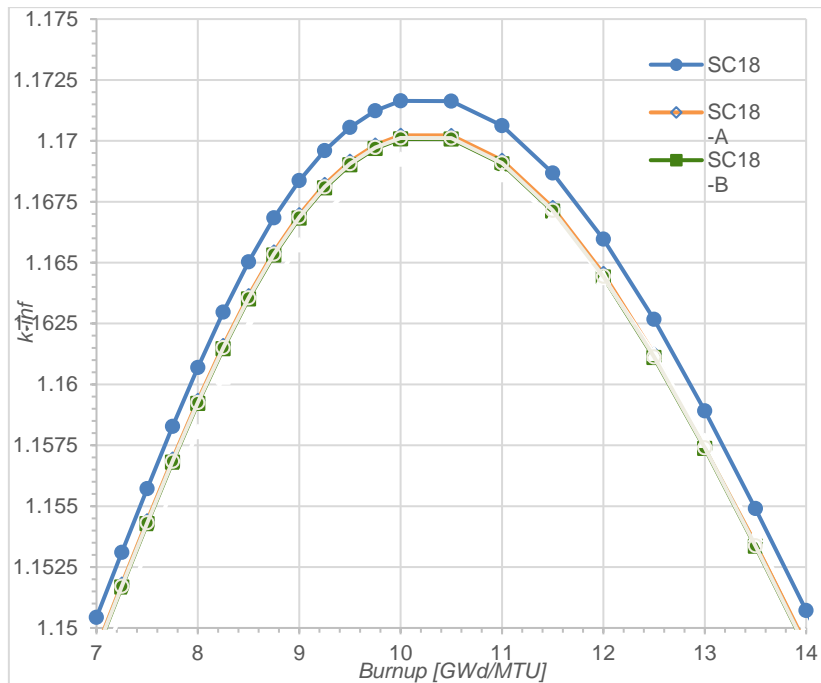
The effect of different solutions and modelling options are illustrated using four additional TRITON/NEWT calculations. These results were not included in the statistical analysis for the benchmark and were used only for sensitivity studies. The reference SC18 model and the model variations are as follows:

- SC18: explicit NEWT transport calculation after each depletion calculation (i.e. no interpolation of results was performed), fine spatial mesh (sides=20, 8x8 pin cell resolution) and Sn=16 quadrature order;
- SC18-A: interpolated  $k_{inf}$  default options;
- SC18-B: the SC18-A model with fine spatial mesh (sides=20, 8x8 pin cell resolution);
- SC18-C: the SC18-A model using a critical spectrum in depletion calculations;
- SC18-D: the SC18-A model high using order scattering (Pn=3).

Results using these models are plotted in Figure 4.114 for the 70% void fraction case. The largest differences are observed between SC18 and SC18-C models. Figure 4.114 shows that the TRITON/NEWT transport solution options can change the results as much as 250

pcm for the same model. Although not as large as other contributing factors, the observed differences likely contribute to some of the variations seen in Figure 4.113.

**Figure 4.114. Comparison of ORNL SCALE(TRITON/NEWT)  $k_{inf}$  results at 70% void fraction in 7-14 GWd/MTU interval**



#### 4.9. Effect of nuclear data libraries

Nuclear data refers to cross section, fission yield and decay data in depletion calculations. Cross-section data are used in transport calculations, while fission yield and decay data are used in depletion calculations. The effect of data libraries on  $k_{inf}$  or predicted nuclide concentrations is difficult to evaluate given that differences in transport solvers and modelling options also cause significant differences in results. Moreover, cross-section processing and deterministic solution options (i.e. spatial mesh, quadrature order) can also change depletion results considerably.

Results from the same depletion code using different libraries or results from different depletion codes using the same libraries can help to identify contributions from different components of depletion calculations to observed differences in  $k_{inf}$  or nuclide concentrations. Therefore, multiple code submissions from institutions are invaluable for this benchmark.

Results of KENOREST codes using different cross-section libraries are shown in Figure 4.115 at 40% void fraction. As discussed in Section 4.3, KE2 (JEFF2.2) results are separated from KE1 (ENDF/B-VII) and KE3 (JENDL/AC) by more than 1 000 pcm difference. Furthermore, VESTA results (Figure 4.116) show that differences in nuclear data libraries have more effect on the  $k_{inf}$  results than differences in MC transports solvers (MCNP6 vs. MORET). VESTA results (VE3P, VE4P) using different MC codes with the same cross-section library agree well ( $\sim 100$  pcm), while VESTA results (VE4P, VE5P3) using the same the same MC code with different cross-section libraries differ more than  $\sim 300$  pcm in  $k_{inf}$ .

Section 4.4 provides an overview of multigroup libraries and trends seen in the deterministic results. The effect of new versus old generations of libraries can be seen in Figures 4.11 and 4.12. When variations in the results of deterministic codes are evaluated with and without inclusion of results using ENDF/B-V and ENDF/B-VI libraries, a large reduction in  $2\sigma$  (1 300 pcm vs. 350 pcm) is observed.

**Figure 4.115. KENOREST  $k_{inf}$  results at 40% void fraction**

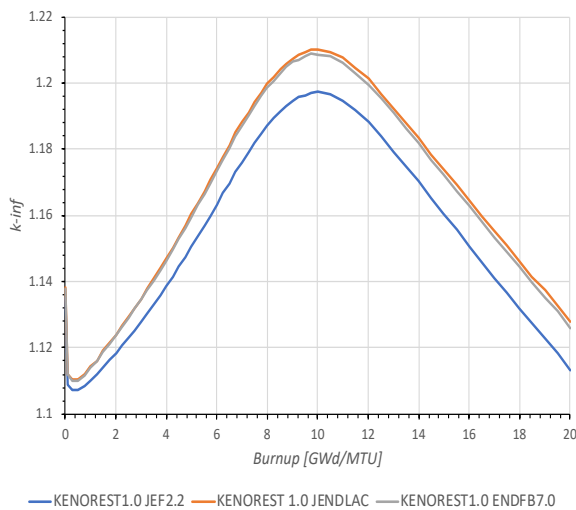
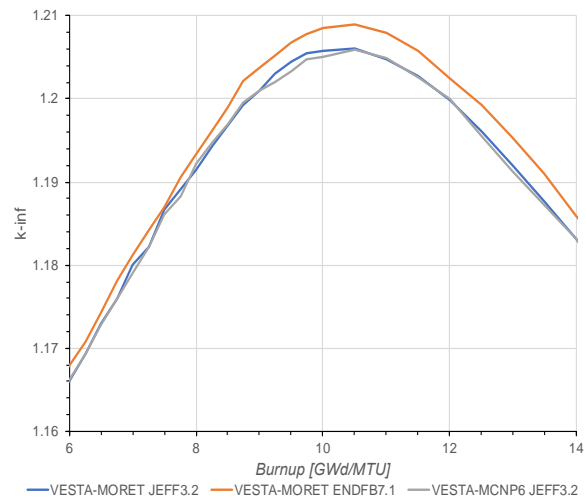


**Figure 4.116. VESTA (predictor only)  $k_{inf}$  results at 40% void fraction in 6-14 GWd/MTU interval**



While not as clearly identifiable as  $k_{inf}$  differences, and difficult to group due to the use of mixed/corrected libraries, the effect of differences in nuclear data libraries can also be observed in calculated nuclide concentrations.

Comparisons of  $^{154}\text{Gd}$  concentrations are discussed in Section 4.5.1 in detail. In general, codes using JEFF libraries predict lower  $^{154}\text{Gd}$  concentrations compared to codes using ENDF/B libraries. Although differences in KENOREST calculated nuclide concentrations are seen in many fission products, the most significant differences are observed in  $^{149}\text{Sm}$  concentrations. KE2 (JEFF2.2) predicts 6% higher concentrations than KE3 (JENDL/AC) and KE1 (ENDF/B-VII.0) codes at peak reactivity. Furthermore, codes with different transport solvers (MC and deterministic) using JEFF3 libraries predict lower  $^{149}\text{Sm}$  concentrations than other codes.

Concentrations of  $^{149}\text{Sm}$  calculated by KE2 and CA1 exhibit a different trend with burnup compared to trends seen in other results. Both codes use JEFF2.2 (CA1 library is a mixture of ENDF/B-VI and JEFF2.2) libraries. Similar agreement between CA1 and KE2 results are also observed in concentrations of  $^{236}\text{U}$  at all void fractions.

$^{155}\text{Eu}$  is another fission product that shows clear grouping in the predicted concentrations based on the cross-section library. Concentrations calculated by HELIOS, SCALE and CA1 using older libraries (ENDF/B-V, ENDF/B-VI and JEFF2.2) are 40% lower than the concentrations calculated by other codes at peak reactivity, and a significant bias between the results of these two groups is observed.

## 5. Conclusions

For this report, the results of 37 submitted depletion calculations were thoroughly compared, and the lattice average actinide and fission product concentrations and the spatial variation of  $^{155}\text{Gd}$  and  $^{157}\text{Gd}$  concentrations in gadolinia rods with burnup were analysed. The statistics for analysed nuclide concentrations and  $k_{inf}$  are provided as a function of burnup and void fraction. In these analyses, several submissions were removed due to suspected input errors in results that were out of trend.

Although results generated with the same depletion code tend to show agreement, trends in nuclide concentrations and  $k_{inf}$  with burnup show that results are more often correlated based on the nuclear data used in calculations. However, more specific conclusions based on nuclear data are not possible because of other non-library parameters that impact the results, as well as the use of mixed/corrected cross-section libraries and different fission yield libraries.

When all code results are considered,  $k_{inf}$  statistics at 10 GWd/MTU (approximate burnup at peak reactivity for all void fractions) show that the maximum relative  $2\sigma$  is 1.33% at 70% void fraction. When results outside the  $2\sigma$  band are removed, the maximum deviation reduces to 0.61% for continuous-energy Monte Carlo (CE MC) code results. The deviation in deterministic code results is around 1.02% when results outside the  $2\sigma$  band are eliminated. However, if the results with earlier generation cross-section libraries, ENDF/B-V and ENDF/B-VI, are removed from statistics, the maximum standard deviation reduces to 0.50% for the deterministic codes. The CE MC codes only used modern and up-to-date libraries.

Higher relative and absolute standard deviations in MC code results could be due to:

1. The large number of submissions using MG SCALE codes, which can lower the standard deviation due to agreement among the same code results.
2. Apparent convergence issues in some MC code results.

Oscillations in  $k_{inf}$  results with burnup, as seen in Figure 4.8, are indications of unconverged  $k_{inf}$  solutions. Considering that  $k_{inf}$  is an integral parameter which is expected to converge faster than spatially varying quantities, i.e. pin powers, ring by ring nuclide concentrations, etc., the effect of an unconverged solution can be more significant on the calculated nuclide concentrations.

Standard deviation in peak reactivity burnup also increases with void fraction. The maximum difference in the predicted burnups varies from 0.5 GWd/MTU to 1.25 GWd/MTU.

Gadolinium isotope concentrations in gadolinia rods were analysed in detail. Because of their large capture cross section,  $^{155}\text{Gd}$  and  $^{157}\text{Gd}$  are the most important isotopes for calculations up to 15 GWd/MTU. At peak reactivity, relative  $2\sigma$  standard deviations in  $^{155}\text{Gd}$  and  $^{157}\text{Gd}$  concentrations are 44% and 21%, respectively. Given that the capture cross section of  $^{157}\text{Gd}$  is four times larger than that of  $^{155}\text{Gd}$ , most of  $^{157}\text{Gd}$  is depleted at peak reactivity. While the highest absolute standard deviation in  $^{157}\text{Gd}$  concentration is observed at 2 GWd/MTU, the highest relative standard deviation in  $^{157}\text{Gd}$  concentration is 60% and is observed at 8 GWd/MTU. Large sensitivity to void fraction is also observed in standard deviations.

The spatial variation of  $^{155}\text{Gd}$  and  $^{157}\text{Gd}$  concentrations were also analysed. While the largest standard deviation in the results is observed in the innermost ring (ring 1), the largest relative standard deviation is observed in the middle rings. Increased standard deviations around peak reactivity (8-10 GWd/MTU) for  $^{155}\text{Gd}$  and  $^{157}\text{Gd}$  concentrations are consistent with increased standard deviations in  $k_{inf}$ .

The smallest variation in actinide concentrations is observed in  $^{238}\text{U}$ . Relative standard deviation in  $^{238}\text{U}$  concentration does not exceed 0.07% throughout the depletion.  $^{236}\text{U}$  concentration shows the largest relative deviation (2.2% at peak reactivity) among all uranium isotopes. Standard deviations in  $^{235}\text{U}$  and  $^{234}\text{U}$  concentrations exhibit similar increasing trends with burnup. At peak reactivity, the maximum relative standard deviations are 0.56% and 0.88% for  $^{235}\text{U}$  and  $^{234}\text{U}$  concentrations, respectively. Unlike other uranium isotopes, the largest standard deviation in  $^{235}\text{U}$  concentration is observed at 0% void fraction as opposed to 70% void fraction.

$^{237}\text{Np}$ ,  $^{239}\text{Pu}$ ,  $^{240}\text{Pu}$ ,  $^{241}\text{Pu}$  and  $^{241}\text{Am}$  concentrations show similar relative standard deviations, with the relative standard deviation around 6% at peak reactivity.  $^{238}\text{Pu}$  (13%) and  $^{242}\text{Pu}$  (10%) concentrations have the largest relative standard deviations among all actinides. A decay time of five years does not change the statistics for actinides significantly. Removing results outside the  $2\sigma$  band reduces the standard deviation for  $^{239}\text{Pu}$  and  $^{241}\text{Pu}$  concentrations by half.

Samarium isotope concentrations, especially  $^{149}\text{Sm}$  and  $^{151}\text{Sm}$  concentrations, show large standard deviations. Relative standard deviations in  $^{147}\text{Sm}$  and  $^{152}\text{Sm}$  concentrations are 1.2% and 4.5%, respectively. Relative standard deviation of  $^{149}\text{Sm}$  and  $^{151}\text{Sm}$  concentrations are around 10% at peak reactivity. The largest relative standard deviations are observed in  $^{155}\text{Eu}$  concentrations (26% at peak reactivity), while  $^{155}\text{Eu}$  also has the lowest concentration in all analysed fission products.



## *References*

- NEA (2016), “Burn-up Credit Criticality Safety Benchmark Phase III-C: Nuclide Composition and Neutron Multiplication Factor of a Boiling Water Reactor Spent Fuel Assembly for Burn-up Credit and Criticality Control of Damaged Nuclear Fuel”, NEA/NSC/DOC(2015)6, OECD Publishing, Paris, [www.oecd-nea.org/jcms/pl\\_19674](http://www.oecd-nea.org/jcms/pl_19674).
- NEA (2002), “OECD/NEA burnup credit criticality benchmarks phase IIIB: Burnup calculations of BWR fuel assemblies for storage and transport”, NEA/NSC/DOC(2002)2, OECD Publishing, Paris, [www.oecd-nea.org/jcms/pl\\_17690](http://www.oecd-nea.org/jcms/pl_17690).
- Bokeh Server Documentation (2018), <https://bokeh.pydata.org/en/latest/>, accessed September 2018.

## Annex A. Participant list

Contact Person	Institution	Email
Ludvyvine Jutier	IRSN (Institut de radioprotection et de sûreté nucléaire)	<a href="mailto:ludvyvine.jutier@irsn.fr">ludvyvine.jutier@irsn.fr</a>
Kenya Suyama	JAEA (Japan Atomic Energy Agency)	<a href="mailto:suyama.kenya@jaea.go.jp">suyama.kenya@jaea.go.jp</a>
Lukasz Koszuk	National Centre for Nuclear Research, Poland	<a href="mailto:l.kozzuk@ncbj.gov.pl">l.kozzuk@ncbj.gov.pl</a>
Dennis Mennerdahl	E Mennerdahl Systems	<a href="mailto:dennis.mennerdahl@ems.se">dennis.mennerdahl@ems.se</a>
Ugur Merturek	ORNL (Oak Ridge National Laboratory)	<a href="mailto:mertureku@ornl.gov">mertureku@ornl.gov</a>
Marcel Tardy	Orano TN	<a href="mailto:marcel.tardy@orano.group">marcel.tardy@orano.group</a>
Stefano Caruso	Nagra	<a href="mailto:stefano.caruso@nagra.ch">stefano.caruso@nagra.ch</a>
Sven Tittelbach	WTI (Wissenschaftlich-Technische Ingenieurberatung GmbH)	<a href="mailto:tittelbach@wti-juelich.de">tittelbach@wti-juelich.de</a>
Carlos Casado Sanchez	ENUSA	<a href="mailto:cbs@enusa.es">cbs@enusa.es</a>
Pedro Ortego	SEA	<a href="mailto:p.ortego@seaingenieria.es">p.ortego@seaingenieria.es</a>
Fabian Sommer	GRS (Gesellschaft für Anlagen- und Reaktorsicherheit)	<a href="mailto:fabian.Sommer@grs.de">fabian.Sommer@grs.de</a>
Anssu Ranta-aho	TVO (Teollisuuden Voima Oyj)	<a href="mailto:anssu.ranta-aho@tvo.fi">anssu.ranta-aho@tvo.fi</a>
Nadia Messaoudi	SCK CEN	<a href="mailto:nmessaou@sckcen.be">nmessaou@sckcen.be</a>
Gwanyoung Kim	KINS (Korea Institute of Nuclear Safety)	<a href="mailto:k722kgy@kins.re.kr">k722kgy@kins.re.kr</a>

## Annex B. Results from all participants

Table B.1.  $K_{inf}$  results from all participants at 0% void fraction (1/4)

Burnup (GWd/MTU)	AL1	AP1	CA1	HE1	HE2	HE3	HE4	KE1	KE2	KE3	MO1	SC1	SC10	SC11	SC12	SC13	SC14	SC15	SC16
0.00	1.1612	1.1545	1.1596	1.1514	1.1668	1.1563	1.1539	1.1649	1.1591	1.1648	1.1575	-	1.1553	1.1561	1.1549	1.1523	1.1583	1.1568	1.1542
0.10	1.1327	1.1267	1.1317	1.1237	1.1385	1.1287	1.1264	1.1370	1.1309	1.1374	1.1299	1.1318	1.1276	1.1296	1.1275	1.1249	1.1314	1.1288	1.1270
0.25	1.1310	1.1256	1.1304	1.1224	1.1371	1.1275	1.1254	1.1349	1.1294	1.1351	1.1291	1.1314	1.1262	1.1279	1.1262	1.1235	1.1291	1.1276	1.1257
0.50	1.1309	1.1258	1.1305	1.1223	1.1368	1.1275	1.1256	1.1347	1.1287	1.1346	1.1299	1.1308	1.1263	1.1271	1.1263	1.1236	1.1306	1.1278	1.1259
0.75	1.1322	1.1275	1.1322	1.1238	1.1380	1.1291	1.1275	1.1354	1.1294	1.1357	1.1323	1.1330	1.1281	1.1279	1.1280	1.1253	1.1313	1.1296	1.1277
1.00	1.1341	1.1298	1.1345	1.1260	1.1399	1.1314	1.1300	1.1375	1.1311	1.1376	1.1340	1.1353	1.1305	1.1300	1.1305	1.1278	1.1340	1.1321	1.1302
1.25	1.1362	1.1324	1.1369	1.1284	1.1420	1.1340	1.1328	1.1395	1.1329	1.1397	1.1364	1.1374	1.1333	1.1326	1.1333	1.1306	1.1367	1.1349	1.1332
1.50	1.1386	1.1351	1.1394	1.1310	1.1443	1.1367	1.1358	1.1416	1.1349	1.1420	1.1400	1.1395	1.1362	1.1354	1.1363	1.1335	1.1401	1.1378	1.1363
1.75	1.1409	1.1378	1.1420	1.1337	1.1466	1.1395	1.1388	1.1441	1.1367	1.1446	1.1421	1.1424	1.1392	1.1383	1.1394	1.1365	1.1442	1.1407	1.1394
2.00	1.1433	1.1406	1.1446	1.1364	1.1490	1.1423	1.1419	1.1469	1.1392	1.1474	1.1446	1.1453	1.1422	1.1413	1.1426	1.1396	1.1464	1.1437	1.1427
2.25	1.1457	1.1433	1.1472	1.1391	1.1514	1.1451	1.1449	1.1498	1.1418	1.1501	1.1480	1.1483	1.1452	1.1443	1.1457	1.1427	1.1493	1.1467	1.1460
2.50	1.1483	1.1461	1.1499	1.1418	1.1538	1.1479	1.1481	1.1527	1.1442	1.1529	1.1514	1.1513	1.1483	1.1474	1.1490	1.1458	1.1526	1.1497	1.1493
2.75	1.1506	1.1490	1.1527	1.1446	1.1562	1.1508	1.1512	1.1560	1.1469	1.1563	1.1544	1.1541	1.1514	1.1506	1.1523	1.1490	1.1555	1.1528	1.1527
3.00	1.1534	1.1518	1.1555	1.1474	1.1587	1.1537	1.1545	1.1585	1.1498	1.1591	1.1581	1.1570	1.1546	1.1536	1.1556	1.1523	1.1588	1.1559	1.1561
3.25	1.1560	1.1548	1.1584	1.1502	1.1612	1.1567	1.1577	1.1622	1.1527	1.1624	1.1609	1.1603	1.1579	1.1568	1.1590	1.1556	1.1612	1.1591	1.1596
3.50	1.1587	1.1578	1.1614	1.1532	1.1638	1.1597	1.1611	1.1654	1.1563	1.1659	1.1642	1.1636	1.1613	1.1601	1.1625	1.1590	1.1653	1.1624	1.1632
3.75	1.1615	1.1609	1.1644	1.1562	1.1664	1.1628	1.1645	1.1693	1.1592	1.1699	1.1677	1.1667	1.1647	1.1634	1.1660	1.1624	1.1682	1.1657	1.1669
4.00	1.1644	1.1640	1.1675	1.1592	1.1691	1.1660	1.1680	1.1731	1.1630	1.1733	1.1715	1.1699	1.1682	1.1669	1.1696	1.1659	1.1721	1.1691	1.1706
4.25	1.1673	1.1673	1.1706	1.1623	1.1719	1.1682	1.1716	1.1768	1.1665	1.1773	1.1747	1.1733	1.1718	1.1704	1.1733	1.1695	1.1757	1.1726	1.1744
4.50	1.1703	1.1706	1.1739	1.1655	1.1747	1.1726	1.1752	1.1809	1.1702	1.1817	1.1781	1.1766	1.1755	1.1740	1.1771	1.1732	1.1790	1.1763	1.1783
4.75	1.1735	1.1740	1.1772	1.1688	1.1777	1.1760	1.1790	1.1849	1.1742	1.1857	1.1819	1.1805	1.1793	1.1777	1.1810	1.1770	1.1835	1.1800	1.1823
5.00	1.1768	1.1775	1.1807	1.1722	1.1806	1.1795	1.1829	1.1895	1.1781	1.1901	1.1858	1.1845	1.1832	1.1815	1.1849	1.1809	1.1867	1.1838	1.1864
5.25	1.1800	1.1811	1.1843	1.1757	1.1837	1.1832	1.1868	1.1941	1.1824	1.1947	1.1890	1.1880	1.1873	1.1854	1.1889	1.1848	1.1922	1.1877	1.1906
5.50	1.1835	1.1848	1.1880	1.1792	1.1869	1.1869	1.1909	1.1982	1.1863	1.1994	1.1945	1.1916	1.1914	1.1894	1.1931	1.1889	1.1955	1.1917	1.1949
5.75	1.1870	1.1887	1.1917	1.1829	1.1901	1.1907	1.1951	2.0033	1.1911	2.0038	1.1979	1.1959	1.1956	1.1936	1.1972	1.1930	1.1995	1.1957	1.1992
6.00	1.1907	1.1926	1.1956	1.1866	1.1935	1.1946	1.1994	2.0078	1.1955	2.0086	2.0023	2.002	1.1999	1.1977	2.0015	1.1972	2.0039	1.1999	2.0037
6.25	1.1943	1.1966	1.1996	1.1904	1.1969	1.1986	2.0037	2.0125	1.1997	2.0133	2.0065	2.0046	2.0043	2.0020	2.0058	2.0015	2.0075	2.0042	2.0082
6.50	1.1982	1.2006	1.2036	1.1944	2.0005	2.0027	2.0081	2.0170	2.0042	2.0178	2.0112	2.0090	2.0088	2.0064	2.0102	2.0068	2.0116	2.0085	2.0128
6.75	1.2022	1.2047	1.2077	1.1983	2.0041	2.0069	2.0126	2.0218	2.0086	2.0224	2.0161	2.0131	2.0132	2.0108	2.0146	2.0101	2.0161	2.0129	2.0173
7.00	1.2062	1.2089	1.2118	2.0023	2.0078	2.0111	2.0171	2.0260	2.0125	2.0267	2.0210	2.0173	2.0177	2.0152	2.0190	2.0144	2.0213	2.0172	2.0218
7.25	1.2104	1.2129	1.2159	2.0064	2.0115	2.0152	2.0214	2.0294	2.0166	2.0307	2.0249	2.0215	2.0220	2.0196	2.0232	2.0185	2.0250	2.0215	2.0262
7.50	1.2144	1.2169	1.2198	2.0103	2.0152	2.0193	2.0256	2.0335	2.0198	2.0342	2.0291	2.0258	2.0260	2.0239	2.0273	2.0225	2.0292	2.0255	2.0302

Table B.2.  $K_{inf}$  results from all participants at 0% void fraction (2/4)

7.75	1.2185	1.2205	1.2235	1.2141	1.2188	1.2231	1.2295	1.2366	1.2232	1.2380	1.2332	1.2296	1.2288	1.2279	1.2311	1.2262	1.2329	1.2292	1.2340
8.00	1.2223	1.2239	1.2270	1.2176	1.2223	1.2266	1.2330	1.2397	1.2261	1.2408	1.2361	1.2334	1.2331	1.2316	1.2345	1.2296	1.2365	1.2326	1.2374
8.25	1.2260	1.2268	1.2301	1.2208	1.2255	1.2298	1.2360	1.2426	1.2290	1.2434	1.2394	1.2365	1.2360	1.2349	1.2375	1.2324	1.2391	1.2356	1.2403
8.50	1.2293	1.2293	1.2328	1.2236	1.2284	1.2325	1.2386	1.2449	1.2312	1.2460	1.2420	1.2395	1.2384	1.2377	1.2401	1.2349	1.2408	1.2380	1.2427
8.75	1.2324	1.2314	1.2360	1.2261	1.2310	1.2348	1.2408	1.2469	1.2330	1.2476	1.2439	1.2416	1.2404	1.2401	1.2422	1.2369	1.2432	1.2400	1.2447
9.00	1.2347	1.2331	1.2369	1.2281	1.2332	1.2367	1.2425	1.2482	1.2342	1.2487	1.2457	1.2437	1.2419	1.2420	1.2438	1.2384	1.2448	1.2416	1.2461
9.25	1.2368	1.2342	1.2383	1.2296	1.2349	1.2381	1.2437	1.2487	1.2364	1.2496	1.2465	1.2448	1.2429	1.2434	1.2449	1.2394	1.2464	1.2427	1.2471
9.50	1.2384	1.2360	1.2393	1.2308	1.2363	1.2391	1.2444	1.2492	1.2366	1.2502	1.2473	1.2459	1.2434	1.2443	1.2455	1.2400	1.2471	1.2433	1.2475
9.75	1.2394	1.2362	1.2398	1.2315	1.2373	1.2396	1.2446	1.2490	1.2365	1.2489	1.2470	1.2464	1.2434	1.2447	1.2457	1.2401	1.2464	1.2435	1.2475
10.00	1.2399	1.2350	1.2399	1.2318	1.2378	1.2397	1.2444	1.2481	1.2348	1.2490	1.2464	1.2469	1.2430	1.2446	1.2455	1.2397	1.2455	1.2432	1.2489
10.50	1.2395	1.2335	1.2387	1.2310	1.2377	1.2386	1.2428	1.2453	1.2322	1.2467	1.2447	1.2450	1.2409	1.2436	1.2438	1.2378	1.2442	1.2415	1.2448
11.00	1.2374	1.2306	1.2363	1.2288	1.2361	1.2361	1.2398	1.2418	1.2289	1.2430	1.2412	1.2418	1.2376	1.2410	1.2408	1.2347	1.2406	1.2385	1.2414
11.50	1.2342	1.2268	1.2327	1.2256	1.2333	1.2326	1.2360	1.2377	1.2241	1.2387	1.2372	1.2377	1.2334	1.2374	1.2370	1.2307	1.2376	1.2345	1.2372
12.00	1.2299	1.2225	1.2285	1.2216	1.2296	1.2284	1.2316	1.2328	1.2196	1.2339	1.2324	1.2334	1.2287	1.2330	1.2326	1.2262	1.2324	1.2300	1.2325
12.50	1.2263	1.2178	1.2239	1.2171	1.2253	1.2237	1.2268	1.2273	1.2143	1.2287	1.2278	1.2283	1.2237	1.2282	1.2278	1.2213	1.2276	1.2251	1.2275
13.00	1.2203	1.2129	1.2190	1.2123	1.2206	1.2189	1.2218	1.2223	1.2088	1.2237	1.2227	1.2231	1.2186	1.2232	1.2228	1.2162	1.2229	1.2201	1.2224
13.50	1.2151	1.2079	1.2139	1.2074	1.2157	1.2139	1.2167	1.2172	1.2037	1.2183	1.2170	1.2176	1.2133	1.2181	1.2178	1.2111	1.2169	1.2150	1.2172
14.00	1.2098	1.2029	1.2088	1.2024	1.2107	1.2088	1.2116	1.2115	1.1983	1.2133	1.2118	1.2125	1.2081	1.2130	1.2127	1.2058	1.2121	1.2098	1.2119
14.50	1.2046	1.1979	1.2037	1.1973	1.2057	1.2037	1.2065	1.2067	1.1929	1.2079	1.2063	1.2077	1.2028	1.2078	1.2075	1.2006	1.2056	1.2046	1.2066
15.00	1.1993	1.1928	1.1985	1.1923	1.2006	1.1986	1.2014	1.2012	1.1875	1.2024	1.2010	1.2021	1.1975	1.2025	1.2024	1.1954	1.2025	1.1994	1.2014
15.50	1.1940	1.1878	1.1934	1.1872	1.1955	1.1935	1.1963	1.1960	1.1823	1.1974	1.1953	1.1965	1.1923	1.1973	1.1972	1.1902	1.1959	1.1943	1.1961
16.00	1.1887	1.1827	1.1882	1.1822	1.1904	1.1885	1.1911	1.1905	1.1770	1.1921	1.1906	1.1914	1.1870	1.1921	1.1921	1.1849	1.1913	1.1891	1.1909
16.50	1.1835	1.1777	1.1831	1.1772	1.1853	1.1834	1.1860	1.1858	1.1717	1.1872	1.1854	1.1863	1.1818	1.1869	1.1870	1.1797	1.1861	1.1839	1.1856
17.00	1.1782	1.1727	1.1780	1.1722	1.1802	1.1783	1.1810	1.1803	1.1665	1.1819	1.1799	1.1809	1.1765	1.1817	1.1819	1.1746	1.1814	1.1788	1.1804
17.50	1.1729	1.1677	1.1729	1.1672	1.1752	1.1733	1.1759	1.1755	1.1615	1.1765	1.1746	1.1758	1.1713	1.1766	1.1768	1.1694	1.1762	1.1737	1.1752
18.00	1.1677	1.1627	1.1679	1.1622	1.1701	1.1683	1.1708	1.1702	1.1564	1.1716	1.1690	1.1708	1.1661	1.1714	1.1717	1.1642	1.1713	1.1685	1.1700
18.50	1.1625	1.1578	1.1628	1.1572	1.1650	1.1632	1.1658	1.1652	1.1509	1.1666	1.1644	1.1655	1.1609	1.1663	1.1666	1.1591	1.1654	1.1634	1.1648
19.00	1.1573	1.1528	1.1578	1.1523	1.1600	1.1582	1.1607	1.1598	1.1462	1.1616	1.1591	1.1605	1.1557	1.1612	1.1615	1.1539	1.1615	1.1583	1.1596
19.50	1.1521	1.1478	1.1527	1.1473	1.1550	1.1532	1.1557	1.1551	1.1407	1.1567	1.1540	1.1552	1.1505	1.1561	1.1564	1.1488	1.1555	1.1532	1.1544
20.00	1.1469	1.1429	1.1477	1.1424	1.1499	1.1482	1.1507	1.1492	1.1362	1.1512	1.1489	1.1491	1.1453	1.1509	1.1513	1.1436	1.1499	1.1481	1.1492

Table B.3.  $K_{inf}$  results from all participants at 0% void fraction (3/4)

Burnup (GWd/MTU)	SC17	SC18	SC19	SC2	SC20	SC3	SC4	SC5	SC6	SC7	SC8	SC9	SE1	SE2	SW1	VE1	VE2	VE3	Avg.	2 $\sigma$ (pcm)
0.00	1.1553	1.1589	1.1557	1.1538	1.1543	1.1552	1.1480	1.1483	1.1508	1.1548	1.1555	1.1566	1.1572	1.1578	1.1633	1.1568	1.1559	1.1585	1.1565	830
0.10	1.1276	1.1306	1.1279	1.1276	1.1271	1.1276	1.1206	1.1212	1.1234	1.1273	1.1280	1.1292	1.1295	1.1303	1.1348	1.1290	1.1293	1.1311	1.1289	807
0.25	1.1262	1.1288	1.1266	1.1260	1.1259	1.1263	1.1194	1.1199	1.1220	1.1260	1.1266	1.1278	1.1287	1.1288	1.1337	1.1278	1.1279	1.1297	1.1275	783
0.50	1.1263	1.1291	1.1268	1.1253	1.1262	1.1264	1.1195	1.1201	1.1220	1.1262	1.1268	1.1280	1.1288	1.1293	1.1342	1.1283	1.1286	1.1304	1.1276	773
0.75	1.1281	1.1307	1.1286	1.1266	1.1281	1.1282	1.1214	1.1220	1.1236	1.1281	1.1286	1.1299	1.1300	1.1303	1.1356	1.1307	1.1303	1.1320	1.1291	742
1.00	1.1305	1.1329	1.1311	1.1289	1.1308	1.1306	1.1238	1.1245	1.1259	1.1306	1.1310	1.1324	1.1325	1.1325	1.1378	1.1328	1.1324	1.1336	1.1315	719
1.25	1.1333	1.1354	1.1339	1.1317	1.1338	1.1334	1.1264	1.1272	1.1284	1.1334	1.1338	1.1352	1.1354	1.1357	1.1407	1.1357	1.1344	1.1368	1.1340	697
1.50	1.1362	1.1381	1.1368	1.1347	1.1369	1.1363	1.1292	1.1301	1.1311	1.1363	1.1366	1.1381	1.1381	1.1386	1.1436	1.1389	1.1380	1.1391	1.1368	680
1.75	1.1392	1.1408	1.1397	1.1378	1.1401	1.1392	1.1320	1.1330	1.1338	1.1393	1.1396	1.1411	1.1406	1.1410	1.1461	1.1414	1.1401	1.1417	1.1396	673
2.00	1.1422	1.1436	1.1427	1.1410	1.1433	1.1422	1.1349	1.1359	1.1366	1.1424	1.1426	1.1442	1.1435	1.1435	1.1489	1.1449	1.1441	1.1451	1.1424	657
2.25	1.1452	1.1464	1.1457	1.1442	1.1466	1.1452	1.1377	1.1389	1.1393	1.1454	1.1456	1.1473	1.1472	1.1465	1.1516	1.1475	1.1461	1.1484	1.1453	659
2.50	1.1483	1.1493	1.1487	1.1475	1.1500	1.1482	1.1406	1.1419	1.1421	1.1486	1.1487	1.1503	1.1496	1.1501	1.1545	1.1507	1.1496	1.1514	1.1483	666
2.75	1.1514	1.1523	1.1517	1.1508	1.1534	1.1514	1.1435	1.1449	1.1450	1.1517	1.1519	1.1537	1.1520	1.1524	1.1572	1.1532	1.1527	1.1544	1.1513	686
3.00	1.1546	1.1552	1.1548	1.1542	1.1569	1.1545	1.1465	1.1480	1.1479	1.1550	1.1551	1.1569	1.1556	1.1553	1.1602	1.1568	1.1555	1.1572	1.1543	675
3.25	1.1579	1.1583	1.1580	1.1576	1.1604	1.1577	1.1495	1.1512	1.1508	1.1582	1.1583	1.1602	1.1588	1.1584	1.1630	1.1596	1.1588	1.1610	1.1574	695
3.50	1.1613	1.1614	1.1612	1.1612	1.1640	1.1610	1.1526	1.1544	1.1538	1.1616	1.1616	1.1637	1.1624	1.1616	1.1662	1.1635	1.1617	1.1640	1.1606	704
3.75	1.1647	1.1647	1.1646	1.1648	1.1677	1.1644	1.1560	1.1576	1.1569	1.1651	1.1651	1.1671	1.1651	1.1645	1.1696	1.1665	1.1652	1.1670	1.1639	731
4.00	1.1682	1.1680	1.1679	1.1684	1.1715	1.1679	1.1594	1.1609	1.1601	1.1686	1.1686	1.1707	1.1685	1.1678	1.1726	1.1706	1.1689	1.1698	1.1673	753
4.25	1.1718	1.1714	1.1714	1.1722	1.1754	1.1714	1.1627	1.1643	1.1633	1.1722	1.1722	1.1744	1.1718	1.1706	1.1757	1.1740	1.1724	1.1731	1.1707	778
4.50	1.1755	1.1749	1.1750	1.1761	1.1794	1.1751	1.1662	1.1679	1.1666	1.1760	1.1758	1.1782	1.1755	1.1748	1.1790	1.1773	1.1762	1.1772	1.1743	807
4.75	1.1793	1.1785	1.1786	1.1800	1.1834	1.1788	1.1697	1.1715	1.1700	1.1798	1.1796	1.1821	1.1787	1.1779	1.1825	1.1811	1.1797	1.1806	1.1779	855
5.00	1.1832	1.1822	1.1824	1.1841	1.1876	1.1827	1.1734	1.1752	1.1735	1.1837	1.1835	1.1860	1.1829	1.1817	1.1858	1.1853	1.1834	1.1847	1.1817	889
5.25	1.1873	1.1860	1.1862	1.1883	1.1918	1.1866	1.1771	1.1790	1.1771	1.1877	1.1875	1.1901	1.1859	1.1857	1.1897	1.1886	1.1868	1.1891	1.1855	948
5.50	1.1914	1.1900	1.1901	1.1925	1.1961	1.1907	1.1809	1.1829	1.1808	1.1919	1.1916	1.1943	1.1904	1.1886	1.1936	1.1925	1.1918	1.1931	1.1894	994
5.75	1.1956	1.1940	1.1942	1.1969	1.2005	1.1948	1.1849	1.1868	1.1846	1.1961	1.1958	1.1986	1.1946	1.1931	1.1970	1.1971	1.1953	1.1970	1.1935	1028
6.00	1.1999	1.1982	1.1983	1.2014	1.2051	1.1991	1.1889	1.1909	1.1884	1.2004	1.2001	1.2030	1.1988	1.1973	1.2011	1.2013	1.1995	1.2015	1.1976	1076
6.25	1.2043	1.2024	1.2025	1.2060	1.2096	1.2034	1.1930	1.1951	1.1924	1.2048	1.2045	1.2074	1.2027	1.2003	1.2051	1.2053	1.2038	1.2051	1.2018	1123
6.50	1.2088	1.2068	1.2067	1.2107	1.2142	1.2078	1.1972	1.1993	1.1965	1.2092	1.2089	1.2120	1.2076	1.2045	1.2091	1.2102	1.2080	1.2098	1.2060	1166
6.75	1.2132	1.2112	1.2110	1.2154	1.2189	1.2123	1.2015	1.2036	1.2006	1.2137	1.2134	1.2165	1.2114	1.2088	1.2131	1.2142	1.2122	1.2145	1.2103	1206
7.00	1.2177	1.2156	1.2152	1.2201	1.2234	1.2167	1.2058	1.2078	1.2047	1.2181	1.2178	1.2210	1.2158	1.2136	1.2172	1.2183	1.2169	1.2184	1.2147	1241
7.25	1.2220	1.2200	1.2194	1.2248	1.2278	1.2210	1.2100	1.2120	1.2089	1.2224	1.2222	1.2254	1.2201	1.2172	1.2211	1.2225	1.2209	1.2232	1.2188	1248
7.50	1.2260	1.2243	1.2234	1.2292	1.2319	1.2252	1.2140	1.2160	1.2129	1.2265	1.2263	1.2295	1.2244	1.2215	1.2253	1.2261	1.2247	1.2271	1.2228	1264
7.75	1.2298	1.2282	1.2271	1.2334	1.2357	1.2290	1.2178	1.2197	1.2168	1.2303	1.2301	1.2333	1.2279	1.2258	1.2298	1.2307	1.2280	1.2309	1.2266	1251
8.00	1.2331	1.2319	1.2305	1.2371	1.2390	1.2325	1.2213	1.2231	1.2203	1.2336	1.2336	1.2367	1.2314	1.2286	1.2323	1.2337	1.2315	1.2344	1.2300	1241

Table B.4.  $K_{inf}$  results from all participants at 0% void fraction (4/4)

0.25	1.2360	1.2351	1.2334	1.2403	1.2418	1.2355	1.2243	1.2260	1.2236	1.2366	1.2368	1.2397	1.2344	1.2319	1.2352	1.2368	1.2344	1.2379	1.2331	1.218
0.50	1.2384	1.2378	1.2359	1.2431	1.2442	1.2381	1.2269	1.2286	1.2264	1.2390	1.2391	1.2422	1.2372	1.2340	1.2379	1.2389	1.2375	1.2399	1.2357	1.193
0.75	1.2404	1.2400	1.2380	1.2453	1.2461	1.2402	1.2290	1.2306	1.2288	1.2410	1.2412	1.2442	1.2392	1.2365	1.2402	1.2413	1.2397	1.2425	1.2379	1.163
9.00	1.2419	1.2417	1.2396	1.2470	1.2475	1.2418	1.2306	1.2323	1.2307	1.2425	1.2427	1.2457	1.2414	1.2371	1.2421	1.2430	1.2414	1.2444	1.2396	1.132
9.25	1.2429	1.2430	1.2407	1.2481	1.2484	1.2429	1.2318	1.2334	1.2323	1.2436	1.2438	1.2467	1.2422	1.2384	1.2437	1.2437	1.2428	1.2454	1.2408	1.093
9.50	1.2434	1.2437	1.2414	1.2488	1.2489	1.2435	1.2325	1.2341	1.2333	1.2442	1.2444	1.2472	1.2427	1.2392	1.2448	1.2445	1.2428	1.2462	1.2417	1.058
9.75	1.2434	1.2439	1.2417	1.2489	1.2488	1.2437	1.2327	1.2344	1.2339	1.2443	1.2445	1.2473	1.2429	1.2394	1.2454	1.2450	1.2436	1.2465	1.2419	1.021
10.00	1.2430	1.2436	1.2415	1.2485	1.2483	1.2434	1.2325	1.2342	1.2341	1.2440	1.2442	1.2469	1.2426	1.2398	1.2455	1.2445	1.2425	1.2459	1.2418	978
10.50	1.2409	1.2417	1.2400	1.2470	1.2461	1.2415	1.2308	1.2326	1.2332	1.2419	1.2423	1.2449	1.2408	1.2373	1.2448	1.2427	1.2408	1.2445	1.2402	938
11.00	1.2376	1.2385	1.2371	1.2440	1.2427	1.2383	1.2278	1.2296	1.2308	1.2387	1.2390	1.2416	1.2381	1.2344	1.2422	1.2396	1.2381	1.2415	1.2373	895
11.50	1.2334	1.2344	1.2332	1.2401	1.2385	1.2342	1.2238	1.2257	1.2273	1.2346	1.2350	1.2374	1.2340	1.2308	1.2391	1.2358	1.2347	1.2372	1.2335	892
12.00	1.2287	1.2297	1.2288	1.2356	1.2338	1.2296	1.2193	1.2212	1.2231	1.2300	1.2303	1.2328	1.2289	1.2266	1.2349	1.2312	1.2297	1.2333	1.2291	876
12.50	1.2237	1.2247	1.2240	1.2307	1.2289	1.2247	1.2145	1.2164	1.2185	1.2251	1.2254	1.2278	1.2244	1.2219	1.2304	1.2264	1.2251	1.2277	1.2243	870
13.00	1.2186	1.2196	1.2190	1.2256	1.2238	1.2196	1.2095	1.2115	1.2136	1.2200	1.2203	1.2227	1.2191	1.2165	1.2255	1.2218	1.2192	1.2231	1.2193	872
13.50	1.2133	1.2143	1.2139	1.2204	1.2186	1.2145	1.2044	1.2064	1.2086	1.2148	1.2152	1.2175	1.2140	1.2114	1.2209	1.2165	1.2149	1.2174	1.2142	863
14.00	1.2081	1.2091	1.2087	1.2152	1.2134	1.2093	1.1994	1.2012	1.2036	1.2096	1.2100	1.2123	1.2085	1.2061	1.2156	1.2111	1.2094	1.2125	1.2090	861
14.50	1.2028	1.2038	1.2035	1.2099	1.2082	1.2041	1.1942	1.1961	1.1985	1.2044	1.2048	1.2070	1.2039	1.2010	1.2103	1.2058	1.2044	1.2074	1.2038	851
15.00	1.1975	1.1985	1.1984	1.2047	1.2030	1.1989	1.1891	1.1910	1.1934	1.1992	1.1996	1.2018	1.1984	1.1957	1.2055	1.2003	1.1990	1.2022	1.1986	858
15.50	1.1923	1.1932	1.1932	1.1995	1.1978	1.1937	1.1839	1.1859	1.1882	1.1940	1.1943	1.1966	1.1934	1.1912	1.2003	1.1952	1.1939	1.1973	1.1934	842
16.00	1.1870	1.1880	1.1880	1.1943	1.1926	1.1885	1.1788	1.1808	1.1831	1.1888	1.1892	1.1914	1.1880	1.1852	1.1954	1.1902	1.1887	1.1917	1.1882	846
16.50	1.1818	1.1828	1.1829	1.1891	1.1875	1.1833	1.1737	1.1757	1.1780	1.1836	1.1839	1.1862	1.1825	1.1802	1.1903	1.1856	1.1839	1.1864	1.1831	848
17.00	1.1765	1.1775	1.1778	1.1839	1.1823	1.1782	1.1686	1.1706	1.1730	1.1785	1.1787	1.1810	1.1774	1.1757	1.1852	1.1799	1.1785	1.1813	1.1780	840
17.50	1.1713	1.1723	1.1727	1.1788	1.1771	1.1730	1.1636	1.1655	1.1679	1.1733	1.1736	1.1758	1.1724	1.1708	1.1802	1.1744	1.1735	1.1767	1.1728	832
18.00	1.1661	1.1671	1.1676	1.1736	1.1720	1.1679	1.1585	1.1604	1.1629	1.1682	1.1684	1.1705	1.1666	1.1656	1.1749	1.1694	1.1679	1.1707	1.1677	827
18.50	1.1609	1.1619	1.1625	1.1684	1.1668	1.1628	1.1535	1.1554	1.1578	1.1630	1.1633	1.1654	1.1618	1.1604	1.1699	1.1637	1.1625	1.1662	1.1626	823
19.00	1.1557	1.1567	1.1574	1.1633	1.1617	1.1577	1.1486	1.1503	1.1528	1.1579	1.1581	1.1602	1.1566	1.1556	1.1648	1.1589	1.1572	1.1602	1.1575	813
19.50	1.1505	1.1515	1.1524	1.1581	1.1566	1.1526	1.1435	1.1453	1.1478	1.1528	1.1530	1.1550	1.1513	1.1504	1.1600	1.1538	1.1525	1.1552	1.1524	819
20.00	1.1453	1.1463	1.1473	1.1529	1.1516	1.1475	1.1385	1.1403	1.1428	1.1476	1.1479	1.1499	1.1464	1.1446	1.1546	1.1493	1.1468	1.1500	1.1472	813

Table B.2.  $K_{inf}$  results from all participants at 40% void fraction (1/4)

Burnup (GWD/MTU)	AL1	AP1	CA1	HE1	HE2	HE3	HE4	KE1	KE2	KE3	MO1	SC1	SC10	SC11	SC12	SC13	SC14	SC15	SC16
0.00	1.1365	1.1307	1.1361	1.1256	1.1494	1.1337	1.1316	1.1379	1.1350	1.1383	1.1335	-	1.1315	1.1340	1.1319	1.1287	1.1344	1.1329	1.1324
0.10	1.1099	1.1047	1.1102	1.0998	1.1226	1.1077	1.1058	1.1121	1.1087	1.1121	1.1078	1.1117	1.1054	1.1090	1.1063	1.1031	1.1082	1.1068	1.1069
0.25	1.1087	1.1040	1.1092	1.0989	1.1214	1.1089	1.1051	1.1101	1.1074	1.1102	1.1073	1.1115	1.1044	1.1076	1.1054	1.1020	1.1075	1.1058	1.1060
0.50	1.1091	1.1046	1.1097	1.0992	1.1213	1.1073	1.1057	1.1101	1.1073	1.1105	1.1086	1.1112	1.1050	1.1072	1.1060	1.1026	1.1082	1.1065	1.1065
0.75	1.1106	1.1066	1.1116	1.1010	1.1226	1.1091	1.1077	1.1115	1.1083	1.1121	1.1106	1.1135	1.1071	1.1085	1.1079	1.1045	1.1109	1.1085	1.1084
1.00	1.1128	1.1091	1.1140	1.1034	1.1244	1.1115	1.1103	1.1139	1.1100	1.1143	1.1128	1.1158	1.1097	1.1108	1.1105	1.1072	1.1143	1.1112	1.1110
1.25	1.1152	1.1118	1.1166	1.1060	1.1264	1.1142	1.1132	1.1162	1.1121	1.1162	1.1155	1.1182	1.1126	1.1135	1.1134	1.1100	1.1165	1.1141	1.1139
1.50	1.1177	1.1146	1.1192	1.1087	1.1286	1.1169	1.1161	1.1186	1.1140	1.1192	1.1183	1.1206	1.1155	1.1164	1.1164	1.1131	1.1199	1.1170	1.1170
1.75	1.1202	1.1173	1.1218	1.1114	1.1308	1.1196	1.1191	1.1211	1.1165	1.1215	1.1219	1.1241	1.1186	1.1193	1.1195	1.1161	1.1227	1.1200	1.1201
2.00	1.1227	1.1201	1.1244	1.1141	1.1329	1.1223	1.1220	1.1237	1.1184	1.1240	1.1250	1.1275	1.1215	1.1223	1.1225	1.1191	1.1254	1.1229	1.1231
2.25	1.1251	1.1228	1.1270	1.1168	1.1351	1.1251	1.1250	1.1263	1.1209	1.1268	1.1281	1.1298	1.1245	1.1252	1.1256	1.1222	1.1282	1.1258	1.1262
2.50	1.1275	1.1255	1.1296	1.1195	1.1372	1.1277	1.1279	1.1291	1.1232	1.1294	1.1316	1.1320	1.1275	1.1282	1.1287	1.1252	1.1312	1.1287	1.1292
2.75	1.1301	1.1282	1.1322	1.1222	1.1394	1.1304	1.1308	1.1318	1.1253	1.1320	1.1342	1.1350	1.1305	1.1312	1.1317	1.1283	1.1344	1.1316	1.1324
3.00	1.1326	1.1310	1.1348	1.1249	1.1414	1.1331	1.1338	1.1346	1.1278	1.1348	1.1368	1.1380	1.1335	1.1341	1.1348	1.1313	1.1377	1.1345	1.1355
3.25	1.1351	1.1337	1.1374	1.1275	1.1435	1.1359	1.1367	1.1374	1.1304	1.1379	1.1398	1.1411	1.1365	1.1371	1.1379	1.1344	1.1408	1.1374	1.1386
3.50	1.1377	1.1364	1.1401	1.1302	1.1457	1.1385	1.1397	1.1404	1.1332	1.1410	1.1434	1.1442	1.1396	1.1401	1.1410	1.1374	1.1439	1.1404	1.1418
3.75	1.1403	1.1392	1.1428	1.1330	1.1478	1.1413	1.1427	1.1435	1.1359	1.1441	1.1462	1.1468	1.1426	1.1431	1.1442	1.1405	1.1468	1.1433	1.1449
4.00	1.1429	1.1420	1.1455	1.1357	1.1499	1.1441	1.1457	1.1463	1.1386	1.1471	1.1488	1.1494	1.1458	1.1462	1.1474	1.1437	1.1498	1.1463	1.1481
4.25	1.1456	1.1449	1.1483	1.1385	1.1521	1.1469	1.1488	1.1497	1.1414	1.1503	1.1526	1.1527	1.1489	1.1493	1.1506	1.1468	1.1528	1.1494	1.1513
4.50	1.1483	1.1478	1.1511	1.1413	1.1543	1.1497	1.1519	1.1529	1.1445	1.1535	1.1552	1.1559	1.1521	1.1525	1.1538	1.1500	1.1563	1.1525	1.1547
4.75	1.1513	1.1507	1.1539	1.1441	1.1566	1.1526	1.1550	1.1562	1.1473	1.1568	1.1588	1.1590	1.1554	1.1557	1.1571	1.1533	1.1600	1.1556	1.1580
5.00	1.1540	1.1537	1.1568	1.1470	1.1589	1.1555	1.1582	1.1595	1.1504	1.1604	1.1621	1.1621	1.1587	1.1590	1.1604	1.1565	1.1627	1.1588	1.1614
5.25	1.1569	1.1567	1.1598	1.1500	1.1612	1.1585	1.1614	1.1631	1.1538	1.1636	1.1651	1.1653	1.1621	1.1623	1.1638	1.1599	1.1668	1.1621	1.1648
5.50	1.1598	1.1598	1.1628	1.1529	1.1636	1.1616	1.1647	1.1665	1.1570	1.1672	1.1691	1.1684	1.1655	1.1657	1.1672	1.1632	1.1692	1.1653	1.1683
5.75	1.1630	1.1630	1.1659	1.1560	1.1661	1.1647	1.1681	1.1698	1.1599	1.1707	1.1723	1.1723	1.1690	1.1691	1.1707	1.1667	1.1725	1.1687	1.1717
6.00	1.1661	1.1662	1.1690	1.1591	1.1685	1.1678	1.1715	1.1735	1.1634	1.1744	1.1764	1.1762	1.1725	1.1726	1.1741	1.1701	1.1763	1.1721	1.1753
6.25	1.1692	1.1694	1.1722	1.1622	1.1711	1.1710	1.1750	1.1770	1.1668	1.1778	1.1797	1.1794	1.1760	1.1761	1.1776	1.1736	1.1796	1.1755	1.1789
6.50	1.1724	1.1727	1.1754	1.1653	1.1737	1.1743	1.1784	1.1804	1.1697	1.1813	1.1836	1.1826	1.1796	1.1797	1.1811	1.1770	1.1834	1.1789	1.1825
6.75	1.1755	1.1760	1.1787	1.1685	1.1763	1.1776	1.1819	1.1839	1.1732	1.1850	1.1871	1.1858	1.1832	1.1833	1.1846	1.1805	1.1877	1.1824	1.1861
7.00	1.1789	1.1793	1.1819	1.1717	1.1790	1.1809	1.1854	1.1870	1.1762	1.1882	1.1906	1.1891	1.1867	1.1869	1.1881	1.1839	1.1907	1.1858	1.1897
7.25	1.1821	1.1825	1.1851	1.1749	1.1817	1.1841	1.1889	1.1904	1.1794	1.1912	1.1940	1.1930	1.1902	1.1905	1.1915	1.1873	1.1939	1.1892	1.1932
7.50	1.1855	1.1857	1.1883	1.1781	1.1844	1.1874	1.1922	1.1932	1.1822	1.1944	1.1978	1.1969	1.1935	1.1940	1.1949	1.1905	1.1969	1.1925	1.1966
7.75	1.1888	1.1887	1.1913	1.1811	1.1871	1.1905	1.1954	1.1961	1.1849	1.1970	2.006	2.002	1.967	1.974	1.980	1.936	2.014	1.956	1.997
8.00	1.1919	1.1916	1.1941	1.1840	1.1898	1.1934	1.1984	1.1986	1.1873	1.1997	2.040	2.035	1.995	2.005	2.009	1.964	2.033	1.984	2.027

Table B.2.  $K_{inf}$  results from all participants at 40% void fraction (2/4)

8.25	1.1960	1.1941	1.1967	1.1867	1.1923	1.1961	1.2011	1.2008	1.1897	1.2020	1.2064	1.2062	1.2021	1.2034	1.2036	1.1989	1.2053	1.2010	1.2063
8.50	1.1978	1.1964	1.1990	1.1891	1.1947	1.1985	1.2034	1.2028	1.1915	1.2044	1.2087	1.2089	1.2043	1.2059	1.2059	1.2011	1.2086	1.2033	1.2075
8.75	1.2003	1.1983	1.2010	1.1912	1.1969	1.2006	1.2054	1.2050	1.1932	1.2057	1.2109	1.2108	1.2061	1.2081	1.2078	1.2030	1.2093	1.2051	1.2094
9.00	1.2026	1.1998	1.2027	1.1930	1.1989	1.2023	1.2070	1.2064	1.1948	1.2073	1.2123	1.2127	1.2075	1.2099	1.2094	1.2044	1.2116	1.2067	1.2109
9.25	1.2044	1.2011	1.2040	1.1944	1.2006	1.2037	1.2083	1.2072	1.1958	1.2086	1.2133	1.2139	1.2086	1.2113	1.2107	1.2055	1.2128	1.2079	1.2121
9.50	1.2059	1.2019	1.2051	1.1955	1.2020	1.2048	1.2093	1.2082	1.1965	1.2092	1.2137	1.2152	1.2093	1.2123	1.2115	1.2063	1.2128	1.2087	1.2128
9.75	1.2069	1.2025	1.2058	1.1963	1.2032	1.2055	1.2098	1.2091	1.1972	1.2100	1.2145	1.2155	1.2097	1.2130	1.2121	1.2067	1.2126	1.2092	1.2133
10.00	1.2077	1.2027	1.2061	1.1968	1.2040	1.2060	1.2100	1.2086	1.1976	1.2101	1.2145	1.2158	1.2098	1.2132	1.2122	1.2067	1.2133	1.2094	1.2133
10.50	1.2079	1.2021	1.2058	1.1967	1.2048	1.2058	1.2095	1.2080	1.1966	1.2096	1.2132	1.2150	1.2089	1.2129	1.2114	1.2057	1.2129	1.2086	1.2122
11.00	1.2068	1.2004	1.2045	1.1955	1.2044	1.2044	1.2077	1.2063	1.1947	1.2076	1.2110	1.2138	1.2066	1.2114	1.2096	1.2037	1.2122	1.2067	1.2101
11.50	1.2045	1.1977	1.2020	1.1933	1.2030	1.2019	1.2050	1.2032	1.1918	1.2047	1.2080	1.2096	1.2035	1.2088	1.2069	1.2008	1.2069	1.2039	1.2070
12.00	1.2014	1.1942	1.1987	1.1902	1.2007	1.1987	1.2015	1.1995	1.1885	1.2014	1.2040	1.2066	1.1996	1.2054	1.2034	1.1971	1.2042	1.2003	1.2033
12.50	1.1973	1.1903	1.1949	1.1865	1.1975	1.1948	1.1975	1.1956	1.1839	1.1968	1.1997	1.2017	1.1954	1.2014	1.1994	1.1930	1.2004	1.1962	1.1990
13.00	1.1931	1.1860	1.1907	1.1824	1.1938	1.1906	1.1931	1.1912	1.1793	1.1924	1.1949	1.1985	1.1908	1.1970	1.1951	1.1885	1.1941	1.1918	1.1945
13.50	1.1885	1.1815	1.1862	1.1781	1.1897	1.1862	1.1886	1.1864	1.1747	1.1879	1.1905	1.1927	1.1861	1.1925	1.1906	1.1839	1.1907	1.1872	1.1898
14.00	1.1838	1.1770	1.1816	1.1736	1.1854	1.1816	1.1840	1.1818	1.1703	1.1835	1.1856	1.1881	1.1813	1.1876	1.1859	1.1792	1.1859	1.1825	1.1850
14.50	1.1789	1.1724	1.1769	1.1690	1.1809	1.1770	1.1793	1.1768	1.1653	1.1784	1.1802	1.1835	1.1765	1.1829	1.1812	1.1744	1.1807	1.1778	1.1802
15.00	1.1742	1.1678	1.1722	1.1644	1.1763	1.1723	1.1746	1.1723	1.1603	1.1739	1.1763	1.1782	1.1717	1.1781	1.1765	1.1696	1.1759	1.1730	1.1754
15.50	1.1694	1.1632	1.1675	1.1598	1.1716	1.1677	1.1699	1.1673	1.1556	1.1692	1.1709	1.1737	1.1669	1.1733	1.1718	1.1648	1.1719	1.1683	1.1706
16.00	1.1645	1.1586	1.1628	1.1552	1.1670	1.1630	1.1652	1.1629	1.1505	1.1644	1.1663	1.1692	1.1621	1.1685	1.1672	1.1601	1.1671	1.1636	1.1658
16.50	1.1597	1.1540	1.1582	1.1506	1.1623	1.1583	1.1605	1.1582	1.1458	1.1598	1.1617	1.1644	1.1573	1.1638	1.1625	1.1553	1.1615	1.1589	1.1611
17.00	1.1549	1.1494	1.1535	1.1461	1.1577	1.1537	1.1559	1.1533	1.1411	1.1553	1.1564	1.1595	1.1526	1.1590	1.1578	1.1506	1.1574	1.1542	1.1563
17.50	1.1502	1.1449	1.1489	1.1415	1.1530	1.1491	1.1513	1.1489	1.1367	1.1508	1.1523	1.1545	1.1479	1.1543	1.1532	1.1459	1.1528	1.1496	1.1515
18.00	1.1454	1.1404	1.1442	1.1370	1.1484	1.1446	1.1467	1.1446	1.1318	1.1464	1.1473	1.1501	1.1432	1.1497	1.1486	1.1413	1.1484	1.1450	1.1469
18.50	1.1407	1.1359	1.1397	1.1325	1.1438	1.1400	1.1421	1.1399	1.1274	1.1415	1.1422	1.1451	1.1385	1.1450	1.1440	1.1366	1.1447	1.1404	1.1422
19.00	1.1360	1.1314	1.1351	1.1280	1.1393	1.1355	1.1376	1.1352	1.1227	1.1373	1.1381	1.1411	1.1339	1.1404	1.1394	1.1320	1.1384	1.1358	1.1376
19.50	1.1313	1.1270	1.1305	1.1236	1.1347	1.1310	1.1330	1.1309	1.1182	1.1328	1.1334	1.1365	1.1293	1.1357	1.1349	1.1274	1.1344	1.1312	1.1329
20.00	1.1267	1.1226	1.1260	1.1192	1.1302	1.1265	1.1285	1.1260	1.1134	1.1279	1.1283	1.1316	1.1247	1.1311	1.1304	1.1228	1.1303	1.1267	1.1283



Table B.2.  $K_{inf}$  results from all participants at 40% void fraction (3/4)

Burnup (GWd/MTU)	SC17	SC18	SC19	SC2	SC20	SC3	SC4	SC5	SC6	SC7	SC8	SC9	SE1	SE2	SW1	VE1	VE2	VE3	Avg.	$2\sigma$ (pcm)
0.00	1.1315	1.1348	1.1321	1.1360	1.1321	1.1314	1.1235	1.1240	1.1264	1.1312	1.1317	1.1339	1.1337	1.1332	1.1390	1.1325	1.1321	1.1340	1.1330	902
0.10	1.1054	1.1082	1.1061	1.1112	1.1065	1.1056	1.0980	1.0987	1.1008	1.1054	1.1059	1.1081	1.1080	1.1087	1.1127	1.1070	1.1071	1.1081	1.1073	866
0.25	1.1044	1.1069	1.1052	1.1099	1.1057	1.1047	1.0972	1.0979	1.0999	1.1046	1.1050	1.1073	1.1068	1.1077	1.1113	1.1060	1.1056	1.1078	1.1063	844
0.50	1.1050	1.1076	1.1058	1.1096	1.1064	1.1053	1.0978	1.0986	1.1003	1.1052	1.1056	1.1080	1.1069	1.1081	1.1126	1.1080	1.1064	1.1085	1.1068	823
0.75	1.1071	1.1095	1.1078	1.1112	1.1085	1.1074	1.0999	1.1007	1.1022	1.1074	1.1077	1.1100	1.1094	1.1103	1.1146	1.1092	1.1082	1.1105	1.1087	804
1.00	1.1097	1.1119	1.1105	1.1136	1.1113	1.1100	1.1025	1.1034	1.1047	1.1100	1.1103	1.1127	1.1114	1.1124	1.1170	1.1119	1.1112	1.1128	1.1112	785
1.25	1.1126	1.1146	1.1133	1.1164	1.1143	1.1129	1.1053	1.1062	1.1074	1.1129	1.1132	1.1156	1.1148	1.1148	1.1201	1.1157	1.1139	1.1158	1.1139	767
1.50	1.1155	1.1174	1.1163	1.1194	1.1174	1.1158	1.1081	1.1092	1.1102	1.1159	1.1162	1.1187	1.1173	1.1183	1.1227	1.1187	1.1171	1.1188	1.1168	754
1.75	1.1186	1.1202	1.1192	1.1224	1.1206	1.1188	1.1110	1.1121	1.1130	1.1189	1.1192	1.1218	1.1204	1.1204	1.1254	1.1208	1.1203	1.1211	1.1196	743
2.00	1.1215	1.1230	1.1222	1.1255	1.1238	1.1218	1.1138	1.1151	1.1157	1.1220	1.1222	1.1248	1.1237	1.1236	1.1287	1.1243	1.1227	1.1243	1.1225	741
2.25	1.1245	1.1258	1.1251	1.1286	1.1269	1.1248	1.1166	1.1180	1.1185	1.1250	1.1252	1.1279	1.1266	1.1269	1.1312	1.1277	1.1264	1.1274	1.1254	741
2.50	1.1275	1.1286	1.1280	1.1317	1.1301	1.1277	1.1193	1.1209	1.1212	1.1280	1.1282	1.1309	1.1282	1.1290	1.1341	1.1299	1.1284	1.1310	1.1282	739
2.75	1.1305	1.1314	1.1308	1.1347	1.1333	1.1307	1.1221	1.1238	1.1240	1.1309	1.1312	1.1340	1.1317	1.1318	1.1366	1.1327	1.1315	1.1339	1.1310	740
3.00	1.1335	1.1343	1.1337	1.1378	1.1365	1.1337	1.1248	1.1267	1.1267	1.1339	1.1342	1.1371	1.1349	1.1352	1.1396	1.1361	1.1347	1.1355	1.1339	746
3.25	1.1365	1.1371	1.1366	1.1409	1.1397	1.1367	1.1277	1.1296	1.1295	1.1370	1.1372	1.1401	1.1376	1.1375	1.1423	1.1390	1.1379	1.1390	1.1368	751
3.50	1.1396	1.1400	1.1396	1.1441	1.1429	1.1397	1.1308	1.1325	1.1322	1.1400	1.1402	1.1433	1.1409	1.1404	1.1449	1.1422	1.1407	1.1416	1.1397	760
3.75	1.1426	1.1430	1.1425	1.1473	1.1462	1.1427	1.1338	1.1354	1.1350	1.1431	1.1433	1.1464	1.1437	1.1437	1.1477	1.1447	1.1435	1.1457	1.1427	765
4.00	1.1458	1.1459	1.1455	1.1505	1.1495	1.1458	1.1367	1.1384	1.1378	1.1462	1.1464	1.1496	1.1467	1.1465	1.1509	1.1479	1.1474	1.1482	1.1456	776
4.25	1.1489	1.1490	1.1485	1.1538	1.1529	1.1489	1.1396	1.1414	1.1407	1.1494	1.1496	1.1529	1.1498	1.1492	1.1538	1.1513	1.1499	1.1514	1.1487	796
4.50	1.1521	1.1520	1.1516	1.1571	1.1563	1.1521	1.1426	1.1445	1.1436	1.1526	1.1528	1.1562	1.1525	1.1525	1.1567	1.1545	1.1529	1.1550	1.1518	811
4.75	1.1554	1.1552	1.1547	1.1605	1.1597	1.1553	1.1456	1.1476	1.1466	1.1559	1.1561	1.1595	1.1555	1.1551	1.1600	1.1574	1.1559	1.1576	1.1549	832
5.00	1.1587	1.1584	1.1579	1.1640	1.1632	1.1586	1.1487	1.1507	1.1495	1.1592	1.1593	1.1629	1.1595	1.1585	1.1630	1.1603	1.1597	1.1612	1.1581	853
5.25	1.1621	1.1616	1.1611	1.1675	1.1667	1.1619	1.1518	1.1539	1.1526	1.1625	1.1627	1.1663	1.1623	1.1607	1.1662	1.1648	1.1629	1.1643	1.1613	878
5.50	1.1655	1.1649	1.1643	1.1710	1.1703	1.1653	1.1549	1.1571	1.1557	1.1659	1.1661	1.1699	1.1656	1.1645	1.1693	1.1677	1.1665	1.1674	1.1646	897
5.75	1.1690	1.1683	1.1676	1.1747	1.1739	1.1687	1.1581	1.1604	1.1589	1.1694	1.1696	1.1734	1.1689	1.1678	1.1724	1.1708	1.1698	1.1713	1.1679	925
6.00	1.1725	1.1717	1.1709	1.1783	1.1776	1.1722	1.1614	1.1637	1.1621	1.1729	1.1731	1.1770	1.1718	1.1708	1.1758	1.1740	1.1735	1.1745	1.1713	956
6.25	1.1760	1.1752	1.1743	1.1821	1.1813	1.1757	1.1647	1.1670	1.1653	1.1764	1.1766	1.1807	1.1763	1.1749	1.1789	1.1780	1.1768	1.1783	1.1748	981
6.50	1.1796	1.1788	1.1777	1.1859	1.1850	1.1793	1.1681	1.1704	1.1686	1.1800	1.1802	1.1843	1.1794	1.1780	1.1826	1.1817	1.1801	1.1819	1.1782	1015
6.75	1.1832	1.1823	1.1811	1.1897	1.1886	1.1829	1.1714	1.1738	1.1719	1.1836	1.1838	1.1880	1.1826	1.1810	1.1856	1.1850	1.1839	1.1850	1.1816	1041
7.00	1.1867	1.1859	1.1845	1.1935	1.1923	1.1864	1.1748	1.1772	1.1752	1.1871	1.1874	1.1916	1.1862	1.1839	1.1885	1.1883	1.1870	1.1890	1.1850	1061
7.25	1.1902	1.1894	1.1878	1.1973	1.1958	1.1899	1.1781	1.1805	1.1785	1.1905	1.1909	1.1952	1.1895	1.1885	1.1921	1.1923	1.1905	1.1927	1.1885	1088
7.50	1.1935	1.1928	1.1910	1.2010	1.1993	1.1933	1.1814	1.1837	1.1817	1.1939	1.1943	1.1986	1.1928	1.1907	1.1953	1.1952	1.1938	1.1958	1.1917	1110
7.75	1.1967	1.1961	1.1941	1.2045	1.2024	1.1965	1.1845	1.1867	1.1848	1.1970	1.1975	1.2018	1.1959	1.1938	1.1985	1.1987	1.1964	1.1991	1.1948	1133
8.00	1.1995	1.1992	1.1969	1.2077	1.2053	1.1995	1.1874	1.1896	1.1878	1.1999	1.2004	1.2048	1.1991	1.1968	1.2013	1.2013	1.1993	1.2017	1.1977	1139
8.25	1.2021	1.2020	1.1995	1.2106	1.2079	1.2021	1.1900	1.1921	1.1905	1.2024	1.2031	1.2074	1.2023	1.1999	1.2040	1.2043	1.2023	1.2048	1.2004	1142

Table B.2.  $K_{inf}$  results from all participants at 40% void fraction (4/4)

8.50	1.2043	1.2044	1.2017	1.2131	1.2101	1.2044	1.1923	1.1944	1.1930	1.2047	1.2053	1.2096	1.2041	1.2015	1.2060	1.2060	1.2037	1.2073	1.2026	1.145
8.75	1.2061	1.2064	1.2036	1.2153	1.2119	1.2064	1.1942	1.1963	1.1951	1.2065	1.2072	1.2115	1.2058	1.2030	1.2080	1.2074	1.2060	1.2090	1.2045	1.133
9.00	1.2075	1.2081	1.2052	1.2170	1.2134	1.2080	1.1958	1.1978	1.1969	1.2080	1.2088	1.2130	1.2074	1.2053	1.2098	1.2093	1.2073	1.2108	1.2062	1.129
9.25	1.2086	1.2094	1.2064	1.2183	1.2145	1.2092	1.1970	1.1990	1.1984	1.2091	1.2099	1.2141	1.2086	1.2066	1.2114	1.2105	1.2085	1.2120	1.2074	1.120
9.50	1.2093	1.2103	1.2073	1.2193	1.2152	1.2100	1.1979	1.1998	1.1995	1.2099	1.2107	1.2148	1.2096	1.2071	1.2120	1.2106	1.2101	1.2125	1.2083	1.101
9.75	1.2097	1.2108	1.2078	1.2198	1.2156	1.2104	1.1984	1.2004	1.2003	1.2104	1.2112	1.2152	1.2102	1.2076	1.2128	1.2120	1.2103	1.2131	1.2089	1.084
10.00	1.2098	1.2110	1.2080	1.2199	1.2156	1.2106	1.1986	1.2006	1.2007	1.2105	1.2113	1.2153	1.2101	1.2073	1.2135	1.2117	1.2104	1.2124	1.2091	1.066
10.50	1.2089	1.2102	1.2074	1.2192	1.2146	1.2098	1.1979	1.2000	1.2007	1.2097	1.2105	1.2144	1.2091	1.2066	1.2130	1.2109	1.2090	1.2128	1.2084	1.043
11.00	1.2066	1.2082	1.2056	1.2174	1.2124	1.2078	1.1960	1.1981	1.1994	1.2076	1.2084	1.2122	1.2072	1.2045	1.2117	1.2088	1.2073	1.2109	1.2067	1.031
11.50	1.2035	1.2051	1.2028	1.2145	1.2092	1.2048	1.1931	1.1953	1.1971	1.2046	1.2054	1.2090	1.2042	1.2014	1.2096	1.2065	1.2042	1.2071	1.2038	992
12.00	1.1996	1.2013	1.1992	1.2109	1.2054	1.2010	1.1897	1.1917	1.1938	1.2009	1.2016	1.2052	1.2003	1.1986	1.2064	1.2027	1.2011	1.2039	1.2003	981
12.50	1.1954	1.1971	1.1952	1.2067	1.2012	1.1969	1.1856	1.1877	1.1901	1.1967	1.1974	1.2010	1.1960	1.1934	1.2026	1.1977	1.1961	1.1998	1.1962	974
13.00	1.1908	1.1925	1.1908	1.2022	1.1967	1.1924	1.1813	1.1834	1.1859	1.1923	1.1929	1.1965	1.1917	1.1899	1.1982	1.1938	1.1921	1.1955	1.1918	968
13.50	1.1861	1.1878	1.1863	1.1975	1.1920	1.1878	1.1768	1.1788	1.1815	1.1877	1.1883	1.1918	1.1873	1.1848	1.1943	1.1886	1.1877	1.1901	1.1872	960
14.00	1.1813	1.1830	1.1816	1.1927	1.1873	1.1831	1.1721	1.1742	1.1770	1.1829	1.1836	1.1870	1.1825	1.1812	1.1898	1.1842	1.1831	1.1856	1.1826	948
14.50	1.1765	1.1782	1.1769	1.1879	1.1826	1.1783	1.1675	1.1696	1.1723	1.1782	1.1788	1.1822	1.1774	1.1754	1.1849	1.1795	1.1779	1.1814	1.1778	946
15.00	1.1717	1.1734	1.1721	1.1831	1.1778	1.1735	1.1627	1.1649	1.1677	1.1734	1.1741	1.1774	1.1726	1.1708	1.1805	1.1751	1.1729	1.1767	1.1731	948
15.50	1.1669	1.1686	1.1674	1.1783	1.1730	1.1687	1.1580	1.1601	1.1630	1.1687	1.1693	1.1727	1.1678	1.1663	1.1756	1.1699	1.1683	1.1719	1.1683	945
16.00	1.1621	1.1638	1.1627	1.1735	1.1683	1.1640	1.1533	1.1555	1.1584	1.1640	1.1646	1.1679	1.1631	1.1614	1.1711	1.1656	1.1634	1.1666	1.1636	948
16.50	1.1573	1.1590	1.1580	1.1687	1.1636	1.1593	1.1488	1.1508	1.1538	1.1592	1.1598	1.1631	1.1582	1.1574	1.1665	1.1611	1.1588	1.1619	1.1589	937
17.00	1.1526	1.1543	1.1533	1.1639	1.1589	1.1546	1.1442	1.1462	1.1492	1.1546	1.1551	1.1584	1.1535	1.1519	1.1619	1.1557	1.1543	1.1573	1.1542	932
17.50	1.1479	1.1495	1.1487	1.1591	1.1542	1.1500	1.1398	1.1416	1.1446	1.1499	1.1505	1.1537	1.1488	1.1476	1.1574	1.1509	1.1497	1.1528	1.1496	922
18.00	1.1432	1.1448	1.1441	1.1544	1.1496	1.1454	1.1354	1.1371	1.1401	1.1453	1.1458	1.1490	1.1440	1.1434	1.1528	1.1461	1.1448	1.1477	1.1449	917
18.50	1.1385	1.1402	1.1395	1.1497	1.1450	1.1408	1.1310	1.1326	1.1356	1.1406	1.1412	1.1444	1.1393	1.1388	1.1482	1.1410	1.1400	1.1431	1.1403	906
19.00	1.1339	1.1355	1.1349	1.1450	1.1404	1.1362	1.1269	1.1281	1.1311	1.1361	1.1366	1.1397	1.1348	1.1339	1.1438	1.1372	1.1353	1.1385	1.1357	901
19.50	1.1293	1.1309	1.1304	1.1403	1.1358	1.1316	1.1224	1.1236	1.1266	1.1315	1.1320	1.1351	1.1297	1.1284	1.1393	1.1323	1.1308	1.1333	1.1311	896
20.00	1.1247	1.1263	1.1259	1.1356	1.1313	1.1271	1.1179	1.1191	1.1222	1.1270	1.1275	1.1305	1.1257	1.1251	1.1346	1.1281	1.1257	1.1293	1.1266	891

Table B.5.  $K_{inf}$  results from all participants at 70% void fraction (1/4)

Burnup (GWD/MTU)	AL1	AP1	CA1	HE1	HE2	HE3	HE4	KE1	KE2	KE3	MO1	SC1	SC10	SC11	SC12	SC13	SC14	SC15	SC16
0.00	1.1104	1.1051	1.1113	1.0983	1.1317	1.1092	1.1066	1.1080	1.1079	1.1086	1.1078	-	1.1061	1.1117	1.1069	1.1044	1.1076	1.1070	1.1083
0.10	1.0859	1.0809	1.0873	1.0744	1.1065	1.0852	1.0827	1.0845	1.0838	1.0848	1.0846	1.0916	1.0817	1.0884	1.0832	1.0806	1.0844	1.0828	1.0847
0.25	1.0850	1.0805	1.0867	1.0738	1.1055	1.0847	1.0823	1.0830	1.0832	1.0829	1.0842	1.0913	1.0810	1.0872	1.0827	1.0798	1.0849	1.0821	1.0839
0.50	1.0856	1.0815	1.0875	1.0746	1.1055	1.0853	1.0832	1.0836	1.0833	1.0837	1.0849	1.0909	1.0820	1.0872	1.0834	1.0806	1.0852	1.0830	1.0847
0.75	1.0874	1.0835	1.0895	1.0765	1.1067	1.0873	1.0853	1.0854	1.0845	1.0856	1.0879	1.0936	1.0841	1.0886	1.0854	1.0826	1.0882	1.0851	1.0866
1.00	1.0895	1.0861	1.0918	1.0789	1.1084	1.0896	1.0878	1.0872	1.0857	1.0875	1.0896	1.0963	1.0866	1.0909	1.0880	1.0852	1.0903	1.0877	1.0890
1.25	1.0919	1.0887	1.0943	1.0815	1.1102	1.0922	1.0906	1.0899	1.0877	1.0897	1.0929	1.0985	1.0894	1.0936	1.0907	1.0880	1.0935	1.0904	1.0918
1.50	1.0943	1.0914	1.0968	1.0841	1.1121	1.0948	1.0934	1.0918	1.0896	1.0920	1.0957	1.1007	1.0922	1.0963	1.0935	1.0909	1.0967	1.0932	1.0945
1.75	1.0966	1.0941	1.0993	1.0868	1.1139	1.0974	1.0961	1.0939	1.0910	1.0943	1.0985	1.1033	1.0951	1.0991	1.0964	1.0937	1.0998	1.0959	1.0973
2.00	1.0990	1.0966	1.1017	1.0894	1.1158	1.0999	1.0989	1.0963	1.0930	1.0969	1.1015	1.1058	1.0978	1.1018	1.0992	1.0965	1.1023	1.0986	1.1001
2.25	1.1014	1.0992	1.1041	1.0919	1.1176	1.1024	1.1015	1.0984	1.0949	1.0987	1.1043	1.1084	1.1005	1.1045	1.1020	1.0993	1.1049	1.1012	1.1028
2.50	1.1036	1.1016	1.1064	1.0944	1.1193	1.1049	1.1042	1.1003	1.0969	1.1010	1.1066	1.1111	1.1032	1.1072	1.1047	1.1020	1.1078	1.1038	1.1055
2.75	1.1058	1.1041	1.1087	1.0968	1.1210	1.1072	1.1068	1.1026	1.0986	1.1029	1.1096	1.1138	1.1058	1.1099	1.1074	1.1047	1.1101	1.1063	1.1081
3.00	1.1081	1.1065	1.1109	1.0992	1.1226	1.1096	1.1093	1.1046	1.1000	1.1047	1.1120	1.1166	1.1084	1.1125	1.1101	1.1073	1.1118	1.1088	1.1107
3.25	1.1103	1.1089	1.1132	1.1016	1.1243	1.1119	1.1118	1.1066	1.1021	1.1074	1.1145	1.1190	1.1110	1.1150	1.1127	1.1100	1.1150	1.1112	1.1133
3.50	1.1126	1.1112	1.1154	1.1039	1.1259	1.1142	1.1143	1.1086	1.1038	1.1094	1.1172	1.1214	1.1136	1.1176	1.1154	1.1126	1.1185	1.1137	1.1159
3.75	1.1148	1.1136	1.1177	1.1063	1.1275	1.1165	1.1167	1.1109	1.1059	1.1115	1.1201	1.1240	1.1162	1.1202	1.1180	1.1152	1.1204	1.1161	1.1184
4.00	1.1170	1.1159	1.1199	1.1086	1.1291	1.1188	1.1192	1.1132	1.1074	1.1139	1.1229	1.1266	1.1187	1.1229	1.1206	1.1178	1.1233	1.1185	1.1210
4.25	1.1193	1.1183	1.1221	1.1109	1.1307	1.1211	1.1217	1.1154	1.1094	1.1156	1.1248	1.1292	1.1213	1.1255	1.1233	1.1204	1.1252	1.1210	1.1236
4.50	1.1216	1.1207	1.1244	1.1132	1.1323	1.1234	1.1242	1.1176	1.1114	1.1182	1.1275	1.1317	1.1239	1.1281	1.1259	1.1230	1.1285	1.1234	1.1261
4.75	1.1239	1.1231	1.1266	1.1156	1.1339	1.1257	1.1267	1.1199	1.1134	1.1203	1.1305	1.1341	1.1265	1.1307	1.1285	1.1256	1.1303	1.1259	1.1287
5.00	1.1262	1.1255	1.1289	1.1179	1.1355	1.1281	1.1292	1.1218	1.1153	1.1228	1.1330	1.1366	1.1292	1.1334	1.1311	1.1282	1.1339	1.1283	1.1313
5.25	1.1286	1.1279	1.1312	1.1203	1.1372	1.1304	1.1318	1.1243	1.1174	1.1251	1.1362	1.1396	1.1318	1.1361	1.1338	1.1308	1.1367	1.1308	1.1339
5.50	1.1310	1.1304	1.1335	1.1227	1.1388	1.1328	1.1343	1.1266	1.1197	1.1274	1.1381	1.1426	1.1345	1.1388	1.1364	1.1334	1.1382	1.1334	1.1366
5.75	1.1333	1.1328	1.1358	1.1251	1.1405	1.1353	1.1369	1.1289	1.1214	1.1299	1.1408	1.1451	1.1372	1.1415	1.1391	1.1361	1.1409	1.1359	1.1392
6.00	1.1358	1.1353	1.1382	1.1275	1.1423	1.1377	1.1395	1.1312	1.1234	1.1323	1.1440	1.1476	1.1399	1.1443	1.1417	1.1387	1.1439	1.1384	1.1419
6.25	1.1382	1.1379	1.1406	1.1299	1.1440	1.1402	1.1421	1.1336	1.1257	1.1345	1.1472	1.1503	1.1426	1.1471	1.1444	1.1414	1.1463	1.1410	1.1446
6.50	1.1407	1.1404	1.1430	1.1323	1.1458	1.1427	1.1448	1.1361	1.1280	1.1367	1.1498	1.1530	1.1453	1.1499	1.1470	1.1440	1.1498	1.1435	1.1472
6.75	1.1432	1.1429	1.1454	1.1348	1.1476	1.1452	1.1474	1.1381	1.1296	1.1393	1.1525	1.1556	1.1480	1.1527	1.1497	1.1466	1.1521	1.1461	1.1499
7.00	1.1459	1.1454	1.1478	1.1372	1.1494	1.1477	1.1500	1.1407	1.1322	1.1415	1.1556	1.1583	1.1506	1.1555	1.1523	1.1492	1.1551	1.1486	1.1525
7.25	1.1483	1.1479	1.1502	1.1396	1.1512	1.1502	1.1526	1.1427	1.1340	1.1439	1.1581	1.1611	1.1533	1.1583	1.1549	1.1518	1.1575	1.1511	1.1551
7.50	1.1508	1.1503	1.1525	1.1420	1.1530	1.1526	1.1552	1.1451	1.1361	1.1459	1.1604	1.1639	1.1568	1.1610	1.1574	1.1542	1.1594	1.1536	1.1577
7.75	1.1532	1.1527	1.1548	1.1443	1.1549	1.1550	1.1577	1.1471	1.1382	1.1480	1.1630	1.1660	1.1583	1.1637	1.1599	1.1566	1.1632	1.1560	1.1601

Table B.6.  $K_{inf}$  results from all participants at 70% void fraction (2/4)

8.00	1.1558	1.1570	1.1466	1.1567	1.1574	1.1600	1.1488	1.1394	1.1500	1.1656	1.1680	1.1606	1.1662	1.1622	1.1589	1.1654	1.1582	1.1625
8.25	1.1582	1.1571	1.1590	1.1487	1.1585	1.1595	1.1622	1.1506	1.1414	1.1519	1.1680	1.1627	1.1686	1.1643	1.1609	1.1679	1.1603	1.1646
8.50	1.1604	1.1590	1.1609	1.1507	1.1603	1.1615	1.1642	1.1524	1.1430	1.1535	1.1700	1.1646	1.1708	1.1663	1.1628	1.1696	1.1622	1.1665
8.75	1.1625	1.1607	1.1626	1.1524	1.1619	1.1633	1.1659	1.1538	1.1445	1.1555	1.1713	1.1755	1.1727	1.1681	1.1644	1.1706	1.1639	1.1682
9.00	1.1644	1.1621	1.1641	1.1539	1.1635	1.1648	1.1674	1.1555	1.1457	1.1567	1.1729	1.1769	1.1743	1.1695	1.1658	1.1731	1.1653	1.1696
9.25	1.1660	1.1633	1.1663	1.1552	1.1649	1.1661	1.1686	1.1563	1.1465	1.1576	1.1740	1.1780	1.1686	1.1757	1.1707	1.1668	1.1732	1.1708
9.50	1.1674	1.1642	1.1662	1.1562	1.1662	1.1671	1.1695	1.1575	1.1478	1.1582	1.1747	1.1792	1.1694	1.1767	1.1717	1.1677	1.1740	1.1717
9.75	1.1684	1.1649	1.1670	1.1570	1.1673	1.1679	1.1702	1.1580	1.1487	1.1597	1.1753	1.1797	1.1700	1.1775	1.1682	1.1752	1.1679	1.1724
10.00	1.1692	1.1653	1.1674	1.1575	1.1682	1.1684	1.1706	1.1590	1.1491	1.1602	1.1753	1.1803	1.1703	1.1780	1.1684	1.1742	1.1683	1.1727
10.50	1.1698	1.1654	1.1676	1.1577	1.1692	1.1687	1.1707	1.1592	1.1497	1.1609	1.1755	1.1807	1.1701	1.1781	1.1681	1.1747	1.1683	1.1725
11.00	1.1695	1.1645	1.1670	1.1572	1.1695	1.1680	1.1698	1.1595	1.1492	1.1604	1.1746	1.1797	1.1690	1.1774	1.1670	1.1737	1.1674	1.1715
11.50	1.1681	1.1628	1.1656	1.1558	1.1658	1.1665	1.1680	1.1583	1.1482	1.1598	1.1722	1.1777	1.1669	1.1759	1.1700	1.1651	1.1718	1.1656
12.00	1.1659	1.1603	1.1633	1.1537	1.1678	1.1643	1.1656	1.1565	1.1463	1.1580	1.1694	1.1746	1.1642	1.1734	1.1675	1.1695	1.1631	1.1671
12.50	1.1631	1.1573	1.1604	1.1509	1.1659	1.1614	1.1625	1.1542	1.1443	1.1556	1.1659	1.1714	1.1608	1.1702	1.1645	1.1650	1.1600	1.1639
13.00	1.1596	1.1538	1.1570	1.1477	1.1634	1.1580	1.1590	1.1513	1.1408	1.1525	1.1619	1.1678	1.1571	1.1666	1.1610	1.1557	1.1618	1.1601
13.50	1.1558	1.1501	1.1533	1.1441	1.1603	1.1542	1.1551	1.1477	1.1377	1.1491	1.1581	1.1632	1.1531	1.1627	1.1572	1.1517	1.1579	1.1562
14.00	1.1518	1.1461	1.1493	1.1402	1.1569	1.1502	1.1511	1.1440	1.1340	1.1453	1.1534	1.1596	1.1489	1.1585	1.1532	1.1476	1.1536	1.1521
14.50	1.1475	1.1420	1.1452	1.1362	1.1531	1.1461	1.1469	1.1399	1.1297	1.1415	1.1494	1.1546	1.1447	1.1542	1.1491	1.1434	1.1500	1.1477
15.00	1.1432	1.1379	1.1410	1.1321	1.1492	1.1419	1.1427	1.1360	1.1256	1.1377	1.1449	1.1500	1.1403	1.1499	1.1449	1.1391	1.1437	1.1435
15.50	1.1387	1.1337	1.1367	1.1279	1.1451	1.1377	1.1384	1.1319	1.1215	1.1332	1.1405	1.1463	1.1360	1.1455	1.1406	1.1348	1.1408	1.1391
16.00	1.1344	1.1295	1.1324	1.1237	1.1409	1.1335	1.1341	1.1276	1.1172	1.1293	1.1357	1.1424	1.1316	1.1411	1.1364	1.1304	1.1364	1.1348
16.50	1.1300	1.1253	1.1281	1.1196	1.1367	1.1292	1.1299	1.1235	1.1130	1.1257	1.1319	1.1371	1.1273	1.1368	1.1321	1.1261	1.1328	1.1305
17.00	1.1256	1.1211	1.1238	1.1154	1.1325	1.1250	1.1256	1.1193	1.1086	1.1213	1.1278	1.1331	1.1230	1.1324	1.1279	1.1218	1.1278	1.1262
17.50	1.1213	1.1170	1.1196	1.1113	1.1283	1.1208	1.1214	1.1153	1.1047	1.1177	1.1233	1.1290	1.1187	1.1281	1.1237	1.1176	1.1236	1.1219
18.00	1.1170	1.1129	1.1154	1.1072	1.1241	1.1166	1.1172	1.1116	1.1006	1.1135	1.1190	1.1251	1.1144	1.1238	1.1195	1.1133	1.1198	1.1176
18.50	1.1128	1.1088	1.1112	1.1031	1.1199	1.1125	1.1131	1.1079	0.9964	1.1093	1.1148	1.1207	1.1102	1.1195	1.1154	1.1091	1.1159	1.1134
19.00	1.1085	1.1047	1.1070	1.0990	1.1157	1.1084	1.1089	1.1035	0.9924	1.1053	1.1103	1.1164	1.1060	1.1153	1.1112	1.1049	1.1121	1.1092
19.50	1.1043	1.1007	1.1029	1.0950	1.1116	1.1043	1.1048	1.0995	0.9883	1.1017	1.1061	1.1115	1.1019	1.1111	1.1071	1.1008	1.1068	1.1050
20.00	1.1000	1.0967	1.0988	1.0910	1.1074	1.1002	1.1008	1.0955	0.9841	1.0974	1.1018	1.1078	1.0977	1.1069	1.1031	1.0967	1.1026	1.1010

Table B.7.  $K_{inj}$  results from all participants at 70% void fraction (3/4)

Burnup (GWD/MTU)	SC17	SC18	SC19	SC2	SC20	SC3	SC4	SC5	SC6	SC7	SC8	SC9	SE1	SE2	SW1	VE1	VE2	VE3	Avg.	2 $\sigma$ (pcm)
0.00	1.1061	1.1089	1.1072	1.1198	1.1084	1.1062	1.0971	1.0984	1.1005	1.1058	1.1062	1.1107	1.1080	1.1041	1.1131	1.1068	1.1069	1.1090	1.1078	1166
0.10	1.0817	1.0843	1.0830	1.0966	1.0845	1.0822	1.0735	1.0749	1.0769	1.0818	1.0822	1.0867	1.0843	1.0801	1.0889	1.0833	1.0826	1.0854	1.0841	1151
0.25	1.0810	1.0834	1.0823	1.0954	1.0841	1.0817	1.0730	1.0745	1.0763	1.0814	1.0817	1.0862	1.0840	1.0796	1.0881	1.0822	1.0825	1.0837	1.0834	1131
0.50	1.0820	1.0842	1.0832	1.0955	1.0850	1.0826	1.0740	1.0756	1.0771	1.0824	1.0826	1.0871	1.0851	1.0809	1.0892	1.0849	1.0834	1.0852	1.0842	1086
0.75	1.0841	1.0862	1.0853	1.0971	1.0872	1.0847	1.0762	1.0778	1.0791	1.0845	1.0848	1.0893	1.0861	1.0812	1.0915	1.0864	1.0854	1.0872	1.0862	1077
1.00	1.0866	1.0886	1.0879	1.0994	1.0898	1.0873	1.0787	1.0804	1.0816	1.0871	1.0874	1.0919	1.0892	1.0835	1.0942	1.0892	1.0880	1.0892	1.0885	1061
1.25	1.0894	1.0912	1.0907	1.1020	1.0927	1.0901	1.0813	1.0832	1.0842	1.0899	1.0901	1.0948	1.0917	1.0863	1.0965	1.0915	1.0906	1.0922	1.0912	1041
1.50	1.0922	1.0939	1.0934	1.1048	1.0956	1.0929	1.0840	1.0860	1.0869	1.0927	1.0930	1.0977	1.0946	1.0885	1.0993	1.0946	1.0939	1.0960	1.0939	1033
1.75	1.0951	1.0966	1.0962	1.1076	1.0985	1.0957	1.0867	1.0888	1.0895	1.0956	1.0958	1.1005	1.0975	1.0901	1.1024	1.0973	1.0965	1.0975	1.0965	1034
2.00	1.0978	1.0992	1.0989	1.1103	1.1014	1.0985	1.0893	1.0915	1.0921	1.0983	1.0986	1.1034	1.0999	1.0925	1.1046	1.1002	1.0993	1.1011	1.0991	1028
2.25	1.1005	1.1018	1.1015	1.1131	1.1043	1.1012	1.0918	1.0942	1.0947	1.1010	1.1013	1.1062	1.1026	1.0946	1.1073	1.1026	1.1027	1.1033	1.1017	1031
2.50	1.1032	1.1043	1.1041	1.1158	1.1071	1.1039	1.0942	1.0968	1.0972	1.1037	1.1040	1.1089	1.1047	1.0966	1.1104	1.1060	1.1045	1.1065	1.1042	1040
2.75	1.1058	1.1068	1.1067	1.1185	1.1098	1.1065	1.0966	1.0994	1.0996	1.1063	1.1066	1.1116	1.1077	1.0996	1.1126	1.1083	1.1076	1.1085	1.1067	1039
3.00	1.1084	1.1093	1.1092	1.1212	1.1126	1.1091	1.0991	1.1019	1.1020	1.1089	1.1093	1.1143	1.1101	1.1007	1.1151	1.1111	1.1100	1.1111	1.1091	1060
3.25	1.1110	1.1118	1.1116	1.1239	1.1153	1.1117	1.1020	1.1043	1.1044	1.1115	1.1119	1.1170	1.1128	1.1032	1.1174	1.1138	1.1130	1.1140	1.1116	1059
3.50	1.1136	1.1142	1.1141	1.1265	1.1180	1.1143	1.1044	1.1068	1.1068	1.1141	1.1145	1.1197	1.1151	1.1052	1.1201	1.1161	1.1151	1.1166	1.1141	1077
3.75	1.1162	1.1167	1.1166	1.1292	1.1208	1.1168	1.1067	1.1092	1.1091	1.1166	1.1170	1.1223	1.1177	1.1067	1.1227	1.1194	1.1174	1.1189	1.1165	1096
4.00	1.1187	1.1192	1.1190	1.1319	1.1235	1.1193	1.1091	1.1117	1.1114	1.1192	1.1196	1.1250	1.1201	1.1087	1.1249	1.1216	1.1201	1.1217	1.1189	1117
4.25	1.1213	1.1217	1.1215	1.1346	1.1262	1.1219	1.1115	1.1141	1.1138	1.1217	1.1222	1.1277	1.1230	1.1112	1.1272	1.1249	1.1229	1.1239	1.1213	1128
4.50	1.1239	1.1242	1.1239	1.1373	1.1289	1.1245	1.1138	1.1166	1.1162	1.1243	1.1248	1.1304	1.1253	1.1131	1.1298	1.1260	1.1251	1.1266	1.1238	1145
4.75	1.1265	1.1267	1.1264	1.1401	1.1317	1.1271	1.1162	1.1191	1.1186	1.1269	1.1275	1.1331	1.1278	1.1151	1.1324	1.1293	1.1280	1.1294	1.1263	1167
5.00	1.1292	1.1293	1.1289	1.1429	1.1345	1.1297	1.1186	1.1216	1.1210	1.1295	1.1301	1.1359	1.1303	1.1169	1.1350	1.1321	1.1305	1.1322	1.1288	1201
5.25	1.1318	1.1318	1.1314	1.1457	1.1372	1.1323	1.1210	1.1241	1.1234	1.1321	1.1328	1.1386	1.1327	1.1194	1.1371	1.1346	1.1330	1.1348	1.1313	1219
5.50	1.1345	1.1344	1.1339	1.1486	1.1400	1.1350	1.1234	1.1266	1.1258	1.1347	1.1354	1.1414	1.1357	1.1210	1.1396	1.1370	1.1362	1.1373	1.1338	1243
5.75	1.1372	1.1371	1.1364	1.1514	1.1428	1.1377	1.1259	1.1291	1.1283	1.1374	1.1381	1.1442	1.1383	1.1228	1.1424	1.1398	1.1389	1.1401	1.1363	1278
6.00	1.1399	1.1397	1.1390	1.1544	1.1456	1.1403	1.1283	1.1316	1.1307	1.1400	1.1408	1.1470	1.1408	1.1259	1.1451	1.1426	1.1413	1.1426	1.1389	1300
6.25	1.1426	1.1424	1.1415	1.1573	1.1484	1.1430	1.1308	1.1341	1.1332	1.1427	1.1435	1.1498	1.1435	1.1275	1.1473	1.1454	1.1437	1.1457	1.1415	1332
6.50	1.1453	1.1450	1.1441	1.1603	1.1512	1.1457	1.1333	1.1367	1.1357	1.1454	1.1463	1.1526	1.1465	1.1295	1.1500	1.1478	1.1463	1.1480	1.1440	1363
6.75	1.1480	1.1477	1.1466	1.1633	1.1540	1.1484	1.1357	1.1392	1.1382	1.1480	1.1490	1.1554	1.1487	1.1324	1.1528	1.1511	1.1492	1.1511	1.1466	1396
7.00	1.1506	1.1504	1.1492	1.1663	1.1568	1.1511	1.1383	1.1417	1.1407	1.1506	1.1517	1.1582	1.1511	1.1339	1.1549	1.1532	1.1518	1.1532	1.1492	1423
7.25	1.1533	1.1531	1.1517	1.1692	1.1595	1.1538	1.1407	1.1442	1.1432	1.1532	1.1543	1.1610	1.1536	1.1362	1.1574	1.1557	1.1549	1.1562	1.1517	1456
7.50	1.1558	1.1557	1.1541	1.1721	1.1622	1.1564	1.1432	1.1466	1.1456	1.1558	1.1569	1.1636	1.1563	1.1377	1.1600	1.1592	1.1567	1.1590	1.1542	1491
7.75	1.1583	1.1583	1.1565	1.1750	1.1647	1.1589	1.1455	1.1490	1.1480	1.1582	1.1594	1.1662	1.1587	1.1406	1.1624	1.1606	1.1596	1.1613	1.1566	1510
8.00	1.1606	1.1607	1.1587	1.1777	1.1671	1.1613	1.1477	1.1512	1.1503	1.1605	1.1618	1.1686	1.1612	1.1417	1.1647	1.1634	1.1622	1.1638	1.1608	1559
8.25	1.1627	1.1630	1.1608	1.1802	1.1692	1.1635	1.1498	1.1533	1.1525	1.1626	1.1640	1.1708	1.1632	1.1439	1.1667	1.1658	1.1640	1.1657	1.1610	1580

Table B.8.  $K_{inj}$  results from all participants at 70% void fraction (4/4)

8.50	1.1646	1.1650	1.1626	1.1824	1.1712	1.1655	1.1517	1.1552	1.1545	1.1645	1.1660	1.1727	1.1655	1.1459	1.1685	1.1677	1.1657	1.1683	1.1630	1600
8.75	1.1662	1.1668	1.1643	1.1844	1.1729	1.1672	1.1534	1.1568	1.1564	1.1661	1.1677	1.1744	1.1675	1.1480	1.1706	1.1688	1.1675	1.1696	1.1647	1593
9.00	1.1676	1.1684	1.1657	1.1861	1.1743	1.1687	1.1548	1.1582	1.1580	1.1675	1.1691	1.1758	1.1685	1.1484	1.1718	1.1698	1.1689	1.1710	1.1661	1613
9.25	1.1686	1.1696	1.1668	1.1874	1.1754	1.1699	1.1560	1.1594	1.1593	1.1687	1.1702	1.1769	1.1695	1.1504	1.1731	1.1708	1.1693	1.1722	1.1672	1605
9.50	1.1694	1.1706	1.1677	1.1885	1.1762	1.1708	1.1569	1.1602	1.1604	1.1695	1.1711	1.1778	1.1704	1.1512	1.1738	1.1719	1.1707	1.1731	1.1682	1602
9.75	1.1700	1.1712	1.1683	1.1892	1.1768	1.1714	1.1576	1.1609	1.1612	1.1702	1.1717	1.1783	1.1707	1.1519	1.1747	1.1728	1.1711	1.1735	1.1689	1592
10.00	1.1703	1.1716	1.1687	1.1897	1.1771	1.1718	1.1580	1.1612	1.1618	1.1705	1.1721	1.1786	1.1714	1.1527	1.1755	1.1728	1.1711	1.1735	1.1693	1573
10.50	1.1701	1.1716	1.1687	1.1897	1.1769	1.1718	1.1582	1.1613	1.1623	1.1705	1.1721	1.1785	1.1715	1.1528	1.1757	1.1720	1.1709	1.1739	1.1694	1557
11.00	1.1690	1.1706	1.1678	1.1887	1.1758	1.1708	1.1574	1.1604	1.1619	1.1696	1.1710	1.1774	1.1700	1.1523	1.1751	1.1715	1.1697	1.1735	1.1686	1525
11.50	1.1669	1.1687	1.1660	1.1869	1.1738	1.1689	1.1556	1.1587	1.1605	1.1677	1.1691	1.1753	1.1683	1.1512	1.1736	1.1691	1.1673	1.1711	1.1669	1483
12.00	1.1642	1.1660	1.1636	1.1842	1.1710	1.1663	1.1531	1.1562	1.1584	1.1651	1.1664	1.1725	1.1652	1.1487	1.1712	1.1670	1.1659	1.1681	1.1645	1452
12.50	1.1608	1.1627	1.1605	1.1809	1.1677	1.1630	1.1501	1.1531	1.1557	1.1619	1.1632	1.1691	1.1625	1.1456	1.1683	1.1639	1.1619	1.1653	1.1614	1415
13.00	1.1571	1.1569	1.1569	1.1772	1.1640	1.1594	1.1466	1.1496	1.1524	1.1563	1.1595	1.1654	1.1584	1.1420	1.1654	1.1602	1.1584	1.1614	1.1579	1405
13.50	1.1531	1.1549	1.1531	1.1731	1.1600	1.1555	1.1429	1.1458	1.1488	1.1544	1.1556	1.1614	1.1548	1.1387	1.1616	1.1566	1.1543	1.1571	1.1541	1369
14.00	1.1489	1.1507	1.1490	1.1688	1.1559	1.1513	1.1389	1.1418	1.1449	1.1503	1.1514	1.1572	1.1506	1.1351	1.1580	1.1513	1.1504	1.1536	1.1501	1357
14.50	1.1447	1.1464	1.1449	1.1645	1.1516	1.1471	1.1348	1.1377	1.1408	1.1461	1.1472	1.1529	1.1456	1.1304	1.1535	1.1481	1.1460	1.1491	1.1459	1353
15.00	1.1403	1.1421	1.1406	1.1600	1.1473	1.1428	1.1310	1.1335	1.1367	1.1418	1.1429	1.1485	1.1411	1.1259	1.1497	1.1441	1.1416	1.1448	1.1416	1335
15.50	1.1360	1.1377	1.1363	1.1555	1.1430	1.1385	1.1272	1.1293	1.1326	1.1375	1.1386	1.1442	1.1376	1.1218	1.1456	1.1386	1.1371	1.1402	1.1373	1326
16.00	1.1316	1.1334	1.1320	1.1511	1.1387	1.1342	1.1229	1.1251	1.1284	1.1332	1.1343	1.1398	1.1327	1.1185	1.1411	1.1346	1.1325	1.1354	1.1330	1307
16.50	1.1273	1.1290	1.1277	1.1466	1.1344	1.1299	1.1187	1.1209	1.1243	1.1290	1.1300	1.1355	1.1287	1.1136	1.1371	1.1305	1.1286	1.1315	1.1288	1303
17.00	1.1230	1.1247	1.1235	1.1421	1.1301	1.1257	1.1145	1.1167	1.1201	1.1247	1.1258	1.1312	1.1246	1.1096	1.1329	1.1259	1.1242	1.1272	1.1245	1296
17.50	1.1187	1.1204	1.1193	1.1377	1.1259	1.1215	1.1104	1.1126	1.1160	1.1205	1.1215	1.1269	1.1198	1.1054	1.1289	1.1216	1.1202	1.1229	1.1203	1282
18.00	1.1144	1.1162	1.1150	1.1333	1.1217	1.1173	1.1062	1.1085	1.1119	1.1163	1.1173	1.1226	1.1155	1.1012	1.1245	1.1171	1.1160	1.1189	1.1161	1276
18.50	1.1102	1.1120	1.1109	1.1289	1.1175	1.1131	1.1021	1.1044	1.1078	1.1121	1.1131	1.1184	1.1107	1.0969	1.1206	1.1131	1.1113	1.1144	1.1119	1271
19.00	1.1060	1.1078	1.1067	1.1245	1.1133	1.1090	1.0980	1.1003	1.1038	1.1080	1.1090	1.1142	1.1070	1.0924	1.1166	1.1087	1.1075	1.1102	1.1078	1266
19.50	1.1019	1.1036	1.1026	1.1202	1.1092	1.1049	1.0940	1.0963	1.0998	1.1039	1.1049	1.1100	1.1030	1.0888	1.1124	1.1048	1.1025	1.1061	1.1036	1240
20.00	1.0977	1.0995	1.0986	1.1159	1.1050	1.1008	1.0900	1.0923	1.0958	1.0999	1.1008	1.1059	1.0984	1.0848	1.1084	1.1004	1.0991	1.1022	1.0995	1237

**Table B.9. <sup>155</sup>Gd concentration results from all participants at 0% void fraction**

Burnup (GWd/MTU)	2.00	4.00	6.00	8.00	10.00	12.00	14.00	16.00	18.00	20.00
AL1	1.379E-04	9.351E-05	5.194E-05	1.975E-05	3.683E-06	4.797E-07	1.493E-07	1.206E-07	1.158E-07	1.125E-07
AP1	1.362E-04	9.015E-05	4.766E-05	1.616E-05	2.829E-06	4.188E-07	1.537E-07	1.264E-07	1.211E-07	1.175E-07
CA1	1.370E-04	9.182E-05	4.970E-05	1.790E-05	3.448E-06	5.267E-07	1.733E-07	1.348E-07	1.282E-07	1.244E-07
HE1	1.375E-04	9.237E-05	5.064E-05	1.883E-05	3.757E-06	5.670E-07	1.710E-07	1.280E-07	1.214E-07	1.180E-07
HE2	1.384E-04	9.469E-05	5.364E-05	2.142E-05	4.699E-06	7.200E-07	1.876E-07	1.285E-07	1.201E-07	1.166E-07
HE3	1.366E-04	9.108E-05	4.909E-05	1.751E-05	3.301E-06	4.925E-07	1.601E-07	1.250E-07	1.192E-07	1.159E-07
HE4	1.355E-04	8.889E-05	4.646E-05	1.554E-05	2.713E-06	4.062E-07	1.489E-07	1.222E-07	1.173E-07	1.141E-07
KE1	1.383E-04	9.206E-05	4.552E-05	1.378E-05	2.310E-06	3.505E-07	1.409E-07	1.200E-07	1.160E-07	1.133E-07
KE2	1.390E-04	9.369E-05	4.746E-05	1.500E-05	2.649E-06	4.097E-07	1.598E-07	1.343E-07	1.293E-07	1.260E-07
KE3	1.383E-04	9.209E-05	4.555E-05	1.380E-05	2.320E-06	3.517E-07	1.410E-07	1.201E-07	1.160E-07	1.133E-07
MO1	1.357E-04	8.874E-05	4.567E-05	1.458E-05	2.349E-06	3.372E-07	1.332E-07	1.137E-07	1.096E-07	1.069E-07
SC1	1.361E-04	8.991E-05	4.736E-05	1.603E-05	2.682E-06	3.696E-07	1.348E-07	1.133E-07	1.092E-07	1.066E-07
SC10	1.356E-04	8.863E-05	4.567E-05	1.472E-05	2.409E-06	3.485E-07	1.351E-07	1.142E-07	1.102E-07	1.075E-07
SC11	1.356E-04	8.858E-05	4.576E-05	1.484E-05	2.421E-06	3.429E-07	1.321E-07	1.121E-07	1.083E-07	1.057E-07
SC12	1.354E-04	8.840E-05	4.585E-05	1.524E-05	2.619E-06	3.832E-07	1.405E-07	1.161E-07	1.115E-07	1.086E-07
SC13	1.355E-04	8.843E-05	4.578E-05	1.509E-05	2.571E-06	3.758E-07	1.381E-07	1.143E-07	1.100E-07	1.074E-07
SC14	1.355E-04	8.883E-05	4.583E-05	1.490E-05	2.499E-06	3.669E-07	1.388E-07	1.161E-07	1.114E-07	1.091E-07
SC15	1.357E-04	8.896E-05	4.627E-05	1.529E-05	2.600E-06	3.789E-07	1.401E-07	1.163E-07	1.119E-07	1.090E-07
SC16	1.350E-04	8.733E-05	4.436E-05	1.387E-05	2.180E-06	3.160E-07	1.298E-07	1.120E-07	1.082E-07	1.056E-07
SC17	1.356E-04	8.863E-05	4.567E-05	1.472E-05	2.409E-06	3.485E-07	1.351E-07	1.142E-07	1.102E-07	1.075E-07
SC18	1.359E-04	8.900E-05	4.626E-05	1.505E-05	2.378E-06	3.254E-07	1.282E-07	1.102E-07	1.066E-07	1.039E-07
SC19	1.358E-04	8.949E-05	4.705E-05	1.597E-05	2.824E-06	4.159E-07	1.481E-07	1.210E-07	1.161E-07	1.131E-07
SC2	1.346E-04	8.670E-05	4.366E-05	1.338E-05	2.072E-06	3.151E-07	1.403E-07	1.229E-07	1.187E-07	1.156E-07
SC20	1.373E-04	8.847E-05	4.418E-05	1.360E-05	2.127E-06	3.113E-07	1.301E-07	1.126E-07	1.088E-07	1.061E-07
SC3	1.356E-04	8.879E-05	4.605E-05	1.505E-05	2.471E-06	3.510E-07	1.337E-07	1.129E-07	1.089E-07	1.061E-07
SC4	1.362E-04	8.989E-05	4.734E-05	1.599E-05	2.753E-06	3.992E-07	1.469E-07	1.218E-07	1.172E-07	1.142E-07
SC5	1.361E-04	8.981E-05	4.725E-05	1.598E-05	2.781E-06	4.070E-07	1.485E-07	1.224E-07	1.177E-07	1.145E-07
SC6	1.372E-04	9.202E-05	4.995E-05	1.811E-05	3.421E-06	4.894E-07	1.512E-07	1.171E-07	1.119E-07	1.089E-07
SC7	1.359E-04	8.907E-05	4.609E-05	1.497E-05	2.477E-06	3.574E-07	1.359E-07	1.143E-07	1.102E-07	1.075E-07
SC8	1.356E-04	8.875E-05	4.593E-05	1.494E-05	2.454E-06	3.515E-07	1.346E-07	1.136E-07	1.096E-07	1.069E-07
SC9	1.356E-04	8.856E-05	4.556E-05	1.461E-05	2.373E-06	3.427E-07	1.341E-07	1.138E-07	1.098E-07	1.071E-07
SE1	1.360E-04	8.954E-05	4.687E-05	1.562E-05	2.666E-06	3.825E-07	1.389E-07	1.148E-07	1.107E-07	1.080E-07
SE2	1.361E-04	8.977E-05	4.714E-05	1.585E-05	2.729E-06	3.921E-07	1.399E-07	1.149E-07	1.105E-07	1.077E-07
SW1	1.373E-04	9.223E-05	5.018E-05	1.835E-05	3.637E-06	5.611E-07	1.786E-07	1.371E-07	1.300E-07	1.262E-07
VE1	1.360E-04	8.963E-05	4.687E-05	1.568E-05	2.769E-06	4.235E-07	1.573E-07	1.294E-07	1.242E-07	1.209E-07
VE2	1.361E-04	8.979E-05	4.708E-05	1.583E-05	2.808E-06	4.294E-07	1.575E-07	1.288E-07	1.233E-07	1.204E-07
VE3	1.360E-04	8.949E-05	4.670E-05	1.548E-05	2.627E-06	3.794E-07	1.386E-07	1.148E-07	1.104E-07	1.076E-07
Average	1.363E-04	8.994E-05	4.703E-05	1.577E-05	2.752E-06	4.034E-07	1.456E-07	1.196E-07	1.149E-07	1.119E-07
2σ	2.054E-06	3.651E-06	4.231E-06	3.494E-06	1.079E-06	1.686E-07	2.867E-08	1.437E-08	1.276E-08	1.218E-08

**Table B.10. <sup>155</sup>Gd concentration results from all participants at 40% void fraction**

Burnup (GWd/MTU)	2.00	4.00	6.00	8.00	10.00	12.00	14.00	16.00	18.00	20.00
AL1	1.380E-04	9.500E-05	5.502E-05	2.356E-05	5.836E-06	9.812E-07	2.431E-07	1.558E-07	1.437E-07	1.394E-07
AP1	1.368E-04	9.263E-05	5.202E-05	2.087E-05	4.993E-06	9.018E-07	2.525E-07	1.644E-07	1.505E-07	1.455E-07
CA1	1.376E-04	9.435E-05	5.411E-05	2.276E-05	5.894E-06	1.125E-06	2.994E-07	1.796E-07	1.607E-07	1.549E-07
HE1	1.376E-04	9.441E-05	5.461E-05	2.332E-05	6.159E-06	1.179E-06	2.992E-07	1.711E-07	1.514E-07	1.461E-07
HE2	1.397E-04	9.875E-05	6.006E-05	2.850E-05	8.781E-06	1.837E-06	4.111E-07	1.863E-07	1.519E-07	1.444E-07
HE3	1.372E-04	9.377E-05	5.365E-05	2.246E-05	5.717E-06	1.066E-06	2.764E-07	1.650E-07	1.480E-07	1.430E-07
HE4	1.363E-04	9.190E-05	5.141E-05	2.063E-05	4.969E-06	9.065E-07	2.496E-07	1.595E-07	1.455E-07	1.409E-07
KE1	1.386E-04	9.602E-05	5.311E-05	2.068E-05	5.158E-06	9.685E-07	2.587E-07	1.609E-07	1.465E-07	1.425E-07
KE2	1.390E-04	9.766E-05	5.520E-05	2.228E-05	5.823E-06	1.134E-06	3.016E-07	1.829E-07	1.650E-07	1.601E-07
KE3	1.385E-04	9.598E-05	5.310E-05	2.070E-05	5.173E-06	9.729E-07	2.601E-07	1.612E-07	1.467E-07	1.425E-07
MO1	1.361E-04	9.093E-05	4.966E-05	1.883E-05	4.140E-06	7.078E-07	2.080E-07	1.450E-07	1.353E-07	1.316E-07
SC1	1.364E-04	9.173E-05	5.079E-05	1.983E-05	4.436E-06	7.411E-07	2.088E-07	1.430E-07	1.335E-07	1.301E-07
SC10	1.362E-04	9.111E-05	5.002E-05	1.924E-05	4.338E-06	7.522E-07	2.154E-07	1.463E-07	1.359E-07	1.322E-07
SC11	1.361E-04	9.100E-05	4.991E-05	1.915E-05	4.247E-06	7.179E-07	2.063E-07	1.425E-07	1.329E-07	1.294E-07
SC12	1.362E-04	9.125E-05	5.053E-05	2.003E-05	4.743E-06	8.465E-07	2.324E-07	1.503E-07	1.379E-07	1.337E-07
SC13	1.360E-04	9.094E-05	5.010E-05	1.963E-05	4.589E-06	8.177E-07	2.269E-07	1.480E-07	1.362E-07	1.324E-07
SC14	1.359E-04	9.101E-05	4.984E-05	1.915E-05	4.373E-06	7.782E-07	2.238E-07	1.491E-07	1.386E-07	1.346E-07
SC15	1.363E-04	9.169E-05	5.093E-05	2.013E-05	4.739E-06	8.446E-07	2.330E-07	1.514E-07	1.391E-07	1.349E-07
SC16	1.362E-04	9.087E-05	4.970E-05	1.897E-05	4.192E-06	7.123E-07	2.058E-07	1.423E-07	1.327E-07	1.292E-07
SC17	1.362E-04	9.111E-05	5.002E-05	1.924E-05	4.338E-06	7.522E-07	2.154E-07	1.463E-07	1.359E-07	1.322E-07
SC18	1.363E-04	9.133E-05	5.035E-05	1.944E-05	4.261E-06	7.011E-07	2.006E-07	1.403E-07	1.314E-07	1.279E-07
SC19	1.365E-04	9.215E-05	5.159E-05	2.076E-05	5.025E-06	9.117E-07	2.482E-07	1.583E-07	1.447E-07	1.403E-07
SC2	1.355E-04	8.986E-05	4.850E-05	1.797E-05	3.836E-06	6.635E-07	2.127E-07	1.559E-07	1.465E-07	1.424E-07
SC20	1.356E-04	8.988E-05	4.868E-05	1.832E-05	4.015E-06	6.885E-07	2.046E-07	1.435E-07	1.341E-07	1.305E-07
SC3	1.361E-04	9.121E-05	5.031E-05	1.955E-05	4.422E-06	7.576E-07	2.137E-07	1.447E-07	1.344E-07	1.308E-07
SC4	1.367E-04	9.240E-05	5.175E-05	2.076E-05	4.933E-06	8.783E-07	2.424E-07	1.579E-07	1.452E-07	1.409E-07
SC5	1.366E-04	9.222E-05	5.160E-05	2.070E-05	4.961E-06	8.942E-07	2.474E-07	1.602E-07	1.469E-07	1.425E-07
SC6	1.376E-04	9.423E-05	5.402E-05	2.276E-05	5.812E-06	1.060E-06	2.642E-07	1.550E-07	1.391E-07	1.348E-07
SC7	1.366E-04	9.181E-05	5.071E-05	1.972E-05	4.506E-06	7.827E-07	2.190E-07	1.462E-07	1.354E-07	1.317E-07
SC8	1.362E-04	9.118E-05	5.019E-05	1.943E-05	4.386E-06	7.551E-07	2.142E-07	1.452E-07	1.349E-07	1.312E-07
SC9	1.361E-04	9.096E-05	4.979E-05	1.901E-05	4.231E-06	7.277E-07	2.108E-07	1.450E-07	1.350E-07	1.313E-07
SE1	1.364E-04	9.168E-05	5.080E-05	1.988E-05	4.583E-06	7.990E-07	2.227E-07	1.481E-07	1.363E-07	1.329E-07
SE2	1.365E-04	9.191E-05	5.106E-05	2.012E-05	4.671E-06	8.168E-07	2.252E-07	1.479E-07	1.367E-07	1.328E-07
SW1	1.375E-04	9.408E-05	5.384E-05	2.265E-05	5.918E-06	1.147E-06	3.062E-07	1.838E-07	1.643E-07	1.583E-07
VE1	1.363E-04	9.165E-05	5.076E-05	1.994E-05	4.719E-06	8.661E-07	2.522E-07	1.677E-07	1.540E-07	1.494E-07
VE2	1.364E-04	9.181E-05	5.095E-05	2.007E-05	4.763E-06	8.815E-07	2.546E-07	1.685E-07	1.553E-07	1.505E-07
VE3	1.363E-04	9.152E-05	5.054E-05	1.964E-05	4.492E-06	7.821E-07	2.200E-07	1.471E-07	1.360E-07	1.322E-07
Average	1.368E-04	9.249E-05	5.160E-05	2.056E-05	4.924E-06	8.880E-07	2.429E-07	1.558E-07	1.427E-07	1.384E-07
2σ	1.936E-06	4.145E-06	4.532E-06	3.884E-06	1.783E-06	4.278E-07	8.216E-08	2.542E-08	1.827E-08	1.697E-08



**Table B.11. <sup>155</sup>Gd concentration results from all participants at 70% void fraction**

Burnup (GWd/MTU)	2.00	4.00	6.00	8.00	10.00	12.00	14.00	16.00	18.00	20.00
AL1	1.385E-04	9.746E-05	5.933E-05	2.869E-05	9.292E-06	2.109E-06	5.009E-07	2.309E-07	1.877E-07	1.782E-07
AP1	1.376E-04	9.576E-05	5.721E-05	2.668E-05	8.456E-06	1.993E-06	5.209E-07	2.470E-07	1.972E-07	1.856E-07
CA1	1.386E-04	9.766E-05	5.950E-05	2.883E-05	9.745E-06	2.436E-06	6.369E-07	2.810E-07	2.137E-07	1.985E-07
HE1	1.382E-04	9.700E-05	5.913E-05	2.870E-05	9.721E-06	2.436E-06	6.287E-07	2.694E-07	2.020E-07	1.874E-07
HE2	1.412E-04	1.031E-04	6.697E-05	3.653E-05	1.488E-05	4.355E-06	1.111E-06	3.689E-07	2.184E-07	1.872E-07
HE3	1.380E-04	9.669E-05	5.856E-05	2.805E-05	9.255E-06	2.251E-06	5.749E-07	2.534E-07	1.945E-07	1.817E-07
HE4	1.372E-04	9.519E-05	5.677E-05	2.652E-05	8.472E-06	2.021E-06	5.251E-07	2.428E-07	1.913E-07	1.798E-07
KE1	1.396E-04	1.018E-04	6.388E-05	3.194E-05	1.186E-05	3.337E-06	8.627E-07	3.204E-07	2.135E-07	1.920E-07
KE2	1.404E-04	1.035E-04	6.608E-05	3.399E-05	1.309E-05	3.828E-06	1.018E-06	3.740E-07	2.446E-07	2.180E-07
KE3	1.396E-04	1.019E-04	6.358E-05	3.202E-05	1.191E-05	3.361E-06	8.736E-07	3.225E-07	2.139E-07	1.921E-07
MO1	1.370E-04	9.425E-05	5.506E-05	2.459E-05	7.289E-06	1.620E-06	4.202E-07	2.112E-07	1.755E-07	1.675E-07
SC1	1.373E-04	9.479E-05	5.581E-05	2.529E-05	7.531E-06	1.634E-06	4.107E-07	2.053E-07	1.713E-07	1.637E-07
SC10	1.372E-04	9.453E-05	5.555E-05	2.522E-05	7.687E-06	1.746E-06	4.485E-07	2.172E-07	1.769E-07	1.681E-07
SC11	1.371E-04	9.430E-05	5.506E-05	2.454E-05	7.218E-06	1.571E-06	4.017E-07	2.034E-07	1.703E-07	1.628E-07
SC12	1.373E-04	9.489E-05	5.622E-05	2.614E-05	8.305E-06	1.955E-06	4.986E-07	2.288E-07	1.806E-07	1.700E-07
SC13	1.370E-04	9.430E-05	5.553E-05	2.552E-05	7.998E-06	1.876E-06	4.839E-07	2.254E-07	1.791E-07	1.692E-07
SC14	1.368E-04	9.429E-05	5.526E-05	2.497E-05	7.615E-06	1.755E-06	4.593E-07	2.236E-07	1.813E-07	1.714E-07
SC15	1.374E-04	9.538E-05	5.685E-05	2.655E-05	8.483E-06	2.016E-06	5.168E-07	2.357E-07	1.851E-07	1.740E-07
SC16	1.378E-04	9.528E-05	5.624E-05	2.567E-05	7.818E-06	1.749E-06	4.398E-07	2.107E-07	1.718E-07	1.634E-07
SC17	1.372E-04	9.453E-05	5.555E-05	2.522E-05	7.687E-06	1.746E-06	4.485E-07	2.172E-07	1.769E-07	1.681E-07
SC18	1.372E-04	9.458E-05	5.563E-05	2.521E-05	7.514E-06	1.629E-06	4.090E-07	2.040E-07	1.701E-07	1.626E-07
SC19	1.375E-04	9.564E-05	5.719E-05	2.688E-05	8.683E-06	2.082E-06	5.356E-07	2.442E-07	1.916E-07	1.803E-07
SC2	1.368E-04	9.358E-05	5.406E-05	2.358E-05	6.705E-06	1.449E-06	3.941E-07	2.172E-07	1.869E-07	1.791E-07
SC20	1.368E-04	9.368E-05	5.455E-05	2.443E-05	7.309E-06	1.634E-06	4.232E-07	2.110E-07	1.745E-07	1.662E-07
SC3	1.371E-04	9.458E-05	5.574E-05	2.547E-05	7.785E-06	1.753E-06	4.443E-07	2.138E-07	1.743E-07	1.657E-07
SC4	1.378E-04	9.594E-05	5.746E-05	2.707E-05	8.705E-06	2.063E-06	5.283E-07	2.422E-07	1.908E-07	1.797E-07
SC5	1.375E-04	9.556E-05	5.711E-05	2.683E-05	8.648E-06	2.069E-06	5.354E-07	2.464E-07	1.939E-07	1.824E-07
SC6	1.385E-04	9.735E-05	5.925E-05	2.877E-05	9.705E-06	2.376E-06	5.897E-07	2.465E-07	1.845E-07	1.718E-07
SC7	1.379E-04	9.559E-05	5.663E-05	2.605E-05	8.081E-06	1.851E-06	4.677E-07	2.190E-07	1.758E-07	1.666E-07
SC8	1.371E-04	9.453E-05	5.562E-05	2.533E-05	7.724E-06	1.743E-06	4.441E-07	2.145E-07	1.749E-07	1.663E-07
SC9	1.370E-04	9.423E-05	5.509E-05	2.472E-05	7.381E-06	1.643E-06	4.232E-07	2.106E-07	1.742E-07	1.660E-07
SE1	1.372E-04	9.487E-05	5.602E-05	2.562E-05	7.883E-06	1.788E-06	4.594E-07	2.203E-07	1.785E-07	1.698E-07
SE2	1.389E-04	9.798E-05	5.975E-05	2.889E-05	9.556E-06	2.267E-06	5.516E-07	2.344E-07	1.791E-07	1.680E-07
SW1	1.381E-04	9.691E-05	5.873E-05	2.828E-05	9.564E-06	2.424E-06	6.452E-07	2.895E-07	2.217E-07	2.061E-07
VE1	1.371E-04	9.467E-05	5.581E-05	2.546E-05	7.923E-06	1.870E-06	5.042E-07	2.490E-07	2.029E-07	1.920E-07
VE2	1.372E-04	9.488E-05	5.603E-05	2.565E-05	8.002E-06	1.902E-06	5.114E-07	2.524E-07	2.046E-07	1.937E-07
VE3	1.371E-04	9.462E-05	5.568E-05	2.526E-05	7.685E-06	1.743E-06	4.498E-07	2.179E-07	1.778E-07	1.687E-07
Average	1.378E-04	9.610E-05	5.753E-05	2.700E-05	8.734E-06	2.110E-06	5.432E-07	2.438E-07	1.892E-07	1.774E-07
2σ	2.057E-06	5.115E-06	6.194E-06	5.578E-06	3.453E-06	1.276E-06	3.332E-07	8.502E-08	3.498E-08	2.647E-08

**Table B.12. <sup>157</sup>Gd concentration results from all participants at 0% void fraction**

Burnup (GWd/MTU)	2.00	4.00	6.00	8.00	10.00	12.00	14.00	16.00	18.00	20.00
AL1	9.832E-05	4.387E-05	1.257E-05	9.748E-07	9.837E-08	8.732E-08	8.472E-08	8.297E-08	8.132E-08	7.980E-08
AP1	9.419E-05	3.867E-05	9.037E-06	4.437E-07	1.057E-07	9.727E-08	9.507E-08	9.321E-08	9.124E-08	8.914E-08
CA1	9.514E-05	3.969E-05	9.742E-06	5.495E-07	1.008E-07	9.125E-08	8.831E-08	8.663E-08	8.494E-08	8.313E-08
HE1	9.595E-05	4.082E-05	1.054E-05	6.841E-07	1.249E-07	1.128E-07	1.097E-07	1.077E-07	1.056E-07	1.034E-07
HE2	9.825E-05	4.364E-05	1.246E-05	1.026E-06	1.240E-07	1.088E-07	1.052E-07	1.032E-07	1.011E-07	9.898E-08
HE3	9.507E-05	3.981E-05	9.811E-06	5.571E-07	1.166E-07	1.066E-07	1.039E-07	1.020E-07	1.001E-07	9.801E-08
HE4	9.333E-05	3.787E-05	8.619E-06	4.118E-07	1.120E-07	1.038E-07	1.013E-07	9.950E-08	9.759E-08	9.554E-08
KE1	8.301E-05	2.467E-05	3.278E-06	2.062E-07	1.188E-07	1.112E-07	1.098E-07	1.085E-07	1.068E-07	1.051E-07
KE2	8.476E-05	2.612E-05	3.729E-06	2.200E-07	1.119E-07	1.037E-07	1.021E-07	1.009E-07	9.959E-08	9.800E-08
KE3	8.299E-05	2.469E-05	3.288E-06	2.067E-07	1.189E-07	1.113E-07	1.097E-07	1.084E-07	1.068E-07	1.050E-07
MO1	9.272E-05	3.694E-05	8.007E-06	3.439E-07	1.054E-07	9.787E-08	9.642E-08	9.479E-08	9.223E-08	9.000E-08
SC1	9.420E-05	3.900E-05	9.319E-06	4.595E-07	9.295E-08	8.459E-08	8.225E-08	8.214E-08	8.048E-08	7.872E-08
SC10	9.246E-05	3.683E-05	8.020E-06	3.467E-07	1.014E-07	9.460E-08	9.264E-08	9.111E-08	8.949E-08	8.776E-08
SC11	9.289E-05	3.749E-05	8.439E-06	3.778E-07	1.018E-07	9.473E-08	9.276E-08	9.126E-08	8.964E-08	8.792E-08
SC12	9.254E-05	3.725E-05	8.471E-06	4.016E-07	1.056E-07	9.799E-08	9.563E-08	9.379E-08	9.186E-08	8.980E-08
SC13	9.248E-05	3.712E-05	8.349E-06	4.055E-07	1.175E-07	1.094E-07	1.071E-07	1.055E-07	1.037E-07	1.018E-07
SC14	9.298E-05	3.721E-05	8.338E-06	3.770E-07	1.073E-07	1.014E-07	9.934E-08	9.568E-08	9.555E-08	9.314E-08
SC15	9.291E-05	3.741E-05	8.397E-06	3.914E-07	1.091E-07	1.014E-07	9.910E-08	9.732E-08	9.543E-08	9.340E-08
SC16	9.148E-05	3.597E-05	7.571E-06	3.019E-07	9.732E-08	9.124E-08	8.939E-08	8.791E-08	8.633E-08	8.463E-08
SC17	9.246E-05	3.683E-05	8.020E-06	3.467E-07	1.014E-07	9.460E-08	9.264E-08	9.111E-08	8.949E-08	8.776E-08
SC18	9.390E-05	3.856E-05	8.950E-06	3.973E-07	9.814E-08	9.127E-08	8.941E-08	8.791E-08	8.631E-08	8.460E-08
SC19	9.338E-05	3.792E-05	8.736E-06	4.361E-07	1.130E-07	1.046E-07	1.021E-07	1.003E-07	9.843E-08	9.642E-08
SC2	9.199E-05	3.634E-05	7.643E-06	2.928E-07	9.980E-08	9.382E-08	9.195E-08	9.042E-08	8.879E-08	8.705E-08
SC20	9.379E-05	3.572E-05	7.444E-06	2.962E-07	1.015E-07	9.527E-08	9.337E-08	9.177E-08	9.006E-08	8.823E-08
SC3	9.328E-05	3.781E-05	8.586E-06	3.898E-07	1.017E-07	9.465E-08	9.266E-08	9.115E-08	8.954E-08	8.781E-08
SC4	9.411E-05	3.875E-05	9.141E-06	4.474E-07	1.029E-07	9.527E-08	9.334E-08	9.198E-08	9.053E-08	8.895E-08
SC5	9.363E-05	3.818E-05	8.852E-06	4.353E-07	1.043E-07	9.651E-08	9.446E-08	9.302E-08	9.148E-08	8.984E-08
SC6	9.564E-05	4.051E-05	1.033E-05	6.262E-07	1.058E-07	9.620E-08	9.387E-08	9.237E-08	9.081E-08	8.912E-08
SC7	9.250E-05	3.684E-05	8.045E-06	3.532E-07	1.006E-07	9.367E-08	9.169E-08	9.018E-08	8.857E-08	8.685E-08
SC8	9.300E-05	3.746E-05	8.385E-06	3.757E-07	1.013E-07	9.434E-08	9.235E-08	9.083E-08	8.921E-08	8.747E-08
SC9	9.243E-05	3.676E-05	7.962E-06	3.396E-07	1.006E-07	9.391E-08	9.192E-08	9.035E-08	8.869E-08	8.692E-08
SE1	9.356E-05	3.806E-05	8.753E-06	4.196E-07	1.073E-07	9.998E-08	9.698E-08	9.630E-08	9.416E-08	9.306E-08
SE2	9.374E-05	3.827E-05	8.884E-06	4.346E-07	1.073E-07	9.949E-08	9.735E-08	9.528E-08	9.321E-08	9.182E-08
SW1	9.466E-05	3.935E-05	9.672E-06	5.716E-07	1.146E-07	1.041E-07	1.013E-07	1.002E-07	9.827E-08	9.647E-08
VE1	9.282E-05	3.712E-05	8.238E-06	3.847E-07	9.920E-08	9.338E-08	9.111E-08	8.925E-08	8.689E-08	8.640E-08
VE2	9.304E-05	3.733E-05	8.366E-06	3.947E-07	1.001E-07	9.377E-08	9.146E-08	8.875E-08	8.820E-08	8.561E-08
VE3	9.327E-05	3.772E-05	8.525E-06	3.986E-07	1.055E-07	9.857E-08	9.703E-08	9.470E-08	9.322E-08	9.101E-08
Average	9.289E-05	3.715E-05	8.446E-06	4.331E-07	1.064E-07	9.840E-08	9.620E-08	9.455E-08	9.286E-08	9.104E-08
2σ	6.351E-06	8.050E-06	3.764E-06	3.429E-07	1.552E-08	1.360E-08	1.346E-08	1.328E-08	1.316E-08	1.298E-08

**Table B.13. <sup>157</sup>Gd concentration results from all participants at 40% void fraction**

Burnup (GWd/MTU)	2.00	4.00	6.00	8.00	10.00	12.00	14.00	16.00	18.00	20.00
AL1	9.894E-05	4.517E-05	1.409E-05	1.602E-06	1.508E-07	1.254E-07	1.209E-07	1.191E-07	1.175E-07	1.156E-07
AP1	9.555E-05	4.087E-05	1.105E-05	9.228E-07	1.551E-07	1.366E-07	1.331E-07	1.312E-07	1.293E-07	1.273E-07
CA1	9.651E-05	4.188E-05	1.179E-05	1.103E-06	1.498E-07	1.283E-07	1.232E-07	1.212E-07	1.196E-07	1.178E-07
HE1	9.706E-05	4.282E-05	1.247E-05	1.282E-06	1.904E-07	1.634E-07	1.578E-07	1.557E-07	1.536E-07	1.516E-07
HE2	1.012E-04	4.777E-05	1.614E-05	2.363E-06	2.159E-07	1.590E-07	1.510E-07	1.482E-07	1.460E-07	1.437E-07
HE3	9.670E-05	4.226E-05	1.201E-05	1.141E-06	1.765E-07	1.534E-07	1.485E-07	1.464E-07	1.446E-07	1.425E-07
HE4	9.523E-05	4.062E-05	1.095E-05	9.202E-07	1.684E-07	1.498E-07	1.455E-07	1.436E-07	1.417E-07	1.397E-07
KE1	8.554E-05	2.859E-05	5.300E-06	4.800E-07	1.868E-07	1.646E-07	1.607E-07	1.595E-07	1.585E-07	1.572E-07
KE2	8.680E-05	3.024E-05	5.963E-06	5.428E-07	1.786E-07	1.548E-07	1.501E-07	1.488E-07	1.480E-07	1.471E-07
KE3	8.549E-05	2.851E-05	5.300E-06	4.818E-07	1.871E-07	1.647E-07	1.606E-07	1.596E-07	1.584E-07	1.569E-07
MO1	9.376E-05	3.885E-05	9.758E-06	7.038E-07	1.550E-07	1.405E-07	1.374E-07	1.347E-07	1.334E-07	1.318E-07
SC1	9.514E-05	4.061E-05	1.087E-05	8.504E-07	1.339E-07	1.186E-07	1.159E-07	1.141E-07	1.138E-07	1.130E-07
SC10	9.382E-05	3.903E-05	9.955E-06	7.381E-07	1.477E-07	1.332E-07	1.301E-07	1.286E-07	1.272E-07	1.255E-07
SC11	9.415E-05	3.955E-05	1.025E-05	7.660E-07	1.469E-07	1.326E-07	1.294E-07	1.280E-07	1.267E-07	1.249E-07
SC12	9.417E-05	3.969E-05	1.059E-05	8.710E-07	1.539E-07	1.373E-07	1.335E-07	1.316E-07	1.297E-07	1.277E-07
SC13	9.387E-05	3.934E-05	1.033E-05	8.510E-07	1.750E-07	1.575E-07	1.538E-07	1.521E-07	1.505E-07	1.487E-07
SC14	9.408E-05	3.919E-05	1.011E-05	7.718E-07	1.599E-07	1.447E-07	1.409E-07	1.410E-07	1.379E-07	1.372E-07
SC15	9.447E-05	3.982E-05	1.050E-05	8.504E-07	1.622E-07	1.452E-07	1.414E-07	1.395E-07	1.377E-07	1.358E-07
SC16	9.343E-05	3.872E-05	9.791E-06	6.985E-07	1.404E-07	1.270E-07	1.240E-07	1.226E-07	1.211E-07	1.195E-07
SC17	9.382E-05	3.903E-05	9.955E-06	7.381E-07	1.477E-07	1.332E-07	1.301E-07	1.286E-07	1.272E-07	1.255E-07
SC18	9.503E-05	4.048E-05	1.079E-05	8.224E-07	1.429E-07	1.283E-07	1.254E-07	1.240E-07	1.225E-07	1.209E-07
SC19	9.487E-05	4.025E-05	1.080E-05	9.169E-07	1.663E-07	1.478E-07	1.437E-07	1.419E-07	1.402E-07	1.383E-07
SC2	9.376E-05	3.886E-05	9.690E-06	6.442E-07	1.427E-07	1.302E-07	1.273E-07	1.258E-07	1.243E-07	1.226E-07
SC20	9.299E-05	3.826E-05	9.564E-06	6.753E-07	1.509E-07	1.372E-07	1.342E-07	1.327E-07	1.310E-07	1.292E-07
SC3	9.462E-05	3.998E-05	1.056E-05	8.239E-07	1.481E-07	1.330E-07	1.298E-07	1.284E-07	1.269E-07	1.253E-07
SC4	9.552E-05	4.102E-05	1.124E-05	9.521E-07	1.498E-07	1.329E-07	1.297E-07	1.285E-07	1.272E-07	1.258E-07
SC5	9.502E-05	4.042E-05	1.091E-05	9.220E-07	1.544E-07	1.369E-07	1.335E-07	1.321E-07	1.308E-07	1.293E-07
SC6	9.687E-05	4.257E-05	1.235E-05	1.230E-06	1.590E-07	1.364E-07	1.322E-07	1.307E-07	1.293E-07	1.277E-07
SC7	9.392E-05	3.913E-05	1.005E-05	7.623E-07	1.455E-07	1.306E-07	1.274E-07	1.259E-07	1.245E-07	1.229E-07
SC8	9.431E-05	3.961E-05	1.033E-05	7.924E-07	1.475E-07	1.326E-07	1.295E-07	1.280E-07	1.265E-07	1.248E-07
SC9	9.373E-05	3.888E-05	9.834E-06	7.122E-07	1.456E-07	1.316E-07	1.284E-07	1.269E-07	1.253E-07	1.235E-07
SE1	9.476E-05	3.998E-05	1.054E-05	8.374E-07	1.587E-07	1.417E-07	1.385E-07	1.380E-07	1.349E-07	1.339E-07
SE2	9.490E-05	4.020E-05	1.068E-05	8.664E-07	1.591E-07	1.425E-07	1.383E-07	1.362E-07	1.356E-07	1.334E-07
SW1	9.566E-05	4.112E-05	1.142E-05	1.073E-06	1.737E-07	1.501E-07	1.456E-07	1.439E-07	1.423E-07	1.401E-07
VE1	9.389E-05	3.899E-05	9.985E-06	7.721E-07	1.488E-07	1.330E-07	1.287E-07	1.288E-07	1.256E-07	1.246E-07
VE2	9.409E-05	3.914E-05	1.007E-05	7.849E-07	1.490E-07	1.328E-07	1.294E-07	1.284E-07	1.262E-07	1.247E-07
VE3	9.425E-05	3.952E-05	1.024E-05	7.872E-07	1.563E-07	1.398E-07	1.378E-07	1.350E-07	1.332E-07	1.328E-07
Average	9.427E-05	3.949E-05	1.044E-05	8.933E-07	1.589E-07	1.402E-07	1.364E-07	1.348E-07	1.332E-07	1.316E-07
2σ	5.939E-06	7.281E-06	3.908E-06	6.594E-07	3.368E-08	2.348E-08	2.241E-08	2.231E-08	2.221E-08	2.212E-08

**Table B.14.** <sup>157</sup>Gd concentration results from all participants at 70% void fraction

Burnup (GWd/MTU)	2.00	4.00	6.00	8.00	10.00	12.00	14.00	16.00	18.00	20.00
AL1	1.007E-04	4.776E-05	1.661E-05	2.764E-06	2.635E-07	1.844E-07	1.742E-07	1.717E-07	1.702E-07	1.688E-07
AP1	9.777E-05	4.407E-05	1.387E-05	1.883E-06	2.460E-07	1.932E-07	1.859E-07	1.838E-07	1.823E-07	1.808E-07
CA1	9.875E-05	4.512E-05	1.468E-05	2.172E-06	2.486E-07	1.819E-07	1.717E-07	1.687E-07	1.674E-07	1.661E-07
HE1	9.908E-05	4.563E-05	1.512E-05	2.351E-06	3.164E-07	2.396E-07	2.282E-07	2.251E-07	2.236E-07	2.223E-07
HE2	1.048E-04	5.284E-05	2.081E-05	4.749E-06	5.139E-07	2.382E-07	2.176E-07	2.117E-07	2.090E-07	2.068E-07
HE3	9.891E-05	4.540E-05	1.481E-05	2.183E-06	2.883E-07	2.224E-07	2.122E-07	2.094E-07	2.079E-07	2.064E-07
HE4	9.770E-05	4.407E-05	1.391E-05	1.915E-06	2.734E-07	2.190E-07	2.100E-07	2.075E-07	2.060E-07	2.045E-07
KE1	9.036E-05	3.537E-05	9.525E-06	1.492E-06	3.557E-07	2.652E-07	2.467E-07	2.426E-07	2.426E-07	2.427E-07
KE2	9.253E-05	3.741E-05	1.058E-05	1.740E-06	3.603E-07	2.522E-07	2.322E-07	2.272E-07	2.272E-07	2.277E-07
KE3	9.040E-05	3.543E-05	9.375E-06	1.507E-06	3.568E-07	2.651E-07	2.470E-07	2.428E-07	2.422E-07	2.423E-07
MO1	9.613E-05	4.214E-05	1.252E-05	1.508E-06	2.430E-07	2.040E-07	1.974E-07	1.952E-07	1.938E-07	1.932E-07
SC1	9.730E-05	4.359E-05	1.350E-05	1.720E-06	2.114E-07	1.698E-07	1.623E-07	1.614E-07	1.598E-07	1.605E-07
SC10	9.630E-05	4.250E-05	1.288E-05	1.624E-06	2.316E-07	1.899E-07	1.832E-07	1.816E-07	1.807E-07	1.796E-07
SC11	9.649E-05	4.259E-05	1.281E-05	1.547E-06	2.227E-07	1.854E-07	1.794E-07	1.777E-07	1.769E-07	1.756E-07
SC12	9.680E-05	4.329E-05	1.363E-05	1.880E-06	2.450E-07	1.939E-07	1.861E-07	1.838E-07	1.823E-07	1.808E-07
SC13	9.633E-05	4.278E-05	1.327E-05	1.814E-06	2.816E-07	2.304E-07	2.222E-07	2.202E-07	2.192E-07	2.181E-07
SC14	9.649E-05	4.258E-05	1.293E-05	1.665E-06	2.550E-07	2.123E-07	2.031E-07	2.006E-07	1.973E-07	1.994E-07
SC15	9.719E-05	4.359E-05	1.370E-05	1.894E-06	2.660E-07	2.127E-07	2.042E-07	2.019E-07	2.006E-07	1.992E-07
SC16	9.634E-05	4.259E-05	1.297E-05	1.630E-06	2.186E-07	1.776E-07	1.712E-07	1.696E-07	1.687E-07	1.677E-07
SC17	9.630E-05	4.250E-05	1.288E-05	1.624E-06	2.316E-07	1.899E-07	1.832E-07	1.816E-07	1.807E-07	1.796E-07
SC18	9.727E-05	4.366E-05	1.360E-05	1.745E-06	2.235E-07	1.816E-07	1.756E-07	1.741E-07	1.732E-07	1.721E-07
SC19	9.738E-05	4.377E-05	1.381E-05	1.932E-06	2.672E-07	2.121E-07	2.034E-07	2.012E-07	2.001E-07	1.988E-07
SC2	9.634E-05	4.222E-05	1.241E-05	1.381E-06	2.104E-07	1.788E-07	1.731E-07	1.714E-07	1.702E-07	1.688E-07
SC20	9.576E-05	4.197E-05	1.260E-05	1.552E-06	2.403E-07	2.005E-07	1.942E-07	1.925E-07	1.913E-07	1.900E-07
SC3	9.706E-05	4.342E-05	1.353E-05	1.782E-06	2.343E-07	1.890E-07	1.822E-07	1.806E-07	1.797E-07	1.787E-07
SC4	9.806E-05	4.466E-05	1.444E-05	2.069E-06	2.438E-07	1.875E-07	1.803E-07	1.788E-07	1.782E-07	1.777E-07
SC5	9.755E-05	4.400E-05	1.401E-05	1.983E-06	2.528E-07	1.968E-07	1.891E-07	1.875E-07	1.868E-07	1.861E-07
SC6	9.919E-05	4.595E-05	1.542E-05	2.446E-06	2.727E-07	1.960E-07	1.868E-07	1.848E-07	1.839E-07	1.830E-07
SC7	9.646E-05	4.270E-05	1.307E-05	1.696E-06	2.289E-07	1.841E-07	1.772E-07	1.755E-07	1.747E-07	1.737E-07
SC8	9.673E-05	4.303E-05	1.326E-05	1.718E-06	2.325E-07	1.887E-07	1.819E-07	1.803E-07	1.793E-07	1.782E-07
SC9	9.608E-05	4.218E-05	1.261E-05	1.529E-06	2.232E-07	1.851E-07	1.787E-07	1.769E-07	1.758E-07	1.745E-07
SE1	9.701E-05	4.325E-05	1.335E-05	1.745E-06	2.557E-07	2.086E-07	1.993E-07	1.984E-07	1.958E-07	1.955E-07
SE2	9.971E-05	4.635E-05	1.554E-05	2.430E-06	2.817E-07	2.070E-07	1.971E-07	1.943E-07	1.953E-07	1.920E-07
SW1	9.779E-05	4.420E-05	1.416E-05	2.081E-06	2.863E-07	2.199E-07	2.116E-07	2.083E-07	2.067E-07	2.067E-07
VE1	9.607E-05	4.209E-05	1.262E-05	1.579E-06	2.366E-07	1.934E-07	1.858E-07	1.825E-07	1.832E-07	1.824E-07
VE2	9.625E-05	4.231E-05	1.273E-05	1.612E-06	2.366E-07	1.932E-07	1.868E-07	1.838E-07	1.840E-07	1.828E-07
VE3	9.643E-05	4.263E-05	1.292E-05	1.627E-06	2.481E-07	2.071E-07	1.975E-07	1.963E-07	1.960E-07	1.929E-07
Average	9.697E-05	4.323E-05	1.353E-05	1.907E-06	2.650E-07	2.042E-07	1.951E-07	1.927E-07	1.917E-07	1.907E-07
2σ	4.913E-06	5.930E-06	3.765E-06	1.142E-06	1.134E-07	4.795E-08	4.177E-08	4.033E-08	4.039E-08	4.073E-08